

## Dissertation

# Resource recovery from fermentation waste streams by membrane technologies with a focus on electrodialysis

submitted in satisfaction of the requirements for the degree of  
Doctor of Science of the TU Wien, Faculty of Civil and Environmental Engineering

by

**Katarina Knežević MSc**

Student Registration Number: 11845277

Under the supervision of

**Univ.-Prof. Dr.-Ing. Jörg Krampe**

and

**Ass. Prof. Dr.rer.nat. Mag.rer.nat Norbert Kreuzinger**

**Examiner:** Univ.-Prof. Dr.-Ing. habil. **Thomas Wintgens**  
Institute of Environmental Engineering  
RWTH Aachen University  
Mies-van-der-Rohe-Straße 1  
52074 Aachen

**Examiner:** Univ.-Prof. Dr.-Ing. **Markus Engelhart**  
Institute of Water Resources Engineering  
Technical University Darmstadt  
Franziska-Braun-Straße 7  
64287 Darmstadt

Vienna, February 2023

**Dissertation**

**Ressourcengewinnung aus Fermentationsabfallströmen  
durch Membrantechnologien mit Schwerpunkt auf  
Elektrodialyse**

ausgeführt zum Zwecke der Erlangung des akademischen Grads eines  
Doktors der technischen Wissenschaften  
eingereicht an der TU Wien, Fakultät für Bau- und Umweltingenieurwesen

von

**Katarina Knežević MSc**

Matr.Nr.: 11845277

Unter der Leitung von  
**Univ.-Prof. Dr.-Ing. Jörg Krampe**  
und

**Ass. Prof. Dr.rer.nat. Mag.rer.nat Norbert Kreuzinger**

Gutachter: Univ.-Prof. Dr.-Ing. habil. **Thomas Wintgens**  
Institut für Siedlungswasserwirtschaft  
RWTH Aachen University,  
Mies-van-der-Rohe-Straße 1  
52074 Aachen

Gutachter: Univ.-Prof. Dr.-Ing. **Markus Engelhart**  
Institut IWAR  
Technische Universität Darmstadt  
Franziska-Braun-Straße 7  
64287 Darmstadt

Wien, im Februar 2023

## ACKNOWLEDGMENT

I would like to begin by expressing my sincere gratitude to Prof. Anton Friedl for providing me with the opportunity to start my journey in TU Wien and for introducing me to the world of scientific research in Austria. My practical work at the Institute of Chemical, Environmental and Bioscience Engineering was a crucial step in my doctoral studies. I am also deeply grateful to my supervisors, Prof. Jörg Krampe and Prof. Norbert Kreuzinger, for selecting me to participate in the Bioactive project at the Institute of Water Quality and Resource Management. Their guidance and support have been of immense importance throughout my research. I want to express my appreciation for the Bioactive project and its leader, Professor Robert Mach. His innovative ideas and efforts have been essential in setting up the project and fostering collaboration among all participants. I would also like to extend my sincere appreciation to all my colleagues within the project for the mutual support and collaboration throughout my research. Their contributions have been instrumental in making this thesis a success. I would like to express my deep appreciation to Prof. Michael Harasek for his scientific input and expertise in the area of electrodialysis. His contribution to my research has been invaluable and I am truly grateful. I would also like to acknowledge the contributions of my colleagues, Daniela Reif and Laura Vanessa Daza Serna, with whom I had an amazing and inspiring collaboration. I am grateful for Zdravka and Ernis Saracevic's thorough examination of thousands of water samples, their insightful discussions, and the hands-on training they provided me. I am also thankful to all the TU Wien colleagues I met during my practical work and doctoral studies for their support and assistance. Finally, I would like to thank my family, friends from fencing, friends in Serbia and new friends from Austria, for their understanding and support throughout this challenging but rewarding process

## Abstract

The recognition of finite and scarce natural resources that are essential for all living organisms on earth as well as industrial production set off a search for alternative approaches to resource procurement. Some of the scarce elements are for example phosphorus and magnesium. In this context, wastewater has been identified as a source of many valuable compounds. The reuse of these compounds could diminish especially the current nutrient scarcity of agricultural fertilizer if appropriate and safe recovery technologies are developed. Treatment of waste streams from industrial processes for nutrient recovery at source embraces technological solutions that lead to a reduction of waste streams and circularity of materials through water and nutrient recycling and reuse on site. This approach also protects the environment from excess nutrient pollution and the eutrophication of natural water bodies.

As a part of the “Bioactive” project, a PhD program established at TU Wien, this thesis focused on electrodialysis as recovery technology, although there is a variety of other emerging technologies for nutrient and water reuse. Electrodialysis is an electro-membrane technology, commonly applied for seawater desalination. But over the last few years, its application has been seen as a promising technique in wastewater treatment too. Due to the significant physical and chemical differences between seawater and wastewater, electrodialysis demands thorough research to test and justify its integration in wastewater treatment or even in biotechnological processes. Waste streams from these productions are heavily polluted with nutrients, carbohydrates, suspended and dissolved solids, micropollutants, and bacteria that increase the risk of premature membrane fouling and malfunctions in electrodialysis. Thus, this thesis researched the performance of electrodialysis for fermentation wastewater treatment and nutrient recovery in a batch lab-scale electrodialysis system PCCell ED 64-004 (PCCell GmbH, Germany) with ten cell pairs. The electrodialysis membrane stack was modified to meet the technological requirements of each research stage.

Limiting current density (LCD) in conventional electrodialysis is one of the main operating parameters, which depends on the feed composition, pH, temperature, flow, membrane characteristics, etc. Previous publications mainly report the methods for determining LCD in NaCl solutions, mimicking the seawater characteristics. Therefore, it was necessary to evaluate existing LCD determination methods when applied to a complex fermentation effluent. The results of five LCD graphical methods, acquired from available literature, revealed complements and divergences between them when applied to feed solutions with increasing ion concentrations and feed complexity. The Cowan and Brown method came up to have the most consistent results, also when applied to feeds containing sulfates, calcium, magnesium, and other ions different from solely Na<sup>+</sup> and Cl<sup>-</sup>. Online electrical conductivity was measured for all performed experiments, and it was linearly correlated with the decreasing ion concentration of the feed solution and corresponding LCD. Thus, the conductivity can be applied for an automatized dynamic control of the operating current density–voltage in the batch electrodialysis.

Other resources, besides nutrients, may be present in waste streams and potentially can be recovered. For example, sulfuric acid is used for the pH control of fermentation with *Sulfolobus acidocaldarius*. Consequently, sulfate ions are the dominating ions in the fermentation waste effluent, which could be recovered by bipolar electrodialysis in a form of sulfuric acid. However, some polluting compounds from the fermentation process end up in the fermentation

effluent too and need to be removed before a subsequent acid/base recovery. Bipolar membranes are especially sensitive to the scaling of calcium and magnesium salts as well as to biofouling caused by microbial growth and linked aspects. In this regard, three pre-treatment technologies were compared for a reduction of divalent cations to a value below 10 ppm and DOC removal from the fermentation wastewater. As a result, both nanofiltration and electro dialysis with monovalent cation exchange membranes were demonstrated to be suitable pre-treatment technologies with 92–96% divalent cation removal and 86–94% DOC removal. Nanofiltration had higher stability in divalent cation rejection and was less energy-consuming, whereas electro dialysis delivered a 1.6-fold concentration factor for sulfate ions, preferable for a subsequent sulfuric acid recovery. The third assessed technology was the ion-exchange resins, which had complete divalent cation removal until the resins' saturation. However, there was no DOC removal and another disadvantage is the need for resins' recovery by chemicals, which adds up additional costs and produces a waste stream.

There is a research gap in recovering nutrients from real wastewater samples by membrane technologies and their actual reuse in biotechnological processes. Moreover, the ability of membranes to retain compounds potentially harmful to fermentation processes is essential, as these compounds are rarely included in experiments with synthetic media. Again, the waste fermentation effluent from the *Sulfolobus acidocaldarius* fermentation was treated in this thesis. This time three pathways for resource recovery were applied: nanofiltration, conventional and bipolar electro dialysis. The recovered media were subjected to batch fermentations for evaluation of suitability in a closed-loop fermentation. Reference fermentation was performed with freshly prepared chemicals. Tests were also obtained with solely microfiltered fermentation effluent, which did not proliferate in microbial growth. Nanofiltration and electro dialysis had high DOC removal and separation of ions from the rest of the media. Further on, 0.11–0.15 M sulfuric acid was recovered by bipolar electro dialysis as described in the previous paragraph. All of the recovered media, used either as a fermentation substrate or for pH regulation, resulted in a similar substrate uptake and microbial growth as the reference fermentation. Nanofiltration had lower energy consumption, but electro dialysis offered selective ion recovery, higher concentration factors, and reuse-specific streams. The removal of nutrients from the fermentation wastewater also reduced the negative environmental impact of the fermentation process.

Optimization of product separation is also a current research topic, along with the recovery and reuse of resources. In this sense, electro dialysis can potentially be used for erythritol separation from the fermentation broth. This approach has a twofold benefit, purifying erythritol and producing a salt concentrate that could be reused for a subsequent erythritol fermentation. In this thesis, four commercial ED membrane stacks were investigated and compared in terms of diffusion of erythritol and by-products, current efficiency, and energy consumption for the same salt removal from a synthetic culture broth. The membrane pair composed of FAS-PET-130 (AEM) and FKS-PET-130 (CEM) (Fumatech GmbH, Germany) had the highest current efficiency (79.1%), high retention of products and by-products (0.53% erythritol losses from feed containing 25 g/L erythritol), and the membrane resistance and energy consumption in the range of other tested membranes. Step-wise voltage control was demonstrated to yield fewer product losses than the commonly applied constant current approach, mainly governed by the reduced contact time between the feed and the ion-exchange membranes. Finally, 2% erythritol

losses were recorded when electro dialysis was operated with a real culture broth containing 25 g/L erythritol.

Concludingly, this thesis first investigated the methods for determining the limiting current density in electro dialysis for the treatment of real waste streams. Followingly, the applicability of electro dialysis for resource recovery from fermentation wastewater in form of nutrient concentrates and recovered acids/bases was demonstrated. Electro dialysis was compared to membrane filtration and ion exchange resins. Finally, electro dialysis was tested for erythritol separation, a product from fermentation, to improve process sustainability. Results were summarized in four peer-reviewed publications.

## Kurzfassung

Die Erkenntnis, dass viele Ressourcen, die für lebende Organismen sowie die industrielle Produktion unerlässlich sind, endlich und knapp sind, führt zu einer Suche nach alternativen Ansätzen zur Ressourcengewinnung. Zu diesen begrenzt verfügbaren Elementen zählen beispielsweise Phosphor und Magnesium, für die Abwasser als alternative Quelle für eine Rückgewinnung identifiziert wurde. Insbesondere die derzeitige Nährstoffknappheit als Grundlage für landwirtschaftlichen Dünger könnte durch eine Nährstoffrückgewinnung aus Abwasser reduziert werden, wenn geeignete und sichere Rückgewinnungstechnologien für diesen Bereich weiterentwickelt werden. Die Rückgewinnung von Nährstoffen aus Abwasserströmen von industriellen Prozessen am Ort der Entstehung umfasst dabei technologische Lösungen, die zu einer Reduzierung von Abwasserströmen und zur Kreislaufführung von Materialien durch Nährstoff- und Wasserrecycling führen. Dieser Ansatz der Kreislaufschließung trägt auch zum Schutz der Umwelt vor übermäßiger Nährstoffbelastung bei und schützt somit natürliche Gewässer vor einer Eutrophierung.

Diese Dissertation, entstanden im Rahmen des Projekts "Bioactive" als ein PhD-Programm der TU Wien, legt den Fokus auf die Elektrodialyse als Rückgewinnungstechnologie. Die Elektrodialyse ist eine elektro-membranbasierte Technologie, die häufig zur Entsalzung von Meerwasser angewendet wird. Seit einigen Jahren wird sie jedoch auch in der Abwasserbehandlung als vielversprechende Technik angesehen. Die erheblichen physikalischen und chemischen Unterschiede zwischen Meerwasser und Abwasser erfordern jedoch umfassende Untersuchungen zur Anwendung der Elektrodialyse bei Abwässern, um ihre Eignung in der Abwasserbehandlung oder in biotechnologischen Prozessen testen zu können. Die Abwässer aus Fermentationsprozessen sind stark mit Nährstoffen, Kohlenhydraten, suspendierten und gelösten Feststoffen, Mikroverunreinigungen sowie Bakterien belastet, die das Risiko eines übermäßigen Membranfoulings sowie von Fehlfunktionen in der Elektrodialyse erhöhen. Im Rahmen dieser Dissertation wurde die Leistung der Elektrodialyse zur Behandlung von Fermentationsabwässern und zur Wiedergewinnung von Nährstoffen im Labormaßstab mit einem Elektrodialyse-System vom Typ PCCell ED 64-004 (PCCell GmbH, Deutschland) mit zehn Zellpaaren untersucht. Der Elektrodialyse-Membranstapel wurden an die technologischen Anforderungen jeder Forschungsfrage angepasst.

Die Grenzstromdichte (LCD) in der konventionellen Elektrodialyse ist einer der wichtigsten Betriebsparameter, die von der Zusammensetzung, der Beschickung, dem pH-Wert, der Temperatur, dem Durchfluss, den Membraneigenschaften usw. abhängen. In früheren Veröffentlichungen werden hauptsächlich die Methoden zur Bestimmung der LCD in NaCl-Lösungen beschrieben, die den Eigenschaften von Meerwasser nachempfunden sind. Daher war es notwendig, die bestehenden Bestimmungsmethoden der LCD auf ein komplexes Fermentationsabwasser anzuwenden. Die Ergebnisse von fünf graphischen LCD-Methoden, die in der Literatur beschrieben sind, zeigten im Falle zunehmender Ionenkonzentrationen und Komplexität der Feed-Lösungen sowohl Synergien als auch Divergenzen untereinander. Die Methode von Cowan und Brown ergab insgesamt sowie hinsichtlich Lösungen, die neben  $\text{Na}^+$  und  $\text{Cl}^-$  auch Sulfate, Calcium, Magnesium und andere Ionen enthielten, die konsistentesten Ergebnisse. Die elektrische Leitfähigkeit wurde online für alle durchgeführten Experimente gemessen und korrelierte linear mit der abnehmenden Ionenkonzentration der Feed-Lösung und

der entsprechenden LCD. Somit kann die Leitfähigkeit für eine dynamische Steuerung der Batch-Elektrodialyse verwendet werden.

Neben Nährstoffen können auch andere Ressourcen in Abwasserströmen vorhanden sein und potenziell zurückgewonnen werden. Beispielsweise wird Schwefelsäure für die pH-Steuerung der Fermentation mit *Sulfolobus acidocaldarius* verwendet. Folglich sind Sulfat-Ionen die dominierenden Ionen im Abwasser der Fermentation, die durch bipolare Elektrodialyse in Form von Schwefelsäure gewonnen werden können. Einige potenziell umweltbelastende Verbindungen aus dem Fermentationsprozess gelangen jedoch auch in das Fermentationsabwasser und müssen vor einer anschließenden Säure-/Basen Wiedergewinnung entfernt werden. Bipolare Membranen sind besonders empfindlich gegenüber der Bildung von Calcium- und Magnesiumsalzen sowie gegenüber Bioverunreinigungen, die durch Mikrobewachstum und weiteren damit verbundenen Aspekten verursacht werden. Für eine Reduzierung der divalenten Kationen auf einen Wert unter 10 ppm und für eine Entfernung von DOC aus dem Fermentationsabwasser wurden drei Vorbehandlungstechnologien miteinander verglichen. Das Ergebnis zeigte, dass sowohl die Nanofiltration als auch die Elektrodialyse mit monovalenten Kationenaustauschmembranen mit Entfernungen von 92-96% der divalenten Kationen und 86-94% des DOC als Vorbehandlungstechnologien geeignet sind. Die Nanofiltration zeigte eine höhere Stabilität im Rückhaltevermögen von divalenten Kationen und eine höhere Energieeffizienz, während die Elektrodialyse einen 1,6-fachen Konzentrationsfaktor für Sulfat-Ionen lieferte, der für eine anschließende Wiedergewinnung von Schwefelsäure vorzuziehen ist. Die dritte untersuchte Technologie waren Ionenaustauschharze, die eine vollständige Entfernung von divalenten Kationen bis zur Sättigung der Harze erreichten. Es gab jedoch keine Entfernung von DOC. Ein weiterer Nachteil besteht darin, dass die Harze mit Chemikalien regeneriert werden müssen, was zusätzliche Kosten verursacht, und Abfall produziert.

Die Wiedergewinnung von Nährstoffen aus realen Abwasserproben durch Membrantechnologien und deren tatsächlicher Wiederverwendung in biotechnologischen Prozessen stellt eine Forschungslücke dar. Die Fähigkeit der Membranen, Verbindungen zurückzuhalten, die für Fermentationsprozesse potenziell schädlich sind, sind dabei von entscheidender Bedeutung. In Experimenten mit synthetischen Medien sind diese Verbindungen jedoch häufig nicht enthalten. In der vorliegenden Dissertation wurde das Abwasser aus der *Sulfolobus acidocaldarius* Fermentation behandelt. Dabei wurden drei Verfahren zur Ressourcenwiedergewinnung angewendet: Nanofiltration, konventionelle und bipolare Elektrodialyse. Die zurückgewonnenen Medien wurden in Batch-Fermentierungen eingesetzt, um die Eignung in einem geschlossenen Kreislauf zu bewerten. Die Referenzfermentation wurde mit frisch zubereiteten Chemikalien durchgeführt. Tests wurden auch mit nur mikrogefiltertem Fermentationsabwasser durchgeführt, das kein mikrobielles Wachstum aufwies. Die Nanofiltration und die Elektrodialyse zeigten eine hohe DOC-Entfernung und Trennung von Ionen von den übrigen Medien. Weiterhin wurde durch bipolare Elektrodialyse wie im vorherigen Absatz 0,11–0,15 M Schwefelsäure zurückgewonnen. Alle recycelten Medien, die entweder als Fermentationssubstrat oder zur pH-Regulierung verwendet wurden, führten zu einer ähnlichen Substrataufnahme und einem ähnlichen mikrobiellem Wachstum wie in der Referenzfermentation. Die Nanofiltration hatte einen geringeren Energieverbrauch, wohingegen die Elektrodialyse eine selektive Ionenrückgewinnung, höhere Konzentrationsfaktoren und spezifische Wiederverwendungsströme bot. Das Entfernen von

Nährstoffen aus dem Fermentationsabwasser reduziert auch potenziell negative Umweltauswirkungen des Fermentationsprozesses.

Ein weiteres, wichtiges Themengebiet stellt die Optimierung der Produktentfernung, zusammen mit der Rückgewinnung und Wiederverwendung der Ressourcen dar. In diesem Sinne kann die Elektrodialyse möglicherweise zur Trennung von Erythrit aus der Fermentationsbrühe verwendet werden. Dieser Ansatz hat einen doppelten Vorteil: Das Erythrit wird gereinigt und ein Salzkonzentrat wird erzeugt, das für eine anschließende Erythrit-Fermentation wiederverwendet werden kann. In dieser Dissertation wurden vier kommerzielle ED-Membranstacks untersucht und hinsichtlich der Diffusion von Erythrit und seinen Nebenprodukten, sowie dem elektrischen Wirkungsgrad und dem Energieverbrauch bei gleicher Salzentfernung aus einer synthetischen Kulturbrühe verglichen. Das Membranpaar, bestehend aus FAS-PET-130 (AEM) und FKS-PET-130 (CEM) (Fumatech GmbH, Deutschland), hatte den höchsten elektrischen Wirkungsgrad (79,1%), einen hohen Rückhalt von Produkten und Nebenprodukten (0,53% Erythritverluste aus einem Feed mit 25 g/L Erythrit) sowie einen Membranwiderstand und einen Energieverbrauch im Bereich der anderen getesteten Membranen. Eine schrittweise Spannungssteuerung ergab weniger Produktverluste als bei der üblichen „constant current“ Steuerung. Diese sind hauptsächlich auf die reduzierte Kontaktzeit zwischen Feed und Ionenaustauschermembranen zurückzuführen. Bei einer Anwendung der Elektrodialyse mit einer realen Kulturbrühe von 25 g/L Erythrit, wurden 2% Erythritverluste gemessen.

Zusammenfassend wurden in dieser Dissertation zunächst Methoden zur Bestimmung der Grenzstromdichte in echten Abfallströmen untersucht. Anschließend wurde die Anwendbarkeit der Elektrodialyse zur Ressourcenrückgewinnung aus Fermentationsabwässern in Form von Nährstoffkonzentraten und wiederhergestellten Säuren / Basen demonstriert. Die Elektrodialyse wurde mit Membranfiltration und Ionenaustauschharzen verglichen. Schließlich wurde die Elektrodialyse für die Trennung von Erythrit, einem Produkt der Fermentation, getestet, um die Prozessnachhaltigkeit zu verbessern. Die Ergebnisse wurden in vier 'Peer-reviewed' Publikationen zusammengefasst.

# Table of Content

Abstract .....	iv
Table of Content.....	x
List of tables .....	xiv
List of figures .....	xv
List of abbreviations.....	xviii
List of publications from the PhD Thesis.....	xx
1 Introduction .....	1
1.1 Aims and Objectives.....	2
1.2 Research questions .....	2
1.3 Structure of the thesis .....	3
2 Bioactive project .....	3
3 Background .....	5
3.1 Scarce resources and future concerns .....	5
3.2 Sustainable development goals and circular economy .....	7
3.3 State-of-the-art fermentation processes .....	8
3.4 Wastewater treatment .....	10
3.4.1 Conventional and industrial wastewater treatment .....	10
3.4.2 Advanced wastewater treatment.....	11
3.5 Resource recovery technologies .....	14
3.6 Electrodialysis for resource recovery .....	15
4 Methodological approach.....	17
4.1 Summary of the scientific papers .....	20
4.2 Scientific contributions.....	22
5 Discussion .....	23
6 Final message and outlook .....	26
References .....	28
Full text published paper I.....	32
1 Introduction .....	32
2 Materials and Methods .....	33
2.1 Experimental Set-Up .....	33

2.2	Description of Assessed LCD Determination Methods .....	35
2.2.1	Isaacson and Sonin (I–S) Method .....	35
2.2.2	Cowan and Brown (C–B) Method .....	35
2.2.3	The pH Method .....	36
2.2.4	Current Efficiency ( $\lambda$ ) Method .....	36
2.2.5	Desalting Efficiency ( $\epsilon$ ) Method .....	36
2.3	Solution Tested .....	37
2.3.1	Solution Level a—Single-Salt Solution (SSS).....	37
2.3.2	Solution Level b—Synthetic Complex Solution (SCS) .....	37
2.3.3	Solution Level c—Real Complex Solution (RCS)—Real Liquid Waste Streams .....	37
2.4	Data Processing .....	38
3	Results and Discussion.....	38
3.1	SSS—Range of NaCl Concentrations .....	38
3.2	Experiments with Different Ionic Compositions but the Same Conductivity .....	42
3.3	Same Ionic Composition but Different Initial Conductivity .....	46
4	Summary .....	47
5	Conclusions .....	48
	Appendix A .....	49
	References .....	51
	<b>Supplement 1 – Assessment of Graphical Methods for Determination of the Limiting Current Density in Complex Electrodialysis-Feed Solutions</b>	
	Full text published paper II .....	65
1	Introduction .....	65
2	Materials and Methods .....	66
2.1	Wastewater – fermentation effluent used in the study .....	66
2.2	Experimental set-up .....	67
2.3	Equipment and membranes for pretreatment experiments .....	67
2.4	Chemical analysis .....	68
2.5	Data analysis.....	68
3	Results and Discussion.....	69
3.1	NF – nanofiltration .....	70
3.2	ED – electrodialysis.....	70
3.3	IER – ion exchange resins .....	70

3.4	Removal of divalent cations and organic compounds by the three investigated technologies .....	71
3.5	Perm-selectivity of monovalent cations .....	71
3.6	Cationic fluxes .....	72
3.7	Behavior of anions .....	73
3.8	Energy consumption .....	73
4	Summary and conclusion .....	74
	References .....	74

**Supplement 2** – Comparison of ion removal from waste fermentation effluent by nanofiltration, electrodialysis and ion exchange for a subsequent sulfuric acid recovery

	Full text published paper III .....	81
1	Introduction .....	81
2	Materials and methods .....	82
2.1	Experimental set-up .....	82
2.2	Pre-treatment .....	82
2.3	ED and EDBM.....	82
2.4	Analytical methods .....	84
2.5	Cultivation of <i>Sulfolobus acidocaldarius</i> in recycled media.....	84
2.6	Data analysis.....	84
3	Results .....	85
3.1	Results of membrane filtration .....	85
3.2	Results from ED .....	85
3.2.1	Salt and water transport.....	85
3.2.2	Concentrating salts from SCB.....	85
3.2.3	Removal of ions in the diluate.....	86
3.3	Results from EDBM .....	87
3.4	Fermentation with <i>S. Acidocaldaius</i> in recycled SCB.....	87
4	Discussion .....	90
4.1	Fermentation.....	90
4.2	Nutrient recovery .....	90
4.3	Acid/base recovery .....	90
4.4	Characteristics of discharged streams.....	91
4.5	Energy requirements.....	91

5	Conclusions .....	91
	References .....	91
<b>Supplement 3 – Circular production – Evaluation of membrane technologies for nutrient recycling from a microbial fermentation effluent</b>		
	Full text submitted paper IV .....	99
1	Introduction .....	100
2	Materials and Methods .....	102
2.1	Technical equipment.....	102
2.2	Membranes .....	103
2.3	Experimental setup .....	104
2.4	Solutions (synthetic and culture broth).....	106
2.5	Analytics.....	107
2.6	Data analysis and calculations .....	108
3	Results and Discussion.....	109
3.1	LCD determination .....	109
3.2	First stage – Membrane selection .....	111
3.2.1	Diffusion of products and by-products.....	111
3.2.2	Desalination of synthetic erythritol broth (SEB).....	111
3.2.3	Product purification.....	112
3.3	Second stage – Effect of the increase in erythritol concentration .....	114
3.3.1	Diffusion of products and by-products.....	114
3.3.2	Erythritol purification and conservation .....	116
3.4	ED operating mode .....	117
3.5	Erythritol culture broth .....	119
4	Conclusion.....	121
	References .....	123

## List of tables

### Paper I:

<b>Table 1.</b> Characteristics of the ion-exchange membranes, as specified by the PCCell producer. ....	<b>34</b>
<b>Table 2.</b> Total organic carbon (TOC) and ionic content of the initial synthetic and real solutions with corresponding conductivity. ....	<b>37</b>
<b>Table 3.</b> List of solutions (SSS—2.3.1) used in the study with corresponding LCDs defined by five methods. ....	<b>38</b>
<b>Table 4.</b> List of solutions used in the study (Sections 2.3.1–2.3.3) with corresponding LCDs defined by four methods. ....	<b>44</b>

### Paper II:

<b>Table 1.</b> Physicochemical analysis of the fermentation effluent .....	<b>66</b>
<b>Table 2.</b> NF membrane characteristics as specified by the producer. ....	<b>67</b>
<b>Table 3.</b> Characteristics of ion-exchange membrane used in the ED experiments, specified by PCCell producer. ....	<b>67</b>
<b>Table 4.</b> Physical and chemical characteristics of Purolite C100E, Purolite MTS9300 and Diaion CR11, as specified by the producer. ....	<b>68</b>
<b>Table 5.</b> The rejection rate for DOC, Ca <sup>2+</sup> , and Mg <sup>2+</sup> from the fermentation effluent, performed via different technologies. ....	<b>71</b>
<b>Table 6.</b> The final composition of the pre-treated fermentation effluent meant to be forwarded to EDBM or DD for acid/base recovery. ....	<b>74</b>

### Paper III:

<b>Table 1.</b> Membranes applied in the pre-treatment of SCB with the specifications of the manufacturers. ....	<b>83</b>
<b>Table 2.</b> Ion exchange membranes and their specifications from the manufacturer. ....	<b>83</b>
<b>Table 3.</b> Overview of shake flask experiments. ....	<b>84</b>
<b>Table 4.</b> Process characteristics of ED2 and ED3. ....	<b>86</b>
<b>Table 5.</b> Fraction of ions from SCB transferred to the concentrate for each ED run separately. Reference values denote the maximum theoretical values for each stage. ....	<b>86</b>
<b>Table 6.</b> Parameters for evaluation of EDBM fed with lower ionic feed concentration (EDBM1) and higher ionic feed concentration (EDBM2). ....	<b>87</b>

### Paper IV:

<b>Table 1.</b> Membrane characteristics of the reference membrane stack (M0) and tested membrane stacks (M1-M3): .....	<b>103</b>
<b>Table 2.</b> Salt fraction of the synthetic erythritol culture broth for membrane testing in LCD, stage one and stage two. ....	<b>106</b>
<b>Table 3.</b> LCDs reached within M0–M3 membrane stacks for salt solutions S1–S4 with their measured electrical conductivities. ....	<b>110</b>
<b>Table 4.</b> Average desalination rate of anions and cations using four different membrane stacks (M0-M3). ....	<b>111</b>

## List of figures

<b>Figure 1.</b> Overview of the Ph.D. positions and tasks for tackling the challenges recognized by the Bioactive project. The position Ph.D. 9 of this thesis is marked with a red frame. (The diagram is adopted from the Bioactive project description). .....	4
<b>Figure 2.</b> Main treatment stages of a conventional wastewater treatment plant. ....	11
<b>Figure 3.</b> a) Sources of energy generation, b) resource recovery possibilities and c) water reuse options from a conventional wastewater treatment plant. ....	13
<b>Figure 4.</b> Conventional electrodialysis with cation- (CEM) and anion-exchanging membranes (AEM) for removal of Na <sub>2</sub> SO <sub>4</sub> from the feed, having dilute and concentrated outlets from the membrane stack. Source: (Kuldeep et al., 2021). ....	16
<b>Figure 5.</b> Membrane stack of bipolar electrodialysis with bipolar membranes (BPM), cation- (CEM) and anion-exchange membranes (AEM) for production of acids (H <sub>2</sub> SO <sub>4</sub> ) and bases (NaOH) from a concentrated Na <sub>2</sub> SO <sub>4</sub> feed. Source: (Kuldeep et al., 2021) .....	17
<b>Figure 6</b> Methodological approach for resolving the research questions, with the depicted scheme of each research stage. ....	18

## Paper I:

<b>Figure 1.</b> A schematic representation of the used experimental set-up, including the ED membrane stack (ED), concentrate (C), diluate (D), electrode rinse (E), centrifugal pumps (1), mixing pipe (2), conductivity and temperature sensors (3), conductivity, temperature, and pH sensors (4), data acquisition box (5). ....	34
<b>Figure 2.</b> Current–voltage curves based on the Isaacson and Sonin method for estimating LCD in (a) three lower concentrated NaCl solutions and (b) two higher concentrated NaCl solutions. The detailed image of the fitting curves and their precision in three less concentrated NaCl solutions can be found in Supplementary Figure S3 and Table S1. ....	39
<b>Figure 3.</b> ED stack resistance–reciprocal current density curves for LCD estimation of the five NaCl solutions based on the Cowan and Brown method. ....	40
<b>Figure 4.</b> Diluate pH–reciprocal current density curves for the LCD estimation for five NaCl solutions based on the pH method. The pH changes plotted against the increasing current density can be found in Supplementary Figure S5. ....	41
<b>Figure 5.</b> Current efficiency ( $\lambda$ )–voltage curves for the LCD estimation of the five NaCl solutions. ....	41
<b>Figure 6.</b> Removal efficiency ( $\epsilon$ ) for the salts present in the feed solution plotted against the applied voltage, for all of the five NaCl solutions. ....	42
<b>Figure 7.</b> Current–voltage curves for five different solutions with the same conductivity. ....	43
<b>Figure 8.</b> ED stack resistance–reciprocal current density curves for the LCD assessment of five different solutions with the same conductivity. ....	44
<b>Figure 9.</b> The $\Delta$ pH values plotted against the reciprocal current density for five different feed solutions. ....	45
<b>Figure 10.</b> Removal efficiency for the salts present in the feed plotted against the applied voltage. ....	46

**Figure 11.** Dependency of the inlet feed conductivities (mS/cm) of the dilutions from different solutions and corresponding LCDs assessed by the Cowan and Brown method. During the batch ED, the feed concentration continuously decreases, consequently, the LCD decreases..... 47

**Paper II:**

**Figure 1.** Process design and the experimental set-up for three technologies tested in this research (in the pink box). MF-microfiltration, NF-nanofiltration, IER-ion exchange resin, ED-electrodialysis with standard AEM and mCEM..... 67

**Figure 2.** Decline of permeate flux over time for two tested membranes: NF(DK) and NF270. Pressure: 23 bar; temperature: 20 °C; circulation flow: 2.2 L/min..... 69

**Figure 3.** a) Evolution of the diluate and concentrate conductivities in the first and second ED run; b) Diluate pH during the demineralization; c) Voltage applied to the ED stack; d) The step-wise current density trend for wastewater demineralization. .... 69

**Figure 4.** Breakthrough point for three types of IER applied for: a) Ca<sup>2+</sup> removal and b) Mg<sup>2+</sup> removal from the fermentation effluent. The temperature was kept at 22 °C ..... 70

**Figure 5.** a) Perm-selectivity between individual monovalent cations (Na<sup>+</sup>, NH<sub>4</sub>- N, or K<sup>+</sup>) and sum of divalent cations (Mg<sup>2+</sup> and Ca<sup>2+</sup>) for the mCEM during the ED operation time; b) fluxes of Mg<sup>2+</sup> and Ca<sup>2+</sup> in the first and the second ED run, depicted over ED operation time. .... 71

**Figure 6.** Characteristics of the NF permeates represented by a) the electrical conductivity and b) the pH measurements. .... 72

**Figure 7.** Average flux of cations through NF(DK), NF270 nanomembranes and mCEM in ED. Flux values for ED are based on two ED runs. .... 72

**Figure 8.** Permeation (migration) of anionic species from the diluate to the concentrate solution through AEM during ED..... 73

**Figure 9.** Energy consumption for pumps in nanofiltration, and for pumps and external electrical field for desalination in ED. .... 73

**Paper III:**

**Figure 1.** Process scheme with four assessed stages: I Pre-treatment by MF or UF/NF, II Conventional electrodialysis (ED), III Electrodialysis with bipolar membranes (EDBM), IV Shake flask fermentation (SF). Other involved technologies: FM – fermentation, F – filtration, MF – microfiltration, UF – ultrafiltration, NF – nanofiltration. Relevant streams: Product, Effluent, C – concentrate, D – diluate, A – acid, B –base, Neutralization, Water, and Base Reuse. Processes with grey lines are not in the scope of this work. .... 83

**Figure 2.** ED1 desalination process with a) conductivity change in the diluate (SCB) and concentrate over ime. Denoted segments correspond to different current densities applied in consecutive steps (dotted line); b) desalination/concentration slopes and their differences for each desalination segment. .... 85

**Figure 3.** Doubling the ionic content of the receiving medium from two different feed solutions: a) with lower initial ionic content (ED<sub>2</sub> = ED<sub>2\_1</sub>+ED<sub>2\_2</sub>) and b) with higher ionic content (ED<sub>3</sub> = ED<sub>3\_1</sub>+ED<sub>3\_2</sub>)..... 86

<b>Figure 4.</b> Removal efficiency of each analyzed ion with the standard deviation bars in the first ED runs (ED1, ED2_1 and ED3_1) for transferring ions, and subsequent ED runs (ED2_2 and ED_3_2) for concentrating ions. ....	<b>86</b>
<b>Figure 5.</b> Conversion of two fermentation effluents with various ionic strengths to corresponding acid/base produced via bipolar membranes in a) EDBM1 and b) EDBM2. ....	<b>87</b>
<b>Figure 6.</b> Results of optical density (OD600) measurements in a) and substrate concentration in b) at each sampling point of cultures grown in ED1, ED2 and NF medium compared to fresh medium (VD). ....	<b>88</b>
<b>Figure 7.</b> Results of optical density (OD600) measurements in a) and substrate concentration in b) at each sampling point of cultures grown in MF, VD + recovered acids and mix of ED1 and recovered acid medium. A1 and A2 are the acids recovered by EDBM. ....	<b>89</b>
<b>Figure 8.</b> Contribution of the recovered ions to the total ionic content of recovered media compared to the fresh media composition. ....	<b>89</b>
<b>Figure 9.</b> Energy consumed per m <sup>3</sup> of treated SCB and the ionic equivalents that were removed from the effluents of the each tested technology. ....	<b>90</b>

#### **Paper IV:**

<b>Figure 1.</b> Scheme of experimental methods for the membrane selection and overall performance of erythritol separation by electro dialysis under various erythritol concentrations and operating conditions. SEB – synthetic erythritol broth containing 5 g/L (SEB <sub>5</sub> ), 15 g/L (SEB <sub>15</sub> ) or 25 g/L (SEB <sub>25</sub> ) erythritol; ECB -erythritol culture broth. ....	<b>104</b>
<b>Figure 2.</b> The resistance of M0–M3 membrane stacks for applied 12V in LCD test of four salt solutions with increasing salt content. S4 is the initial solution to be treated, whereas S1 represents the desired final solution after the ED treatments. ....	<b>110</b>
<b>Figure 3.</b> Comparison of current efficiency and energy consumption for desalination of erythritol broth among four tested membranes (M0–M3). ....	<b>113</b>
<b>Figure 4.</b> a) Diffusion of erythritol and glycerol from the feed towards concentrate depending on the erythritol concentration in the feed; b) Evolution of erythritol and glycerol diffusion over circulation time. "Ery" stays for erythritol and "Gly" for glycerol. ....	<b>116</b>
<b>Figure 5.</b> Diffusion of erythritol from the feed containing 5 g/L, 15 g/L and 25 g/L of erythritol towards the concentrate solution (black circles); Erythritol flux in the ED desalination that includes convective diffusion and co-transport with ionic species driven by the external electrical field (white circles). ....	<b>117</b>
<b>Figure 6.</b> Evolution of erythritol in the concentrate during the desalination of 25 g/L erythritol broth by ED with applied step-wise voltage vs. constant current. ....	<b>118</b>
<b>Figure 7.</b> Evolution of the erythritol (Ery) and glucose (Glu) molar fluxes from the feed to the concentrate in the ED desalination of the real erythritol culture broth. The evolution of Ery and Glu concentrations in the concentrate is on the right y-axis. ....	<b>120</b>

## List of abbreviations

DD – diffusion dialysis

DOC – dissolved organic carbon

ED – electrodialysis (conventional)

EDBM – electrodialysis with bipolar membranes (bipolar electrodialysis)

EDm – electrodialysis with monovalent selective cation-exchange membrane

IEM – ion exchange membrane

IER – ion-exchange resins

LCD – limiting current density

MF – microfiltration

NF – nanofiltration

SCB – spent culture broth

UF – ultrafiltration

VD – reference medium

$\%p^{NF}$ , % – ion permeation in nanofiltration membrane

CE, % – current efficiency

E, kWh/kg – energy consumption

F, sA/mol – Faraday constant (96485 sA/mol)

I, A – electrical current

$J^{NF}$ , mol/(m<sup>2</sup>h) – ionic flux in nanofiltration membrane

N, - – number of cell pairs

$R_d$ , % – demineralization rate (total removal efficiency)

RE, % – removal efficiency

$R^{NF}$ , % – rejection rate for an ion in nanofiltration membrane

$R_s$ , % – recovery/conversion rate

$S_n^i$  - - membrane perm-selectivity

U, V – electrical potential

$w_i$  - - mass fraction

$z_i$  - - ion valence

## List of publications from the PhD Thesis

The following papers have either been published or submitted for publishing:

### Paper I:

*“Assessment of Graphical Methods for Determination of the Limiting Current Density in Complex Electrodialysis-Feed Solutions”*

Published in **Membranes**

Submitted on 17 January 2022; Published on 18 February 2022

Open access

doi: 10.3390/membranes12020241

<https://doi.org/10.3390/membranes12020241>

### Paper II:

*“Comparison of ion removal from waste fermentation effluent by nanofiltration, electrodialysis and ion exchange for a subsequent sulfuric acid recovery”*

Published in **Journal of Environmental Chemical Engineering**

Submitted on 28 May 2022; Published on 10 August 2022

Open access

doi: 10.1016/j.jece.2022.108423

<https://doi.org/10.1016/j.jece.2022.108423>

### Paper III:

*“Circular production – Evaluation of membrane technologies for nutrient recycling from a microbial fermentation effluent”*

Published in **Journal of Cleaner Production**

Submitted on 28 April 2022; Published on 4 October 2022

Open access

doi: 10.1016/j.jclepro.2022.134436

<https://doi.org/10.1016/j.jclepro.2022.134436>

### Paper IV:

*“Investigation of ion-exchange membranes and erythritol concentration for the desalination of erythritol culture broth by electrodialysis”*

Submitted to **Chemical Engineering and Processing – Process Intensification**

Submitted on 11 September 2022

# 1 Introduction

Pharmaceutical and food industries generate a large amount of wastewater, which may contain valuable nutrients, but at the same time, toxic substances may be present. Valuable nutrients, such as phosphorus and nitrogen, are considered pollutants if they are discharged uncontrolled into the environment. Thus, wastewater treatment is necessary for the removal of potentially harmful substances and nutrients emerging from cultivation processes to prevent the imbalances of natural processes. Commonly, biological treatment is performed in centralized wastewater treatment plants, where microorganisms remove / transform nitrogenous and carbonic compounds from wastewater e.g. in nitrification/denitrification processes. Phosphorus in wastewater is partially removed by microorganisms and partially needs to be chemically precipitated. Precipitated phosphorus requires further treatment for its recovery, safe disposal, or reuse. Industrial wastewater is either separately treated or forwarded to urban wastewater treatment plants, often with a pre-treatment step at the industry location. Biological treatment is, however, susceptible to changes in wastewater characteristics and loads, so inflow of inhibiting compounds, fluctuations in temperature, or stormwater events may hamper the activity of microorganisms. This may further cause hazards in natural water bodies and living organisms.

Instead of forwarding wastewater-correlated issues to a centralized wastewater treatment plant, this thesis evaluates technologies for integrated wastewater treatment and resource recovery at the source. In this sense, membrane technologies were seen as a potential solution for reducing the environmental impacts of industrial fermentation processes. More specifically, electro dialysis and electro dialysis with bipolar membranes were investigated for the recovery of valuable compounds from fermentation media. Electro dialysis is an electro-membrane process with ion-exchange membranes, which allows the separation of charged particles from the rest of the aqueous medium. Thus, wastewater might be effectively split into a concentrate solution with charged particles, while the uncharged particles remain in the diluate. Bipolar electro dialysis works on a similar principle to conventional electro dialysis, but it includes bipolar membranes in addition to ion-exchange membranes. Thus, acids or bases can be in situ produced from salt-containing media. Finally, concentrate, acid, or base streams produced from waste fermentation media may be reused in fermentation processes.

To prove the concept of electro dialysis application in the treatment of fermentation wastewater, laboratory experiments were performed with fermentation media from two different sources. Firstly, the recovery of sulfuric acid was primarily investigated, along with other compounds, using fermentation with *Sulfolobus acidocaldarius*, an organism that is the focus of the Bioactive program. At the same time, potentially harmful compounds in the effluent originating from the fermentation must be removed. *S. acidocaldarius* is recognized as a future industrial microorganism in the pharmaceutical branch. Current developments for optimal fermentation conditions should be supported by conscious nutrient management, which is often neglected when only the final product is in focus.

Secondly, the separation of erythritol from the rest of the cultivation medium by electro dialysis was assessed. Erythritol is a sugar substitute, which is declared safe for consumption by people suffering from diabetes. To produce erythritol, high concentrations of salts need to be prepared

for the fermentation process. Thus, electrodialysis may deliver pure erythritol solution, while removing and recovering salts, which can be applied for succeeding fermentations.

Beside electrodialysis, this thesis evaluates ion-exchange resins, micro- and nanofiltration, as individual or pre-treatment technologies before electrodialysis. Efforts were put into resolving the research gaps on the application of membrane technologies for fermentation wastewater treatment, recovery of valuable compounds from waste streams, and their actual reuse in subsequent purposes.

## 1.1 Aims and Objectives

The aims of this research were defined by requirements from the framing Bioactive project and the need to establish environmentally friendly production processes with waste reduction and nutrient utilization. The main aims were:

- Closing the material loop in fermentation processes by nutrient and water recovery from waste streams
- Exploring the recent technological developments in advanced wastewater treatment and selecting the most promising technology for the nutrient/water recovery
- Diminishing polluting compounds evolved during fermentation processes that could be harmful to the process/environment
- Reducing the waste generated during the product purification steps in biotechnological processes

The following objectives were defined:

- 1) To identify recent developments for nutrient and water recovery from waste streams
- 2) To assess the applicability of electrodialysis and graphical limiting current density methods on complex synthetic solutions and real wastewater
- 3) To find an optimal pre-treatment method as upstream technology for subsequent bipolar electrodialysis for acid/base recovery, that will remove dissolved organic carbon and divalent cations while retaining or even concentrating sulfates and monovalent cations from waste fermentation effluent
- 4) Proof-of-concept for circular production of fermentation with *Sulfolobus acidocaldarius* and nutrient recycling from waste fermentation effluent
- 5) To assess the performance of electrodialysis for erythritol broth desalination and investigate erythritol diffusion through ion-exchange membranes

## 1.2 Research questions

Preliminary research indicated a possibility for applying membrane technologies, more specifically electrodialysis, for resource recovery from waste fermentation effluents. Thus, the following research questions were put into context for resolving the stated objectives:

- 1) What are the core operating parameters of electrodialysis, the selected nutrient/water recovery technology, and which effects it might have when applied in wastewater treatment?

- 2) How can the selected technology be optimized for the specific use as it was assigned by the Bioactive project requirements?
- 3) Can recovered products enable microbial growth and production rate in fermentation processes similar to standard cultivation media?
- 4) Can the selected technology lead to waste reduction when applied to a position different than the end-of-pipe, such as for the downstream process in a biotechnological production?
- 5) Can ion-exchange membranes retain erythritol while removing ions from the fermentation broth?

### 1.3 Structure of the thesis

This thesis researches the application of electrodialysis for resource recovery from fermentation wastewater and product purification in erythritol production. The results of the research are summarized in four scientific papers, of which three are peer-reviewed and published in scientific journals, whereas the fourth paper is submitted for peer review.

- 1) The first chapter introduces the aims, objectives, and research questions of this thesis, as a part of the Bioactive project.
- 2) The second chapter briefly describes the Bioactive project and broadly introduces the problematic of current pharmaceutical production. The structure and the workflow of the project are presented.
- 3) The third chapter gives a background of this thesis, explaining the current and future issues of scarce resources and measurements to tackle them, such as the development of sustainable production processes and a circular economy. State-of-the-art fermentation processes, and conventional and advanced wastewater treatment are further discussed. Finally, resource recovery technologies are introduced, with a focus on electrodialysis and electrodialysis with bipolar membranes.
- 4) The fourth chapter describes the methodological approach for resolving the research questions of this thesis, followed by the summary of four publications and the scientific contribution of each of the scientific publications that are part of this thesis.
- 5) The fifth chapter discusses the outcomes of the scientific papers and resolves the stated research questions.
- 6) The sixth chapter summarizes the final messages of the thesis and gives an outlook for future research.

After the sixth chapter, the published/submitted scientific papers are attached in the original format.

## 2 Bioactive project

This thesis was performed as a part of the Bioactive project. The Bioactive project was an PhD program established at TU Wien to discover and produce novel bioactive substances for medical application, such as antibiotics, antifungals, anti-cancer and anti-inflammatory drugs based on innovative framing fermentation process technologies. Current industrial productions are time- and resource-consuming, laborious, expensive, unsustainable, with huge CO<sub>2</sub> footprints and numerous side-products. Thus, the Bioactive project aimed to revolutionize pharmaceutical production by fast identification of novel bioactive substances using

bioinformatics and synthetic biology, cost-efficient and renewable substrates, eliminating side-products, valorizing CO<sub>2</sub>, and fostering resource recovery and reuse.

The interdisciplinary nature of the problems occurring during the current pharmaceutical production approaches instigated the Bioactive project to organize cooperative teamwork for achieving ambitious research goals. Therefore, ten Ph.D. students were gathered from the field of bioinformatics, molecular and synthetic biology, microbiology, system biology, bioprocess engineering, bio-resource and natural product, biophysics and microscopy, CO<sub>2</sub> utilization, and waste stream utilization to collaboratively solve ongoing challenges that were recognized by the Bioactive project. The topics of each Ph.D. position and their position within the project approach as well as their dependencies can be seen in Figure 1. The workflow of the project was divided according to the three main challenges as described in the following paragraphs.

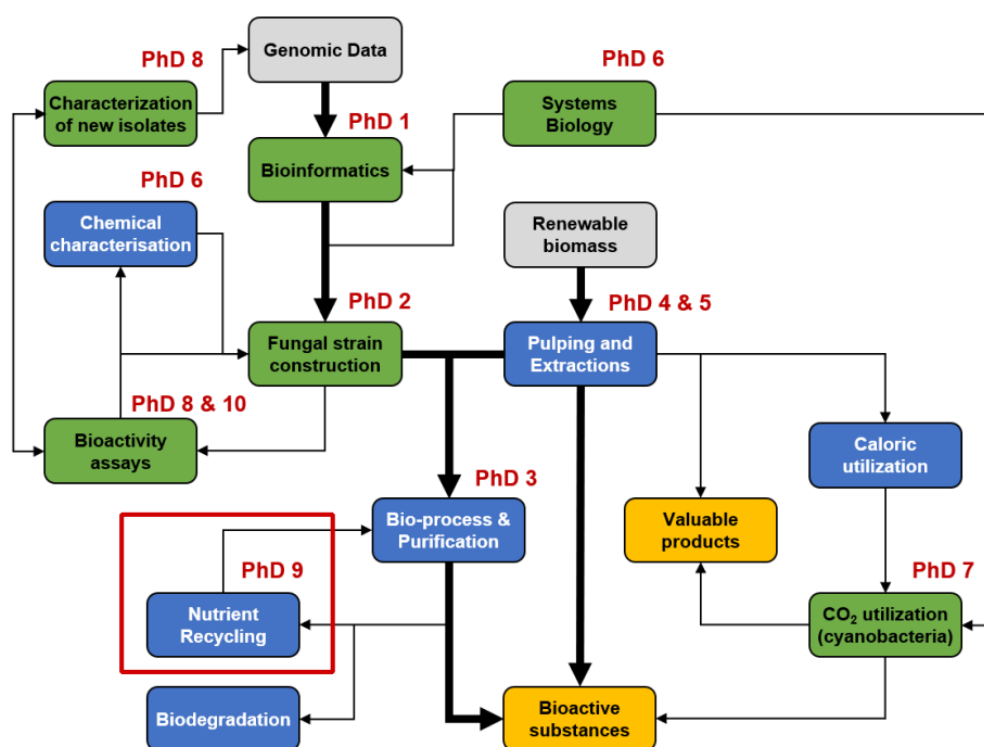


**Figure 1.** Overview of the Ph.D. positions and tasks for tackling the challenges recognized by the Bioactive project. The position Ph.D. 9 of this thesis is marked with a red frame. (The diagram is adopted from the Bioactive project description).

The first topic of research was the discovery of yet undescribed genes encoding for potentially bioactive substances, followed by the production of fungal bioactive substances under laboratory/biotechnological conditions. This demand was initialized by the worldwide threat of antibiotic resistance in the environment. Antibiotics are secondary metabolites of microorganisms that are widely used to fight infectious diseases in humans, livestock industries, and agriculture (Ben et al., 2019). Extensive use of antibiotics led to their loading in water and the land environment through the discharge of municipal wastewater, manufacturing industries, and landfill leachates of antibiotic disposal (Ashbolt et al., 2013). The uncontrolled occurrence of antibiotics in the environment caused genetic or mutational changes in normally sensitive bacteria, allowing the bacteria to survive and further proliferate as antibiotic-resistant bacteria

that carry antibiotic-resistant genes (Martinez, 2009). Thus, antibiotic therapy with currently used bioactive substances is becoming ineffective and there is a need for discoveries to fight diseases caused by bacteria.

The second core topic of the Bioactive project was the establishment of sustainable biofermentation processes, including the extraction of nutrients needed as cultivation media from unused plant biomass, in contrast to the current processes of the pharmaceutical industry. The base of state-of-the-art manufacturing industries lies in the abundance of natural resources. However, recent studies point out the finite amount of mineral resources, e.g. 30 materials were recognized as critical raw materials in 2020 (European Commission (EC), 2020). Further on, ores of critical materials such as phosphorus, magnesium, and cobalt are located outside of Europe, resulting in dependency on the global political and economic situation. Thus, strategic planning and foresight of resource management along with the adaptation of manufacturing processes are needed to meet the new challenges and reach a climate-neutral economy.

The third challenge of the Bioactive project was waste minimization, with the main focus on recycling inorganic nutrients and other salts from the waste fermentation streams. Further efforts were put into CO<sub>2</sub> valorization and life-cycle-assessment to identify all main and side streams of each production step. 5R strategy (reduction, replacement, reuse, recovery, and recycling) may diminish resource scarcity and set the foundations for a circular economy.

Research findings of each Ph.D. position contribute to resolving the challenges recognized by the Bioactive project. Findings are distributed in form of scientific publications and finally summarized in a cumulative Ph.D. thesis. The present thesis belongs to resolving the challenges from the third group of the Bioactive project, denoted as position Ph.D. 9 in Figure 1, and it focused on the treatment of liquid waste streams from fermentation processes for the production of new bioactive substances and erythritol as a zero-calorie sugar substitute

### 3 Background

Starting from the wider scope of the Bioactive project that includes research for discovering and producing novel bioactive substances and establishing environmentally friendly and cost-reduced processes in the pharmaceutical industry, this Ph.D. thesis narrows down to developing a circular production and closing material flows by fostering resource recovery and reuse. To clarify the drivers for the development of resource recovery technologies, scarce resources, sustainable development goals, circular economy, state-of-the-art fermentation processes, wastewater treatment technologies, and resource recovery technologies are elaborated in the following paragraphs.

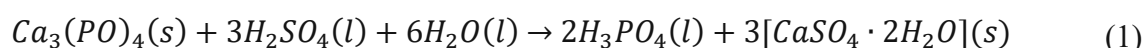
#### 3.1 Scarce resources and future concerns

Phosphorus is a fundamental element for all living organisms on earth. It is essential for energy transfer on a cellular level, and it is incorporated in the genetic material (DNA and RNA), in cellular membranes and proteins in plants, animals, and humans. Crucial to life on earth and yet declared as a scarce element, phosphorus reserves in form of phosphate deposits are predicted to be exhausted in the near future, accounting for 29 to 110 years (Cordell & White, 2014; Liu et al., 2021). Besides the physical aspect, phosphorus scarcity includes economic, managerial, geopolitical, and institutional scarcity, which contributes to further shortages as

e.g. in food production (Cordell & White, 2014). These are also interconnected with other global issues which were recognized by United Nations and listed under sustainable development goals (SDGs) for resolving them (United Nations, 2022). Phosphate deposits for exploitation are non-renewable and are mainly located in Morocco and Western Sahara, with remaining only 30 % distributed over other countries (Liu et al., 2021). On the other hand, phosphorus is responsible for severe environmental issues through eutrophication and subsequent further deteriorating effects. The source of phosphorus pollution originates from insufficient, inadequate, or complete lack of elimination in wastewater treatment, and intrusion of untreated wastewater to surface water. The awareness of these opposing manifestations, scarcity of raw phosphate versus its undesired occurrence in water bodies, led to a quite obvious strategical approach for future phosphorus management. This was to put an accent on developing technologies for phosphorus recovery and recycling from waste streams.

Phosphorus naturally enters the P-cycle through plant uptake of inorganic phosphorus, mainly orthophosphate, from the soil. Due to population growth, the need for higher crop yields grew respectively, which further led to increased application of fertilizers. Although fertilization of arable land was practiced since ancient times, it was initially not known that phosphates are the key component for increased productivity. At the beginning of the 19<sup>th</sup> century, Justus Liebig recognized nitrogen and phosphorus as essential plant nutrients and formulated the "law of the minimum" where plant growth is limited by the most scarce nutrient resource. This discovery quickly led to the targeted application of fertilizers to increase crop yields - including phosphorus. Since then, a vast of phosphorus enters the global phosphorus flows through fertilizers: direct application rock (DAR), single superphosphate, triple superphosphate, monoammonium phosphate (MAP), diammonium phosphate (DAP), and combined nitrogen, phosphorus, potassium (NPK) fertilizers. Further on, phosphorus is extensively used in food and pharma industries, e.g., phosphoric acid for direct food manufacturing or as biocompliant preservatives, and polyphosphoric acid as a reagent in organic chemistry. Sodium phosphates are often used in baking and leavening products, for pH adjustment and buffering, dough conditioning and enrichment, as growth factors for yeasts, or in meat production. Phosphorus sulfides and phosphorus chlorides are used as agrochemicals, flame retardants, and lubricant additives. Potassium triphosphate is applied in detergents and as a cleaning component. So, there are many ways for phosphorus to enter the environment, either directly from the phosphorus mining, and manufacturing processes, or after animal and human digestion.

The increased demand for phosphoric acid pulled along the consumption of sulfuric acid. 60 % of total sulfuric acid consumption is spent on the production of phosphate fertilizers (King et al., 2013). The most common reaction of sulfuric acid is with phosphate rock to produce phosphoric acid as follows:



Afterward, phosphoric acid reacts with ammonia to produce monoammonium phosphate (MAP) and diammonium phosphate (DAP) (King et al., 2013). Other uses of sulfuric acid are e.g., for the production of detergents, the glass and paper industry, production of other chemicals, as catalysts for polymer manufacturing, and petroleum refining. The majority of sulfuric acid is produced from burning elemental sulfur, whereas the remainder comes from

SO<sub>2</sub> in smelter, roaster, and spent acid regeneration furnace off-gases. According to a report from Donau Chemie from 2021 (Fortelny & Inmann, 2021), sulfuric acid was massively affected by shortages during the Covid pandemic. At that time, oil production was extremely reduced due to the sharp decline in air and road traffic, which further lead to a disruption of the liquid sulfur production in refineries. Apart from the Covid pandemic, oil and gas production in Europe is declining. The import of liquid sulfur and other resources from distant refineries and mines further increases prices and economical as well as environmental burdens for a chain of industries operating on the European continent. It should be mentioned that sulfuric acid production from refineries is solely a by-product and modern refineries prefer to refine sweet oil with a low sulfur content rather than sour crude oil with a high content. Sweet crude oil has processing and environmental advantages due to its lower density and sulfur content. Thus, the transformation of refineries to greener production will result in the availability of fewer liquid sulfur sources.

Similar to phosphorus, nitrogen is an essential element for life on earth. Although nitrogen gas is abundant in Earth's atmosphere, making up 78% of its volume, nitrogen is hardly available in forms required for plants, animals, and humans. Energy-intensive processes, such as the Haber Bosch process, were developed to synthetically fix nitrogen in a plant-usable form, mainly ammonia (Kirova-Yordanova, 2004). Through the human and animal consumption of food and medicines, runoffs from agricultural fields, and fertilizer production, nitrogen species are entering freshwater streams and therein causing various environmental problems such as eutrophication or even acute toxicity. Other environmental issues stem from energy consumption, CO<sub>2</sub> emissions and natural gas requirements in the fertilizer industry (Beckinghausen et al., 2020). On the one hand, wastewater treatment plants are collecting ammonia in wastewater, which is a result of the anthropogenic excretion of urea from the metabolism of nitrogen within proteins. On the other hand, wastewater treatment plants are emitters of free dinitrogen during the nitrification/denitrification process. Hence, recent research in sanitary engineering is shifting toward nitrogen and phosphorus recovery from wastewater treatment plants, in order to prevent eutrophication, and save energy and natural resources through nitrogen and phosphorus reuse (Perera et al., 2019).

### **3.2 Sustainable development goals and circular economy**

The United Nations developed an agenda for sustainable development on the global level through 17 Goals (United Nations, 2022). The first milestones for eradicating poverty and hunger, improving health and education, providing basic services, are set for implementation until the year 2030. This research addresses the sustainable development goal 6 – SDG6 clean water and sanitation. Indirectly are targeted: SDG2 – Zero hunger (depends on food production which is further related to the available water sources); SDG9 – Industry, innovation and infrastructure (industries produce a lot of waste and wastewater, thus the technological improvements towards cleaner production can directly contribute to clean water and sanitation); SDG11 – Sustainable cities and communities (nutrient recovery from municipal or industrial waste stream supports the development of sustainable cities); SDG12 – Responsible consumption and production (the reduction of mineral resources consumption to the minimal required level would have a positive impact on the total environment); SDG14 – Life below water (reduction of pollutants originating from wastewater directly reduces eutrophication and

maintains freshwater ecosystem in balance); SDG15 – Life on land (clean water is one of the main elements that enables life on land).

The term “Circular economy” appeared already in 1988 (Kneese, 1988), and the European Union adopted the Circular economy action plan in 2015 (European Commission, 2015). The New Circular Economy Action Plan finally was published in 2020 (European Union, 2020). The principles of circular economy are based on the circularity of products and materials, elimination of waste and pollution, and regeneration of nature, to fight the global challenges of climate change, biodiversity loss, waste, and pollution. Reducing material usage in the first place lowers the negative environmental impacts of material production, consumption and disposal. The following measurements include the usage of materials and products in their initial form as long as possible, then their refurbishment, and only afterward is considered material recycling and reuse. The circular economy has to be integrated into social, technical, economical, political, and environmental sectors and presents a new perspective on resource extraction, fabrication methods, product consumption, and disposal. The European Environmental Agency and the United States Environmental Protection Agency are among leading organizations in initiating and implementing a circular economy approach instead of the traditional linear one. However, the term “circular” does not always mean “sustainable”, as the recirculation of some materials may be harmful to the environment, such as additives used in polymers (Blum et al., 2020) and energy consuming. Therefore, it is suggested that academia develops assessment tools accounting for material circularity, and economic, environmental, and social sustainability, preferably in a collaboration with practitioners (Blum et al., 2020). Such a holistic approach will allow informative decision-making for favored circular economy activities and sustainable development.

### 3.3 State-of-the-art fermentation processes

Bio-fermentation processes are significant for producing a spectrum of valuable products in pharmacy, cosmetics, food and beverage industries. Microorganisms are commonly engaged for the production of biologically active substances that can fight diseases in humans and animals, or for food production via fermentation. Some of the well-known fermentation products produced by various microorganisms are beer, cheese, yogurt, glycerol, ethanol, penicillin, citric acid, etc. A mixture of macro- and micronutrients is needed for microbial growth and generation of fermentation products. Microbial growth should not be limited by the availability of nutrients; thus, culture media are commonly prepared with surplus of compounds needed for optimal cellular growth. Consequently, a share of nutrients ends up in waste fermentation effluents, which could be recovered and reused. Beside that, the pharmaceutical and food industry have in common large water consumption and heavily polluted wastewater. Thus, optimized treatment steps could be implemented in the downstream processes to purify the products from fermentation with simultaneous nutrient and water recovery. In this way, forwarding excess nutrients to mere waste streams can be omitted.

This work focuses on closing the material flows of industrial production processes for pharmaceuticals and food by assessing their wastewater and possibilities for wastewater reduction and nutrient utilization. Production processes include multiple steps, starting from the raw material, followed by biological, chemical, or mechanical process steps to obtain the desired final product. As an example of the application of nutrient recycling approaches, two

liquid waste streams from bio-fermentation processes were particularly analyzed in this thesis. The first waste stream treated was from the fermentation with *Sulfolobus acidocaldarius*, an archaeon that has a high potential for extended future industrial use. The second application for the nutrient recycling and cleaner production was assessed for the optimization of erythritol separation in the downstream handling of the osmophilic yeast biotechnological process. Often industrially engaged microorganisms for erythritol production are *Yarrowia lipolytica*, *Moniliella pollinis*, *Zygosaccharomyces*, or *Hansenula*.

The genus *Sulfolobus* incorporates extreme thermoacidophilic Archaea, which became interesting for research since 1970s due to their capability to carry out microbial process and biotransformations at extremely low pH (2–3) and high temperature (75–80°) (Quehenberger et al., 2017). *Sulfolobus acidocaldarius* is one of the *Sulfolobus* species that is less researched than e.g., *Sulfolobus solfataricus*. In general, *Sulfolobus* species are seen as a source of thermostable enzymes for food, feed, textile, cleaning, pulp and paper industry, but they are still in the research phase, without actual industrial application. Enzymes of *Sulfolobus* can enhance industrial processes by their great catalytic diversity, for e.g., enzymatic hydrolysis of lactose for the generation of saccharides (Reuter et al., 1999), or for the chiral production of halo-carboxylic acids (Rye et al., 2009). Sulfolobocins are antibiotic proteins and peptides produced by *Sulfolobus*, which act as potent and highly specific growth inhibitors to species closely related to the producing organism (Prangishvili et al., 2000). Trehalose is another metabolite of *Sulfolobus*, which is used for preservation of enzymes and antibodies, and in food and cosmetic industry (Ohtake & Wang, 2011). Thermophilic *Sulfolobus* cells have lower growth and protein expression rates than conventional bioprocesses. However, many advantages are recognized in engaging *Sulfolobus* in bioprocessing: source of stable enzymes and unique biomaterials, reduced risk of contamination due to the high operating temperature and low pH, increased solubility of substrates, reduced need for cooling of the fermenter and thus reduced energy consumption, the production of volatile compounds such as alcohols, which can be continuously recovered.

Erythritol production was assessed within this thesis to purify final product while at the same time recovering nutrients from the culture broth. Erythritol is a sugar alcohol (polyol), similar to xylitol, which is synthesized in fermentation with fungus or bacteria and isolated in multiple treatment steps. Polyols are promising alternative for white sugar (Mäkinen, 2011), which provide a sweet taste of food but are preventing the onset of sugar-born diseases in humans. Multiple human diseases are correlated to overconsumption of commonly used white sugar, starting from less serious such as dental caries, to life-threatening as cardiovascular disease, diabetes, and obesity (Malik & Hu, 2022; Yang et al., 2014). White sugar in nutrition is sucrose extracted from sugar beet and sugar cane (Mariotti & Lucisano, 2014). The white crystals are further isolated by different processes of carbonation, decolorization, evaporation, centrifugation, and drying. The final product enriches a variety of food products with a sweet taste and can act as a food preservative by retardation of bacterial and mold growth (Mariotti & Lucisano, 2014). Therefore, the most recent research focused on finding sugar alternatives and optimizing biotechnological processes for their production. In both sugar and sugar substitutes production, nutrients are required for the product manufacturing; fertilizers are needed for sugar beet and cane crops, whereas biotechnological processes require a mixture of macro- and

micronutrients for microbial growth and excretion of polyols. The application of nutrients for crops or bio-fermentation often results in an eventual escape of unused nutrients to the environment, which indicates a possibility for a guided recovery and reuse of the excess nutrients.

In both fermentation with *Sulfolobus* and erythritol production, a culture broth rich in nutrients needs to be prepared for microbial cultivation and product generation. Furthermore, acids/bases are continuously dosed to the cultivation broth to maintain stable pH values, required for optimal microbial growth. The matrix and the accumulation of valuable compounds during the fermentation process are distinguished between the two assessed biotechnological processes. The enzymes or products of *Sulfolobus extremophiles*: protease, esterases/lipases, chaperonins, liposomes, archaeal membrane components, sulfoblasticins, and trehalose, are contained in the microbial cells (Quehenberger et al., 2017). In contrast, erythritol is an extracellular product of osmophilic yeasts, excreted as a protective response to the high osmotic environment. Thus, technical approaches for product extraction and purification differ among the intra- and extracellular products, as well as with the product type and required purity. Biomass is usually separated by centrifugation or membrane processes, whereas the erythritol and similar extracellular products are separated from the cultivation medium by ion-exchange resins for the removal of ionic species and concentrated by rotary evaporation to allow erythritol crystallization in the very final step (Rakicka et al., 2016). The downstream processes impact the final product costs, and current solutions are cost-intensive and have side streams reach in “leftover” nutrients from the fermentation processes, including N, P, and  $Mg^{2+}$  species. Thus, it would be beneficial to integrate technologies for simultaneous product purification, nutrient recycling, and waste minimization.

### 3.4 Wastewater treatment

The continuously increasing world population is driving demand for an expanded production of food, pharmaceuticals, and in other industrial sectors that provide a variety of consumer products (Tripathi et al., 2019). On the one hand, these products enable, ease, and support human life and development. On the other hand, a huge amount of waste streams emerges from production processes, and stress is put on water and finite natural resources. The resulting waste streams need to be treated for safe disposal. Otherwise, substances and chemicals in waste streams can cause adverse effects on the environment and eventually present a risk to human health as well.

#### 3.4.1 Conventional and industrial wastewater treatment

In general, wastewater can be divided into two main groups, municipal and industrial wastewater. Municipal wastewater is household wastewater collected either by separate sanitary sewers or by combined sewers for both municipal wastewater and stormwater runoffs. Sewage systems transport wastewater to a treatment plant but in some places, it is still directly discharged to water bodies. Municipal wastewater is treated in conventional wastewater treatment plants (WWTP) with the removal of suspended solids, pathogens, and biological degradation and/or conversion of compounds to acceptable levels, meeting the effluent standards of the permitting rules in place. Commonly, a WWTP comprises a preliminary (screening and grit removal), primary (sedimentation), and secondary (biological) treatment, as shown in Figure 2. Depending on legal requirements, also further treatment by disinfection or

advanced processes (activated carbon adsorption and/or ozonation) is applied when the receiving water conditions require higher-quality effluent. Main control parameters for WWTP effluents among others include onsite measurements of pH, turbidity, dissolved oxygen, ammonium concentration, and laboratory analysis of biochemical oxygen demand (BOD), chemical oxygen demand (COD), total suspended solids (TSS), total nitrogen (TN) and total phosphorus (TP).

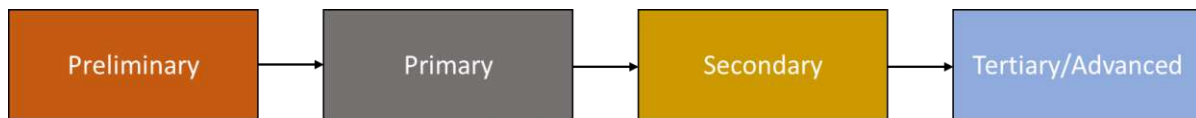


**Figure 2.** Main treatment stages of a conventional wastewater treatment plant.

Industrial discharges are frequently heavily loaded with high-polluting and low-degradable chemicals, which require special treatment according to the industry's best available technology. Treatment of industrial wastewater is industry specific and some of the used technologies, besides conventional biological-based treatment, are membrane bioreactors, including micro- and ultra-membrane filtration, ozonation, chemical precipitation, ion exchange, dissolved air flotation, etc.

In both sectors, municipal and industrial, continuous research and improvement are supported by scientific sectors to enhance already existing technologies, improve their energy efficiency, and establish new technologies for wastewater treatment and water monitoring.

### 3.4.2 Advanced wastewater treatment

Recently, wastewater is not seen solely as a waste stream that has to be treated for minimum impact on the receiving environment, but as a source of energy, water, and a variety of nutrients (Mo & Zhang, 2013). Economic and environmental benefits can be accomplished via nutrient removal and recovery, water reuse, and energy production in wastewater treatment facilities. Figure 3 demonstrates the possibilities of energy generation, resource recovery, and water reuse in a conventional WWTP, according to the general treatment stages depicted in Figure 2. Chemical, thermal and hydro energy can be generated from treated sludge or wastewater flow, as shown in Figure 3a. WWTPs occupy a large surface, allowing the implementation of solar panels and wind turbines for additional green energy production, to meet WWTP energy requirements.

Resources can be recovered from multiple WWTP stages, as shown in Figure 3b, and applied as constructing material or for other innovative solutions. Nutrient recovery, of mainly phosphorus and nitrogen, maintains the controlled nutrient flow with twofold benefits. Firstly, the polluting impact of wastewater is reduced or completely eliminated due to nutrient removal. Secondly, recovered nutrients can be reused in on-site processes or applied off-site for other purposes, e.g., as fertilizer. In WWTP the majority of the nitrogen (N) gets removed as nitrogen gas during the denitrification process while the majority of phosphorus (P) ends up in the solid sludge after incorporation into biomass and chemically induced precipitation. The sludge can

be anaerobically digested to produce biogas and heat (Morero et al., 2017). The degassed sludge still containing significant amounts of nutrients can further be used as a fertilizer on soil if there are no high levels of heavy metals. (Faragò et al., 2021). Nitrogen can be captured together with phosphorus by chemical struvite precipitation, or by stripping processes (Rahimi et al., 2020). Activated carbon can be derived from wastewater screenings using hydrothermal carbonization (Benstoem et al., 2018), or from the sludge (Hadi et al., 2015).

Water reuse from the preliminary and primary treatment stage is not recommended due to the high concentration of polluting organic compounds. However, the purified water after the secondary or tertiary treatment can be reused as shown in Figure 3c. The water reuse depends on the quality of the recovered water. Common applications are for irrigation of food or non-food crops, and for recharging groundwater. Purified water can also be used as technical water for rinsing purposes in WWTPs or for industrial cooling. Smart cities tend to implement water recovery systems for urban irrigation or even direct/indirect potable use, depending on the applied advanced technological solutions for wastewater treatment.

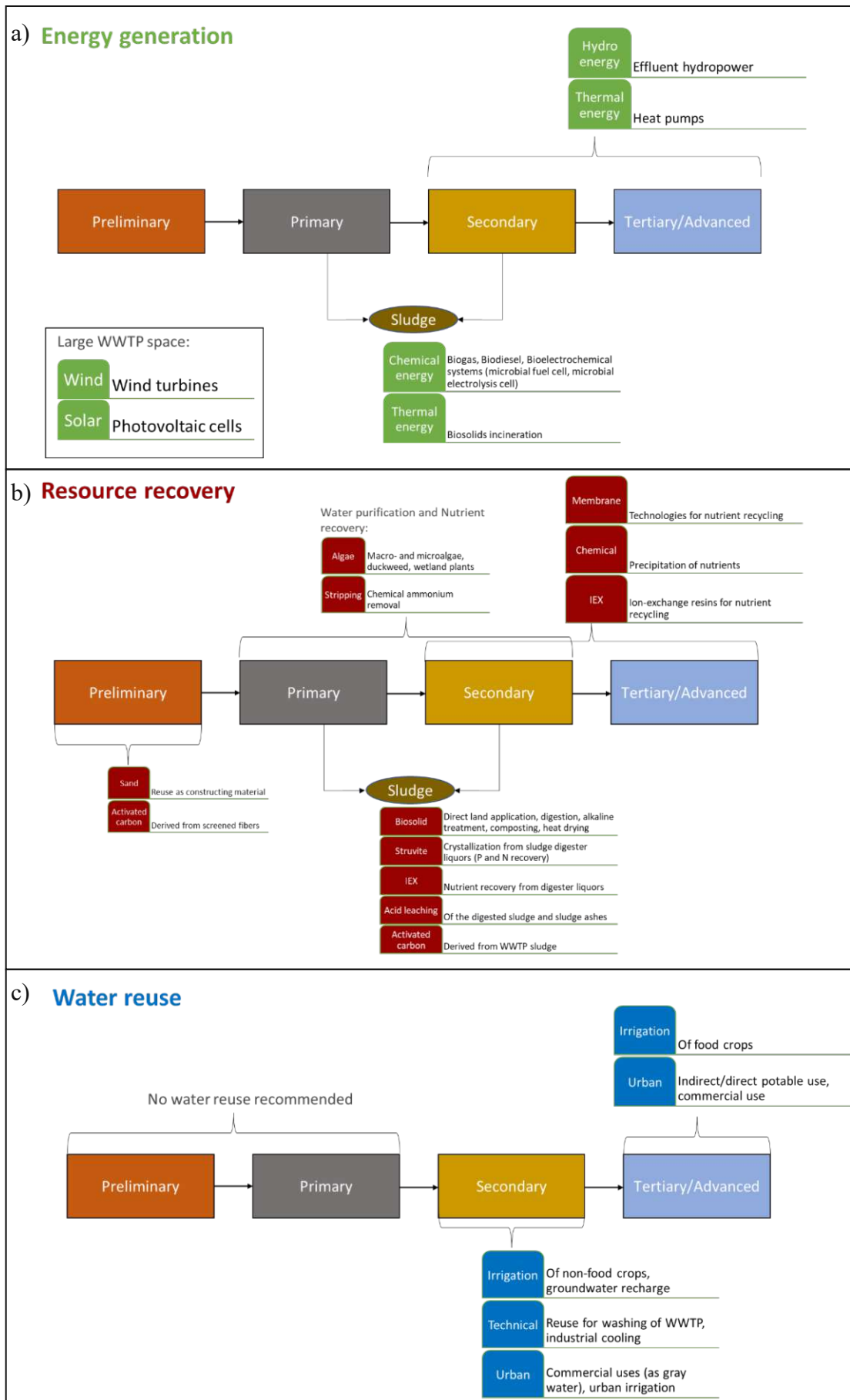


**Figure 3.** a) Sources of energy generation, b) resource recovery possibilities and c) water reuse options from a conventional wastewater treatment plant.

Still, there are many concerns to be overcome for the safe and effective reuse of resources recovered from WWTPs. In the first line, there are technological developments, followed by the acceptance of society, farmers, and citizens, for the purchase and application of recovered products. Wastewater is a fluid susceptible to changes in quantitative and qualitative composition due to uncontrolled events such as heavy rains, and household or industrial contaminations. This rises risks of contamination of recovered products and complicates the operation and control of technical processes. Ultimately, human and environmental health may be threatened through contact or consumption of products that rely on recovered sources.

Technological developments in the detection of chemicals brought up the subject of environmental micropollutants. Micropollutants comprise a collective term for organic household and industrial chemicals, pharmaceuticals, biocides, and pesticides occurring in  $\mu\text{g/l}$  or  $\text{ng/l}$  concentration range. Although present in these low concentrations, micropollutants can still cause severe damage to biota in receiving environments.

As conventional WWTPs only remove micropollutants to a certain degree, they need to be retrofitted to meet the latest requirements in effluent quality as e.g. stated in the recent publication of the first draft of the newly adopted EU-urban wastewater directive (European Commission, 2022). Frequently, disinfection, ozonation, and activated carbon are suggested and implemented as technological steps for advanced WWTP (Pistocchi et al., 2022). Membrane technologies can also eliminate micropollutants and meet high standards. In general, secondary and tertiary treatment make up 50 % of the complete energy consumption of a whole WWTP, which accounts mainly for oxygen transfer and chemical demand, and which increases the total operating costs (Rahimi et al., 2020).

It is of immense importance to tackle the environmental issues at the very beginning of their emergence, rather than shifting them to conventional WWTPs. This leads to improvements in the production processes, where nutrient management, emerging waste streams, and pollutants should be analyzed and properly addressed already in the production design. The aim should be to bring the resource requirements to the lowest value, with an awareness of the implications of the production processes to environmental safety and harmony. Only conscious nutrient management can lead to sustainable environmental protection and prosperity. Material flow analysis is a good approach to identifying sensitive areas and the impact of various environmental factors. Wastewater treatment technologies need to be further developed and integrated with resource recovery to offer an optimal treatment solution in accordance with a specific geographical area, industrial branch, or communal region.

### **3.5 Resource recovery technologies**

Waste fermentation effluents usually contain higher concentrations of nutrients compared to municipal wastewater. Nevertheless, the same technological approaches for the recovery of valuable compounds may be applied in both wastewater streams. There are many nutrient recovery technologies in the research phase or already in operation at WWTPs. Some of the technologies marked from the review study of Perera et al. (Perera et al., 2019) are:

*P recovery:* ion-exchange/adsorption, magnetic microsorbents, reactive filtration with coprecipitation, adsorption and physical filtration, struvite precipitation, electro dialysis,

chemical precipitation by addition of metal ions, biological phosphorus recovery by phosphate accumulating organisms, algae harvesting, electrochemical P recovery with anodes for enhanced chemical precipitation.

*N recovery*: ion-exchange/adsorption, electrodialysis, electrochemical nitrogen recovery with cathodes for ammonium stripping and adsorption into an acid, bioelectrochemical with biologically catalyzed oxidation of organic substrate on the anode and ammonium stripping at the cathode, struvite precipitation, stripping and adsorption by air stripping of ammonia, gas permeable membranes, direct conversion to livestock feed and protein from nitrogen in wastewater by heterotrophic microorganisms.

Each nutrient recovery technology has advantages and disadvantages, and depending on the target of application has to be analyzed based on multiple factors for individual purposes and wastewater characteristics. This thesis strived for both phosphorus and nitrogen recovery, but also to recover sulfates, and other ions from the fermentation waste effluent, as well as for total waste minimization. Struvite precipitation is a possible way of recovering phosphorus and nitrogen, but it demands the application of chemicals for the precipitation reaction and it is not a solution for other elements of fermentation waste effluent. Among the listed technologies, electrodialysis offers a solution for both, phosphorus and nitrogen recovery, and potentially other requirements for cleaner pharmaceutical and food production, as defined by the scope of the Bioactive project. Therefore, electrodialysis was selected as a key technology for nutrient recycling in this thesis.

### **3.6 Electrodialysis for resource recovery**

This work assessed electrodialysis within a sustainable production of bioactive compounds in the Bioactive project. Electrodialysis is an electro-membrane process that is commonly used for water desalination, similar to reverse osmosis. While reverse osmosis is a pressure-driven membrane technology, electrodialysis is an electrically driven separation process that allows the selective removal of charged compounds from the rest of the wastewater stream. Although electrodialysis is an already existing and applied technology, it has only recently been recognized as a process suitable for wastewater treatment. It is composed of alternately assembled cation- and anion exchange membranes with spacers in between (Figure 4). The working fluids are circulating between the ion-exchange membranes in chambers defined by the spacers. Ions of the opposite charge to the membrane charge (counter-ions) can migrate through the membrane matrix, while the ions of the same charge (co-ions) remain retained on the membrane surface. The assembly of membranes and spacers is called a membrane stack and it is placed between a cathode and an anode. Electron movement is initialized by external electrical fields and further transferred from electrodes to the movement of mobile ions within the ion-exchange membranes and in the working fluids.

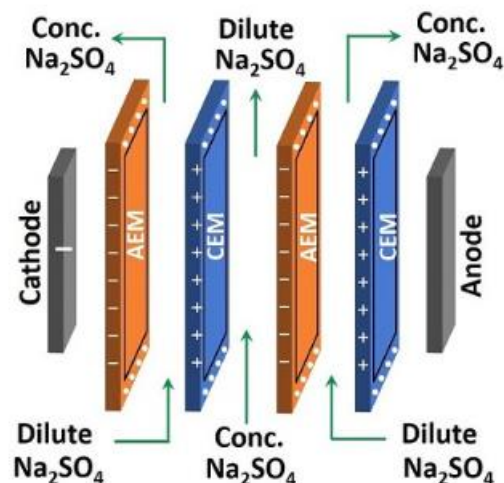


**Figure 4.** Conventional electrodesalination with cation- (CEM) and anion-exchanging membranes (AEM) for removal of  $\text{Na}_2\text{SO}_4$  from the feed, having dilute and concentrated outlets from the membrane stack. Source: (Kuldeep et al., 2021)

Ions are selectively removed from the feed by conventional electrodesalination, resulting in two separate streams as outlets: a diluate stream scarce in ions and a concentrate stream rich in ions. This approach allows wastewater treatment with near-to-zero waste generation, providing the use of the diluate stream with low substance content as technical water and the reuse of the concentrated stream in the production process (origin of wastewater) or as e.g., a fertilizer. There are modifications of conventional electrodesalination, such as reverse electrodesalination, where the electrodes can be reversed, switching the moving direction of cations and anions of working fluids. This approach allows a prolonged lifetime of ion-exchange membranes, reducing the membrane fouling and requirement for cleaning in place. Another subdivision of electrodesalination is bipolar electrodesalination, which contains bipolar membranes between the ion-exchange membranes (Figure 5). Bipolar membranes initiate the splitting of water molecules into hydrogen and hydroxyl ions. These ions are then combined with anions and cations removed from the treated wastewater, respectively. Therefore, in-situ acid/base production can be achieved.

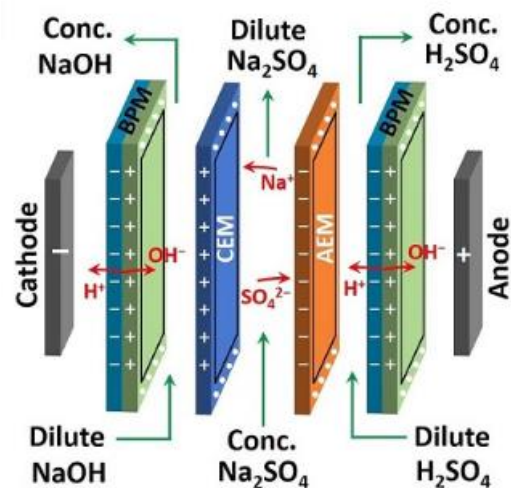


**Figure 5.** Membrane stack of bipolar electrodes with bipolar membranes (BPM), cation- (CEM) and anion-exchange membranes (AEM) for production of acids ( $\text{H}_2\text{SO}_4$ ) and bases (NaOH) from a concentrated  $\text{Na}_2\text{SO}_4$  feed. Source: (Kuldeep et al., 2021)

The mentioned features of electrodes indicate the suitability of its application within a sustainable production for fermentation processes and waste reduction through nutrient recovery. However, thorough research is needed in order to prove and justify the application of electrodes in the treatment of waste fermentation effluents. Therefore, this research concentrates on the assessment and optimization of electrodes applied in the treatment of wastewater originating from fermentation processes for nutrient recovery. The applicability of nutrients recovered from wastewater falls also within the scope of this research. Not solely centered on the end treatment of waste streams, this thesis also investigated methods to reduce emerging waste products. Thus, an example of cleaner production was demonstrated in the production of erythritol, where the benefit of electrodes was twofold. Firstly, a fermentation product erythritol is separated by electrodes. Secondly, salts from the erythritol culture broth are removed and concentrated by electrodes, offering their further application or reuse in the production step and quantitative waste reduction.

## 4 Methodological approach

This research was performed in four stages, encompassing the stated aims and objectives. The systematic approach for resolving the research questions, including objectives, methods of literature research and laboratory experiments, and respective outcomes are depicted in Figure 6. Each of the research stages was eventually summarized in an individual peer reviewed publication.



**Figure 6** Methodological approach for resolving the research questions, with the depicted scheme of each research stage.

To resolve the stated objectives following methods were adopted:

The **first scientific paper** included literature research on the application of electro dialysis for desalination and wastewater treatment. Further on, operating parameters in electro dialysis were investigated, and limiting current density was found to be one of the main parameters for the electro dialysis control. In the paper, graphical methods for determining limiting current density were analyzed in depth. After gaining theoretical knowledge, an electro dialysis stack was assembled for the limiting current density tests. Various synthetic solutions and real wastewater samples were prepared for experimental research in the laboratory. Experimental data were recorded and analyzed. Results were discussed following the theory of electro dialysis operation and available scientific literature. Outcomes and recommendations for the application of graphical limiting current density methods in electro dialysis for complex media and wastewater treatment were clearly stated.

The **second scientific paper** engaged three technologies for the pre-treatment of fermentation wastewater before electro dialysis with bipolar membranes. A high volume of fermentation effluent from studies within the Bioactive program was collected and prepared for succeeding experimental research. Two nanofiltration membranes, three ion-exchange resins, and electro dialysis with monovalent selective cation-exchange membranes were contrasted for the removal of dissolved organic carbon and divalent cations from the feed. Chemical analyses of obtained samples were performed to determine the dissolved organic carbon and ion concentrations. Results were compared, discussed, and the advantages/disadvantages of each pre-treatment method were defined.

The **third scientific paper** assessed three pathways for nutrient recovery from fermentation wastewater again derived from within the Bioactive program. Wastewater samples were collected from the fermentation with *Sulfolobus acidocaldarius* which is performed and researched in the TU Wien biotechnological laboratory. Samples were treated by nanofiltration, electro dialysis, and electro dialysis with bipolar membranes. Recovered products were then tested in the biotechnological laboratory to grow *S. acidocaldarius* cells and examine whether there is cellular proliferation. Cultivation in recovered media was compared to the cultivation in standard medium and solely microfiltered fermentation effluent. Chemical analyses were performed to determine the behavior of ions and cells in electro dialysis and fermentation processes, respectively. Waste streams and energy requirements of membrane technologies were investigated. Obtained data were analyzed, discussed, and corresponding conclusions were made.

The **fourth scientific paper** investigated the application of electro dialysis in the purification of erythritol from the cultivation broth. Synthetic cultivation media were prepared, containing increasing concentrations of erythritol. Four ion-exchange membranes were tested for the desalination of feed solutions and retention/diffusion of erythritol. Two operating modes of electro dialysis were tested, one by application of constant current and the other with step-wise voltage. Finally, real erythritol broth was desalinated in laboratory conditions. All the samples were chemically analyzed to measure the concentrations of products and by-products in treated media. Obtained data were evaluated, discussed, and conclusions were defined.

## 4.1 Summary of the scientific papers

Each of the peer-reviewed papers is dedicated to solving the research objectives presented in the first chapter and Figure 6, and comprises the following content:

The **first published manuscript** (<https://doi.org/10.3390/membranes12020241>) with the title “**Assessment of Graphical Methods for Determination of the Limiting Current Density in Complex Electrodialysis-Feed Solutions**” investigated the operating parameters of conventional electrodialysis. In the literature, the term “limiting current density” is often mentioned as one of the main driving parameters for electrodialysis control. Limiting current density (LCD) has a direct impact on process efficiency. LCD depends on the ionic content of the treated fluid, temperature, flow, membrane characteristics, and spacers. LCD is a sign of the boundary layer formation on the membrane/fluid surface, indicating a depleted concentration of counter-ions on the diluate side and a concentration saturation of co-ions on the concentrate side. Followingly, an increased electrical field leads to the dissociation of water molecules to  $H^+$  and  $OH^-$  ions on the diluate side, which further leads to drastic pH changes, a drop in the current efficiency, and an increase in energy consumption. The formation of hydrogen and hydroxyl ions may lead to membrane scaling and their permanent structural changes. Thus, various approaches were investigated in the available literature to define LCD for the treated medium. The most established methods are graphical approaches as follows: Isaacson and Sonin, Cowan and Brown, pH method, current efficiency and desalination efficiency method. However, these methods are based on experiments performed with synthetic media, usually containing  $Na^+$  and  $Cl^-$  ions only. As the Bioactive project aimed at producing bioactive substances and, thus, treating real waste streams of the fermentation processes, the first article comprised elaborative experiments with synthetic and real wastewater and analysis of LCD graphical methods to confirm their applicability in real media as well. This paper integrated the following research steps: (I) The applicability of the graphical LCD methods to a wide range of monovalent salt concentrations because the salt content of waste streams varies strongly; (II) The applicability of the graphical LCD methods to each type of feed representing an increasing complexity because the real waste streams contain also multivalent ions and uncharged compounds, however, the initial ionic strength among treated solutions was the same (same electrical conductivity); (III) Expanded experimental work to the solutions with the same ionic species but different initial conductivity to observe the LCD behavior; (IV) Investigating the potential for using a simple measurement, such as the conductivity, for a quick LCD determination of simple and complex synthetic media as well as real complex solutions.

The **second published manuscript** (<https://doi.org/10.1016/j.jece.2022.108423>) with the title “**Comparison of ion removal from waste fermentation effluent by nanofiltration, electrodialysis and ion exchange for a subsequent sulfuric acid recovery**” focused on pretreatment methods of the real fermentation waste effluent for an enhanced sulfuric acid recovery. The microorganism involved in a fermentation process requires a stable pH of the cultivation medium in addition to the carbon sources and nutrients. Thus, acids or bases are continually dosed to maintain the optimal conditions for microbial growth and production rate. In the case of *Sulfolobus acidocaldarius* cultivation sulfuric acid was used for maintaining the pH 3 of the fermentation broth. This approach led to increased sulfate concentration in the waste fermentation effluent, after the biomass separation. The application of bipolar electrodialysis or

diffusion dialysis allows direct recovery of sulfuric acid from the sulfate-containing waste stream. However, the waste stream contains other polluting and potentially harmful compounds that need to be removed before the bipolar electrodialysis. Further on, increasing the sulfate concentration is beneficial for achieving higher sulfuric acid concentrations. The second paper gives an insight into the fouling potential of IEMs - colloidal fouling, organic fouling, inorganic scaling, and biofouling. Three different technologies were analyzed to diminish the fouling of IEMs caused by organic and inorganic compounds of a bio-fermentation effluent from the archaea *Sulfolobus acidocaldarius*. The aim was to remove divalent cations to a value below 10 ppm and to reduce DOC content. Experiments were first performed with nanofiltration membranes from two manufacturers. A particular ED stack was assembled for the second step of the study, containing standard anion-exchange membranes (AEM) and monovalent cation-exchange membranes (mCEM). This assembly provided an optimized feed for bipolar or diffusional dialysis through enrichment of feed with specific ions and reduction of organic molecules. The third approach investigated three types of chelating ion-exchange resins for the removal of divalent cations. Results obtained from the three investigated technologies were studied in terms of their removal efficiency for DOC,  $Mg^{2+}$ , and  $Ca^{2+}$ , selectivity between mono- and divalent ions, ionic fluxes, and energy consumption.

The **third published manuscript** (<https://doi.org/10.1016/j.jclepro.2022.134436>) with the title “**Circular production – Evaluation of membrane technologies for nutrient recycling from a microbial fermentation effluent**” integrated membrane technologies for wastewater treatment resulting from fermentation processes. A decentralized wastewater treatment may allow the disintegration of liquid waste streams to their main components, splitting valuable nutrients and polluting compounds from water molecules. Thus, isolated components may be returned to the production process (fermentation), safely disposed or applied for other purposes such as irrigation or crop fertilization. Industries are currently required to treat their waste streams adequately to protect the environment and natural ecosystem. The rigorous governmental demands for wastewater treatment can be turned into benefits for industry by engaging nutrient and water recycling from evolved waste streams. Closing the production loop would decrease the initial supply demand of nutrients and water. Alternatively, wastewater-born products may be sold once the market for recycled products has been established at a country and global level. Therefore, the paper comprises membrane technologies: nanofiltration, conventional electrodialysis and electrodialysis with bipolar membranes, for the treatment of the bio-fermentation effluent from the archaea *Sulfolobus acidocaldarius*. Real wastewater from the *S. acidocaldarius* cultivation was treated in three different ways to recycle nutrients or produce acid/base while removing potentially harmful compounds and carbon sources. Nutrient recovery is an ongoing topic in the literature; however, it is often performed with synthetic media, and the recovered products are hardly applied for their consumption in follow-up processes. Thus, this paper went a step further by reusing the products recovered from the fermentation effluent in subsequent fermentation batches. The cultivation on the nanofiltered medium and the medium recovered by ED was possible and resulted in microbial growth similar to the reference medium prepared with newly purchased chemicals. An improved growth curve compared to the reference medium was achieved with the use of the acid recovered by EDBM. The applied membrane technologies were compared for their DOC removal, concentration factors for nutrients, membrane selectivity, and energy consumption.

Further on, concerns that might appear during the application of different nutrient-recovery pathways were discussed in the paper.

The **fourth manuscript** (submitted for publication) with the title “**Investigation of ion-exchange membranes and erythritol concentration for the desalination of erythritol culture broth by electro dialysis**” has a different approach compared to the previous three papers. While the previous publications focused on wastewater treatment by membrane technologies at the process endpoint, this paper dealt with the application of electro dialysis in an earlier stage of the fermentation process, for product separation, nutrient recycling, and waste minimization. The product of the fermentation was erythritol, a zero-calorie sweetener. On the one hand, downstream of the erythritol fermentation broth by electro dialysis offers desalination of the broth. On the other hand, a salt concentrate composed of salts removed from the fermentation broth can be returned in the production step. The twofold benefit of electro dialysis in erythritol production was first confirmed in a collaborative study within the Bioactive project and resulted in a publication by Daza-Serna et al (Daza-Serna et al., 2022). The follow-up study published in this fourth manuscript tested different commercially available ion-exchange membranes to identify diffusional phenomena of erythritol and by-products through the membranes towards the salt concentrate. Every erythritol diffusion means product losses, and both erythritol and by-product diffusion mean the contamination of the salt concentrate. Thus, diffusional phenomena should be brought to zero in the electro dialysis process to obtain high-quality products. The study addressed the convectational diffusion of 5 – 25 g/L erythritol without the application of an external electrical field and electrically driven co-diffusion with the ionic migration through the IEMs. Commercially produced ion-exchange membranes were investigated with the synthetic erythritol culture broth. Once the diffusional phenomena, membrane resistance, current efficiency, separation duration, and energy consumption were calculated, the best-performing membrane was selected for further analysis. The research was rounded by the treatment of a real erythritol broth to assess the ED feasibility in this specific application.

## 4.2 Scientific contributions

The following chapters are a summary of the main scientific contributions of this Ph.D. work documented by the peer reviewed publications:

- 1) The first paper comprises literature research on the existing methods for electro dialysis control, main operating and control parameters, and experimental results. Outcomes of the literature study on the experiments obtained with electro dialysis, mainly with sodium chloride solution, indicated:
  - a. the importance of the limiting-current-density parameter (LCD) for process control and current efficiency,
  - b. the existence of different methods to determine LCD, among which graphical methods, and
  - c. the lack of reliability tests for established LCD-determination methods on the multi-ionic complex matrixes and real wastewater.

Thus, this research involved ED experiments in solutions with increasing grades of complexity for LCD tests and compared the LCDs obtained by various graphical LCD methods. The value of the research lies in resolving the best-available graphical LCD

method for complex synthetic media and real wastewater, which are important for further ED research in the domain of wastewater treatment and nutrient recovery technologies.

- 2) The second paper is a part of the pathway to discover an optimal pre-treatment technology for mainly sulfuric acid recovery but also base production from the “leftover” ions in the waste fermentation effluent. “Leftover” ions include the ions from the culture media that were not consumed by microorganisms, from the microbial excretions, and from the chemicals used for the pH control. The experimental results were obtained by applying three technologies: nanofiltration, electro dialysis with monovalent cation-exchange membranes, and ion-exchange resins, which are significant for the future acid/base recovery from liquid waste streams. The manuscript gives an overview of the technological performance regarding divalent cation and DOC removal efficiency, membrane selectivity between mono- and divalent cations, ionic fluxes, and energy consumption. The results are also useful for the downstream biotechnological processes, as these often include membrane technologies or ion-exchange resins. The outcomes of this research provide information for decision-making regarding technology selection and process design in both wastewater treatment and biotechnology.
- 3) The third paper is a proof-of-concept study that applies membrane technologies to close the production loop of the future industrial and pharmaceutical microorganism *Sulfolobus acidocaldarius*, aiming at near-to-zero liquid and waste discharge. Products recovered from the fermentation effluent by nanofiltration, electro dialysis, or electro dialysis with bipolar membranes were tested for their applicability in batch fermentations. The results bring the pathways for nutrient recovery from real wastewater, the ability of membranes to retain harmful compounds, and the actual applicability of recovered nutrients in biotechnological processes. The concept of circular production should be adopted in most industries, as it would lead to more conscious nutrient management, reduction of waste, and reduced risk of environmental pollution by industrial waste streams.
- 4) The fourth paper offers an alternative for the purification of erythritol utilizing electro dialysis instead of conventionally used ion-exchange resins. Investigation of four commercially available ion-exchange membrane stacks led to the selection of one membrane pair with low membrane resistance, low energy consumption, high current efficiency, and high retention of products and by-products. These parameters are important for scaling up the electro dialysis application from the laboratory to the pilot plant, or even industrial scale. Besides the technological importance of the obtained results, the research also supports the development of industrial erythritol production, which is recognized as a safe zero-calorie sugar substitute, also suitable for people with diabetes disease.

## 5 Discussion

In the following section, each scientific paper was analyzed and summed up in order to answer the research questions introduced in chapter 1:

1) What are the core operating parameters of electro dialysis, the selected nutrient/water recovery technology, and which effects it might have when applied in wastewater treatment?

- This work demonstrated the applicability of electro dialysis (ED) for wastewater treatment regarding simultaneous nutrient recovery and water purification. Limiting current density (LCD) was identified as one of the core operating ED parameters. Graphical methods for the LCD detection in the ED operating mode were valid for the feed concentrations  $\leq 0.03$  M NaCl. However, wastewater is a complex mixture, containing high concentrations of dissolved organic and inorganic compounds, multivalent ions, etc. and in contrast, the graphical methods were developed in past for the seawater with sodium chloride dissolved in water as the main constituent. Results of the study indicate the preferable use of the Cowan and Brown method for the wastewater samples due to its applicability to a wide range of solutions with varying ionic compositions, concentrations, and matrix complexities. LCD is primarily influenced by the ionic content of a medium and this study tested the correlation of the electrical conductivity measured in the treated fluid with the detected LCD, for future automatized LCD evaluation and ED control. ED control with the online conductivity measurements was applicable for the batch ED control of one solution matrix, while LCD linearly correlated with the decreasing conductivity. Otherwise, measuring only the conductivity is not suitable for current density adjustment unless combined with other characteristics of the treated medium, such as the pH, type of ions, and organic content.

2) How can the selected technology be optimized for the specific use as it was assigned by the Bioactive project requirements?

- Electro dialysis with bipolar membranes (EDBM) is a process developed from conventional electro dialysis, with the ability to directly produce acids/bases from the anions/cations contained in the treated liquid. This study aimed at achieving higher ionic concentrations, removing dissolved organic carbon, and reducing divalent cations from the waste fermentation effluent in order to deliver pure and higher concentrated acids/bases. Three pre-treatment technologies were tested: nanofiltration (NF), electro dialysis with monovalent cation-exchange membranes (EDm), and ion-exchange resins (IER). Results indicate trade-offs that need to be considered before the process design in wastewater treatment or biotechnological downstream treatment. NF had high removal of organic compounds, and divalent cations, but also for sulfates. In this process constellation, the removal of sulfates is negative as it reduces the final acid concentration produced by EDBM. EDm had the highest removal of organic compounds and lower removal of divalent cations compared to NF and IER, and a concentration factor of 1.9 for monovalent cations and 1.6 for sulfates. IER had a complete divalent cation removal until the resin's saturation and no removal of organic compounds and anions. From the perspective of energy consumption, NF was the most cost-effective treatment, followed by electro dialysis. Ion-exchange resins were the least feasible pre-treatment option due to the absence of DOC removal and requirements for additional posttreatment and chemicals for resin regeneration.

- 3) Can recovered products enable microbial growth and production rate in fermentation processes similar to standard cultivation media?
- The recovery of nutrients and sulfuric acid from the waste fermentation effluent was performed by membrane technologies to finally reintroduce the recovered products to the fermentation process. Regarding that, nanofiltration (NF) and conventional electrodialysis (ED) provided recovered fermentation substrates with microbial growth- and production-rate similar to the reference medium. Whereas ED enabled higher concentration factors of recovered nutrients and higher DOC removal than NF. Phosphorus removal was observed to depend on the feed pH, indicating a potential for selective ED separation of phosphates from other ions of the feed. Electrodialysis with bipolar membranes (EDBM) recovered 0.11–0.15 M sulfuric acid from the sulfates contained in the fermentation wastewater. Anions other than sulfates were also present in the recovered acid and co-ion transport was detected, supplying the fermentation substrate with additional P and N sources. Thus, the growth curve was improved when the recovered acid was applied for the cultivation compared to the reference medium. Economic feasibility must be included in the circular process design. NF is at least 10 times less cost intensive compared to ED/EDBM, for the same treated medium. The advantages of ED/EDBM are the selective ion separation, higher concentration factors, and recovery of high-value products. Implementation of renewable energy sources to power electro-membrane processes and increased market for recovered resources may justify the application of ED/EDBM in the industrial fermentation processes.
- 4) Can the selected technology lead to waste reduction when applied to a position different than the end-of-pipe, such as for the downstream process in a biotechnological production?
- Shifting the electro-membrane processes to an earlier stage of the biotechnological downstream process, other than the treatment of the final wastewater, may have mutual economic and environmental benefits. Electrodialysis (ED) was tested for downstream treatment in erythritol production to integrate product purification, resource recovery, and waste minimization. Desalination rate of 94 % in synthetic and real erythritol culture broth led to the separation of uncharged particles, including erythritol, from the ionic content. This practice resulted in a salt concentrate, which can be reused in further cultivations. The concentration factor of the ions in the concentrate was 1.8.
- 5) Can ion-exchange membranes retain erythritol while removing ions from the fermentation broth?
- ED operation control by step-wise voltage, following the removal trend of the ions from the cultivation broth, performed with fewer product losses than the conventionally applied constant current control (0.53 % compared to 0.78 % erythritol losses). There is a variety of ion-exchange membranes on the market that need to be tested for a particular application. This work assessed commercial membranes to provide a downstream process with the least product losses caused by the diffusional effects of uncharged particles through the ion exchange membranes. Step-wise voltage control was adopted for further ED experiments. When the feed contained 5 g/L erythritol, membrane pairs from Fumatech GmbH,

Germany, retained the erythritol completely, whereas other tested membranes had 1.3 – 2 % erythritol losses. With increased erythritol concentrations to 15 g/L and 25 g/L the erythritol diffusion was 0.36 % and 0.41 % through Fumatech membranes, respectively. With the application of external electrical field, erythritol losses reached 0.53 %. When the real culture broth with 25 g/L erythritol was treated by ED with Fumatech membranes 2 % erythritol losses were detected. Concludingly, erythritol diffusion depends on the initial erythritol concentrations, ion-exchange membrane characteristics, ED operating mode and desalination time.

## 6 Final message and outlook

This thesis aimed at recovering and reusing resources from wastewater of industrial fermentation processes in the pharmaceutical and food industry. For this purpose, membrane technologies were investigated, wherein the focus was placed on electrodialysis (ED) and electrodialysis with bipolar membranes (EDBM).

Limiting current density (LCD) is one of the core parameters for ED operation, and the results of the first publication justify the applicability of the Cowan and Brown graphical method to determine LCD in ED treating complex synthetic media and even real wastewater.

Fermentation wastewater treated in this thesis contained high concentrations of dissolved organic carbon (~ 1.8 g/L DOC) and ionic strength measured as the electrical conductivity of 19 – 30 mS/cm. Thus, pre-treatment before ED/EDBM is necessary to protect the ion-exchange membranes from fouling and scaling. Microfiltration is usually sufficient pre-treatment for electrodialysis, whereas the results of the second publication recommend the application of nanofiltration or ED with monovalent cation-exchange membranes before EDBM. Contrary, ion-exchange resins are not advised due to the absence of DOC removal and requirements for additional posttreatment and chemicals for resin regeneration.

In general, ED performed well in lab-scale batch experiments for recovering nutrients from fermentation wastewater and purification of the wastewater. The final products were in the form of concentrated ionic solution without, or with a very low concentration of organic compounds. EDBM recovered low-concentrated sulfuric acid, however, in a combination with other acids produced from anions of the fermentation wastewater. The mixture of bases, according to the cations present in the fermentation wastewater, was also produced by EDBM. In contrast to microfiltration, ED, EDBM, and nanofiltration were able to remove inhibiting metabolites from the waste fermentation effluent. Concentrated ionic solutions were successfully utilized as substrates for batch fermentation tests, yielding similar microbial growth and production rate as the reference medium composed of industrially produced chemicals. Recovered acids/bases enabled pH control of the tested batch fermentations.

In the downstream processes, ED had very low erythritol losses (up to 2%), while the ions were effectively concentrated for further reuse. Thus, ED can substitute commonly used ion-exchange resins for erythritol purification and contribute to a more sustainable biotechnological production process.

Although ED and EDBM provided high-value recovered products, the technology is more energy-consuming than e.g. nanofiltration. Powering electrodialysis with renewable energy sources can decrease the negative environmental effect of this technology.

Further research should focus on

- Improvement of selectivity for ion-exchange membranes
- Manufacturing membranes for ion fractionation
- Cost-effective monitoring methods for ionic species of wastewater
- Application of electrodialysis for a continuous resource recovery
- Long-term application of electrodialysis in wastewater treatment, fouling effects and optimal membrane cleaning methods
- Developing a life cycle assessment tool for a holistic insight into electrodialysis application, which can support decision-making for an optimal treatment technology
- Ways to expand the awareness of nutrient recycling necessity and the market for recovered resources

## References

- Ashbolt, N. J., Am, ézquita A., Backhaus, T., Borriello, P., Brandt, K. K., Collignon, P., Coors, A., Finley, R., Gaze, W. H., Heberer, T., Lawrence, J. R., Larsson, D. G. J., McEwen, S. A., Ryan, J. J., Sch, önfeld J., Silley, P., Snape, J. R., Van, den E. C., & Topp, E. (2013). Human Health Risk Assessment (HHRA) for Environmental Development and Transfer of Antibiotic Resistance. *Environmental Health Perspectives*, *121*(9), 993–1001. <https://doi.org/10.1289/ehp.1206316>
- Beckinghausen, A., Odlare, M., Thorin, E., & Schwede, S. (2020). From removal to recovery: An evaluation of nitrogen recovery techniques from wastewater. *Applied Energy*, *263*, 114616. <https://doi.org/10.1016/j.apenergy.2020.114616>
- Ben, Y., Fu, C., Hu, M., Liu, L., Wong, M. H., & Zheng, C. (2019). Human health risk assessment of antibiotic resistance associated with antibiotic residues in the environment: A review. *Environmental Research*, *169*, 483–493. <https://doi.org/10.1016/j.envres.2018.11.040>
- Benstoem, F., Becker, G., Firk, J., Kaless, M., Wuest, D., Pinnekamp, J., & Kruse, A. (2018). Elimination of micropollutants by activated carbon produced from fibers taken from wastewater screenings using hydrothermal carbonization. *Journal of Environmental Management*, *211*, 278–286. <https://doi.org/10.1016/j.jenvman.2018.01.065>
- Blum, N. U., Haupt, M., & Bening, C. R. (2020). Why “Circular” doesn’t always mean “Sustainable.” *Resources, Conservation and Recycling*, *162*, 105042. <https://doi.org/10.1016/j.resconrec.2020.105042>
- Cordell, D., & White, S. (2014). Life’s Bottleneck: Sustaining the World’s Phosphorus for a Food Secure Future. *Annual Review of Environment and Resources*, *39*(1), 161–188. <https://doi.org/10.1146/annurev-environ-010213-113300>
- Daza-Serna, L., Knežević, K., Kreuzinger, N., Mach-Aigner, A. R., Mach, R. L., Krampe, J., & Friedl, A. (2022). Recovery of Salts from Synthetic Erythritol Culture Broth via Electrodialysis: An Alternative Strategy from the Bin to the Loop. *Sustainability*, *14*(2), Article 2. <https://doi.org/10.3390/su14020734>
- European Commission. (2015). *COMMUNICATION FROM THE COMMISSION TO THE EUROPEAN PARLIAMENT, THE COUNCIL, THE EUROPEAN ECONOMIC AND SOCIAL COMMITTEE AND THE COMMITTEE OF THE REGIONS Closing the loop—An EU action plan for the Circular Economy* (COM(2015) 614 final). [https://eur-lex.europa.eu/resource.html?uri=cellar:8a8ef5e8-99a0-11e5-b3b7-01aa75ed71a1.0012.02/DOC\\_1&format=PDF](https://eur-lex.europa.eu/resource.html?uri=cellar:8a8ef5e8-99a0-11e5-b3b7-01aa75ed71a1.0012.02/DOC_1&format=PDF)

- European Commission. (2022). *Proposal for a DIRECTIVE OF THE EUROPEAN PARLIAMENT AND OF THE COUNCIL concerning urban wastewater treatment (recast)* (COM(2022) 541 final). <https://environment.ec.europa.eu/system/files/2022-10/Proposal%20for%20a%20Directive%20concerning%20urban%20wastewater%20treatment%20%28recast%29.pdf>
- European Commission (EC). (2020). *Communication from the Commission to the European Parliament, the Council, the European Economic and Social Committee and the Committee of the Regions. Critical Raw Materials Resilience: Charting a Path towards greater Security and Sustainability* (COM(2020) 474 Final). European Commission (EC), Brussels, Belgium. <https://eur-lex.europa.eu/legal-content/EN/TXT/PDF/?uri=CELEX:52020DC0474&from=EN>
- European Union. (2020). *Circular Economy Action Plan. For a cleaner and more competitive Europe*. European Union (EU), European Commission (EC), Brussels, Belgium. [https://ec.europa.eu/environment/pdf/circular-economy/new\\_circular\\_economy\\_action\\_plan.pdf](https://ec.europa.eu/environment/pdf/circular-economy/new_circular_economy_action_plan.pdf)
- Faragò, M., Damgaard, A., Madsen, J. A., Andersen, J. K., Thornberg, D., Andersen, M. H., & Rygaard, M. (2021). From wastewater treatment to water resource recovery: Environmental and economic impacts of full-scale implementation. *Water Research*, 204, 117554. <https://doi.org/10.1016/j.watres.2021.117554>
- Fortelny, M., & Inmann, K. (2021). Sulphuric acid: Why the acid all-rounder is affected by extreme shortage. *Donau Chemie AG & Donauchem GmbH*, 10.
- Hadi, P., Xu, M., Ning, C., Sze Ki Lin, C., & McKay, G. (2015). A critical review on preparation, characterization and utilization of sludge-derived activated carbons for wastewater treatment. *Chemical Engineering Journal*, 260, 895–906. <https://doi.org/10.1016/j.cej.2014.08.088>
- King, M. J., Davenport, W. G., Davenport, W. G., & Moats, M. S. (2013). *Sulfuric acid manufacture: Analysis, control, and optimization* (Second edition). Elsevier.
- Kirova-Yordanova, Z. (2004). Exergy analysis of industrial ammonia synthesis. *Energy*, 29(12), 2373–2384. <https://doi.org/10.1016/j.energy.2004.03.036>
- Kneese, A. V. (1988). The Economics of Natural Resources. *Population and Development Review*, 14, 281–309. <https://doi.org/10.2307/2808100>
- Kuldeep, Badenhorst, W. D., Kauranen, P., Pajari, H., Ruismäki, R., Mannela, P., & Murtomäki, L. (2021). Bipolar Membrane Electrodialysis for Sulfate Recycling in the

Metallurgical Industries. *Membranes*, 11(9), Article 9.  
<https://doi.org/10.3390/membranes11090718>

- Liu, H., Hu, G., Basar, I. A., Li, J., Lyczko, N., Nzihou, A., & Eskicioglu, C. (2021). Phosphorus recovery from municipal sludge-derived ash and hydrochar through wet-chemical technology: A review towards sustainable waste management. *Chemical Engineering Journal*, 417, 129300. <https://doi.org/10.1016/j.cej.2021.129300>
- Mäkinen, K. K. (2011). Sugar Alcohol Sweeteners as Alternatives to Sugar with Special Consideration of Xylitol. *Medical Principles and Practice*, 20(4), 303–320. <https://doi.org/10.1159/000324534>
- Malik, V. S., & Hu, F. B. (2022). The role of sugar-sweetened beverages in the global epidemics of obesity and chronic diseases. *Nature Reviews Endocrinology*, 18(4), Article 4. <https://doi.org/10.1038/s41574-021-00627-6>
- Mariotti, M., & Lucisano, M. (2014). Sugar and Sweeteners. In *Bakery Products Science and Technology* (pp. 199–221). John Wiley & Sons, Ltd. <https://doi.org/10.1002/9781118792001.ch11>
- Martinez, J. L. (2009). The role of natural environments in the evolution of resistance traits in pathogenic bacteria. *Proceedings of the Royal Society B: Biological Sciences*, 276(1667), 2521–2530. <https://doi.org/10.1098/rspb.2009.0320>
- Mo, W., & Zhang, Q. (2013). Energy–nutrients–water nexus: Integrated resource recovery in municipal wastewater treatment plants. *Journal of Environmental Management*, 127, 255–267. <https://doi.org/10.1016/j.jenvman.2013.05.007>
- Morero, B., Vicentin, R., & Campanella, E. A. (2017). Assessment of biogas production in Argentina from co-digestion of sludge and municipal solid waste. *Waste Management*, 61, 195–205. <https://doi.org/10.1016/j.wasman.2016.11.033>
- Ohtake, S., & Wang, Y. J. (2011). Trehalose: Current Use and Future Applications. *Journal of Pharmaceutical Sciences*, 100(6), 2020–2053. <https://doi.org/10.1002/jps.22458>
- Perera, M. K., Englehardt, J. D., & Dvorak, A. C. (2019). Technologies for Recovering Nutrients from Wastewater: A Critical Review. *Environmental Engineering Science*, 36(5), 511–529. <https://doi.org/10.1089/ees.2018.0436>
- Pistocchi, A., Andersen, H. R., Bertanza, G., Brander, A., Choubert, J. M., Cimbritz, M., Drewes, J. E., Koehler, C., Krampe, J., Launay, M., Nielsen, P. H., Obermaier, N., Stanev, S., & Thornberg, D. (2022). Treatment of micropollutants in wastewater: Balancing effectiveness, costs and implications. *Science of The Total Environment*, 850, 157593. <https://doi.org/10.1016/j.scitotenv.2022.157593>

- Prangishvili, D., Holz, I., Stieger, E., Nickell, S., Kristjansson, J. K., & Zillig, W. (2000). Sulfolobocins, Specific Proteinaceous Toxins Produced by Strains of the Extremely Thermophilic Archaeal Genus *Sulfolobus*. *Journal of Bacteriology*, *182*(10), 2985–2988. <https://doi.org/10.1128/JB.182.10.2985-2988.2000>
- Quehenberger, J., Shen, L., Albers, S.-V., Siebers, B., & Spadiut, O. (2017). *Sulfolobus* – A Potential Key Organism in Future Biotechnology. *Frontiers in Microbiology*, *8*, 2474. <https://doi.org/10.3389/fmicb.2017.02474>
- Rahimi, S., Modin, O., & Mijakovic, I. (2020). Technologies for biological removal and recovery of nitrogen from wastewater. *Biotechnology Advances*, *43*, 107570. <https://doi.org/10.1016/j.biotechadv.2020.107570>
- Rakicka, M., Rukowicz, B., Rywińska, A., Lazar, Z., & Rymowicz, W. (2016). Technology of efficient continuous erythritol production from glycerol. *Journal of Cleaner Production*, *139*, 905–913. <https://doi.org/10.1016/j.jclepro.2016.08.126>
- Reuter, S., Rusborg Nygaard, A., & Zimmermann, W. (1999).  $\beta$ -Galactooligosaccharide synthesis with  $\beta$ -galactosidases from *Sulfolobus solfataricus*, *Aspergillus oryzae*, and *Escherichia coli*. *Enzyme and Microbial Technology*, *25*(6), 509–516. [https://doi.org/10.1016/S0141-0229\(99\)00074-5](https://doi.org/10.1016/S0141-0229(99)00074-5)
- Rye, C. A., Isupov, M. N., Lebedev, A. A., & Littlechild, J. A. (2009). Biochemical and structural studies of a l-haloacid dehalogenase from the thermophilic archaeon *Sulfolobus tokodaii*. *Extremophiles*, *13*(1), 179–190. <https://doi.org/10.1007/s00792-008-0208-0>
- Tripathi, A. D., Mishra, R., Maurya, K. K., Singh, R. B., & Wilson, D. W. (2019). Chapter 1— Estimates for World Population and Global Food Availability for Global Health. In R. B. Singh, R. R. Watson, & T. Takahashi (Eds.), *The Role of Functional Food Security in Global Health* (pp. 3–24). Academic Press. <https://doi.org/10.1016/B978-0-12-813148-0.00001-3>
- United Nations. (2022). *The Sustainable development Goals Report 2022*. United Nations. <https://unstats.un.org/sdgs/report/2022/The-Sustainable-Development-Goals-Report-2022.pdf>
- Yang, Q., Zhang, Z., Gregg, E. W., Flanders, W. D., Merritt, R., & Hu, F. B. (2014). Added Sugar Intake and Cardiovascular Diseases Mortality Among US Adults. *JAMA Internal Medicine*, *174*(4), 516–524. <https://doi.org/10.1001/jamainternmed.2013.13563>

## Article

# Assessment of Graphical Methods for Determination of the Limiting Current Density in Complex Electrodialysis-Feed Solutions

Katarina Knežević <sup>1,\*</sup> , Daniela Reif <sup>1</sup> , Michael Harasek <sup>2</sup> , Jörg Krampe <sup>1</sup>  and Norbert Kreuzinger <sup>1</sup> 

<sup>1</sup> Institute for Water Quality and Resource Management, TU Wien, 1040 Vienna, Austria; dreif@iwag.tuwien.ac.at (D.R.); jkrampe@iwag.tuwien.ac.at (J.K.); norbkreu@iwag.tuwien.ac.at (N.K.)

<sup>2</sup> Institute of Chemical, Environmental and Bioscience Engineering, TU Wien, 1060 Vienna, Austria; michael.harasek@tuwien.ac.at

\* Correspondence: katarina.knezevic@tuwien.ac.at

**Abstract:** Electrodialysis (ED) is a promising technology suitable for nutrient recovery from a wide variety of liquid waste streams. For optimal operating conditions, the limiting current density (LCD) has to be determined separately for each treated feed and ED equipment. LCD is most frequently assessed in the NaCl solutions. In this paper, five graphical methods available in literature were reviewed for LCD determination in a series of five feed solutions with different levels of complexity in ion and matrix composition. Wastewater from microbial fermentation was included among the feed solutions, containing charged and uncharged particles. The experiments, running in the batch ED with an online conductivity, temperature, and pH monitoring, were conducted to obtain data for the comparison of various LCD determination methods. The results revealed complements and divergences between the applied LCD methods with increasing feed concentrations and composition complexity. The Cowan and Brown method had the most consistent results for all of the feed solutions. Online conductivity monitoring was linearly correlated with the decreasing ion concentration in the feed solution and corresponding LCD. Therefore, the results obtained in this study can be applied as a base for the automatized dynamic control of the operating current density–voltage in the batch ED. Conductivity alone should not be used for the ED control since LCD depends on the ion exchange membranes, feed flow, temperature and concentration, ionic species, their concentration ratios, and uncharged particles of the feed solution.

**Keywords:** electrodialysis; limiting current density; wastewater treatment; nutrient recovery



**Citation:** Knežević, K.; Reif, D.; Harasek, M.; Krampe, J.; Kreuzinger, N. Assessment of Graphical Methods for Determination of the Limiting Current Density in Complex Electrodialysis-Feed Solutions. *Membranes* **2022**, *12*, 241. <https://doi.org/10.3390/membranes12020241>

Academic Editors: August Bonmati and Miriam Cerrillo

Received: 17 January 2022

Accepted: 14 February 2022

Published: 18 February 2022

**Publisher's Note:** MDPI stays neutral with regard to jurisdictional claims in published maps and institutional affiliations.



**Copyright:** © 2022 by the authors. Licensee MDPI, Basel, Switzerland. This article is an open access article distributed under the terms and conditions of the Creative Commons Attribution (CC BY) license (<https://creativecommons.org/licenses/by/4.0/>).

## 1. Introduction

Electrodialysis (ED) is an electro-membrane ion separation process widely used to demineralize, concentrate, and/or convert salt-containing solutions [1–4]. Moreover, ED appears as an emerging technology for nutrient recovery in wastewater treatment [5–8]. The driving force for the salt separation is the application of an electrical potential across an ED membrane stack, whereby charged particles are removed from the feed solution. An ED membrane stack comprises alternately placed cation- and anion-exchange membranes. During ED, the feed stream is separated into two streams, one with a reduced concentration of ions (diluate), and the other enriched with ions (concentrate). From the techno-economical point of view, it is important to run ED under optimal operating conditions [9–12]. Various parameters, such as feed solution composition, temperature, flow, membrane characteristics, spacers, applied power, and current density, impact the ED process efficiency [2,13–18]. One of the core parameters for the ED process design is the limiting current density (LCD) [19–23]. The experimentally determined LCD is commonly used for deriving the process essential boundary layer thickness, and it is directly proportional to the ion concentration and diffusivity [20,22,24]. The boundary layer is a thin layer of the

solution adjacent to the membrane surface, with a concentration decrease of counter-ions on the diluate side and a concentration increase of co-ions on the concentrate side, compared to the bulk concentration [16]. The LCD indicates the electric current density that leads to the depletion of ions in the boundary layer on the diluate side, as a result of the concentration polarization [24]. With a further increase of the current density above a certain threshold, a dissociation of water molecules to  $H^+$  and  $OH^-$  ions occurs in the boundary layer as an undesired effect, causing an increase of the overall current density and subsequently a decrease in the current efficiency. Two additional transport mechanisms, gravitational convection and electroconvection, were proven to significantly affect the generation of current in the over limiting conditions [2,21,25–27]. The LCD increases with the increasing flow, temperature, and ion concentration of the solution [16,28–31].

The LCD values are difficult to predict for complex solutions, such as municipal or industrial wastewater, and must be determined in advance for each treated feed solution in lab-scale experiments. In the past, batch ED processes had been mostly operated under constant current conditions, which were chosen based on the LCD of the targeted diluate concentration. However, recent publications propose a dynamic current density control, dependent on the actual diluate compositions and ED stack characteristics [32,33]. Considerable research focused on defining the boundary layer formation, resolving the problems it causes and determining the LCD in advance for optimal process design and operation [19,20,22,34–36]. Graphical methods are most commonly suggested in the literature to determine the LCD and corresponding operating current density [2,16,19,35,37–40]. However, the obtained results are often contradictory. Furthermore, most of the developed methods were conducted with simplified matrices as sodium chloride solutions and rarely with "real-life" media. Since ED is emerging as an interesting method for nutrient recovery from various liquid waste streams, there is a need to assess the applicability of the existing LCD determination methods on complex feed solutions.

This paper assessed the applicability of five established LCD graphical methods from the literature to feed solutions with increasing grades of complexity. The considered graphical methods are Isaacson and Sonin [15,37], Cowan and Brown [35], the pH method [38], a method based on the current efficiency ( $\lambda$ ) proposed by La Cerva et al. [19], and on the desalting efficiency ( $\epsilon$ ) proposed by Meng et al. [36]. The feed solution complexity investigated in this paper was divided into three levels: (a) Single-salt ( $NaCl$ ,  $Na_2SO_4$ ) solutions, (b) complex synthetic media (various ions added in changing ratios), and (c) real liquid waste streams from a microbial fermentation process. All of the LCD experiments were performed with the same ED set-up in the batch mode, only varying the feed matrix. The diluate concentration decreases continuously during the ED ion separation process in the batch mode. Consequently, the LCD changes as well, leading to the requirements for a consecutive adaptation of the operating conditions. Therefore, the concentration ranges were assessed on the LCD, and the online conductivity measurement, as a direct correlation to the ionic concentration, was applied for the monitoring. The experimental data were analyzed using the methods mentioned above. This study aimed at answering the following questions: (I) Are the applied methods for the LCD determination equally applicable to a wide range of salt concentrations; (II) Are the methods equally applicable to each type of feed representing an increasing complexity; (III) Do the solutions with the same conductivity but different ionic composition and level of complexity, reach the same LCD; (IV) Is there a potential for using a simple measurement, such as the conductivity, for a quick LCD determination of simple and complex synthetic media as well as real complex solutions.

## 2. Materials and Methods

### 2.1. Experimental Set-Up

A 10-cell pair lab-scale ED 64-004 unit (PCCell GmbH, Heusweiler, Germany) was used for the experimental work. The utilized membranes were 10 anion-exchange membranes (AEM, PC SA) and nine cation-exchange membranes (CEM, PC SK) from the same producer, with an active membrane area of  $8 \times 8 \text{ cm}^2$  per membrane. The membrane characteristics

are in Table 1, and the relative contribution of the membranes to the whole ED stack resistance is in Supplementary Material. Polypropylene spacers (PCCell) had a thickness of 0.45 mm. Both of the end membranes were set up as cation-exchange membranes to minimize the chloride ion transport towards the electrodes. Pt/Ir-coated titanium anode and V4A steel cathode were placed in the polypropylene electrode housing material. A DC power supply was applied for adjusting the constant current–voltage operating mode. The two double-wall feed tanks (2 L), one for the diluate and one for the concentrate, were filled with identical feed solutions at the beginning of each experiment. Cooling water was circulated through the outer layer of the double-wall tanks, maintaining the feed temperature at a constant level. Online measurements of the conductivity, temperature, and pH of the diluate outlet, and the conductivity and temperature (JUMO GmbH and Co., Fulda, Germany) of the concentrate outlet were measured every 2 s. Operational data were automatically recorded in a csv-file via the data acquisition box, as originally supplied by the producer.

**Table 1.** Characteristics of the ion-exchange membranes, as specified by the PCCell producer.

Membrane	Type	Thickness, $\mu\text{m}$	Transference Number	Resistance, $\text{Ohm cm}^2$	Water Content (wt%)	pH Stability
PC SA	Anion-exchange	100–110	>0.95	1.8	14	0–9
PC SK	Cation-exchange	100–120	>0.95	2.5	9	0–11
PC MTE	End membrane	220	>0.94	4.5	-	1–13

The ED unit was operated in a batch mode and the operating conditions could be adjusted only manually. For all of the performed LCD tests, both of the obtained streams, the diluate and the concentrate stream, were continuously mixed again after the membrane stack to maintain the feed concentration at a constant level during the experiments (Figure 1). Flows of the diluate and concentrate solutions were maintained with centrifugal pumps (ITS-Betzel, Hattersheim, Germany) by applying a constant flow rate of 15 L/h, with an average velocity of 0.012 m/s in each diluate/concentrate chamber. A 0.25 M  $\text{Na}_2\text{SO}_4$  (5 L) electrolyte solution was circulated between the electrodes with a flow rate of 150 L/h. The applied voltage was increased stepwise from 3–5 V to a maximum of 29 V, in 0.5–1 V increments.

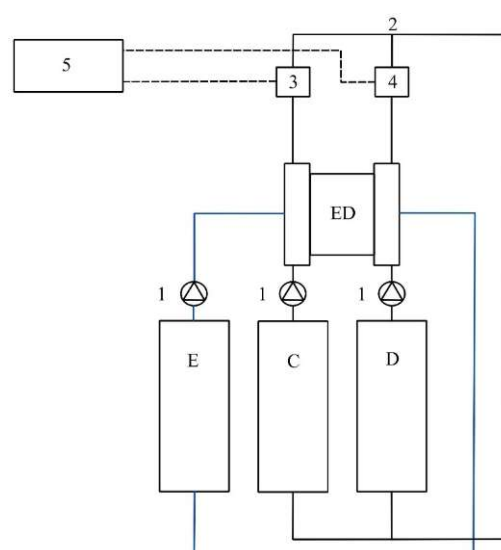


**Figure 1.** A schematic representation of the used experimental set-up, including the ED membrane stack (ED), concentrate (C), diluate (D), electrode rinse (E), centrifugal pumps (1), mixing pipe (2), conductivity and temperature sensors (3), conductivity, temperature, and pH sensors (4), data acquisition box (5).

## 2.2. Description of Assessed LCD Determination Methods

Commonly, the feed stream circulates inside the diluate chamber in the ED batch mode until the desired demineralization rate is reached. This indicates that the diluate salt concentration, as well as its conductivity, are continuously decreasing. Since the salt concentration directly impacts the LCD, the lowest current density should be applied throughout the ED desalting process or the current density should be gradually reduced. Therefore, the ranges of the salt concentrations were subjected to a diapason of current densities (voltages) and analyzed via graphical LCD methods.

Various measured parameters, such as current density, voltage, conductivity, and pH, can indicate the properties and behavior of the treated solution. Several authors correlated these parameters to lead to knowledge in the ED. Therefore, the LCD has been defined as a crucial parameter for understanding the treated solution behavior and ED process control. The applied graphical LCD methods are described in the following sections, and their graphical presentations can be found in Appendix A.

### 2.2.1. Isaacson and Sonin (I-S) Method

Isaacson and Sonin (I-S) method analyzes the current density (mA/cm<sup>2</sup>) behavior depending on the voltage applied to the ED cell [37]. Three different regions (I–III) are defined by this method (Appendix A, Figure A1). (I) is the Ohmic region with a linear correlation of the current density with the applied voltage. (II) is a region where the linear dependence starts leveling out. Here, the operational mode is transfiguring to the limiting current density region, indicating an energy loss due to the increased voltage resulting in the dissociation of water molecules to H<sup>+</sup> and OH<sup>−</sup> ions, gravitational convection due to density differences, and electroconvection [21,41]. This occurs due to the boundary layer formation adjacent to the membrane surface on the diluate side. The intersection point of the two slopes belonging to the Ohmic and the second (plateau) region indicates the LCD. One way to extend the Ohmic region would be to increase the feed flow, allowing for better mixing of the ions present in the treated solution and reduction of near-membrane boundary layer formation [42]. The third region (III) extends over the increasing positive slope, where a second intersection point can be determined. This region can be explained by the contribution of already split water molecules to the conducting electricity through the ED cell, gravitational convection, electroconvection, and the current carried by the salt counter-ions.

In this research, the head and the tail of the experimental data were fitted by a linear equation, as presented in Appendix A, Figure A1. The LCD was found at their intersecting point, calculated as:

$$y(i_{lim}) = m_1 \cdot \frac{b_2 - b_1}{m_1 - m_2} + b_1 \quad (1)$$

where the  $m_1$  and  $m_2$  are the slopes of the first and second fitting equation, respectively, and  $b_1$  and  $b_2$  are the intercepts of the first and second fitting equation, respectively.

### 2.2.2. Cowan and Brown (C-B) Method

Cowan and Brown (C-B) [35] presented their data differently than Isaacson and Sonin. Rather than analyzing a direct current density–voltage dependency, the ED cell resistance is plotted against the reciprocal current density (Appendix A, Figure A2). LCD manifests at a polarization voltage as a rapid change of the slope. The ED cell resistance is decreasing with the increase of the current density up to a certain point. At this point, with a further increase of the current density (applied voltage), regions with higher resistance in the ED cell evolve, drawing a negative slope on the diagram. The intersection of the positive and negative slope represents the LCD. In this study, the experimental data were fitted by an inverse second-order polynomial function, and the LCD is determined as the function minimum:

$$f(x) = y_0 - \frac{a}{x} + \frac{b}{x^2} \quad (2)$$

Values of the function coefficients ( $y_0$ ,  $a$  and  $b$ ),  $R^2$ , intersection of the slopes, and current density ( $1/x$ ) for minimum resistance can be found in Supplementary Table S2.

### 2.2.3. The pH Method

Cowan and Brown noticed that the pH of the diluting stream starts to decrease at a current value very close to the value at which the resistance slope changes [35]. Consequently, the authors [38] define the limiting current density for the pH method as a point where the pH value of the diluting stream shows a decrease of 0.2 pH units. This breaking point can be seen on the diluate pH–reciprocal current density diagram (Appendix A, Figure A3). However, the initial pH of the tested feed solutions varies strongly, and in some of the experiments it actually increases with the increasing current density. Therefore,  $\Delta pH$  was introduced to compare the pH trends among the solutions with different levels of complexity, calculated as follows:

$$\Delta pH = pH_{dil}^{OUT} - pH_{dil}^{IN} = -\log \frac{[H^+]_t}{[H^+]_0} \tag{3}$$

where the subscripts  $pH_{dil}^{IN}$  and  $pH_{dil}^{OUT}$  are the pH values of the diluate inlet and outlet, respectively. When the diluate pH drops, the  $H^+$  ion concentration increases and  $\Delta pH$  is  $<0$ , and vice versa.

### 2.2.4. Current Efficiency ( $\lambda$ ) Method

La Cerva et al. [19] examined the research of Kwak et al. [43] and suggested plotting the current efficiency ( $\lambda$ ) against the current density, wherein the LCD appears at the maximum  $\lambda$  (%) (Appendix A, Figure A4). This method is an alternative to the desalting efficiency method proposed by Meng et al. [36] for determining the optimal operating current. The following equation was used to calculate  $\lambda$ :

$$\lambda = \frac{zFQ_{dil}(C_{dil}^{IN} - C_{dil}^{OUT})}{NI} \cdot 100\% \tag{4}$$

where  $z$  is the ionic charge,  $F$  is Faraday constant (96485.33 sA/mol),  $Q_{dil}$  is the flow of the diluate stream (L/s),  $C_{dil}^{IN}$  and  $C_{dil}^{OUT}$  are the inlet and outlet concentrations of the diluate stream (mol/L),  $I$  is the current value (A), and  $N$  is the number of the ED cell pairs. NaCl concentrations are calculated based on the NaCl concentration–conductivity correlation (Supplementary, Figure S2).

### 2.2.5. Desalting Efficiency ( $\epsilon$ ) Method

Meng et al. [36] proposed a method for determining the optimal operating current based on the desalting efficiency ( $\epsilon$ ):

$$\epsilon = \frac{S_{dil}^{IN} - \kappa_{dil}^{OUT}}{\kappa_{dil}^{IN}} \cdot 100\% \tag{5}$$

where  $\kappa_{dil}^{IN}$  is the initial conductivity (mS/cm) of the feed to be treated, and  $\kappa_{dil}^{OUT}$  is the conductivity (mS/cm) of diluate generated by the ED. Values of the desalting efficiency are plotted against the current density, wherein the LCD appears as the maximum  $\epsilon$  (%), representing the optimal operating current (Appendix A, Figure A5).

In this research, the  $\epsilon$  values were plotted against the voltage, since the experimental data had similar trends to the C–B curves. Therefore, the head and tail of the experimental data were fitted by a linear equation and the LCD was found at their intersecting point. The  $\epsilon$ – $i$  plots can be found in Supplementary Material.

### 2.3. Solution Tested

To assess the five methods for determining the LCD, a set of experimental ED runs with different synthetic and real feed media were performed. All of the reagents used in this study were purchased from Merck KGaA (Darmstadt, Germany). The pH values of the synthetically prepared solutions are rather low (~5) due to the absorption of atmospheric carbon dioxide and the production of carbonic acid in the deionized water used for the NaCl solution preparation [43].

#### 2.3.1. Solution Level a—Single-Salt Solution (SSS)

Analytical grade NaCl was added to the deionized water to meet the concentration ranges between the surface waters and seawater in five concentrations between 0.005 and 0.5 M. The corresponding measured electrical conductivities ranged from 1–48.7 mS/cm, respectively. In further experiments, 0.03 M NaCl solution with a conductivity of 5.5 mS/cm was assigned as SSS1 (see Table 2) for comparison to the other analyzed solutions. In the next approach, analytical grade Na<sub>2</sub>SO<sub>4</sub> (SSS2) was added to the deionized water to meet the conductivity of 5.5 mS/cm and to compare its behavior during the LCD experiments to the other treated solutions (see Table 2). Sulfate-containing salt was chosen due to the high SO<sub>4</sub><sup>2-</sup> content in the real complex solutions investigated in a later step (see Section 2.3.3). Additionally, the impact of the ionic radii and ionic mobility on the LCD can be studied when NaCl and Na<sub>2</sub>SO<sub>4</sub> solutions with the same conductivity (ionic strengths) are subjected to the same conditions for the LCD assessment.

**Table 2.** Total organic carbon (TOC) and ionic content of the initial synthetic and real solutions with corresponding conductivity.

Solution	TOC	PO <sub>4</sub> -P	Cl <sup>-</sup>	SO <sub>4</sub> <sup>2-</sup>	NH <sub>4</sub> -N	Na <sup>+</sup>	K <sup>+</sup>	Ca <sup>2+</sup>	Mg <sup>2+</sup>	Conductivity
	mg/L									
SSS1	0	0	53.6	0	0	53.8	0	0	0	5.5
SSS2	0	0	0	19.5	0	9.4	0	0	0	5.5
SCS1	0	13.2	12.0	12.1	12.8	11.9	13.2	0	2.8	5.5
SCS2	0	4.3	2.01	71.0	92.2	25.7	2.8	0.8	1.0	13.8
RCS	1060	4.1	2.2	85.1	94.4	37.5	4.7	1.3	2.5	18.4

#### 2.3.2. Solution Level b—Synthetic Complex Solution (SCS)

Two model solutions based on the ionic content of the waste streams from two different fermentation processes (SCS1 and SCS2) without any organic matter content were prepared with the analytical grade salts (see Table 2). SCS1 (5.5 mS/cm) solution has already been studied in a previous research [44]. Organic compounds, commonly present in real waste streams, were not added to these model solutions in order to avoid their interference in LCD determination. Dilution ranges from the initial model solutions (SCS1 and SCS2) were chosen and prepared for the LCD assessment, keeping in mind the decreasing LCD with decreasing salt content in the diluate stream during the batch ED. The following conductivities for the dilution steps used as feed solutions were obtained: 2.9, 1.4, and 0.2 mS/cm for the SCS1 serial; and 7.7, 5.3, 2.8, and 1.9 mS/cm for the SCS2 serial. The pH value of the SCS2 was adjusted to 3 by adding 20% of sulfuric acid.

#### 2.3.3. Solution Level c—Real Complex Solution (RCS)—Real Liquid Waste Streams

As macro- and micro-nutrients are usually added to fermentation media in excess, their unused residuals remain in the liquid waste at the end of the process. There is a high potential to recover these elements via ED and reuse them in a new fermentation process. As an example for this application, a real waste stream from fermentation with *Sulfolobus acidocaldarius* was used and analyzed in dilution ranges [45,46]. *S. acidocaldarius* is recognized as a key organism in future biotechnology due to its multiple commercial products [47]. The initial characteristics of the fermentation media (RCS) are shown in

Table 2. The fermentation effluent was microfiltered before the ED application as a barrier to residual bacterial cells. The waste streams of the fermentation processes often vary in salt concentration. Therefore, the dilution ranges were selected to meet specific conductivities (11.2, 7.5, 5.1, 2.7, 1.9 mS/cm).

### 2.4. Data Processing

R Studio (version 3.6.1) was used for data processing. An R-script was written, taking the ED unit’s text-file output as a script input, processing data based on the five LCD assessment methods, and displaying LCD values for each method and media used. Numeric data were consolidated by diagrammatic visualization of the data.

## 3. Results and Discussion

Results of experimental LCD tests are categorized into three sections. First, graphical LCD methods were proven for the feed NaCl dilution ranges. Second, LCD was assessed for feed solutions with the different ionic complexity, but the same initial conductivity. Third, one LCD method was selected for the LCD–conductivity correlation between the solutions with varying ionic complexity and inlet conductivity.

### 3.1. SSS—Range of NaCl Concentrations

Starting from a simple NaCl solution, five LCD assessment methods were applied to five increasing NaCl concentrations and compared to each other (LCD values in Table 3). LCD was mostly studied in the ED application for seawater desalination. Therefore, ion transport mechanisms, such as migration and diffusion, along with the occurring phenomena appearing, such as osmosis and electro-osmosis, in the limiting and over limiting regions are available in literature [16,21,48]. LCD is expected to be seen in a flattening of the I–U curve (I–S), sudden ED stack resistance increase (C–B), sudden diluate pH drop (pH-method), maximum point in the current efficiency ( $\lambda$ ), and desalting efficiency ( $\epsilon$ ) followed by a sudden drop of the current/desalting efficiency.

Table 3. List of solutions (SSS—2.3.1) used in the study with corresponding LCDs defined by five methods.

Solution	NaCl 1	NaCl 2	NaCl 5.5	NaCl 30.6	NaCl 48.7
NaCl concentration [mol/L]	0.005	0.004	0.03	0.3	0.5
Conductivity [mS/cm]	1	2	5.5	30.6	48.7
Average temperature T [°C]	19.1	19.2	20.2	20.4	21.0
Initial pH	5.16	5.23	5.21	5.20	4.80
<b>LCDs [A/m<sup>2</sup>]</b>					
I–S	30.1	58.8	175.5	/	/
C–B	23.5	41.7	130.9	/	/
pH Method	43.8	78.1	209.6	771.2	/
Max pH *	43.8	72.9	203.1	554.7	693.6
pH decrease **	34.2	67.2	198.4	382.8	459.7
$\lambda$ Method ***	43.7	67.6	107.8	108.0	78.1
$\epsilon$ Method	23.4	42.8	167.5	/	/

\* LCD values as the maximum measured pH value subtracted by 0.2 pH units. \*\* LCD values recorded for the first diluate pH decline. \*\*\* LCD values as the maximum  $\lambda$  values.

Overall slopes increased with the increasing salt concentrations, since the current density increases with the increasing ionic content of the feed solution. In the voltage–current density plots (Figure 2a), slope changes described by the I–S method can be observed for the NaCl solutions with the lower conductivities of 1, 2, and 5.5 mS/cm. Numerous plateaus were observed in the NaCl 1 mS/cm solution. The ion scarcity in this solution induced a high ED cell resistance and the absence of the Ohmic region. In contrast, the NaCl 2 mS/cm solution had a linear Ohmic region, followed by repetitive plateaus. Multiple

appearances of ion-depleted regions, exhibited as numerous plateaus in both of the low concentrated NaCl solutions, indicate the hydrodynamic instabilities in the over limiting current regime [41,49]. Electroconvection is a predominant mechanism for the current transfer in dilute solutions, but with the increasing voltage the water splitting increases, suppressing electroconvection [21,39,50,51]. However, the gravitational convection has a minor effect on the LCD for the NaCl solutions of 0.02 M and lower ( $\leq 0.2$  mS/cm) [50]. The NaCl 5.5 mS/cm solution did not reach the exact plateau. Nevertheless, the slope change can be clearly seen, indicating that LCD was reached (Figure 2a). The NaCl 30.6 and 48.7 mS/cm solutions remained in the Ohmic region during the whole experimental time. However, the slopes slightly increased after applying 20 and 15 V (Figure 2b) in the NaCl 30.6 and 48.7 mS/cm, respectively. This can be due to the increased ion mobility caused by Joule heat production resulting from the high current density [52]. The temperature in the NaCl 30.6 mS/cm experiment increased from 19.9 to 20.7 °C for applied 20–24.5 V, whereas in the NaCl 48.7 mS/cm it increased from 20.6 to 21 °C for applied 15–20.5 V. Of note, the highest applied voltage to solutions 4 and 5, was 24.5 and 20.5 V, respectively. At these points, the maximum allowed amperage of 5 A was reached, as a limiting current specified by the PCell supplier.

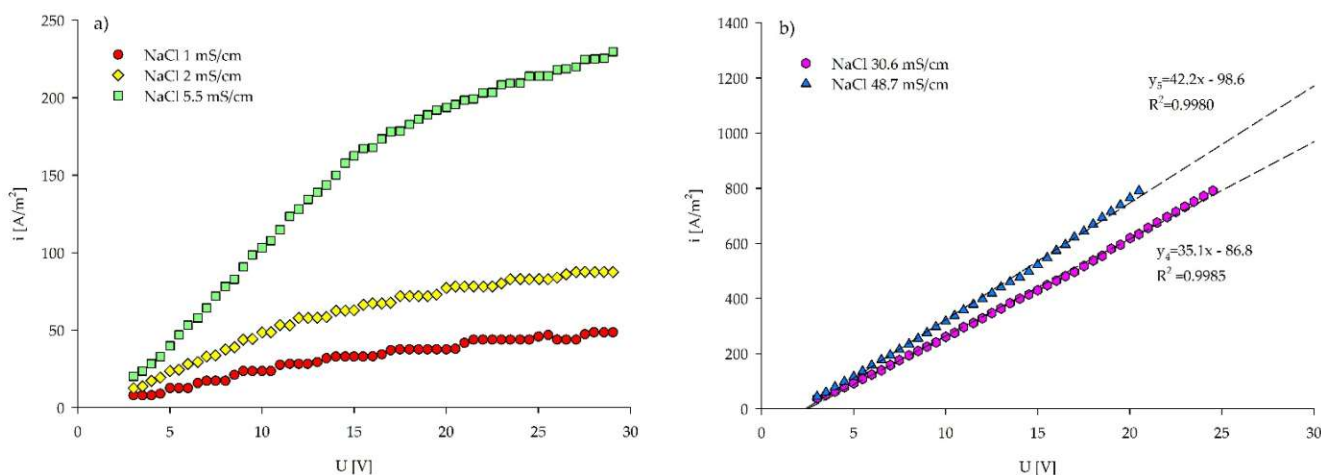


**Figure 2.** Current–voltage curves based on the Isaacson and Sonin method for estimating LCD in (a) three lower concentrated NaCl solutions and (b) two higher concentrated NaCl solutions. The detailed image of the fitting curves and their precision in three less concentrated NaCl solutions can be found in Supplementary Figure S3 and Table S1.

The considerable scatter in the two lower concentrated NaCl solutions can be observed in the C–B plots, similar to the I–S plots (Figure 3). Clear inflection points, indicating LCDs, for the NaCl solutions with the lower conductivities ( $\leq 5.5$  mS/cm) can be deduced using the C–B approach. On the contrary, for the solutions with higher conductivities (30.6 and 48.7 mS/cm) LCD was not reached, which is in line with the results obtained from the I–S method. Experimental data were fitted by the inverse polynomial function of a second order, and LCDs were found as a function minimum for the NaCl solutions with the conductivities  $\leq 5.5$  mS/cm (Table 3). Fitting functions and the detailed image of the NaCl solutions of 30.6–48.7 mS/cm can be found in Supplementary Table S2 and Figure S4.

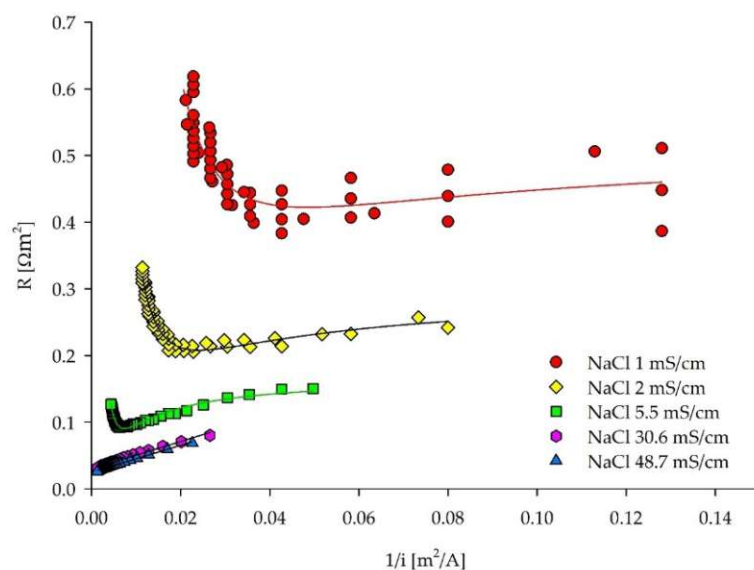


**Figure 3.** ED stack resistance–reciprocal current density curves for LCD estimation of the five NaCl solutions based on the Cowan and Brown method.

Interestingly, LCDs assessed by the pH method could be successfully carried out for all of the five treated solutions, including the highest NaCl concentrations when the pH values of the same experiments were plotted (Figure 4). This behavior can be explained by the different mobilities of the  $\text{Cl}^-$  and  $\text{Na}^+$  ions [53]. Kooistra et al. [54] reported the lower LCD of a cation-exchange membrane compared to an anion-exchange membrane, as the transport number of  $\text{Na}^+$  is less than  $\text{Cl}^-$  in a NaCl solution. Moreover, the higher mobility and lower hydration number of the  $\text{Cl}^-$  anions would change the equilibrium state of the NaCl solution in the diluate chamber, with a sudden increase of free  $\text{H}^+$  ions, generating the decrease of the solution's pH value [50]. Yet, another explanation could be found in correlation to the ED channel length. As the treated solution flows through the membrane stack, ions are removed from the diluate chamber along the whole path. With high current densities, the ions may be removed with this velocity from the frontal part of the channel, in which the solution with the depleted ions flows further through the membrane stack. Basically, at the membrane stack outlet, water dissociation occurs, induced by the low ion concentrations and high electrical potential. Research conducted on a microscale ED [42] showed concentration profiles at limiting and over limiting current densities along the length of the membrane stack. Therein, the term “vortex instability” is introduced by Kwak et al. [42]. The vortices appear in the depletion zone, and the boundary layer fluctuates with the increased current density and changes in ion concentrations along the channel. Another observation from the same research was the increase of current efficiency ( $\lambda$ ) in the limiting regime and the occurrence of the maximum efficiency in the initial stage of the over limiting regime. Yet, La Cerva et al. [19] observed an inflection point in the  $\lambda$ –current density plots, with the maximum  $\lambda$  corresponding to the LCD.

In Figure 5, current efficiency  $\lambda$  is plotted against the applied voltage rather than the current density to allow for a comparison between the different NaCl concentrations. However, the trend of  $\lambda$  values in  $\lambda$ –current density plot remains the same, whereas the solutions with higher NaCl concentrations develop higher current densities for the same applied voltage (Supplementary Figure S6). According to the method, the LCD can be found as the  $\lambda$  maximum (Table 3). However, there are no clear  $\lambda$  peaks indicating the over limiting current regions. This behavior deviates from the method description. Similar to the I–S plots, high  $\lambda$  fluctuations appear for  $\text{NaCl} \leq 2$  mS/cm, caused by water splitting. All of the solutions show poor  $\lambda$  for applied voltages lower than 3.5 V since the Faradic current is negligible beneath these voltages, similar to the results obtained by Kwak et al. [42]. For voltages above 3.5 V, all of the solutions have rather high  $\lambda$ , similar to the values obtained

by La Cerva et al. [19] when both the concentrate and the diluate are fed with the same solutions. The highest concentrated NaCl solution manifests the lowest  $\lambda$  values for all of the applied voltages. This behavior is in accordance with the study of Sadrzadeh et al. [55], where  $\lambda$  increases with the increasing feed concentration to a maximum value and the further increase of the concentration decreases it. A sudden  $\lambda$  drop occurred when 5–10 V were applied to the NaCl 48.7 mS/cm solution, since the current transported by ions was not efficiently used for ionic removal from the diluate. The evolution of the current density and the ionic removal stabilized with voltages above 10 V, resulting in the stable current efficiency. Similarly, this applies to the NaCl 30.6 mS/cm solution. From the aspect of the current efficiency observed in Figure 5, optimal feed solution conductivities for the ED treatment should range from 5–30.6 mS/cm (0.03–0.3 M NaCl), for the ED set-up used in this research.

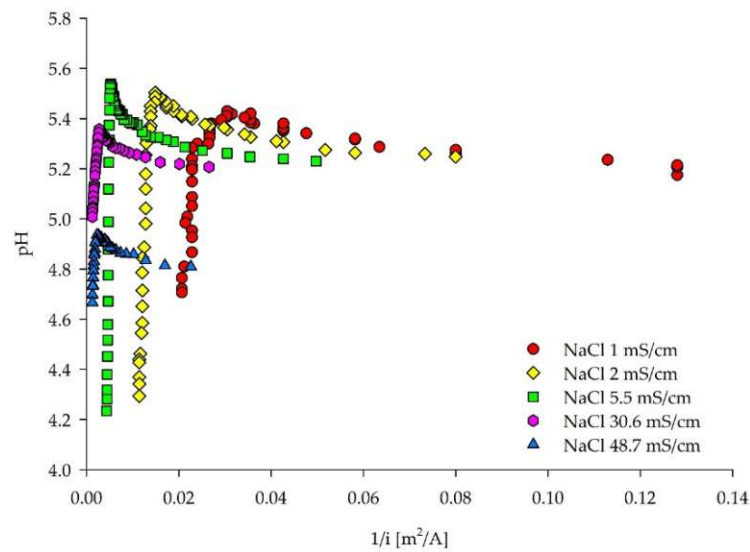


**Figure 4.** Diluate pH–reciprocal current density curves for the LCD estimation for five NaCl solutions based on the pH method. The pH changes plotted against the increasing current density can be found in Supplementary Figure S5.

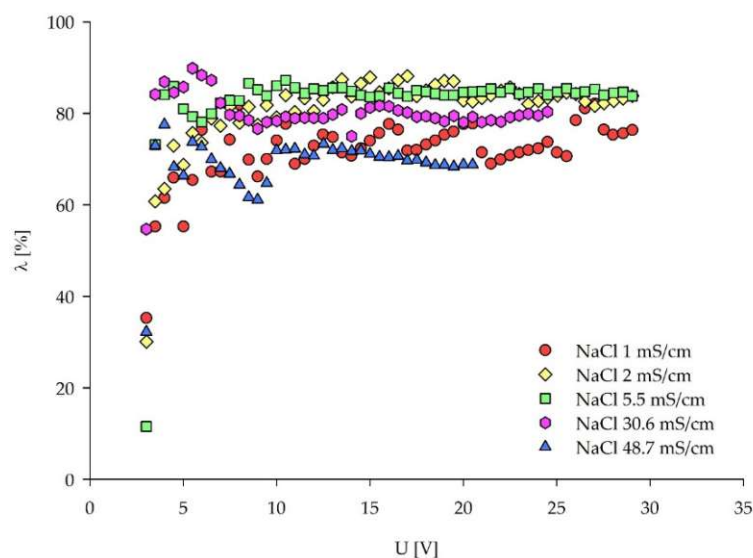


**Figure 5.** Current efficiency ( $\lambda$ )–voltage curves for the LCD estimation of the five NaCl solutions.

LCD assessment via the removal efficiency ( $\epsilon$ ) approach (Figure 6) does not exhibit the maximum value followed by an inflection point, as described by Meng et al. [36]. However,

the removal efficiency graph has similarities in this specific case with the I–S plots. Namely, a linear region (similar to the Ohmic region) can be seen for all of the feed solutions, whereas for the NaCl concentrations  $\leq 5.5$  mS/cm, a flattening of the curve introduces the second region (limiting region). Therefore, the LCDs via the removal efficiency ( $\epsilon$ ) approach can be determined as the cross-sections of these two regions. The  $\epsilon$  values plotted against current density can be found in Supplementary Figure S7.

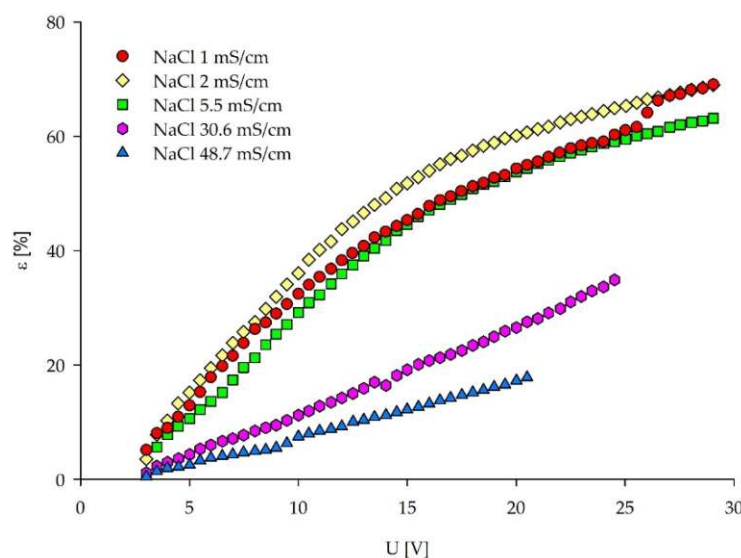


**Figure 6.** Removal efficiency ( $\epsilon$ ) for the salts present in the feed solution plotted against the applied voltage, for all of the five NaCl solutions.

Values for the specific LCDs derived from all of the applied LCD assessment methods are summarized in Table 3. Temperatures vary slightly among the tested NaCl solutions. C–B LCD values are determined in three ways (Supplementary Table S3), and values denoted in Table 3 are based on the function minimum (see Section 2.2.2). The inflection point in the I–S curves was not always clearly visible in the multi-cell ED stack used in this study. The change of the overall ED stack resistance was distinctly indicated in the C–B plots. The C–B method showed the lowest LCD values compared to the other methods. Only the pH method displays LCDs for all of the five solutions if the maximum measured pH is subtracted by 0.2 pH units or the first value of the diluate pH declines. Hereby, slight increases of the diluate pH before the sudden drop can be seen in Figure 4 and Figure S3. Based on the other methods, LCD could not be determined for the NaCl  $\geq 30.6$  mS/cm.

### 3.2. Experiments with Different Ionic Compositions but the Same Conductivity

The graphical LCD methods were previously compared to the simple NaCl solutions to evaluate the methods and understand their coherence. The current efficiency ( $\lambda$ ) method strongly deviated from the method description, as defined in Section 3.1. When the feed contains multiple ionic species, the  $\lambda$  method becomes rather impractical compared to the other graphical methods due to the required elaborate ionic analysis of the ED effluent. Consequently, this method was excluded during the subsequent analysis.

Five feed solutions (two from SSS 2.3.1, two from SCS 2.3.2, and one from RCS 2.3.3), with various ionic compositions but the same conductivity (5.5 mS/cm), were subjected to the LCD experiments and LCD assessment. The aim was to assess whether the aforementioned LCD methods apply to each type of feed representing the increasing complexity and whether the solutions with the same conductivity but different ionic compositions and complexity have the same LCD. The purpose of this approach was two-fold. The first was to evaluate the applicability of the LCD graphical methods on the more complex feed solutions, as performed for the NaCl solutions. Second, the interactions between the different ionic species as well as between the charged and uncharged molecules were

expected to influence the LCD, even though the feed conductivities were the same. If this is not the case, the conductivity of the feed solution could be used as an easy-to-measure online parameter for adjusting current density during the operation under initially defined ED configurations. A 5.5 mS/cm conductivity was applied since the corresponding NaCl solution yielded LCD values by all of the used LCD graphical methods.

An inflection point can be seen in the voltage–current density plots for all of the solutions in Figure 7, indicating the LCDs (for specific values, see Table 4). Only SCS1 does not have a clear inflection point. When the ionic composition of SCS1 and SCS2 is compared (Table 2), it can be seen that SCS1 has higher  $\text{PO}_4\text{-P}$  and  $\text{Cl}^-$  concentrations, whereas SCS2 has around a double concentration of  $\text{SO}_4^{2-}$  ions. Yan et al. [56] researched the competing transport of monovalent and multivalent ions based on their concentration ratios. In another study [57], lower LCDs were observed when some of the  $\text{Cl}^-$  was substituted with  $\text{SO}_4^{2-}$  anions. Namely, sulfates have lower ionic diffusivities ( $0.923 \times 10^{-9} \text{ m}^2/\text{s}$ ) compared to chlorides ( $1.77 \times 10^{-9} \text{ m}^2/\text{s}$ ) [57]. From these studies, it can be concluded that the interactions between the ions and their molar ratio, accompanied with the elevated temperature for 2 °C, lead to the increased LCD in the SCS1 compared to the SCS2. Previous research conducted with the SCS1 solution [44] demonstrated the influence of the concentration of ions, mobility of ions, electrical potential, and the energy applied on the ion-removal rate. In those experiments,  $\text{Cl}^-$  showed the highest removal rate in the initial phase of the ED separation process when the higher voltage (10 V) was applied. Therefore, it can be assumed that the chloride anions were removed in the first section of the ED channel, after which other ions transport the current in the second part of the ED channel, maintaining the Ohmic region at higher voltages. Furthermore, Galama et al. [58] concluded the preferential removal of multivalent over monovalent ions at low current densities, after the demineralization rate of ~60% has been reached. Yet, another study from Benneker et al. [28] analyzed the impact of temperature gradients on the selectivity of the separation, resulting in the higher transport of divalent  $\text{Mg}^{2+}$  than the monovalent  $\text{K}^+$  and  $\text{Na}^+$  ions with an elevated solution temperature. This behavior may impact the ionic transport since the temperature inside the ED stack increases with the increasing current density. However, they assessed the temperature gradient of  $\pm 20$  °C, whereas in our experiments it does not exceed  $\pm 2$  °C, and thus can be neglected.

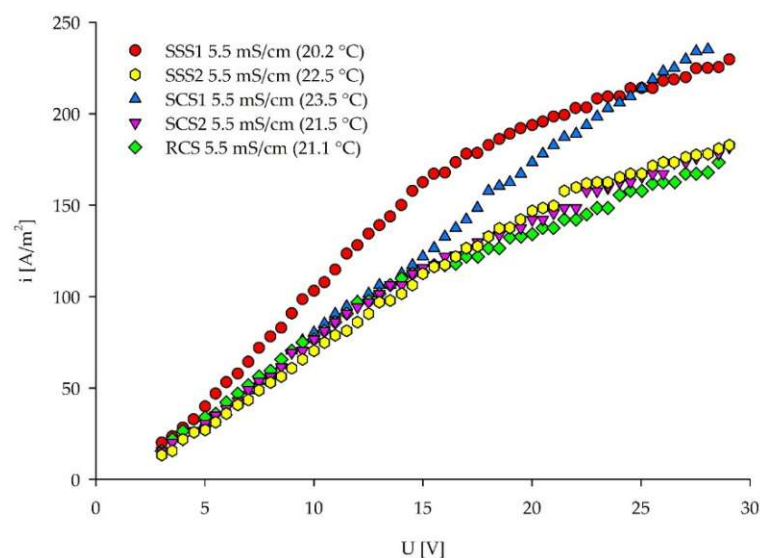


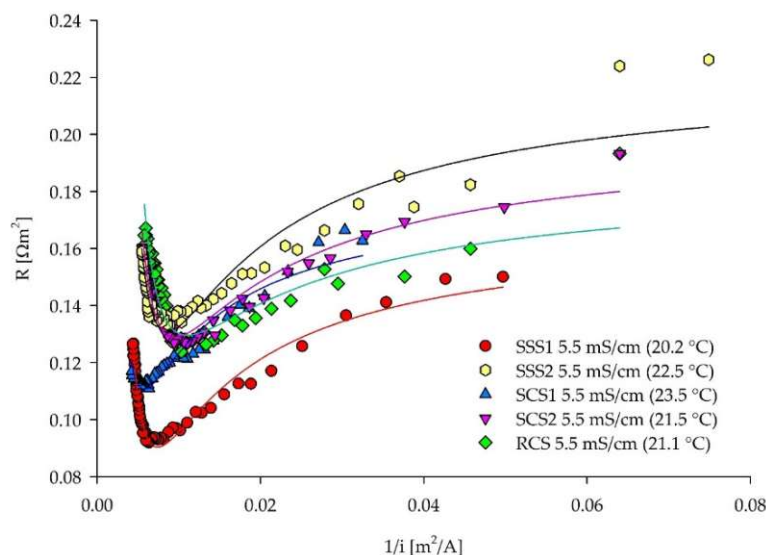
Figure 7. Current–voltage curves for five different solutions with the same conductivity.

**Table 4.** List of solutions used in the study (Sections 2.3.1–2.3.3) with corresponding LCDs defined by four methods.

Solution	SSS1 (NaCl)	SSS2 (Na <sub>2</sub> SO <sub>4</sub> )	SCS1	SCS2	RCS
Conductivity [mS/cm]	5.5	5.5	5.5	5.5	5.5
Average temperature [°C]	20.2	22.5	23.5	21.5	21.1
Initial pH	6.31	8.49	4.59	3.24	2.25
	LCD [A/m <sup>2</sup> ]				
I&S	175.5	153.2	179.0	135.7	117.2
C&B	130.9	119.3	176.8	102.3	89.6
pH method	209.6	137.6	90.5	(112.5) *	(76.5) *
ε Method	167.5	158.3	137.4	118.0	112.9

\* LCD values corresponding to the increase of the measured pH by 0.2 pH units from the initial value.

For all of the solutions, an exact inflection point can be identified by applying the C–B approach (Figure 8). With the increasing solution resistance, LCD is generally decreasing (Table 4). The SSS1 (NaCl) solution has the lowest resistance, showing the higher mobility of the Na<sup>+</sup> and Cl<sup>−</sup> ions, compared to the SSS2 (Na<sub>2</sub>SO<sub>4</sub>) solution and complex media (SCS1–2) with the same measured conductivity. The SSS2 solution has the highest resistance, followed by the real fermentation wastewater sample (RCS), with the same conductivity of 5.5 mS/cm. These high resistances can be explained in the first order by the presence of SO<sub>4</sub><sup>2−</sup> ions. The dominant presence of SO<sub>4</sub><sup>2−</sup> ions was the main reason for the higher solution resistance and lower LCDs, as can be seen in Figures 7 and 8, especially comparing SSS1 (NaCl) and SSS2 (Na<sub>2</sub>SO<sub>4</sub>) solution. When SCS2 and RCS are compared, other non-charged substances (e.g., organic carbon) originating from culture media and microbial excretions seem not to affect the overall resistance. Different ionic species in various quantities significantly impact on the solution’s resistance in the membrane stack.

**Figure 8.** ED stack resistance–reciprocal current density curves for the LCD assessment of five different solutions with the same conductivity.

A  $\Delta pH$  axis (see Section 2.2.3) was applied for the LCD assessment by the pH method (Figure 9), since the initial pH values of compared solutions vary strongly between each other (pH 2.2–8.5). Culture media for fermentation usually include buffering compounds, such as phosphates for pH stability [59]. The gradual dilute pH drop of the SCS1 (Figure 9) can be explained by its dominant PO<sub>4</sub><sup>3−</sup> concentrations (Table 2), acting as a buffer, accepting that H<sup>+</sup> ions evolved due to the “water splitting” effect. Similarly, ammonium can buffer

$\text{OH}^-$  ions that are evolved on the CEM-side by donating a proton to form water molecules. On the contrary, the pH drop is rather sudden in the case of single salt solutions (SSS1–2). An increase of the diluate pH can be seen with the increasing current density (voltage) when comparing the model (SCS2) and real fermentation wastewater (RSC). The initial pH increase in the SCS2 was followed by a sudden pH drop induced at  $112.5 \text{ A/m}^2$ , which is not the case for the RSC. This indicates the effect of the other compounds present in the real samples on the solution characteristics and behavior during the ED treatment, resulting in a continuous pH increase. Organic nitrogen can also provide a buffering capacity, such as proteins [60], present in the RCS but not in the SCS2, preventing steep pH changes. The LCD could be defined only by a modified pH method requirement, with  $\pm 0.2$  pH units change in the diluate. Therefore, Table 4 (pH method) shows that the LCD decreases with the increase of the solution complexity.

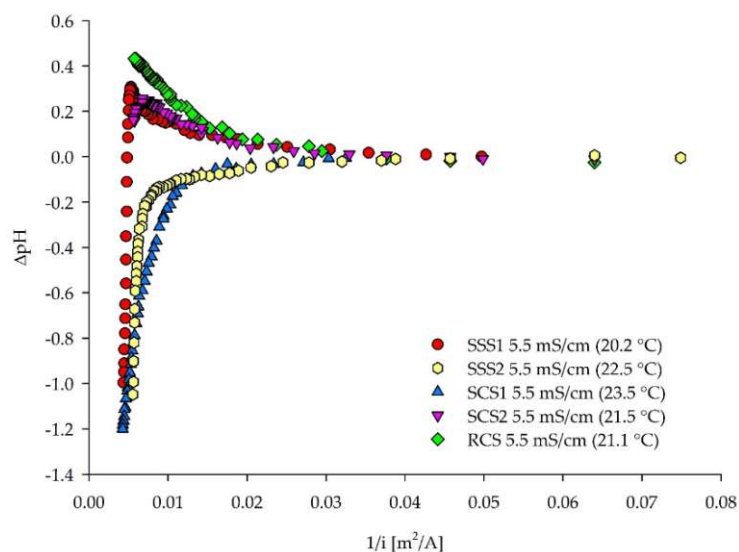


**Figure 9.** The  $\Delta\text{pH}$  values plotted against the reciprocal current density for five different feed solutions.

With the increasing applied voltage, the salt removal efficiency (Figure 10) can be divided into two stages according to the I–S current–voltage curves, with a linear region (Ohmic dependency) transfiguring into the limiting region (flattening of the curve). LCD was detected at the intersection of these two stages (Table 4). SSS1 (NaCl) achieved the highest removal efficiencies, whereas SSS2 had the lowest. The presence of the  $\text{SO}_4^{2-}$  is impeding the removal efficiency, due to the higher overall resistance of the ED stack and prevailing concentration polarization effect at the membrane surface, although the initially measured conductivities were the same for all of the tested solutions. The removal efficiencies ( $\epsilon$ ) of complex solutions are in the same range, corresponding to their similar content of equivalent multivalent anions (Table 2). The  $\epsilon$  values plotted against current density can be found in Supplementary Figure S8. In these plots, the maximum  $\epsilon$  was not followed by an inflection point, which would indicate the occurrence of the LCD.

Table 4 summarizes the final LCD values for the solutions derived from the graphical assessment (Figures 7–10) of the previous diagrams. The removal efficiency method ( $\epsilon$ ) had a similar trend to the I–S method, facing the same LCD estimation problems of distinguishing between the Ohmic and limiting regions. On the one hand, the pH changes were an indicator for different removal velocities of anionic and cationic species. On the other hand, the changes indicated “water splitting” and unfavorable  $\text{H}^+$  production. However, the pH changes depend on the initial solution pH and composition. Therefore, the pH method should be used as a secondary LCD measurement. The C–B method expressed the most reliable and unique values, as the sudden increase of the ED stack resistance was clearly visible for all of the solutions with different complexities. This inflection point can be correlated with the boundary layer formation on the diluate side. The standard

error of experimental data analyzed by the C–B method was less than 0.03, providing good quality LCD assessment fitted with the inverse second-order polynomial function (Supplementary). The I–S method yielded higher LCD values, and a clear inflection point was not always visible. Therefore, estimation of the LCD was not unambiguous. The quality of the LCD assessment by the I–S method depends on the length of the data points selected for the estimation of the intersecting point and the intersection of two linear functions. As a result, the error of the data analysis can be higher compared to the C–B method. Finally, the detection of the LCD was more pronounced in the C–B method than in the I–S method. The LCD values assessed via the C–B method were used to compare the conductivity–composition–LCD relations among the analyzed solutions. The SSS2 ( $\text{Na}_2\text{SO}_4$ ) solution had lower LCD ( $119.3 \text{ A/m}^2$ ) compared to the SSS1 ( $\text{NaCl}$ ) solution ( $130.9 \text{ A/m}^2$ ), even though the conductivities were the same. Due to the larger  $\text{SO}_4^{2-}$  size, and their lower mobility, compared to the  $\text{Cl}^-$ , the overall resistance was higher, and the boundary layer formed earlier. The SCS1 solution had a higher LCD than SSS1 according to Table 4, although the solution comprised various ions and had higher overall resistance. This was not the case when the LCDs tracked as the resistance minimum were compared (Supplementary Table S4), with  $159.7$  and  $157.8 \text{ A/m}^2$  for SSS1 and SCS2, respectively. Moreover, one smaller inflection point of SCS1 can be seen at  $0.011 \text{ m}^2/\text{A}$  ( $90.5 \text{ A/m}^2$ ) (Figure 8). Since both the model and real fermentation wastewater had a high  $\text{SO}_4^{2-}$  concentration (Table 2), the lower LCDs correspond to the lower LCD of the SSS2, as denoted above. The negatively charged organic molecules, most probably present in the real wastewater [1], may also impact the reduction of the LCD by blocking the way of the anionic migration through the anion-exchange membranes. More in-depth research on a molecular level is necessary to understand the behavior of complex feed solutions in the limiting and over limiting regions. Nevertheless, this work focuses on the general approach for LCD determination and the solutions assessed here had the same trend in the C–B plots.

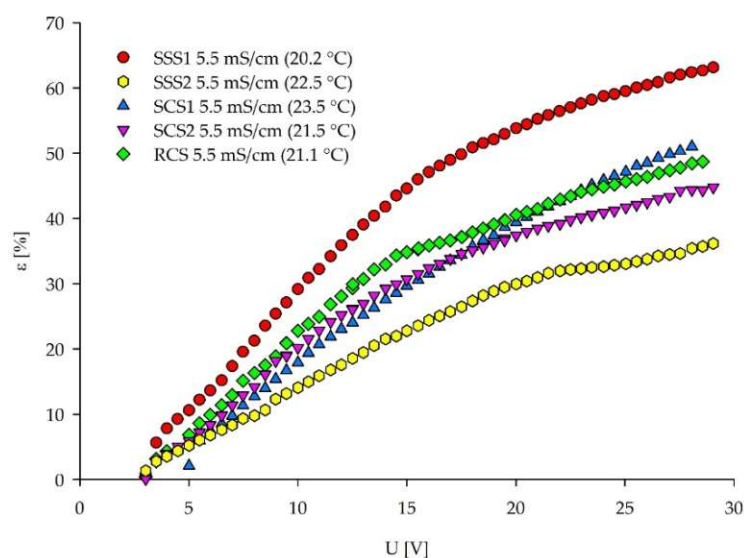


**Figure 10.** Removal efficiency for the salts present in the feed plotted against the applied voltage.

### 3.3. Same Ionic Composition but Different Initial Conductivity

Due to the unambiguity of the results obtained in Sections 3.1 and 3.2, the C–B method was applied to a span of feed solutions (SSS, SCS, RCS) with increasing–decreasing salt concentrations. The dilution ranges for the LCD experiments were prepared to mimic the decreasing ionic content of the diluate in the batch ED. The LCD values were successfully obtained by the C–B method for all of the tested solutions with the inlet feed conductivities  $\leq 18 \text{ mS/cm}$  (Figure 11). LCD correlates linearly to the feed conductivity, with a high fitting accuracy of  $R^2 = 0.99$  for SSS1, SCS1, SCS2, and RCS, similar to the literature values [16,32,53].

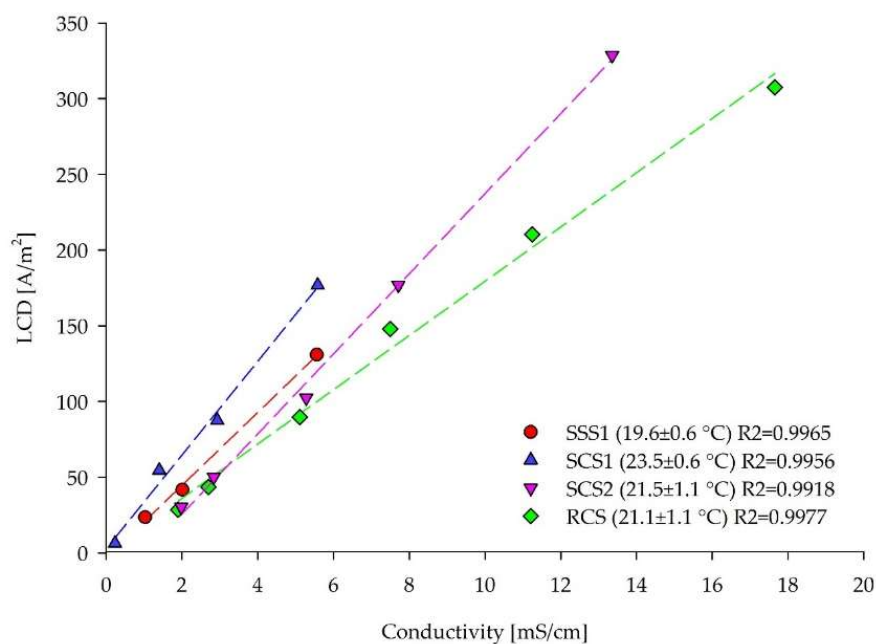


**Figure 11.** Dependency of the inlet feed conductivities (mS/cm) of the dilutions from different solutions and corresponding LCDs assessed by the Cowan and Brown method. During the batch ED, the feed concentration continuously decreases, consequently, the LCD decreases.

As shown in Figure 11, the LCD–conductivity correlation for RCS has the smallest slope, compared to the model solutions containing only salts (SSS, SCS). The SCS2 solution had 1.3 times higher LCDs for every increase of 1 mS/cm of measured inlet conductivity compared to the RCS, whereas for SSS1 and SCS1 this ratio was 1.2 and 1.7, respectively. This behavior clearly indicates the retarding effect of other compounds present in real waste streams, such as organic molecules, on the ionic removal from the feed solution. Therefore, the LCD decreased, even though the ionic strength was the same. The current density applied to the ED membrane stack could be gradually reduced with the decreasing diluate concentration in the batch ED process for one type of feed solution and set-up. However, ion size and mobility, ion concentration, concentration ratios of the different ions, and organic components of the treated feed impact the LCD and ion removal ratio. Therefore, conductivity alone cannot be used for the LCD determination among various feed solutions.

#### 4. Summary

This work focused on comparing five graphical methods for the limiting current density (LCD) assessment in the batch electro dialysis desalination process (ED). The applied methods were: Isaacson and Sonin (current density–voltage), Cowan and Brown (ED stack resistance–reciprocal current density), pH method (diluate pH–reciprocal current density),  $\lambda$  method (current efficiency–voltage),  $\epsilon$  method (removal efficiency–voltage).

First, five methods were applied to five different NaCl concentrations, representing the solutions with the lowest level of complexity. The  $\lambda$  method did not exhibit strict LCD values, as described by the method. The pH method revealed LCDs for all of the five concentration levels, indicating “water splitting” occurrence. The other three methods demonstrated LCD only for the lower NaCl concentrations ( $\leq 0.03$  M NaCl), whereas for the concentrations  $\geq 0.3$  M NaCl limiting values could not be obtained, as the ED equipment has the maximum tolerating amperage of 5 A.

Second, the applicability of four LCD methods ( $\lambda$  method was excluded from this part) was tested in solutions with the same conductivity but different levels of complexity (synthetically prepared and real waste streams). Due to the presence of different ionic species, comprising different sizes and mobilities, the resistances of the ED stack differed,

although the measured conductivities were the same. Therefore, the obtained LCDs varied, as well. The presence of the  $\text{SO}_4^{2-}$  anions may be lowering the solution's LCD. However, in-depth research on the molecular level is necessary, to understand the behavior of complex feed solutions in the limiting and over limiting regions. Other compounds, such as large organic molecules in the real waste streams, decrease the LCD. The pH method applied to the fermentation wastewater did not reveal a sudden pH drop of the diluate with the increased voltages, deviating from the typical behavior of the NaCl solution. Other methods worked in accordance with the assessments conducted on the simple NaCl solution.

Third, a linear dependence of the LCD determined by the Cowan and Brown method and the measured solution conductivity was concluded for various dilution steps of each solution type. However, the gradual decrease of the current density applied to the ED stack cannot be conducted solely by monitoring the diluate conductivity, since the LCD depends on the present ionic species and other compounds, such as organic molecules in the real waste stream.

## 5. Conclusions

Based on the initially presented research questions, the following conclusions can be drawn from this research:

- All of the assessed graphical methods showed LCDs for the feed concentrations  $\leq 0.03$  M NaCl. The current efficiency ( $\lambda$ ) method did not have a clear peak at the LCD as defined by the method. Only the pH method revealed LCDs for feed concentrations  $\geq 0.3$  M NaCl.
- Four out of five LCD methods were applicable to each type of feed with increasing complexity. The current efficiency ( $\lambda$ ) method was excluded, and the pH method was modified ( $\pm 0.2$  pH units from the initial feed pH). The C–B method had the most consistent results for all of the different types of feed solutions, and lower LCD values compared to the I–S method. In conclusion, the usage of the C–B method is highly recommended due to its applicability to a wide range of solutions with varying ionic compositions, concentrations, and matrix complexities.
- Solutions with the same conductivity but different ionic compositions do not reach the same LCD, as it is strongly influenced by the type and concentration of ionic species, and the presence of uncharged compounds.
- In one solution matrix, LCD linearly correlates with the decreasing conductivity. Therefore, the online conductivity measurement could be used for the batch ED control of one specific medium with a known composition. Otherwise, measuring only the conductivity is not suitable for current density adjustment unless combined with other characteristics of the feed solution.
- The obtained results bring knowledge to the existing graphical LCD methods and the complex medias' behavior during electro dialysis membrane separation processes. The conclusions obtained in this work are useful for the selection of an appropriate LCD method in real feed solutions, LCD assessment, and future automatization of the electro dialysis.

**Supplementary Materials:** The following supporting information can be downloaded at: <https://www.mdpi.com/article/10.3390/membranes12020241/s1>, Figure S1: 10-cell pair lab-scale ED unit (PCCell ED 64-004, Heusweiler, Germany); Figure S2: NaCl concentration-conductivity diagram; Figure S3: The intersection of two fitting linear functions for the LCD determination in (a) NaCl 1 mS/cm solution; (b) NaCl 2 mS/cm solution; (c) NaCl 5.5 mS/cm solution; Figure S4: ED stack resistance–reciprocal current density curves for LCD of two high concentrated NaCl solutions based on the Cowan and Brown method. With the increasing current density, the resistance is decreasing and the inflection point does not appear for these two solutions; Figure S5: Change of the diluate pH with (a) current density and (b) applied voltage; Figure S6: Current efficiency ( $\lambda$ )–current density curves for LCD estimation of five NaCl solutions; Figure S7: Removal efficiency ( $\epsilon$ ) for the salts present in the feed solution plotted against current density, for all five NaCl solutions; Figure S8:

Removal efficiency for the salts present in the feed plotted against current density. Table S1: The slopes (m), intercepts (b) and the coefficient of determination ( $R^2$ ) for two fitting linear equations in experimental data of three NaCl solutions for the LCD determination; Table S2: Coefficients of the inverse polynomial function of a second order for estimating LCDs based on Cowan and Brown method presented in the research paper; Table S3: List of solutions (SSS–2.3.1) used in the study with corresponding LCDs defined by Cowan and Brown method in three ways (a/b/c); Table S4: List of solutions used in the study (Chapters 2.3.1., 2.3.2., 2.3.3.) with corresponding LCDs defined by Cowan and Brown method in three ways (a/b/c).

**Author Contributions:** Conceptualization, K.K. and N.K.; methodology, K.K. and D.R.; validation, K.K., D.R., N.K., M.H. and J.K.; formal analysis, K.K.; investigation, K.K.; resources, J.K. and N.K.; data curation K.K.; writing—original draft preparation, K.K.; writing—review and editing, D.R., M.H., J.K. and N.K.; visualization, K.K.; supervision, N.K., M.H. and J.K.; project administration, J.K.; funding acquisition, J.K. and N.K. All authors have read and agreed to the published version of the manuscript.

**Funding:** This research received no external funding.

**Institutional Review Board Statement:** Not applicable.

**Informed Consent Statement:** Not applicable.

**Acknowledgments:** The authors want to acknowledge the TU Wien and the Institutional Open Access Program (IOAP) for financial support (Open Access Funding by TU Wien). The authors would like to express their thanks to the “Bioactive” Doctoral College of the TU Wien, under which the research was performed, for its financial support and to the Bioactive Journal Club members for the insights of the manuscript.

**Conflicts of Interest:** The authors declare no conflict of interest. The funders had no role in the design of the study; in the collection, analyses, or interpretation of data; in the writing of the manuscript, or in the decision to publish the results.

## Appendix A

This section describes the graphical LCD methods used to determine LCDs in various solutions and compares their outcomes to find the most reliable LCD method for the real feed streams.

### *Appendix A.1. Method by Isaacson and Sonin*

The Isaacson and Sonin (I–S) method analyzes the current density ( $\text{mA}/\text{cm}^2$ ) behavior depending on the voltage applied to the ED cell. Three different regions (I–III) are defined by this method (Figure A1). (I) is the Ohmic region with a linear correlation of the current density with the applied voltage. (II) is a region where the linear dependence starts leveling out. Here, the operational mode is transfiguring to the limiting current density region, indicating an energy loss due to the increased voltage resulting in the splitting of water molecules to  $\text{H}^+$  and  $\text{OH}^-$  ions, gravitational convection, and electroconvection. The intersection point of the two slopes belonging to the Ohmic and the second (plateau) region indicates the LCD. The third region (III) extends over the increasing positive slope, where a second intersection point can be determined. This region can be explained by the contribution of already split water molecules to the conducting electricity through the ED cell, gravitational convection, and electroconvection.

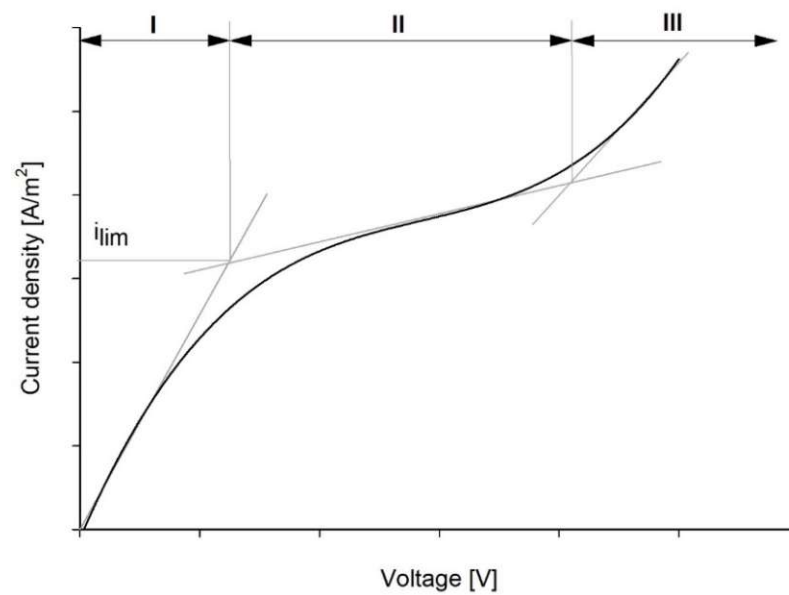


**Figure A1.** Current–voltage curve for an ED stack, showing LCDs of an electrolyte solution according to the Isaacson and Sonin method [37].

*Appendix A.2. Method by Cowan and Brown*

In the LCD method by Cowan and Brown (C–B), the ED cell resistance from the experimental data is plotted against the reciprocal current density (Figure A2). LCD manifests at a polarization voltage as a rapid change of the slope. The ED cell resistance decreases with the increase of the current density up to a certain point. At this point, with further increase of the current density (applied voltage), regions with higher resistance in the ED cell evolve, drawing a negative slope on the diagram. The intersection of the positive and the negative slope represents the LCD.

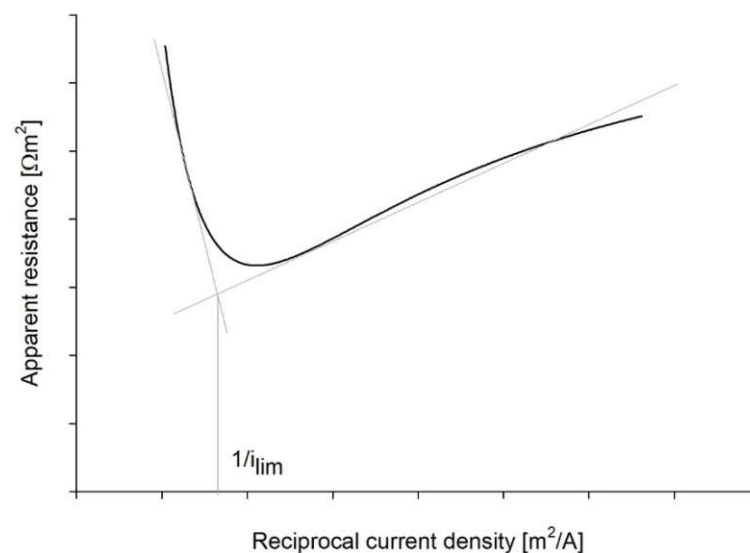


**Figure A2.** LCD assessed according to the Cowan and Brown method [35], correlating the reciprocal current density and ED stack resistance.

*Appendix A.3. The pH Method*

It was first noticed by Cowan and Brown (Cowan and Brown 1959) that the pH of the diluting stream starts to decrease at a current value very close to the value at which the resistance slope changes. Therefore, the authors (Melin and Rautenbach 2007) define the

limiting current density for the pH method as a point where the pH value of the diluting stream shows a decrease of 0.2 pH units. This breaking point can be seen on the diluate pH–reciprocal current density diagram (Figure A3).

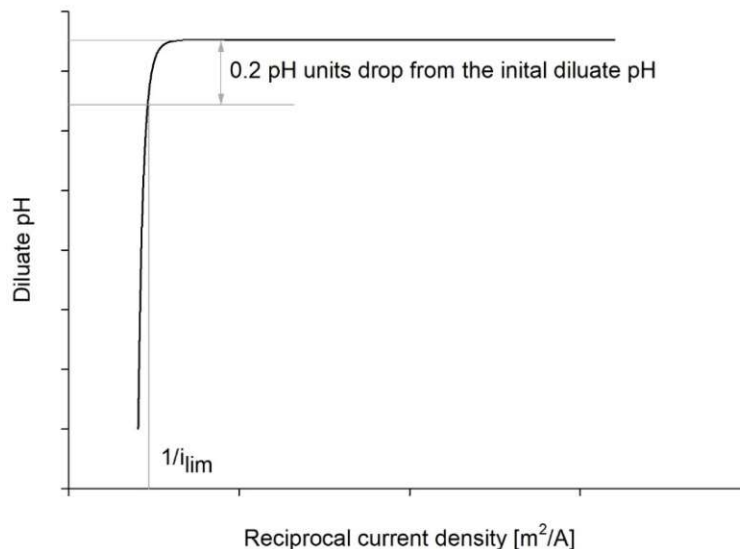


**Figure A3.** LCD determined as the sudden pH drop of the diluate solution with the increased current density [38].

*Appendix A.4. Current Efficiency Method*

La Cerva et al. (La Cerva et al. 2018) examined the research of Kwak et al. (Kwak et al. 2013) and suggested plotting the current efficiency ( $\lambda$ ) against the current density, wherein the LCD appears at the maximum  $\lambda$  (%) (Figure A4). The  $\lambda$  was calculated according to the following equation:

$$\lambda = \frac{zFQ_{dil}(C_{dil}^{IN} - C_{dil}^{OUT})}{NI} \cdot 100 \% \tag{A1}$$

where  $z$  is the ionic charge,  $F$  is Faraday constant (96485.33 sA/mol),  $Q_{dil}$  is the flow of the diluate stream (L/s),  $C_{dil}^{IN}$  and  $C_{dil}^{OUT}$  are the inlet and outlet concentrations of the diluate stream (mol/L),  $I$  is the current value (A), and  $N$  is the number of the ED cell pairs.

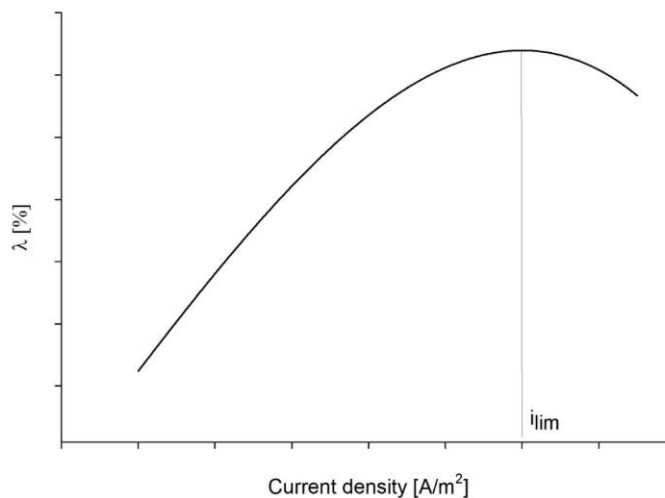


**Figure A4.** LCD determined as the maximum current efficiency, according to the method proposed by La Cerva et al. [19].

### Appendix A.5. Desalting Efficiency Method

Meng et al. (Meng et al. 2005) proposed a method for the determination of the optimal operating current based on the desalting efficiency ( $\varepsilon$ ):

$$\varepsilon = \frac{\kappa_{dil}^{IN} - \kappa_{dil}^{OUT}}{\kappa_{dil}^{IN}} \cdot 100 \% \quad (A2)$$

where  $\kappa_{dil}^{IN}$  is the initial conductivity (mS/cm) of the feed to be treated, and  $\kappa_{dil}^{OUT}$  is the conductivity (mS/cm) of diluate generated by the ED. Values of the desalting efficiency are plotted against the current density, wherein the LCD appears as the maximum  $\varepsilon$  (%), representing the optimal operating current (Figure A5).

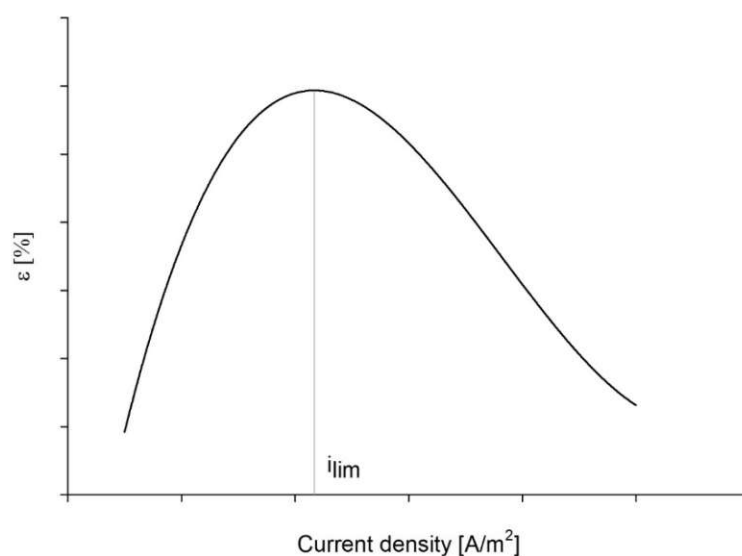


**Figure A5.** LCD appearing at the maximum desalting efficiency, according to the method proposed by Meng et al. [36].

### References

1. Al-Amshawee, S.; Yunus, M.Y.B.M.; Azoddein, A.A.M.; Hassell, D.G.; Dakhil, I.H.; Hasan, H.A. Electrodialysis desalination for water and wastewater: A review. *Chem. Eng. J.* **2020**, *380*, 122231. [[CrossRef](#)]
2. Campione, A.; Gurreri, L.; Ciofalo, M.; Micale, G.; Tamburini, A.; Cipollina, A. Electrodialysis for water desalination: A critical assessment of recent developments on process fundamentals, models and applications. *Desalination* **2018**, *434*, 121–160. [[CrossRef](#)]
3. van der Bruggen, B.; Milis, R.; Vandecasteele, C.; Bielen; van San, E.; Huysman, K. Electrodialysis and nanofiltration of surface water for subsequent use as infiltration water. *Water Res.* **2003**, *37*, 3867–3874. [[CrossRef](#)]
4. Xu, T.; Huang, C. Electrodialysis-based separation technologies: A critical review. *AIChE J.* **2008**, *54*, 3147–3159. [[CrossRef](#)]
5. Gurreri, L.; Tamburini, A.; Cipollina, A.; Micale, G. Electrodialysis Applications in Wastewater Treatment for Environmental Protection and Resources Recovery: A Systematic Review on Progress and Perspectives. *Membranes* **2020**, *10*, 146. [[CrossRef](#)]
6. Mohammadi, R.; Tang, W.; Sillanpää, M. A systematic review and statistical analysis of nutrient recovery from municipal wastewater by electrodialysis. *Desalination* **2021**, *498*, 114626. [[CrossRef](#)]
7. Ward, A.J.; Arola, K.; Brewster, E.T.; Mehta, C.M.; Batstone, D.J. Nutrient recovery from wastewater through pilot scale electrodialysis. *Water Res.* **2018**, *135*, 57–65. [[CrossRef](#)]
8. Xie, M.; Shon, H.K.; Gray, S.R.; Elimelech, M. Membrane-based processes for wastewater nutrient recovery: Technology, challenges, and future direction. *Water Res.* **2016**, *89*, 210–221. [[CrossRef](#)]
9. Al-Karaghoul, A.; Kazmerski, L.L. Energy consumption and water production cost of conventional and renewable-energy-powered desalination processes. *Renew. Sustain. Energy Rev.* **2013**, *24*, 343–356. [[CrossRef](#)]
10. Sosa-Fernandez, P.A.; Post, J.W.; Ramdhan, M.S.; Leermakers, F.A.M.; Bruning, H.; Rijnaarts, H.H.M. Improving the performance of polymer-flooding produced water electrodialysis through the application of pulsed electric field. *Desalination* **2020**, *484*, 114424. [[CrossRef](#)]
11. Tanaka, Y. Mass transport and energy consumption in ion-exchange membrane electrodialysis of seawater. *J. Membr. Sci.* **2003**, *215*, 265–279. [[CrossRef](#)]

12. Wu, D.; Chen, G.Q.; Hu, B.; Deng, H. Feasibility and energy consumption analysis of phenol removal from salty wastewater by electro-electrodialysis. *Sep. Purif. Technol.* **2019**, *215*, 44–50. [[CrossRef](#)]
13. Ankoliya, D.; Mudgal, A.; Sinha, M.K.; Davies, P.; Licon, E.; Alegre, R.R.; Patel, V.; Patel, J. Design and optimization of electro-dialysis process parameters for brackish water treatment. *J. Clean. Prod.* **2021**, *319*, 128686. [[CrossRef](#)]
14. Generous, M.M.; Qasem, N.A.A.; Akbar, U.A.; Zubair, S.M. Techno-economic assessment of electro-dialysis and reverse osmosis desalination plants. *Sep. Purif. Technol.* **2021**, *272*, 118875. [[CrossRef](#)]
15. Kucera, J. (Ed.) *Desalination: Water from Water*; John Wiley & Sons: Hoboken, NJ, USA, 2014.
16. Lee, H.-J.; Strathmann, H.; Moon, S.-H. Determination of the limiting current density in electro-dialysis desalination as an empirical function of linear velocity. *Desalination* **2006**, *190*, 43–50. [[CrossRef](#)]
17. Li, F.; Jia, Y.; He, J.; Wang, M. Effects of electro-dialysis conditions on waste acid reclamation: Modelling and validation. *J. Clean. Prod.* **2021**, *320*, 128760. [[CrossRef](#)]
18. Strathmann, H. Chapter 6 Electro-dialysis and related processes. In *Membrane Science and Technology*, 2nd ed.; Noble, R.D., Stern, S.A., Eds.; Elsevier: Amsterdam, The Netherlands, 1995; pp. 213–281. [[CrossRef](#)]
19. La Cerva, M.F.; Gurreri, L.; Tedesco, M.; Cipollina, A.; Ciofalo, M.; Tamburini, A.; Micale, G. Determination of limiting current density and current efficiency in electro-dialysis units. *Desalination* **2018**, *445*, 138–148. [[CrossRef](#)]
20. Nakayama, A.; Sano, Y.; Bai, X.; Tado, K. A boundary layer analysis for determination of the limiting current density in an electro-dialysis desalination. *Desalination* **2017**, *404*, 41–49. [[CrossRef](#)]
21. Nikonenko, V.; Kovalenko, A.; Urtenov, M.K.; Pismenskaya, N.D.; Han, J.; Sifat, P.; Pourcelly, G. Desalination at overlimiting currents: State-of-the-art and perspectives. *Desalination* **2014**, *342*, 85–106. [[CrossRef](#)]
22. Pawlowski, S.; Sifat, P.; Crespo, J.G.; Velizarov, S. Mass transfer in reverse electro-dialysis: Flow entrance effects and diffusion boundary layer thickness. *J. Membr. Sci.* **2014**, *471*, 72–83. [[CrossRef](#)]
23. Strathmann, H. Electro-dialysis, a mature technology with a multitude of new applications. *Desalination* **2010**, *264*, 268–288. [[CrossRef](#)]
24. Doyen, A.; Roblet, C.; L'Archevêque-Gaudet, A.; Bazinet, L. Mathematical sigmoid-model approach for the determination of limiting and over-limiting current density values. *J. Membr. Sci.* **2014**, *452*, 453–459. [[CrossRef](#)]
25. Rösler, H.-W.; Maletzki, F.; Staude, E. Ion transfer across electro-dialysis membranes in the overlimiting current range: Chronopotentiometric studies. *J. Membr. Sci.* **1992**, *72*, 171–179. [[CrossRef](#)]
26. Rubinstein, I. Electroconvection at an electrically inhomogeneous permselective interface. *Phys. Fluids A: Fluid Dyn.* **1991**, *3*, 2301–2309. [[CrossRef](#)]
27. Zabolotsky, V.I.; Urtenov, M.K. Coupled transport phenomena in overlimiting current electro-dialysis. *Sep. Purif. Technol.* **1998**, *14*, 255–267. [[CrossRef](#)]
28. Benneker, A.M.; Klomp, J.; Lammertink, R.G.H.; Wood, J.A. Influence of temperature gradients on mono- and divalent ion transport in electro-dialysis at limiting currents. *Desalination* **2018**, *443*, 62–69. [[CrossRef](#)]
29. Mahendra, C.; Sai, P.M.S.; Babu, C.A. Current–voltage characteristics in a hybrid electro-dialysis–ion exchange system for the recovery of cesium ions from ammonium molybdophosphate-polyacrylonitrile. *Desalination* **2014**, *353*, 8–14. [[CrossRef](#)]
30. Min, K.J.; Kim, J.H.; Park, K.Y. Characteristics of heavy metal separation and determination of limiting current density in a pilot-scale electro-dialysis process for plating wastewater treatment. *Sci. Total Environ.* **2021**, *757*, 143762. [[CrossRef](#)]
31. Xutoi, S.; Guang, C. The calculation of limiting current density of electro-dialysis under the influence of water quality and temperature. *Desalination* **1983**, *46*, 263–274. [[CrossRef](#)]
32. van Linden, N.; Spanjers, H.; van Lier, J.B. Application of dynamic current density for increased concentration factors and reduced energy consumption for concentrating ammonium by electro-dialysis. *Water Res.* **2019**, *163*, 114856. [[CrossRef](#)]
33. He, W.; le Henaff, A.-C.; Amrose, S.; Buonassisi, T.; Peters, I.M.; Winter, A.G. Voltage- and flow-controlled electro-dialysis batch operation: Flexible and optimized brackish water desalination. *Desalination* **2021**, *500*, 114837. [[CrossRef](#)]
34. Bittencourt, S.D.; Marder, L.; Benvenuti, T.; Ferreira, J.Z.; Bernardes, A.M. Analysis of different current density conditions in the electro-dialysis of zinc electroplating process solution. *Sep. Sci. Technol.* **2017**, *52*, 2079–2089. [[CrossRef](#)]
35. Cowan, D.A.; Brown, J.H. Effect of Turbulence on Limiting Current in Electro-dialysis Cells. *Ind. Eng. Chem.* **1959**, *51*, 1445–1448. [[CrossRef](#)]
36. Meng, H.; Deng, D.; Chen, S.; Zhang, G. A new method to determine the optimal operating current (I<sub>lim</sub>) in the electro-dialysis process. *Desalination* **2005**, *181*, 101–108. [[CrossRef](#)]
37. Isaacson, M.S.; Sonin, A.A. Sherwood Number and Friction Factor Correlations for Electro-dialysis Systems, with Application to Process Optimization. *Ind. Eng. Chem. Proc. Des. Dev.* **1976**, *15*, 313–321. [[CrossRef](#)]
38. Melin, T.; Rautenbach, R. *Membranverfahren: Grundlagen der Modul-und Anlagenauslegung*, 3th ed.; Springer: Berlin/Heidelberg, Germany, 2007.
39. Rubinstein, I.; Shtilman, L. Voltage against current curves of cation exchange membranes. *J. Chem. Soc. Faraday Trans. 2 Mol. Chem. Phys.* **1979**, *75*, 231–246. [[CrossRef](#)]
40. Valerdi-Pérez, R.; Ibáñez-Mengual, J. Current–voltage curves for an electro-dialysis reversal pilot plant: Determination of limiting currents. *Desalination* **2001**, *141*, 23–37. [[CrossRef](#)]
41. Krol, J.J.; Wessling, M.; Strathmann, H. Chronopotentiometry and overlimiting ion transport through monopolar ion exchange membranes. *J. Membr. Sci.* **1999**, *162*, 155–164. [[CrossRef](#)]

42. Kwak, R.; Guan, G.; Peng, W.K.; Han, J. Microscale electro dialysis: Concentration profiling and vortex visualization. *Desalination* **2013**, *308*, 138–146. [[CrossRef](#)]
43. Dortwegt, R.; Maughan, E.V. The chemistry of copper in water and related studies planned at the Advanced Photon Source. In Proceedings of the 2001 Particle Accelerator Conference (Cat. No.01CH37268), Chicago, IL, USA, 18–22 June 2001; Volume 2, pp. 1456–1458. [[CrossRef](#)]
44. Daza-Serna, L.; Knežević, K.; Kreuzinger, N.; Mach-Aigner, A.R.; Mach, R.L.; Krampe, J.; Friedl, A. Recovery of Salts from Synthetic Erythritol Culture Broth via Electrodialysis: An Alternative Strategy from the Bin to the Loop. *Sustainability* **2022**, *14*, 734. [[CrossRef](#)]
45. Jacobsen, A.-C.; Jensen, S.M.; Fricker, G.; Brandl, M.; Treusch, A.H. Archaeal lipids in oral delivery of therapeutic peptides. *Eur. J. Pharm. Sci.* **2017**, *108*, 101–110. [[CrossRef](#)]
46. Quehenberger, J.; Albersmeier, A.; Glatzel, H.; Hackl, M.; Kalinowski, J.; Spadiut, O. A defined cultivation medium for *Sulfolobus acidocaldarius*. *J. Biotechnol.* **2019**, *301*, 56–67. [[CrossRef](#)]
47. Quehenberger, J.; Shen, L.; Albers, S.-V.; Siebers, B.; Spadiut, O. Sulfolobus—A Potential Key Organism in Future Biotechnology. *Front. Microbiol.* **2017**, *8*, 2474. [[CrossRef](#)]
48. Sun, B.; Zhang, M.; Huang, S.; Wang, J.; Zhang, X. Limiting concentration during batch electro dialysis process for concentrating high salinity solutions: A theoretical and experimental study. *Desalination* **2021**, *498*, 114793. [[CrossRef](#)]
49. Zaltzman, B.; Rubinstein, I. Electro-osmotic slip and electroconvective instability. *J. Fluid Mech.* **2007**, *579*, 173–226. [[CrossRef](#)]
50. Pismenskaya, N.D.; Nikonenko, V.; Belova, E.I.; Lopatkova, G.Y.; Sizat, P.; Pourcelly, G.; Larshe, K. Coupled convection of solution near the surface of ion-exchange membranes in intensive current regimes. *Russ. J. Electrochem.* **2007**, *43*, 307–327. [[CrossRef](#)]
51. Rubinstein, I.; Zaltzman, B. Electro-osmotically induced convection at a permselective membrane. *Phys. Rev. E* **2000**, *62*, 2238–2251. [[CrossRef](#)]
52. Sun, B.; Zhang, M.; Huang, S.; Su, W.; Zhou, J.; Zhang, X. Performance evaluation on regeneration of high-salt solutions used in air conditioning systems by electro dialysis. *J. Membr. Sci.* **2019**, *582*, 224–235. [[CrossRef](#)]
53. Długołęcki, P.; Anet, B.; Metz, S.J.; Nijmeijer, K.; Wessling, M. Transport limitations in ion exchange membranes at low salt concentrations. *J. Membr. Sci.* **2010**, *346*, 163–171. [[CrossRef](#)]
54. Kooistra, W. Characterization of ion exchange membranes by polarization curves. *Desalination* **1967**, *2*, 139–147. [[CrossRef](#)]
55. Sadrzadeh, M.; Mohammadi, T. Treatment of sea water using electro dialysis: Current efficiency evaluation. *Desalination* **2009**, *249*, 279–285. [[CrossRef](#)]
56. Yan, H.; Li, W.; Zhou, Y.; Irfan, M.; Wang, Y.; Jiang, C.; Xu, T. In-Situ Combination of Bipolar Membrane Electro dialysis with Monovalent Selective Anion-Exchange Membrane for the Valorization of Mixed Salts into Relatively High-Purity Monoprotic and Diprotic Acids. *Membranes* **2020**, *10*, 135. [[CrossRef](#)]
57. Geraldes, V.; Afonso, M.D. Limiting current density in the electro dialysis of multi-ionic solutions. *J. Membr. Sci.* **2010**, *360*, 499–508. [[CrossRef](#)]
58. Galama, A.H.; Daubaras, G.; Burheim, O.S.; Rijnaarts, H.H.M.; Post, J.W. Seawater electro dialysis with preferential removal of divalent ions. *J. Membr. Sci.* **2014**, *452*, 219–228. [[CrossRef](#)]
59. Lu, C.; Tahir, N.; Li, W.; Zhang, Z.; Jiang, D.; Guo, S.; Wang, J.; Wang, K.; Zhang, Q. Enhanced buffer capacity of fermentation broth and biohydrogen production from corn stalk with Na<sub>2</sub>HPO<sub>4</sub>/NaH<sub>2</sub>PO<sub>4</sub>. *Bioresour. Technol.* **2020**, *313*, 123783. [[CrossRef](#)]
60. Stanbury, P.F.; Whitaker, A.; Hall, S.J. *Principles of Fermentation Technology*, 3th ed.; Elsevier: Amsterdam, The Netherlands, 2017.

## Supplement 1 – Assessment of Graphical Methods for Determination of the Limiting Current Density in Complex Electrolysis-Feed Solutions

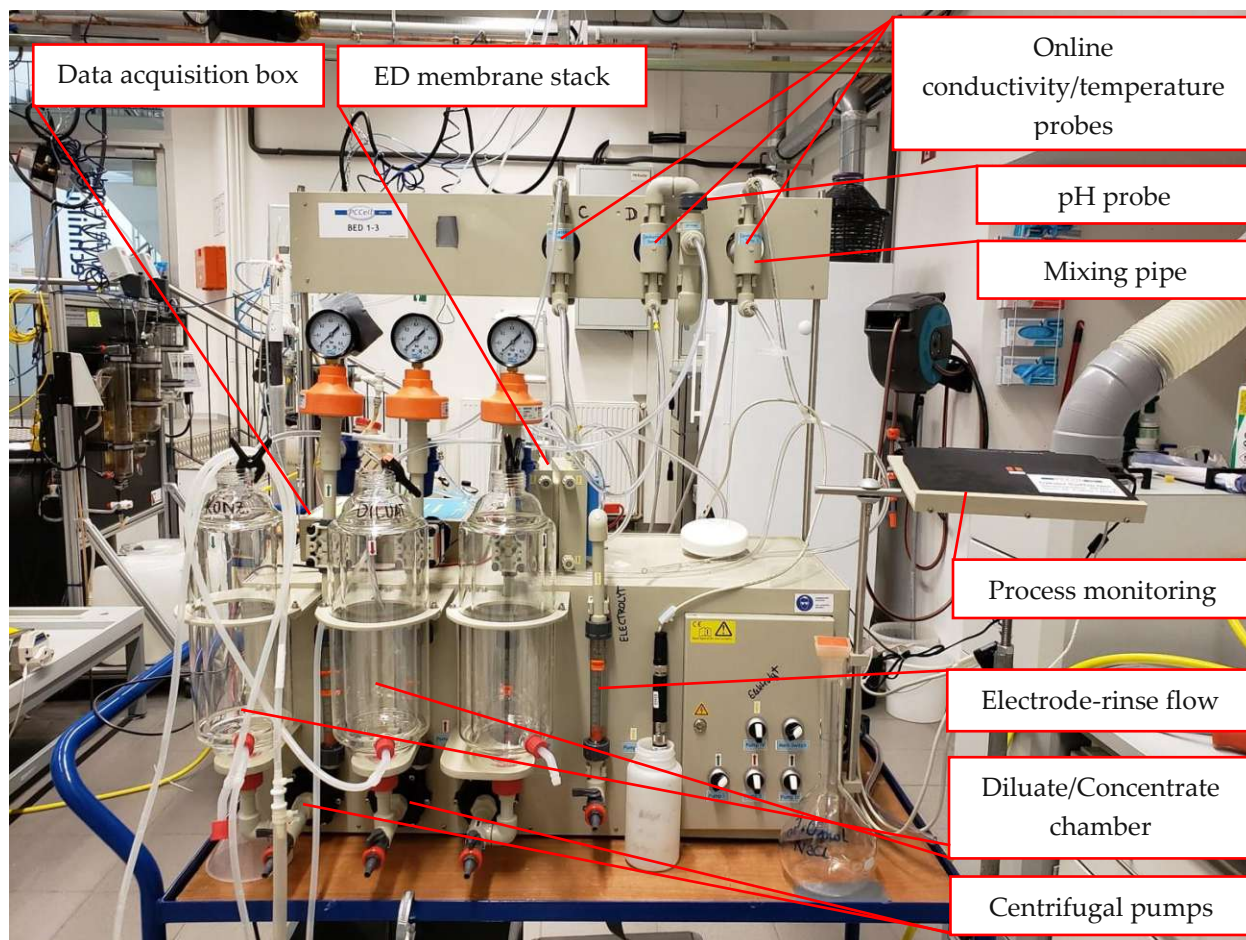


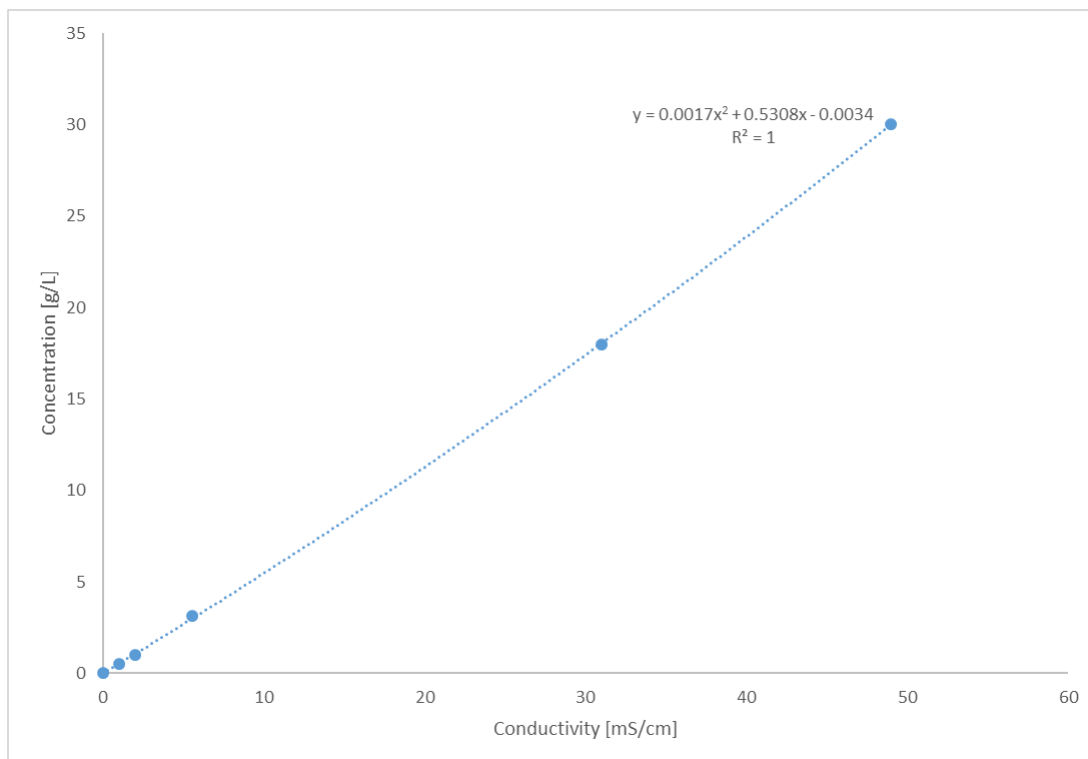
**Figure S1.** 10-cell pair lab-scale ED unit (PCCell ED 64-004, Heusweiler, Germany)

The resistance of an ED stack depends on the number and type of the ion-exchange membranes (cation, anion and end membranes), the specific membrane resistance and active membrane area, the type and ionic concentration of the feed solution, spacers and the resistance of the electrode-rinsing solution and electrodes. The membrane active area in the used ED stack was  $64 \text{ cm}^2$ , and for the nine cation-exchange membranes, ten anion-exchange membranes and two end membranes the total resistance was  $0.8 \Omega$ . The specifications of membranes are in the main document in Table 1. The resistance of the  $0.25 \text{ M Na}_2\text{SO}_4$  electrode-rinse solution is estimated to be  $4.2 \Omega$ . These values are taken as constant values for the used ED stack. The resistance of the electrodes and spacers is often neglected in the calculations of the total ED stack resistance. Further on, the resistance of the diluate and concentrate chamber are calculated from the online conductivity measurements as follows:

$$R = \frac{1}{\kappa} \cdot \frac{h}{A_{eff}} \quad (S1)$$

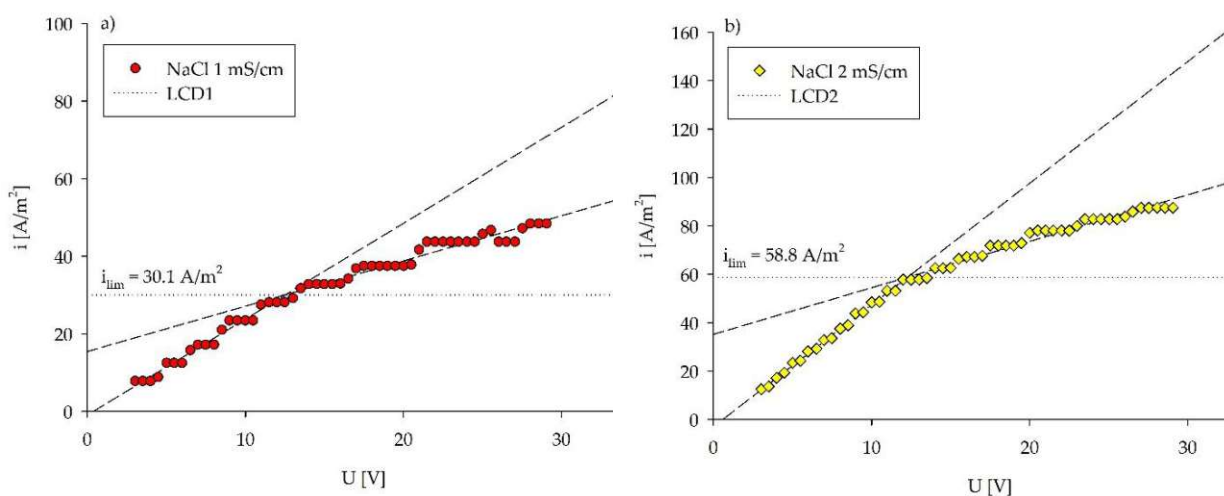
Where the  $\kappa$  (mS/cm) is the specific conductivity of a solution in either diluate or concentrate chamber;  $h$  (cm) is the distance between the membranes, and  $A_{eff}$  (cm<sup>2</sup>) is the active membrane area. From Equation S1 can be seen that the resistance of the treated solution changes during the ED demineralization time, increasing in the diluate chamber and decreasing in the concentrate chamber. Also, the resistances of the solutions employed in this study differed strongly among NaCl solutions with the conductivities of 1–48.7 mS/cm. The contribution of the solution resistance varied from 26–6% of the total ED stack resistance for the NaCl solutions of 1–48.7 mS/cm, respectively. The total ED stack resistance can be clearly seen in the Cowan & Brown plots. Therefore, the relative contribution of the membranes' resistance to the total ED stack's resistance increased averagely from 1–15% with increasing salt concentration represented by the increasing conductivities of 1–48.7 mS/cm, respectively. For example, the contribution of the membrane resistance was 4.6% and of the solution resistance was 20.4% in the NaCl 5.5 mS/cm solution. The formation of the boundary layer can be seen at the resistance inflection point in the Cowan & Brown plots for the NaCl solutions with the conductivity  $\leq 5.5$  mS/cm. The contribution of the boundary layer resistance to the total ED stack resistance increased with the further voltage increase.

For the preparation of the NaCl dilution steps measured conductivities and NaCl concentrations were recorded, having a linear dependency (Figure S2).



**Figure S2.** NaCl concentration - conductivity diagram

In Figure S2 are the experimental data of the NaCl solutions with the conductivities  $\leq 5.5$  mS/cm. The data were fitted to linear functions to find the LCD based on the I&S method.



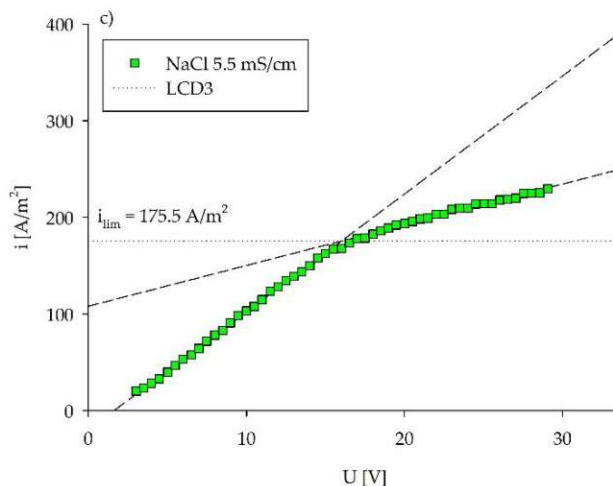


**Figure S3.** The intersection of two fitting linear functions for the LCD determination in a) NaCl 1 mS/cm solution; b) NaCl 2 mS/cm solution; c) NaCl 5.5 mS/cm solution.

In Table S1 are the parameters of linear functions  $f(x) = mx + b$  that were used for fitting the experimental data points in the NaCl solutions with the conductivities  $\leq 5.5$  mS/cm.

**Table S1.** The slopes ( $m$ ), intercepts ( $b$ ) and the coefficient of determination ( $R^2$ ) for two fitting linear equations in experimental data of three NaCl solutions for the LCD determination.

Solution	$m_1$	$b_1$	$R_1^2$	$m_2$	$b_2$	$R_2^2$
NaCl 1 mS/cm	2.4744	-0.9438	0.9619	1.1678	15.4490	0.9455
NaCl 2 mS/cm	5.0314	-2.9481	0.9947	1.9238	35.2072	0.9670
NaCl 5.5 mS/cm	12.2057	-19.7312	0.9990	4.2176	108.0440	0.981

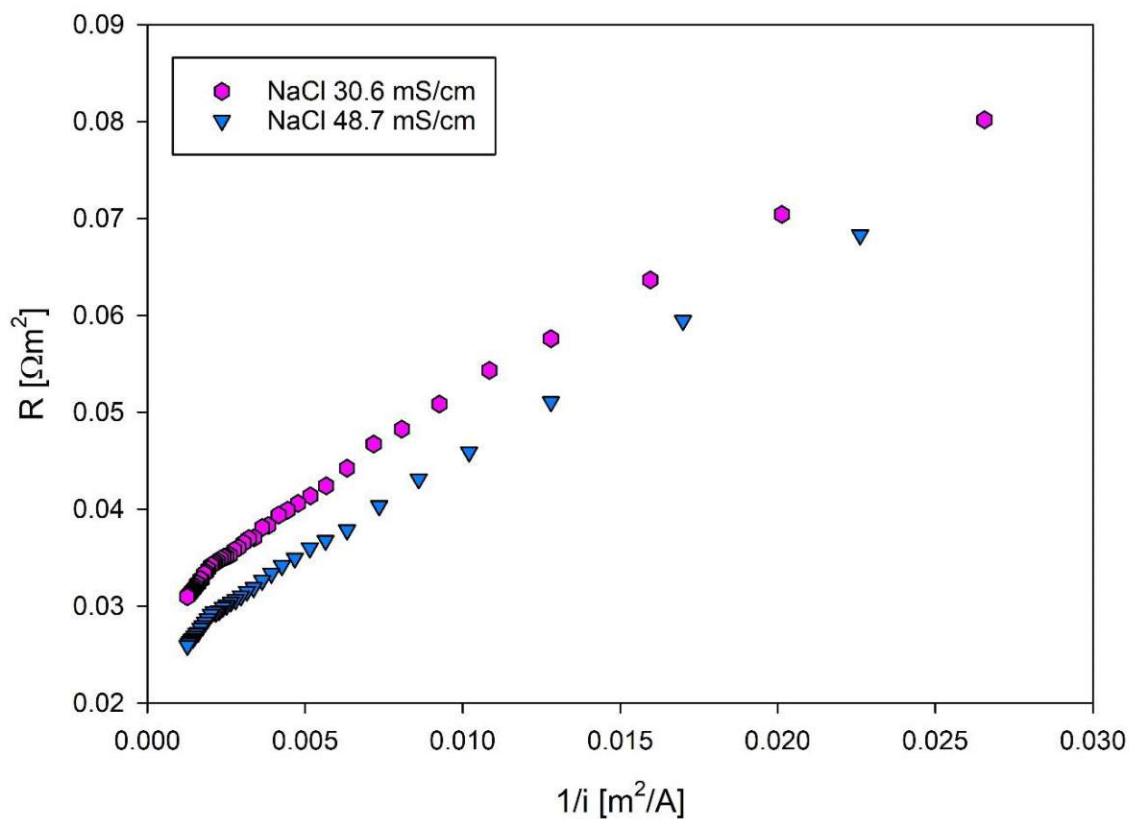


**Figure S4.** ED stack resistance – reciprocal current density curves for LCD of two high concentrated NaCl solutions based on the Cowan and Brown method. With the increasing current density, the resistance is decreasing and the inflection point does not appear for these two solutions

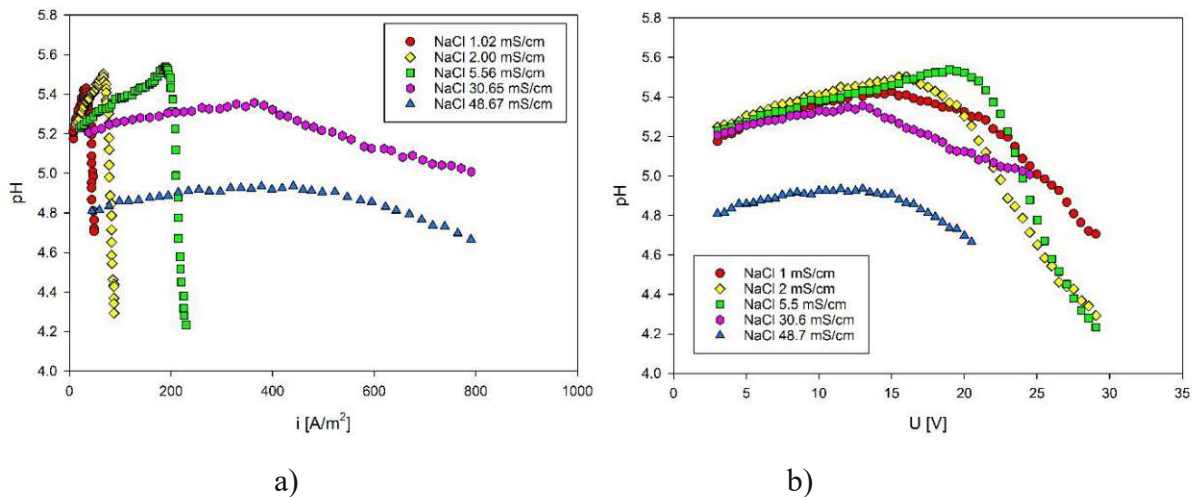


**Figure S5.** Change of the diluate pH with a) current density and b) applied voltage

The more intuitive approach of LCD assessment based on the pH value is shown in Figure S4, where the diluate pH is correlated either to the applied voltage (Figure S4a) or to the current density (Figure S4b). A clear drop in the diluate pH can be seen for all five treated NaCl solutions. The corresponding LCD values are in the Table 2, estimated in three ways. The LCD values adopted for the first diluate pH decline have the values between pH Method (drop for 0.2 pH units) and Max pH (max pH value subtracted for 0.2 pH units). Still, all LCDs indicate higher values compared to the C&B method.

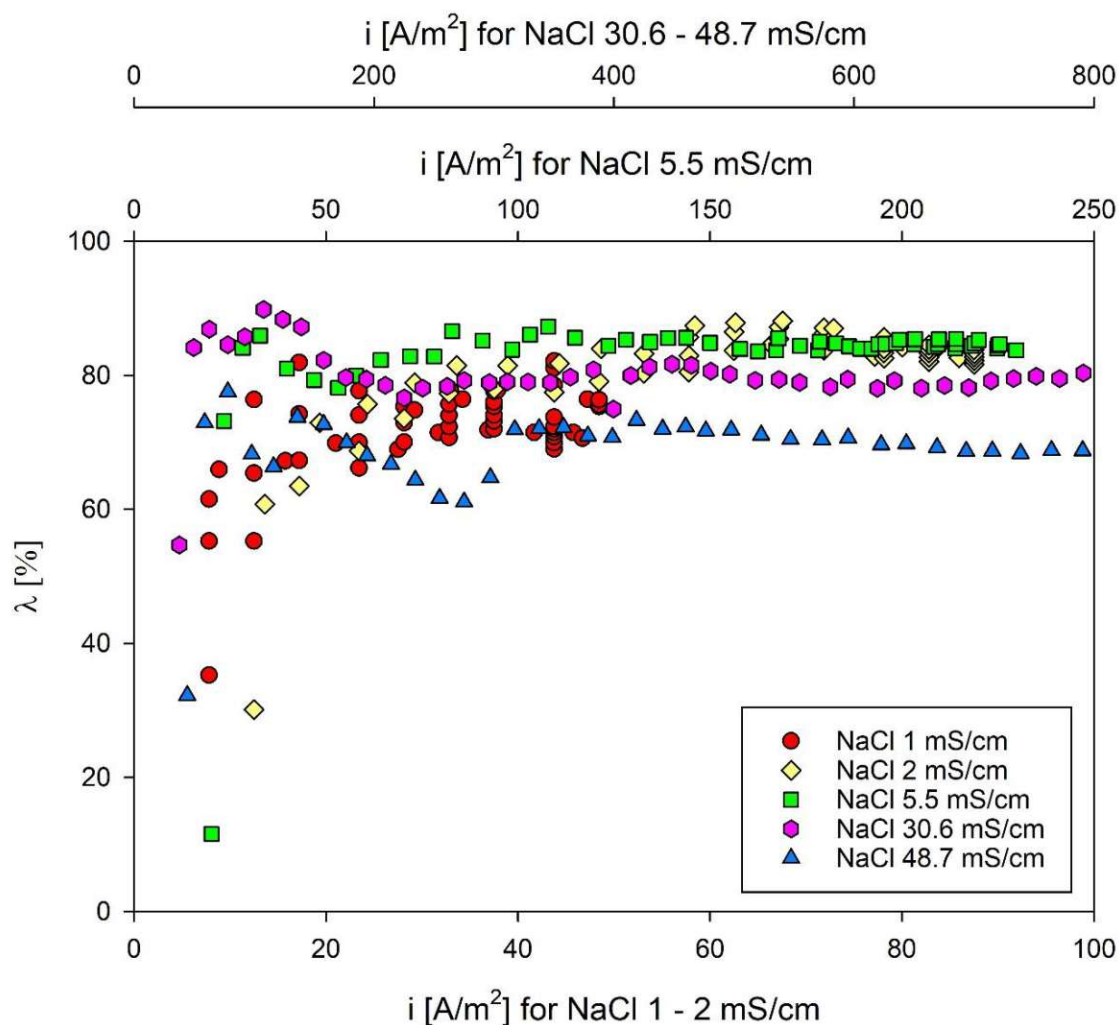


**Figure S6.** Current efficiency ( $\lambda$ ) – current density curves for LCD estimation of five NaCl solutions

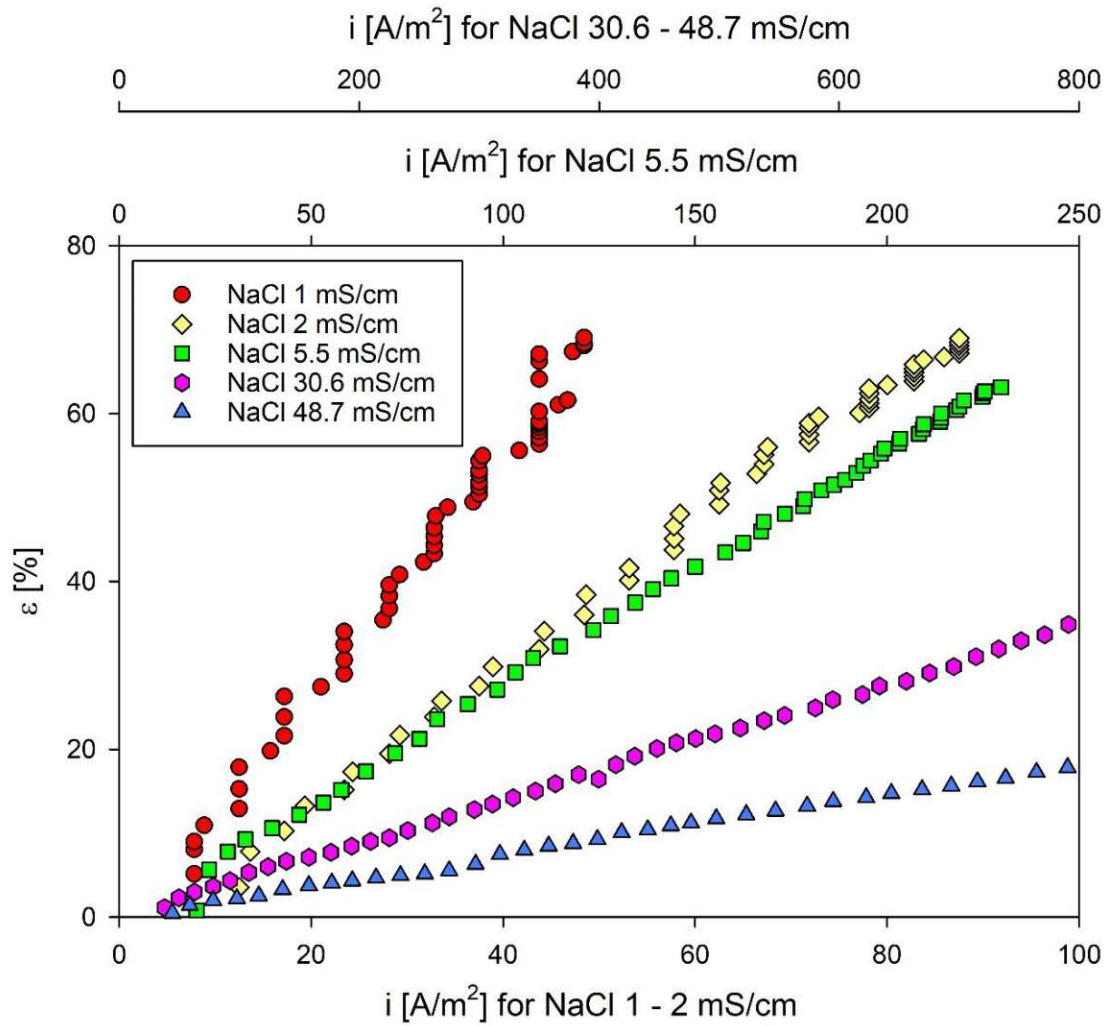


**Figure S7.** Removal efficiency ( $\epsilon$ ) for the salts present in the feed solution plotted against current density, for all five NaCl solutions.

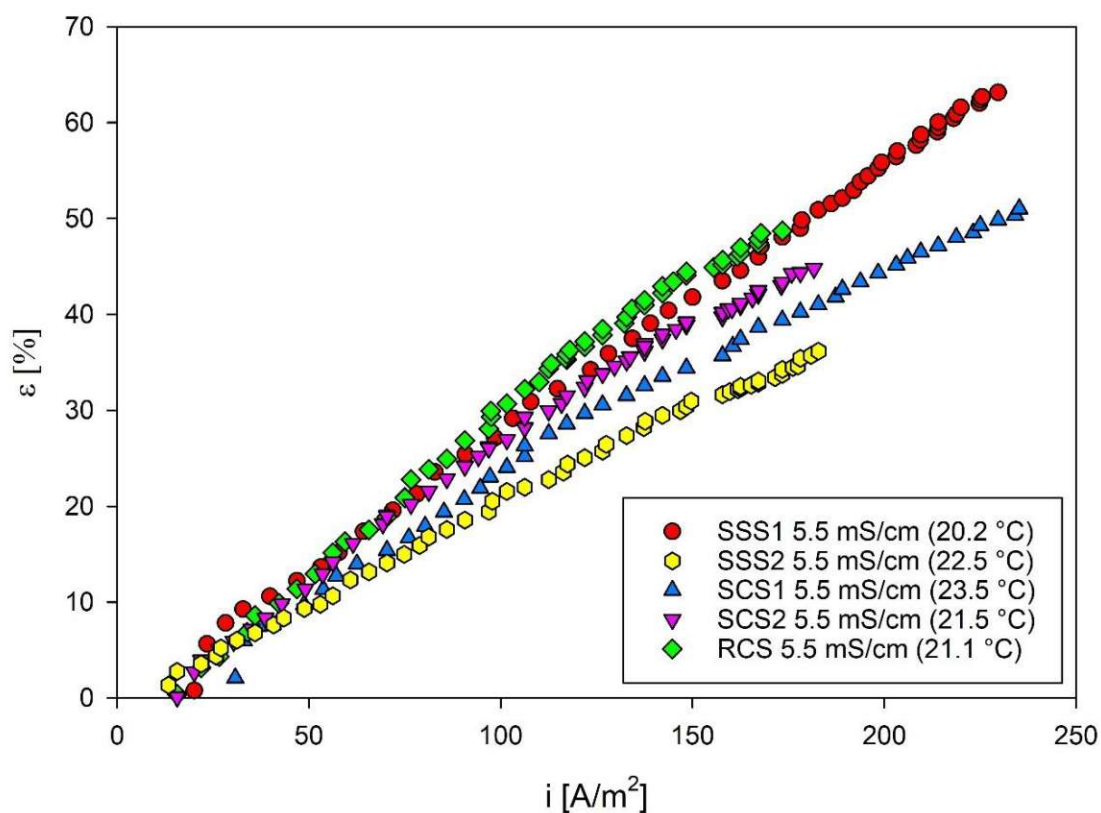


**Figure S8.** Removal efficiency for the salts present in the feed plotted against current density.

Fitting inverse polynomial function of a second order from SigmaPlot, determined from experimental data:

$$f(x) = y_0 - \frac{a}{x} + \frac{b}{x^2} \tag{1}$$

LCD is calculated as the function minimum in following steps:

$$f'(x) = x^{-2}(a - 2bx^{-1}) = 0 \tag{2}$$

$$LCD = x^{-1} = -\frac{a}{2b} \tag{3}$$

**Table S2.** Coefficients of the inverse polynomial function of a second order for estimating LCDs based on Cowan and Brown method presented in the research paper:

Solution		$y_0$	a	b	$R^2$	Std.Error
NaCl mS/cm	1	0.5195	-0.0094	0.0002	0.7463	0.0321
NaCl mS/cm	2	0.2962	-0.0043	5.1606E-005	0.9556	0.0080
NaCl mS/cm	5.5	0.1677	-0.0011	4.2029E-006	0.9710	0.0026
NaCl mS/cm	30.6	0.0300	2.0476	/	0.9881	0.0012
NaCl mS/cm	48.7	0.0248	2.0209	/	0.9937	0.0008
SSS1 mS/cm	5.5	0.1677	-0.0011	4.2029E-006	0.9710	0.0026
SSS2 mS/cm	5.5	0.2224	-0.0016	6.7065E-006	0.8929	0.0066
SCS1 mS/cm	5.5	0.1797	-0.0008	2.2618E-006	0.9337	0.0037
SCS2 mS/cm	5.5	0.1993	-0.0013	6.3531E-006	0.9190	0.0042
RCS mS/cm	5.5	0.1845	-0.0012	6.6920E-006	0.8343	0.0060
SCS1 mS/cm	1.4	0.6089	-0.0109	0.0001	0.7464	0.0218
SCS1 mS/cm	2.02	0.6083	-0.0111	0.0001	0.8104	0.0250
SCS1 mS/cm	2.93	0.3200	-0.0026	1.4863E-005	0.8831	0.0072
SCS2 mS/cm	2	0.5565	-0.0121	0.0002	0.8542	0.0195
SCS2 mS/cm	3	0.3445	-0.0042	4.1966E-005	0.7568	0.0145
SCS2 mS/cm	8	0.1763	-0.0011	3.1077E-006	0.9284	0.0056
SCS2 mS/cm	13.8	0.1070	-0.0004	6.0847E-007	0.8947	0.0041
RCS mS/cm	2	0.3408	-0.0057	0.0001	0.9240	0.0157
RCS mS/cm	3	0.2806	-0.0037	4.2574E-005	0.9215	0.0105

RCS mS/cm	8	0.1478	-0.0008	2.7060E-006	0.9658	0.0020
RCS mS/cm	12	0.1068	-0.0003	7.1280E-007	0.8662	0.0031
RCS mS/cm	18	0.0877	-0.0002	3.2515E-007	0.9099	0.0028

Experimental data plotted on C&B diagrams were assessed for occurrence of LCD in three ways: a—as the intersection of slopes for decreasing/increasing ED stack resistance; b—based on the current density corresponding to the minimum measured ED stack resistance; c—as the minimum of the inverse polynomial function of a second order fitted to the experimental data.

**Table S3.** List of solutions (SSS – 2.3.1) used in the study with corresponding LCDs defined by Cowan and Brown method in three ways (a/b/c):

<b>NaCl concentration [g/L]</b>	0.3	0.9	3.1	18.3	29.3
<b>Conductivity [mS/cm]</b>	1	2	5.5	30.6	48.7
<b>Average temperature T [°C]</b>	19.1	19.2	20.2	20.4	21.0
<b>Initial pH</b>	5.16	5.23	5.21	5.20	4.80
<b>LCDs [A/m<sup>2</sup>]</b>					
<b>C&amp;B a*</b>	28.4	56.8	175.0	/	/
<b>C&amp;B b*</b>	23.4	44.3	157.8	/	/
<b>C&amp;B c*</b>	23.5	41.7	130.9	/	/

\*a/b/c – cross section of the slopes/data minimum/function minimum

**Table S4.** List of solutions used in the study (Chapters 2.3.1., 2.3.2., 2.3.3.) with corresponding LCDs defined by Cowan and Brown method in three ways (a/b/c):

<b>Solution</b>	<b>SSS1 (NaCl)</b>	<b>SSS2(Na<sub>2</sub>SO<sub>4</sub>)</b>	<b>SCS1</b>	<b>SCS2</b>	<b>RCS</b>
<b>Conductivity [mS/cm]</b>	5.5	5.5	5.5	5.5	5.5
<b>Average temperature [°C]</b>	22.6	22.5	23.5	21.5	21.1
<b>Initial pH</b>	6.31	8.49	4.59	3.24	2.25
<b>LCD [A/m<sup>2</sup>]</b>					

<b>C&amp;B a*</b>	153.6	152.4	184.2	108.8	132.5
<b>C&amp;B b*</b>	159.7	112.5	157.8	106.2	96.9
<b>C&amp;B c*</b>	148.0	119.3	176.8	102.3	89.6

\*a/b/c – cross section of the slopes/data minimum/function minimum



# Comparison of ion removal from waste fermentation effluent by nanofiltration, electro dialysis and ion exchange for a subsequent sulfuric acid recovery

Katarina Knežević<sup>\*</sup>, Ernis Saracevic, Jörg Krampe, Norbert Kreuzinger

*Institute for Water Quality and Resource Management, TU Wien, Vienna, Austria*

## ARTICLE INFO

Editor: G. Palmisano

### Keywords:

Pretreatment  
Nanofiltration  
Electrodialysis  
Ion-exchange resins  
Nutrient recycling  
Fermentation wastewater  
Downstream process

## ABSTRACT

Nutrient recovery from wastewater in the form of acids/bases by electro dialysis with bipolar membranes or diffusion dialysis facilitates the current demand for a green economy and circular production. However, bipolar membranes are sensitive to scaling, mainly by calcium and magnesium salts, as well as to biofouling caused by microbial growth and linked aspects. This work aimed to reduce divalent cations to a value below 10 ppm and DOC content of a residual liquid waste stream after microbial fermentation and before a bipolar electro dialysis/diffusion dialysis step for nutrient and acid/base recovery. In this context, three pretreatment technologies were analyzed: nanofiltration, electro dialysis with monovalent cation-exchange membranes, and ion-exchange resins. Nanofiltration and electro dialysis with monovalent cation-exchange membrane were demonstrated to be suitable pretreatments with 92–96 %  $Mg^{2+}$  and  $Ca^{2+}$  removal and 86–94 % DOC removal. Ion-exchange resins had excellent divalent cation removal but no DOC removal, therefore requiring additional treatment to remove organic substances and prevent membranes' biofouling. Electro dialysis with monovalent cation-exchange membranes was preferable over nanofiltration due to the 1.6-fold concentration factor for sulfate ions. In contrast, nanofiltration had lower energy consumption and higher stability in divalent cation rejection. Results obtained in this study are valuable for selecting an appropriate treatment for resource recovery and water reclamation from industrial wastewater and for biotechnological downstream processes.

## 1. Introduction

Liquid wastes of different industrial production processes often contain high concentrations of nutrients and ions which need to be removed in conventional wastewater treatment plants before the discharge to the environment. Otherwise, nutrient loading into water bodies can cause eutrophication, toxic effect and other health issues [1], [2]. Alternatively, nutrients could be recovered for reuse, following the European Green Deal for a zero-pollution ambition [3].

Several membrane processes, such as electro dialysis (ED), bipolar electro dialysis (EDBM) and diffusion dialysis (DD), have been recognized as feasible technologies for resource recovery at source from diverse wastewaters [4–9]. Moreover, these technologies comprise numerous cation- and anion-exchange membranes for selective ionic transport. ED and EDBM are electro-membrane processes that require an electrical field as a driving force for ionic removal. On the contrary, the driving force in the DD process is a concentration gradient. Furthermore,

ions from industrial waste streams can be recovered as acids/bases by EDBM and DD [10–14].

Besides cation- and anion-exchange membranes commonly applied in conventional ED and DD, EDBM contains bipolar membranes where an external electrical field initializes water splitting. Evolved protons and hydroxyl ions combined with their counter-ions occurring in the feed result in a corresponding acidic or caustic stream. In DD, the ions transfer through the membrane by dissolution and then diffusion down a concentration gradient, while the ion exchange membranes (IEM) reject the larger co-ions [15], [16]. However, small size co-ions with low valence ( $H^+$  and  $OH^-$ ) can migrate through the IEM [14]. Both EDBM and DD offer resource recovery and reuse even in the same processes e.g. for pH control, ion-exchange resin regeneration, etc. [17–19].

The competitiveness between ED and DD was lately researched regarding the acid recovery rate, metal rejection rate, energy consumption and the process economy [20]. EDBM can achieve much larger acid/base concentrations and recovery ratios in a short time, allowing a

<sup>\*</sup> Corresponding author.

E-mail address: [katarina.knezevic@tuwien.ac.at](mailto:katarina.knezevic@tuwien.ac.at) (K. Knežević).

<https://doi.org/10.1016/j.jece.2022.108423>

Received 28 May 2022; Received in revised form 6 August 2022; Accepted 9 August 2022

Available online 10 August 2022

2213-3437/© 2022 The Authors. Published by Elsevier Ltd. This is an open access article under the CC BY license (<http://creativecommons.org/licenses/by/4.0/>).

higher treatment capacity than DD. On the other hand, the advantages of DD are lower energy consumption, lower membrane fouling and higher environmental friendliness [16], [20]. Although DD membranes are less prone to fouling, both EDBM and DD require pretreatment to protect IEMs when applied in wastewater treatment. Additionally, adequate pretreatment can increase acid/base concentrations and recovery ratio in both technologies.

Industrial liquid waste streams often contain significant amounts of additional organic and inorganic substances that cause fouling as a general term on IEMs. In fact, IEM fouling can be classified into four groups – colloidal fouling, organic fouling, inorganic scaling, and biofouling [21]. The formation of deposits on and in the IEMs has adverse effects on the process performance – especially on membrane characteristics, increasing electrical resistance, decreasing membrane permeability and selectivity, and altering its physical properties [22]. Colloids in wastewater are non-dissolved suspended solids ranging in particle size from 1  $\mu\text{m}$  to 1 nm. Organic fouling is caused by the dissolved organic matter of a treated solution, such as carbohydrates, proteins, and humic acids [21], [23], [24].  $\text{Mg}^{2+}$  and  $\text{Ca}^{2+}$  are the major scaling ions that tend to precipitate on the membrane surface mainly as carbonates, especially in the EDBM system, due to the strong pH changes of the produced streams [25–27]. Precipitation of  $\text{Al}(\text{OH})_3$  on the membrane can occur in NaOH extraction by DD [28]. Finally, biofouling is particularly disturbing as bacteria form biofilms on IEMs, increasing the membrane thickness and reducing the available area for ion exchange.

Fouling is not only a problem in IEMs but also in pressure-driven membrane processes for drinking water production and wastewater treatment [29–32]. Latter has been more researched considering the broad and long applications of pressure-driven membranes in diverse applications. In contrast, IEM fouling mechanisms and cleaning procedures gained more attention only in recent years [21], [33]. Ion exchange resin is not excluded from the issues mentioned above. Namely, their capacity decreases over time due to fouling phenomena, particularly by organic foulants in the water purification assembly [34].

Different strategies for preventing or reducing IEM fouling have already been studied [21]. There are approaches in IEM modifications [35–37], implementation of advanced membrane spacers [38], changes in ED/EDBM operating conditions [26], mechanical and chemical cleaning methods [33], [39], as well as the pretreatment of feed solutions [40], [41].

Frequently, pressure-driven membrane processes are used for ED/EDBM/DD pretreatment, including micro-, ultra-, and nanofiltration [28], [42]. Micro- and ultrafiltration can remove colloids from wastewater and reduce organic matter, providing sufficient pretreatment for the ED feed. In the study of Wang et al. [10], ultrafiltration was applied for removing proteins, mycelium, and carbohydrates from a microbial fermentation broth, followed by activated carbon for discoloration before further treatment via EDBM. However, feeds containing scaling ions demand more sophisticated pretreatment because IEMs of EDBM/DD systems are more prone to scaling. In some studies, ion-exchange resins have also been coupled with EDBM, e.g., to remove hydroxycarboxylic acids and thiosulfates from spent pulping liquors [18] and to remove nickel ions [43]. Developed strategies for antifouling of IEMs, including e.g., synthesis of nanocomposite materials [44] and periodic air sparging [45], indicate even the feasibility of a direct ED application before EDBM/DD in the treatment of some industrial wastewater.

In general, ED is an emerging membrane separation technology beneficial for its selective ion separation from various feeds and near-to-zero liquid discharges [46]. IEMs are ongoingly investigated, modified, and optimized for specific usages, such as separating monovalent and multivalent ions [35] or enhancing ionic flux and ion perm-selectivity [47]. The fabrication of the monovalent-selective membranes offers a multitude of innovative ED applications in seawater desalination, acid recovery in hydrometallurgy, and removal of specific ions from liquid

**Table 1**  
Physicochemical analysis of the fermentation effluent.

Parameter	Fermentation effluent
pH	2.83
Conductivity (mS/cm)	19.2 $\pm$ 1.4
DOC (mg/L)	1058.7 $\pm$ 68.9
Na <sup>+</sup> (mg/L)	1195.5 $\pm$ 164.5
K <sup>+</sup> (mg/L)	319.3 $\pm$ 122.2
NH <sub>4</sub> -N (mg/L)	1709.6 $\pm$ 113.1
Ca <sup>2+</sup> (mg/L)	36.8 $\pm$ 2.8
Mg <sup>2+</sup> (mg/L)	44.5 $\pm$ 0.9
Cl <sup>-</sup> (mg/L)	122.5 $\pm$ 51.2
SO <sub>4</sub> <sup>2-</sup> (mg/L)	9541.8 $\pm$ 663.9
PO <sub>4</sub> -P (mg/L)	146.8 $\pm$ 5.7

waste [35].

The main drawbacks of electro-membrane compared to pressure-driven processes are still the increased specific energy consumption costs, especially for feeds with TDS  $\geq$  5000 ppm, and higher membrane and maintenance costs [48], [49]. The greater capital and operating costs of ED/EDBM/DD can be, however, outweighed by their advantages when applied for nutrient recycling after conventional wastewater treatment, selective ion separation, water-saving, and quantitative reduction of waste streams.

This research analyzed the performance of three pretreatment technologies applied to a bio-fermentation effluent from the archaea *Sulfolobus acidocaldarius* before an EDBM or DD treatment. As described above, an adequate EDBM/DD pretreatment may decrease the IEM fouling and increase the concentration and recovery ratio of the sulfuric acid retrieved from the fermentation broth. Emphasis was put on the ED pretreatment technology for the selective ionic separation and concentrating ions from the treated waste stream. A particular ED stack was assembled for this study, containing standard anion-exchange membranes (AEM) and monovalent cation-exchange membranes (mCEM), that provide an optimized feed for EDBM/DD by resulting in enrichment with specific ions and reduction of organic molecules. The removal of the divalent cations to a value below 10 ppm and a DOC reduction from the fermentation effluent is necessary due to the afore-mentioned IEMs fouling issues occurring in EDBM systems. The first technology applied was nanofiltration, assessing membranes from two manufacturers. The second technology investigated was ED stacked with AEM and mCEM configuration, which enables to pre-concentrate sulfates for a more efficient subsequent sulfuric acid production by EDBM/DD. Thirdly, three types of chelating ion-exchange resins were applied to remove divalent cations. Results obtained from the three technologies were studied in terms of their removal efficiency for DOC,  $\text{Mg}^{2+}$  and  $\text{Ca}^{2+}$ , selectivity between mono- and divalent ions, ionic fluxes and energy consumption.

## 2. Materials and methods

### 2.1. Wastewater – fermentation effluent used in the study

Wastewater samples were collected from the residual fermentation broth after a bio-fermentation with the archaea *S. acidocaldarius* in a lab-scale [50]. After fermentation, the residual broth was microfiltered via  $\text{Al}_2\text{O}_3$ -coated ceramic filter (0.2  $\mu\text{m}$  pore size, Deltapore, Netherlands) to separate the biomass containing the desired fermentation products from the surrounding medium. The waste permeates from several fermentation replicates were collected and mixed to obtain sufficient material with uniform conditions for the EDBM experiments. The high-volume sample was then split into 5 L subsamples and stored at  $-20^\circ\text{C}$ . Samples were thawed at room temperature separately before applying various subsequent pretreatment technologies. Additional ionic analyses were done for each thawed subsample to ensure that the ionic composition did not change e.g., by precipitation during freezing. These

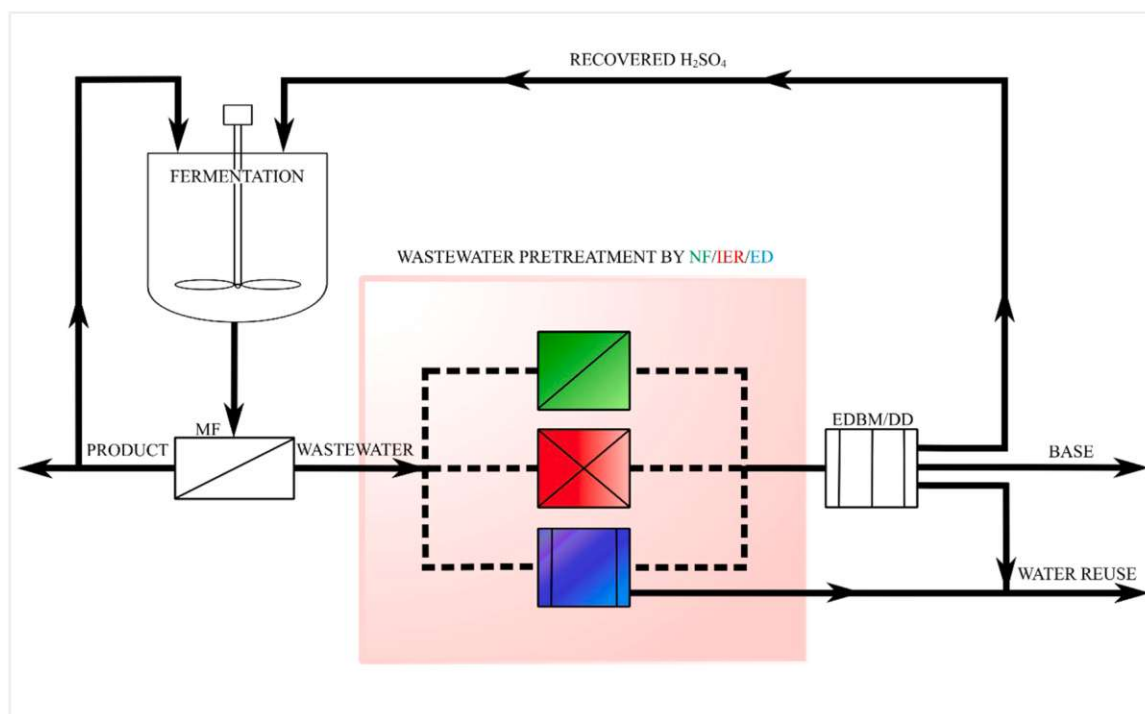


**Fig. 1.** Process design and the experimental set-up for three technologies tested in this research (in the pink box). MF-microfiltration, NF-ion exchange resin, ED- electro dialysis with standard AEM and mCEM.

**Table 2**  
NF membrane characteristics as specified by the producer.

Membrane class	Manufacturer	Model	Material	Stabilized salt rejection (%)	pH 25°C	MWCO (Da)	Max P (bar)	Max. Temp. °C
NF	SUEZ	DK	PA-TFC	98 % MgSO <sub>4</sub>	2–10	200	40	80
NF	DUPONT	NF270	PA-TFC	> 97 % MgSO <sub>4</sub>	2–11	200–400	41	45

re-measurements are the base for characterizing the chemical composition of the fermentation effluent provided in [Table 1](#).

## 2.2. Experimental set-up

The whole process scheme depicting the fermentation, product separation by microfiltration, wastewater source (fermentation effluent), three tested pretreatment technologies, and intended final treatment by either EDBM or DD (out of the research scope) is shown in [Fig. 1](#). A sufficient amount of the fermentation effluent stored in the freezer was thawed at room temperature before applying the pretreatment technology to be tested. Experiments were performed individually for NF (DK) and NF270 filtration, ED, and three types of IER (C100E, MTS9300, and CR11). The aim was to obtain a treated solution with less than 10 ppm of divalent cations and reduced DOC values for further recovery of sulfuric acid by EDBM/DD. Experimental conditions are described in the following sections of the study, and samples were taken accordingly. Chemical analysis of collected samples and data analysis of all obtained results were done as described in the following section.

**Table 3**  
Characteristics of ion-exchange membrane used in the ED experiments, specified by PCCell producer.

Membrane	Type	Thickness, μm	Transference number	Resistance, Ohm cm <sup>2</sup>	Water content (wt %)	pH stability
PC SA	Anion exchange	100–110	> 0.95	1.8	14	0–9
PC MVK*	Cation exchange	100–120	–	–6	–	0–11
PC MTE	Cation exchange	220	> 0.94	4.5	–	1–13

\* monovalent cation-selective membrane

## 2.3. Equipment and membranes for pretreatment experiments

**Nanofiltration (NF).** A cross-flow test cell (OSMO Membrane Systems GmbH, Korntal-Münchingen, Germany) with a membrane active area of 80 cm<sup>2</sup> was used for the batch NF experiments. The experimental conditions were: 1.7 L of treated feed, a pressure of 23 bars, 20 °C and a circulation flow of 2.2 L/min. Two membranes were tested for the retention of divalent cations and DOC removal from the fermentation effluent until 1.5 L of permeate was gained. The NF membrane characteristics are summarized in [Table 2](#). Both membranes were kindly provided by the manufacturers, the NF(DK) by SUEZ Group (Paris, France), and NF270 DuPont (Wilmington, Delaware, US).

**Electrodialysis (ED).** ED experiments were done in a batch laboratory-scale ED system PCCell ED 64–004 (PCCell GmbH, Germany) with ten cell pairs. Applied membranes were standard anion-exchange membranes (AEM) and monovalent selective cation-exchange membranes (mCEM), with specifications shown in [Table 3](#). One cell pair was comprised of one AEM, spacer, mCEM and again a spacer. Spacers defined repeating diluate and concentrate compartments and allowed better mixing of treated streams. PC MTE cation exchange membrane

**Table 4**

Physical and chemical characteristics of Purolite C100E, Purolite MTS9300 and Diaion CR11, as specified by the producer.

Parameter	Purolite C100E	Purolite MTS9300	Diaion CR11
Polymer structure	Gel polystyrene crosslinked with divinylbenzene	Macroporous polystyrene crosslinked with divinylbenzene	Highly porous styrene-divinylbenzene
Optical appearance	Spherical beads	Spherical beads	Spherical beads
Functional group	Sulfonic acid	Iminodiacetic	Iminodiacetate
Ionic form, as shipped	Na <sup>+</sup> form	Na <sup>+</sup> form	Na <sup>+</sup> form
Total capacity (eq/L)	1.9 (Na <sup>+</sup> form)	nd	nd
Moisture retention	46–50 % (Na <sup>+</sup> form)	52–60 % (Na <sup>+</sup> form)	55–60
Particle size range (µm)	300–1200	425–1000	355–1180
Reversible swelling	10 % (Na <sup>+</sup> to H <sup>+</sup> )	35 % (H <sup>+</sup> to Na <sup>+</sup> )	28 % (H <sup>+</sup> to Na <sup>+</sup> )
Specific gravity	1.27	1.18	nd
Shipping density (g/L)	800–840	750–800	730
Effective pH range	6–10	nd	2–6
Temperature limit	120 C	80	120

was used as an end-membrane in the ED stack (Table 3). The effective membrane area was 64 cm<sup>2</sup>. Spacer thickness was 0.45 mm. Electrodes were Pt/Ir-coated titanium anode and V4A steel cathode, placed in the polypropylene electrode housing material. The process was controlled by a step-wise application of current density based on the limiting current densities estimated via Cowan and Brown curves [51] (Appendix A). Electrode-rinse solution (0.25 M Na<sub>2</sub>SO<sub>4</sub>) was circulated at 120 L/h flowrate. 1.53 L of the fermentation effluent and 0.81 L of the synthetic solution with 250 mg/L Na<sub>2</sub>SO<sub>4</sub> dissolved in deionized water were circulated at a 15 L/h flowrate (linear velocity of 0.012 m/s) in the diluate and concentrate chamber, respectively. The synthetic solution in the concentrate was used to retain the organic substances from the feed solution and attain the ionic species containing macronutrients such as P, N and S. The 1.9 vol ratio between the diluate and the concentrate was selected to concentrate ions from the fermentation effluent. ED experiments were done as duplicates to obtain in total ~1.6 L of concentrate solution. Conductivity and temperature were continuously monitored and recorded at the ED stack outlet for both streams. Additionally, the pH of the diluate was also continuously measured.

**Ion exchange resins (IER).** Three types of IER were used in the experiments, kindly provided by Mitsubishi Chemical (Tokyo, Japan) and by Purolite Corporation (Pennsylvania, USA). The physicochemical properties of the chelating resins are given in Table 4. For each experiment, 50 mL of resins were put in glass columns with an internal diameter of 1.5 cm. The total bed volume (BV) height was 16 cm, including 1 cm glass wool to avoid loss of resins, 0.5 cm glass pearls (diameter 1 mm) for even distribution of the feed and 14.5 cm resin material. The fermentation effluent was manually fed on the top of the column, having gravitational down-flow through the filter bed. The flow was regulated by a bottom valve and maintained at 8.4 BV/h (7 mL/min). The resins were rinsed with 20 BV deionized water before the start of the experiments. Samples of the column effluent for cation analysis were taken every 20 min. The conductivity, pH, and temperature of the column effluent were continuously measured. The endpoint of experiments was achieved when a volume of 1.7 L of treated fermentation effluent was gained.

nd - not defined.

## 2.4. Chemical analysis

Water samples were analyzed for PO<sub>4</sub>-P and NH<sub>4</sub>-N with continuous flow analysis and photometrical detection (Skalar, Netherlands) according to DIN EN ISO 6878 and DIN EN ISO 11732 standards, respectively. Anions (Cl<sup>-</sup>, SO<sub>4</sub><sup>2-</sup>) were analyzed according to DIN EN ISO 10304-1 and cations (Na<sup>+</sup>, K<sup>+</sup>, Ca<sup>2+</sup>, Mg<sup>2+</sup>) according to DIN EN ISO 14911 standard, using high performance ion chromatography (Metrohm AG, Switzerland). Dissolved organic carbon (DOC) was analyzed using the combustion method according to DIN EN 1484 standard.

## 2.5. Data analysis

The following equations were used to compare process efficiencies and characteristics among the investigated three different pretreatment technologies.

The rejection rate of a specific ion in the NF ( $R^{NF}$ ) and ED ( $R^{ED}$ ) system was calculated from:

$$R^{NF} = \left(1 - \frac{c_p}{c_f}\right) \times 100\% R^{ED} = \left(1 - \frac{(c_c^t - c_c^0)V_c}{c_d^0 V_d}\right) \times 100\% \quad (1)$$

where  $c_f$  and  $c_p$  (mol/L) are the concentrations of ion  $i$  in the feed and in the permeate, respectively, in the NF system. In the ED system, removal of ion  $i$  was calculated based on the ion concentration  $c$  (mol/L) and volume  $V$  (L) in the diluate  $d$  and concentrate  $c$ , denoted in subscript, at the time 0 and  $t$ , denoted in superscript.

The ion permeation in NF (% $p^{NF}$ ) and ED (% $p^{ED}$ ) was obtained according to:

$$\%p^{NF} = \frac{c_p}{c_f} \times 100\% \quad \%p^{ED} = \frac{(c_c^t - c_c^0)V_c}{c_d^0 V_d} \times 100\% \quad (2)$$

where the permeation of ions in ED refers to ion migration from the diluate to the concentrate chamber.

The ionic flux in NF ( $J^{NF}$ ) and ED ( $J^{ED}$ ) was calculated using:

$$J^{NF} = \frac{c_p V_p}{A t} \quad J^{ED} = \frac{(c_c^t - c_c^0)V_c}{A t} \quad (3)$$

where  $V_p$  (L) is the permeate volume.  $V_c$  (L) in ED is the concentrate volume.  $A$  (m<sup>2</sup>) is the effective membrane area and  $t$  (h) the process duration time.

The membrane perm-selectivity between monovalent cation  $i$  and divalent cations  $n^{2+}$  (Mg<sup>2+</sup> and Ca<sup>2+</sup>) in NF was obtained according to:

$$S_{n^{2+}}^i = \left(\frac{c_f^{n^{2+}} / c_f^i}{c_p^{n^{2+}} / c_p^i}\right) \quad (4)$$

where  $c$  (mol/L) is the ion concentration, for monovalent ion  $i$  and divalent ions  $n^{2+}$ , denoted in superscript, and in feed  $f$  and permeate  $p$ , denoted in subscript. As  $S_{n^{2+}}^i$  increases, the monovalent selectivity of the membrane increases.

The membrane perm-selectivity between monovalent ion species  $i$  and divalent cations  $n^{2+}$  (Mg<sup>2+</sup> or Ca<sup>2+</sup>) in ED was obtained according to:

$$S_{n^{2+}}^i = \frac{J_i c_{n^{2+}}}{J_{n^{2+}} c_i} \quad (5)$$

Where  $J$  (mol/(cm<sup>2</sup> s)) is the ionic flux and  $c$  (mol/L) is the average ion concentration in the diluate chamber during experiment, for monovalent ion  $i$  and divalent ions  $n^{2+}$ , denoted in the subscripts. As  $S_{n^{2+}}^i$  increases, the monovalent selectivity of the membrane increases.

Current efficiency in the ED process was calculated from the following equation:

$$CE = \frac{F \times \sum_i z_i (c_i - c_0) \times V}{N \times I \times t} \quad (6)$$

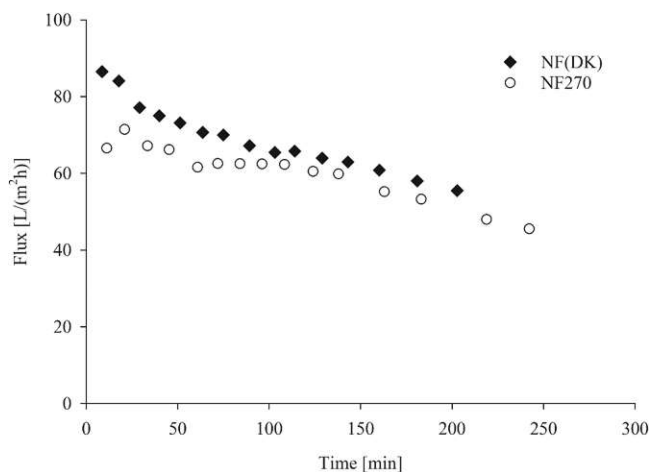


Fig. 2. Decline of permeate flux over time for two tested membranes: NF(DK) and NF270. Pressure: 23 bar; temperature: 20 °C; circulation flow: 2.2 L/min.

where  $F$  is the Faraday constant (96,485 sA/mol),  $z_i$  the valance of ion  $i$ ,  $N$  the number of ED cell pairs (10 in this study),  $I$  (A) applied current.

In the ED the energy is consumed for the feed desalination ( $E_d$ ) and for the pumps of the diluate, concentrate and electrode-rinsing solutions

( $E_p$ ). Therefore, the total energy consumption for the experimental conditions of the batch ED mode were calculated as follows:

$$E = E_d + E_p = \frac{U \times I \times t}{V} + \frac{Q \times \Delta p}{\eta \times V} \quad (7)$$

where  $U$  (V) is the applied voltage,  $I$  (A) is the applied current,  $t$  (h) is the desalination duration, and  $V$  ( $m^3$ ) is the treated volume of the feed solution. Energy consumed by the pumps ( $E_p$ ) in the diluted, concentrated, and electrode-rinsing solutions was calculated accordingly, where  $Q$  ( $m^3/s$ ) is the flow of the diluted, concentrated, or electrode-rinsing solution,  $\Delta p$  (Pa) is the differential pressure between the inlet and outlet of the ED stack,  $\eta$  is the pump efficiency (assumed as 75 % for all three pumps), and  $V$  ( $m^3$ ) is the treated volume of the diluted solution. The same  $E_p$  equation was used for calculating energy consumption in nanofiltration.

### 3. Results and discussion

The following section presents the results obtained from the treatment of the fermentation effluent by nanofiltration, electrodialysis and ion-exchange resins. The investigated parameters were subsequently compared to define the quality of the streams obtained by three different technologies.

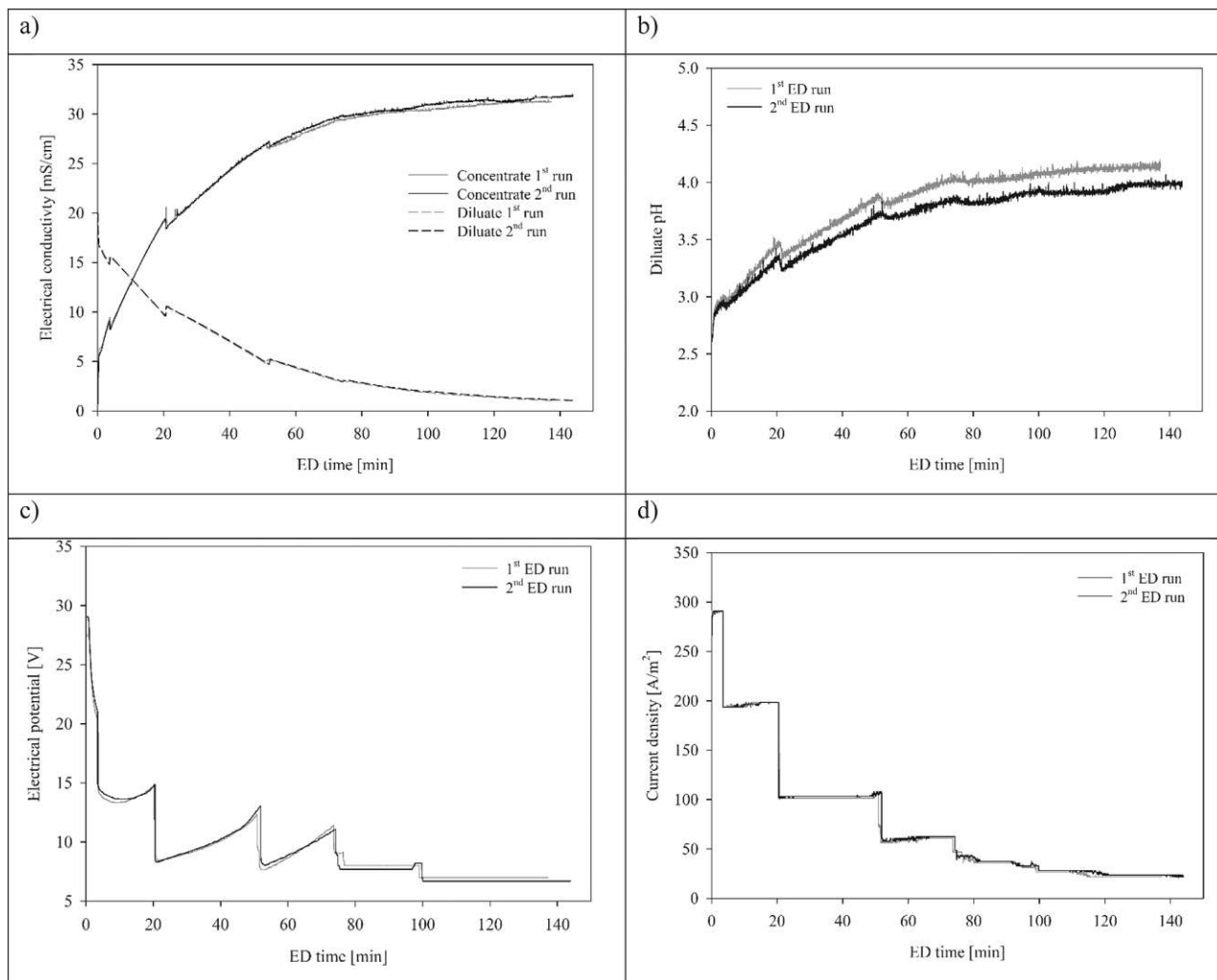


Fig. 3. a) Evolution of the diluate and concentrate conductivities in the first and second ED run; b) Diluate pH during the demineralization; c) Voltage applied to the ED stack; d) The step-wise current density trend for wastewater demineralization.

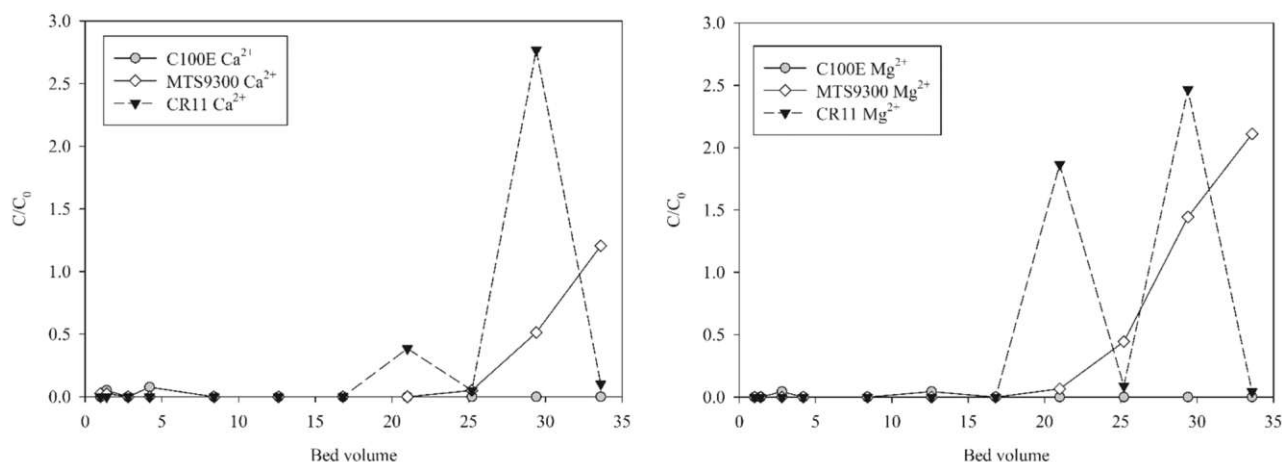


Fig. 4. Breakthrough point for three types of IER applied for: a)  $\text{Ca}^{2+}$  removal and b)  $\text{Mg}^{2+}$  removal from the fermentation effluent. The temperature was kept at 22 °C.

### 3.1. NF - nanofiltration

NF was performed in batch mode, using NF(DK) and NF270 membranes to treat the fermentation effluent. The filtration time for NF(DK) and NF270 was 203 min and 242 min, respectively. Fig. 2 shows the evolution of the permeate flux for two NF membranes tested until 1.5 L of the filtrate was obtained. The measured fluxes are similar to the values obtained from literature [52–55]. The permeate flux continuously declined due to the continually higher concentrations in the feed and organic fouling of the membranes. The more the organic molecules adsorbed on the membrane, the higher the decline in the flux [56]. The mass balance of DOC revealed adsorption of 1.3 g DOC to the NF(DK) surface and 1.1 g DOC to the NF270 surface, from 1.7 L of the treated feed containing  $1 \pm 0.07$  g/L DOC. The molar quantities retained by NF (DK) and NF270 from the feed were 0.20 mol and 0.34 mol, respectively. The volume reduction factor of 8.5 led to retentate densities of 1.07 g/mL for NF(DK) and 1.49 g/mL for NF270, both rich with  $\text{Mg}^{2+}$ ,  $\text{Ca}^{2+}$  and  $\text{SO}_4^{2-}$  ions and organic matter. The water recovery factor was 90 % and 87 % for NF(DK) and NF270, respectively.

### 3.2. ED - electro dialysis

ED experiments were done in batch mode and duplicates. Initial volumes were 1.5 L of the fermentation effluent in the diluate chamber and 0.81 L of 250 mg/L  $\text{Na}_2\text{SO}_4$  model solution in the concentrate chamber. The demineralization rate of the diluates was 94.7 % and ED lasted  $140.6 \pm 3.3$  min. The concentrate/diluate volumes were monitored to restrain volume variations during ED. Thus, ED was aborted when the diluate reached a conductivity of 1.05 mS/cm. This value prevented significant concentrate volume increments but still provided a diluate fulfilling the irrigation water requirements (e.g. diluate conductivity < 3 mS/cm) [57]. Otherwise, the large difference between the diluate and concentrate conductivities initializes osmotic water flux from the diluate towards concentrate [58]. Consequently, the uncharged pollutants from the feed may increasingly diffuse towards the concentrate [59]. The final concentrate conductivity was  $31.5 \pm 0.3$  mS/cm. Conductivity trends, representing the total ionic strength, are shown in Fig. 3a for the diluate and concentrate of both ED runs. In the ED set-up, the mCEM retained divalent cations in the diluate, whereas the standard AEM allowed the transport and concentration of sulfates toward the concentrate solution. The molar quantities of salt removed from the diluate were  $0.44 \pm 0.003$  mol and transferred to the concentrate  $0.41 \pm 0.002$  mol. The remaining difference makes up for the retained divalent cations (0.0039 mol) and ion leakage to the electrode-rinsing solution (explained in 3.5 and 3.7). A total concentration factor of

$1.59 \pm 0.02$  was achieved, comparing the initial diluate and concentrate conductivities. The concentration factor of sulfates was  $1.6 \pm 0.1$ . Diluate pH rose from 2.6 to 4 pH with increased ion removal (Fig. 3b). Step-wise current was applied for the ED control, as described in Appendix A. Trends of electrical potential and current density can be seen in Fig. 3c and Fig. 3d. The current efficiency CE for anion removal from the diluate was  $72.7 \pm 7.1$  %, whereas the cationic removal CE was  $61.3 \pm 3.5$  % due to the retention of divalent cations. CE values are in the range provided in literature [4], [60], [61].

### 3.3. IER - ion exchange resins

Three types of chelating cation exchange resins were tested for the removal of divalent cations in the scope of this research. In initial experiments, the content of anions in the treated fermentation effluent was proven to remain unchanged as expected. Thus, the IER column outlet samples were analyzed for cations only. A volume of 1.7 L was collected after 240 min (33.6-bed volumes) with the wastewater down-flow rate of 7 mL/min. The measured  $\text{Ca}^{2+}$  and  $\text{Mg}^{2+}$  concentrations in the column outlet were divided by their inlet concentration and plotted against the bed volume in Fig. 4. The breakthrough curves for  $\text{Ca}^{2+}$  removal (Fig. 4a) and  $\text{Mg}^{2+}$  removal (Fig. 4b) were observed for MTS9300 and CR11 resins, while the C100E resins remained unsaturated. Thus, the C100E resins had complete removal of divalent cations (0.0046 mol), whereas the molar quantities removed by MTS9300 and CR11 resins before the breakthrough point were 0.0028 mol and 0.0023 mol, respectively.

The ion breakthrough in the CR11 resins started at around 20 BV for both magnesium and calcium, followed by subsequent adsorption of these ions at 25 BV, another desorption at 30 BV and again adsorption at 33 BV. The desorption of divalent cations is possible due to the 34 times higher monovalent cation equivalents compared to divalent cation equivalents in the fermentation effluent and low adsorption in the resin. The behavior of the resins could also be affected by a possible nonideal fluid mixing and flow through the column geometry. For all resins, the selectivity for cations was:  $\text{Ca}^{2+} > \text{Mg}^{2+} > \text{K}^+ > \text{NH}_4^+ > \text{Na}^+$ . The dynamic ion exchange capacity for divalent cations was  $\text{C100E} > \text{MTS9300} > \text{CR11}$ , with exchange capacities between 0.12 eq/L and above 0.19 eq/L of resins. The sorption of divalent cations depends on the solution pH values and can reach higher or lower values for the pH other than 2.8 [62], [63]. A recent study by Suwannahong et al. [64] indicated a decreased adsorption ability of the iminodiacetic acid functional group in IERs when treating highly acid solutions, similar to the MTS9300 and CR11 chelating resins researched in this paper. In contrast, C100E resins have sulfonic acid as the functional group

**Table 5**

The rejection rate for DOC,  $\text{Ca}^{2+}$ , and  $\text{Mg}^{2+}$  from the fermentation effluent, performed via different technologies.

R (%)	NF (DK)	NF270	ED1&2	IER		
				C100E	MTS9300	CR11
DOC	85.9	85.6	94.1 ± 0.14	~0	~0	~0
Ca	93.9	97.6	89.3 ± 6.0	100	100	100
Mg	93.5	95.3	95.3 ± 2.2	100	100	100

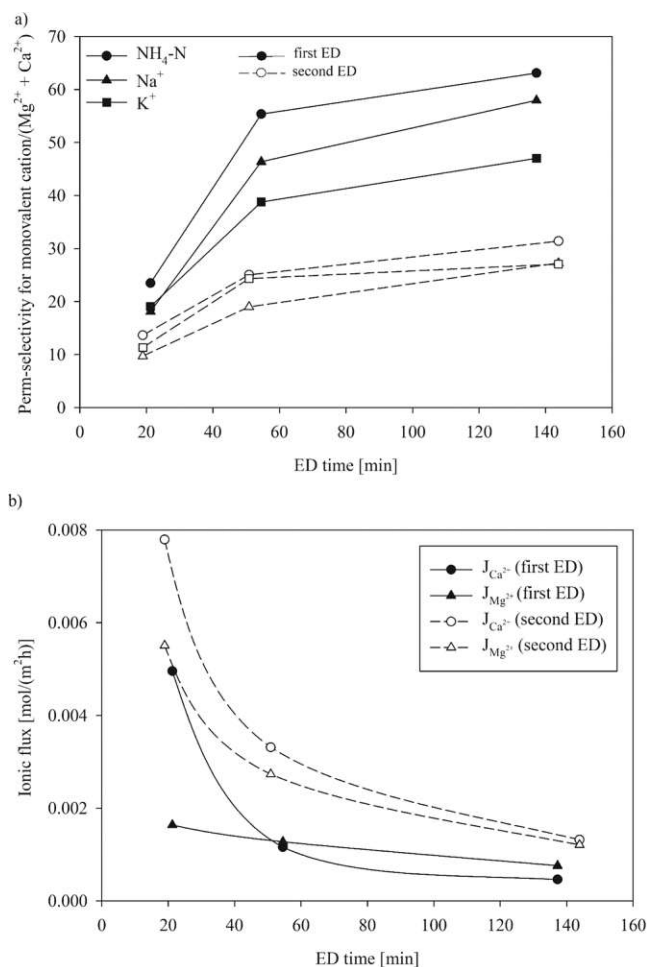


**Fig. 5.** a) Perm-selectivity between individual monovalent cations ( $\text{Na}^+$ ,  $\text{NH}_4\text{-N}$ , or  $\text{K}^+$ ) and sum of divalent cations ( $\text{Mg}^{2+}$  and  $\text{Ca}^{2+}$ ) for the mCEM during the ED operation time; b) Fluxes of  $\text{Mg}^{2+}$  and  $\text{Ca}^{2+}$  in the first and the second ED run, depicted over ED operation time.

(Table 4) and exhibited the highest softening capacity for the wastewater treated within this study. The obtained results indicate preferential application of the resins with the sulfonic acid functional group to remove divalent cations from the fermentation effluent with a low pH value.

### 3.4. Removal of divalent cations and organic compounds by the three investigated technologies

This aspect of the research focused on removing divalent cations and DOC from the fermentation effluent via three technologies under investigation.  $\text{Mg}^{2+}$  and  $\text{Ca}^{2+}$  removal was obtained by their rejection rate in NF and mCEM and the exchange rate in IER. The obtained removal efficiencies are summarized in Table 5 and decreased in the following order for DOC: ED>NF(DK)>NF270>IER; for  $\text{Ca}^{2+}$ :

IER>NF270>NF(DK)>ED and for  $\text{Mg}^{2+}$ : IER>ED=NF270>NF(DK). IER had 100 % removal of divalent cations; however, the organic matter remained in the column effluent. Therefore, IERs require additional posttreatment, such as activated carbon, for DOC reduction and discoloration. Both NF membranes and ED had very high DOC and divalent cation removal values.

### 3.5. Perm-selectivity of monovalent cations

The monovalent cations together with hydroxide anions in the EDBM system result in a caustic stream. As the fermentation effluent mainly contains  $\text{NH}_4^+$  and  $\text{Na}^+$  ions (Table 1), the bases produced via bipolar membranes are predominantly  $\text{NH}_4\text{OH}$  and  $\text{NaOH}$ , and at a lower rate  $\text{KOH}$ . In order to increase the yield for the caustic stream, it is desired to have high concentrations of monovalent cations after the pre-treating step before forwarding it to EDBM.

The mCEM retains divalent cations in the diluate and shifts monovalent cations towards the concentrate. The concentrate is supposed to be fed to the EDBM for the acid/base production. Fig. 5 shows the development of the mCEM perm-selectivity between individual mono- and the sum of divalent cations in ED against the operation time. A detailed picture of perm-selectivities determined individually for  $\text{Mg}^{2+}$  and  $\text{Ca}^{2+}$  ions can be found in Appendix B. Perm-selectivities were determined for three sampling points during the ED process, at average current densities of 209.4  $\text{A/m}^2$ , 143.8  $\text{A/m}^2$  and 78.1  $\text{A/m}^2$ , for both first and the second ED run (Fig. 5a). The perm-selectivity between monovalent ( $\text{NH}_4\text{-N}$ ,  $\text{Na}^+$  or  $\text{K}^+$ ) and divalent cations increased with the ED demineralization time, reaching maximum values of 63.1, 58.0 and 47.0 for  $\text{NH}_4\text{-N}$ ,  $\text{Na}^+$ , and  $\text{K}^+$ , respectively. With decreasing diluate ion concentration and current density, the perm-selectivities were increasing, indicating a positive effect of these two parameters on the overall membrane selectivity. Further on, prolonged ED operation time led to a progressive diffusion boundary layer formation near mCEM on the diluate side. This layer promoted diffusional transport mechanisms, favoring the transport of monovalent over multivalent counter-ions.

However, the perm-selectivities decreased drastically (~50 %) in the second ED run. Effects of ion concentrations and current densities on the mCEM selectivity can be excluded, as the exact same conditions were applied in the first and the second ED run. The mCEM has a specified 0–11 pH stability (Table 3), therefore excluding the impact of the low feed solution pH (pH 3) on the membrane properties. When the fluxes of divalent cations through the mCEM of the first and the second ED run were compared, a significant increase was observed in the second ED run (Fig. 5b). The increased fluxes of  $\text{Mg}^{2+}$  and  $\text{Ca}^{2+}$  ions indicate the damage of the mCEM surface layer that usually hinders the transport of divalent ions and the absence of its electrostatic repulsion towards multivalent ions. The strong binding of divalent cations to the sulfonic acid group led to the inactivation of mCEM exchange layer [65]. Once the divalent cations enter the membrane matrix, the membrane characteristics alter strongly. Adsorption of organic molecules may have also impacted the mCEM characteristics in the second ED run, as the instability of the IEM charged layer during ED has already been noticed [65–67]. These behaviors need further research. In this study, commercial IEMs were used, but recent studies show the improvements of the modified monoselective IEMs compared to the commercial ones, with promising selectivity, stability and antifouling potential [47], [68], [69].

Nevertheless, the perm-selectivities obtained in the second ED run were in the range of those obtained in NF experiments. Perm-selectivities for  $\text{NH}_4\text{-N}$ ,  $\text{Na}^+$ , and  $\text{K}^+$  were 12.6, 12.2 and 16.7 in NF (DK) and 7.1, 9.6 and 9.1 for NF270, respectively, and similar to the literature values [25]. NF(DK) membrane had relatively high perm-selectivity for monovalent over divalent cations. The differences in the permeates obtained by NF(DK) and NF270 can be seen in the change of the conductivity (Fig. 6a) and in pH measurement (Fig. 6b). The conductivity of the NF270 permeate is significantly lower compared to

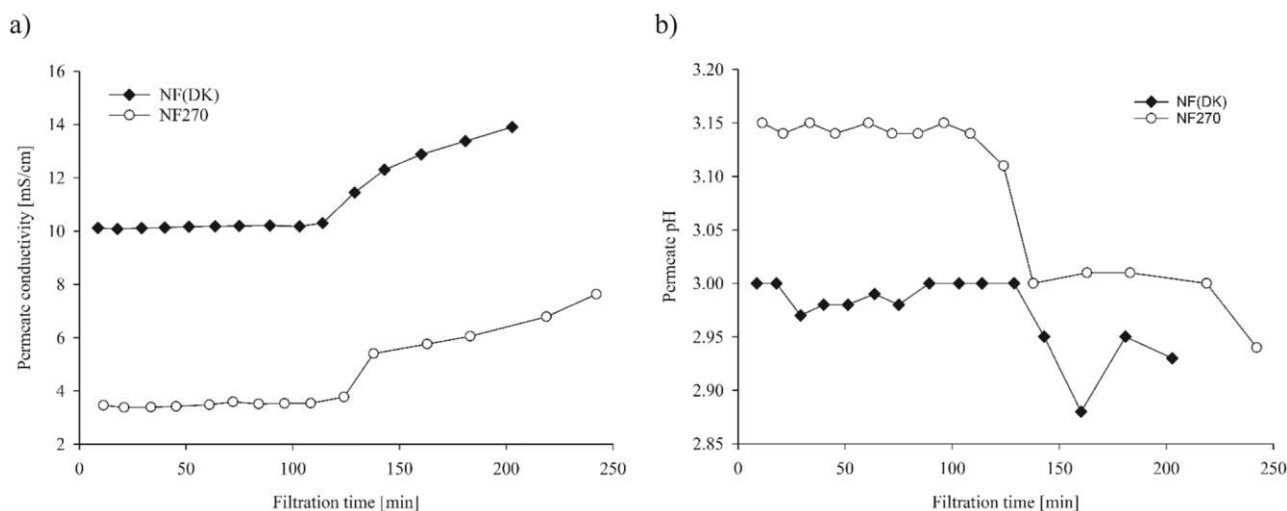


Fig. 6. Characteristics of the NF permeates represented by a) the electrical conductivity and b) the pH measurements.

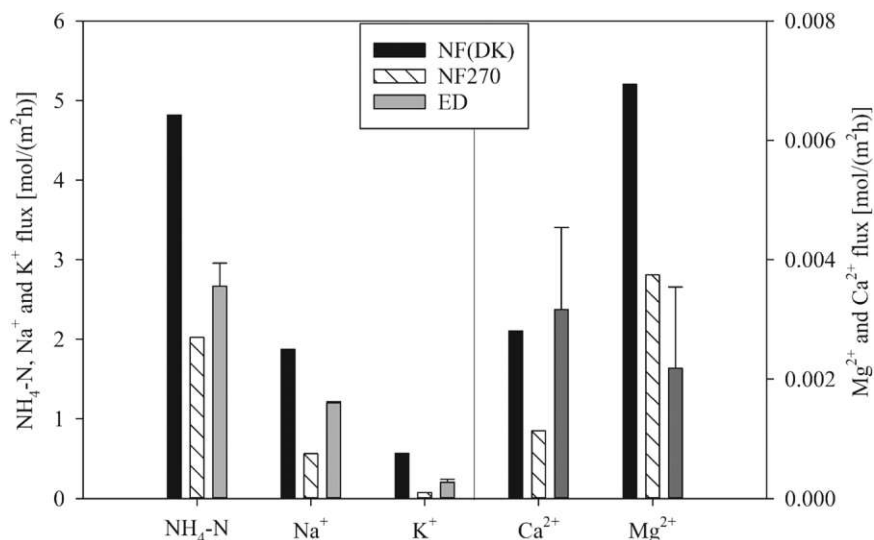


Fig. 7. Average flux of cations through NF(DK), NF270 nanomembranes and mCEM in ED. Flux values for ED are based on two ED runs.

the NF(DK) permeate because more ions were retained. The high retention of monovalent cations (e.g. 63 % for NH<sub>4</sub>-N, 65 % for K<sup>+</sup>) by NF270 membrane is comparable to the literature results [70]. An increase of the conductivity in both permeates occurred after a water recovery ratio of ~50 %, indicating the impact of the ion concentration in the retentate on the permeation of ions. High retention and concentration of Mg<sup>2+</sup>, Ca<sup>2+</sup>, and SO<sub>4</sub><sup>2-</sup> ions in the retentate forced other ions from the fermentation medium to permeate through the NF membranes.

### 3.6. Cationic fluxes

The perm-selectivity of mCEM and NF membranes was demonstrated in the previous section, and the ionic fluxes of mono- and divalent ions strongly influence it. Ionic fluxes through the applied membrane depend on the membrane and feed physicochemical characteristics, ion concentrations, driving force, operating conditions, etc. Thus, cationic fluxes were compared among the tested pretreatment technologies. Fig. 7 reveals higher cationic fluxes for the more concentrated cations in the feed (Table 1) for both pressure-driven and ion-exchange membrane processes.

The fluxes obtained correspond to the molar ratios between NH<sub>4</sub><sup>+</sup> against Na<sup>+</sup> and K<sup>+</sup> ions in the feed, which led to flux reduction factors

of 0.4 and 0.1 for Na<sup>+</sup> and K<sup>+</sup>, respectively, compared to the NH<sub>4</sub><sup>+</sup> flux:

$$M_{(\text{Na})}/M_{(\text{NH}_4)} = 0.4 \rightarrow J_{(\text{Na})} = 0.4 * J_{(\text{NH}_4)}$$

$$M_{(\text{K})}/M_{(\text{NH}_4)} = 0.1 \rightarrow J_{(\text{K})} = 0.1 * J_{(\text{NH}_4)}$$

The only exemption was in the case of the NF270 membrane, with 1.2–2.5 lower fluxes than through the NF(DK) membrane, for both mono- and divalent cations. The lowest Ca<sup>2+</sup> and Mg<sup>2+</sup> fluxes during the NF270 filtration step were beneficial for divalent cation removal. However, the NF270 membrane retained a significant amount of monovalent cations, as seen in their low fluxes in Fig. 7. The low mono- and divalent cationic fluxes can be assigned to the positively charged NF270 membrane surface when the solution pH is less than 3.3–4 [71], as is the case for the fermentation effluent treated in this study. The resulting electric charge repulsion increased the retention of the monovalent cations that otherwise pass through the NF membrane at neutral conditions [72].

The average fluxes of the monovalent cation through mCEM were between the ranges of fluxes through NF(DK) and NF270. Ca<sup>2+</sup> flux was higher, whereas Mg<sup>2+</sup> flux was lower in ED compared to NF membranes. According to Fig. 7 selection of NF(DK) membrane is preferential due to the highest monovalent cation flux and higher capacity than the other tested technologies for the same membrane area.

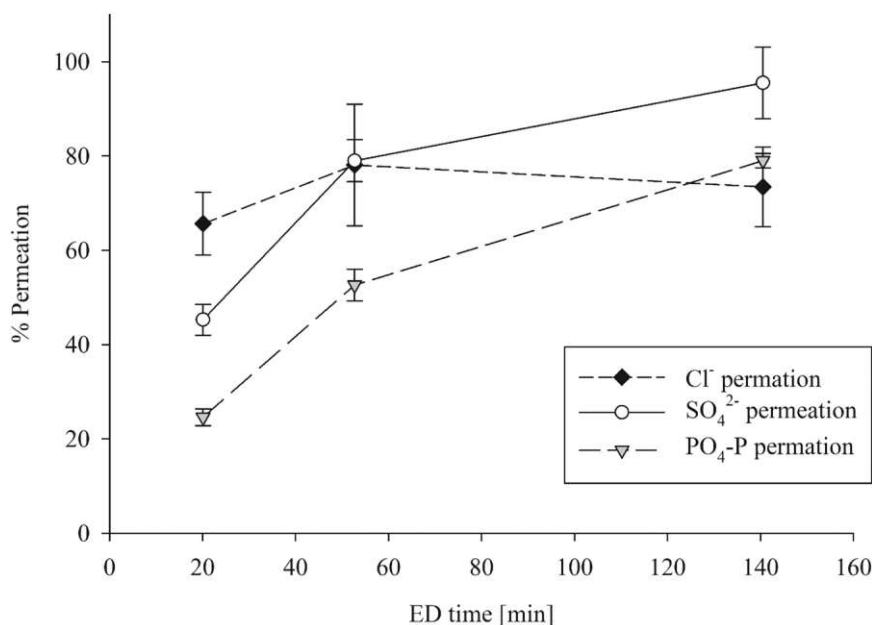


Fig. 8. Permeation (migration) of anionic species from the diluate to the concentrate solution through AEM during ED.

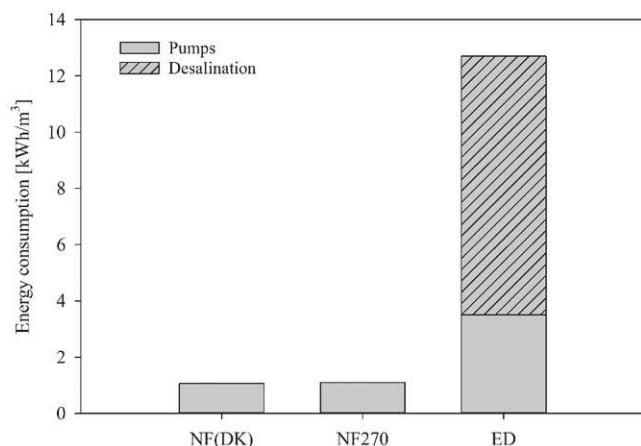


Fig. 9. Energy consumption for pumps in nanofiltration, and for pumps and external electrical field for desalination in ED.

### 3.7. Behavior of anions

Retaining a high concentration of anions in the pre-treated fermentation medium is important because it directly affects the concentration of the acid produced by the subsequent EDBM treatment. The fermentation effluent contains a high concentration of sulfates (~9.5 g/L), whereas the molar concentration of chlorides and phosphates is about 40 times lower. Therefore, the acid produced by EDBM is mainly composed of H<sub>2</sub>SO<sub>4</sub> and significantly less of H<sub>3</sub>PO<sub>4</sub> and HCl. The concentration of the anions in the purified fermentation medium varies considering the technology applied for its pretreatment. Therefore, this section compares the performance of NF, ED, and IER regarding anions by calculating the permeation of anionic species.

Fig. 8 shows the anion migration over time through the anion-exchange membranes (AEM) in ED. The permeation of SO<sub>4</sub><sup>2-</sup> and PO<sub>4</sub>-P increased during the ED process time and ultimately reached 95.5 ± 5 % and 79.0 ± 1 %, respectively. Cl<sup>-</sup> was less concentrated than the other anions and was already efficiently removed (78.1 ± 9 %) in the first 60 min of the ED process. Afterward, the Cl<sup>-</sup> permeation decreased to 73.4 ± 6 %, most probably due to the co-ion leakage through the end-

membrane towards the electrode-rinsing solution [20], [73], [74]. The electrical conductivity of the electrode-rinsing solution increased by 0.8 mS/cm until the end of the demineralization.

Permeation of Cl<sup>-</sup>, SO<sub>4</sub><sup>2-</sup> and PO<sub>4</sub>-P was 95.8 %, 68.6 % and 89.2 % for NF(DK) and 90.5 %, 28.8 % and 73.3 % for NF270, respectively. The obtained values are comparable to the ones from literature [75]. Anionic content of the feed treated by IER remained unchanged.

SO<sub>4</sub><sup>2-</sup> permeation through the AEM in ED was the highest. Comparing NF membranes, SO<sub>4</sub><sup>2-</sup> permeation was 2.4 times higher in the NF(DK) than in the NF270 membrane. Thus, if applying a pressure-driven membrane process before EDBM, NF(DK) membrane would be preferable.

### 3.8. Energy consumption

A simplified economic evaluation was conducted based only on the energy consumption calculations for NF and ED technologies but not for IER. Results are presented in Fig. 9. The energy consumption for the pumps in the NF(DK) process was 1.06 kWh/m<sup>3</sup> of the treated waste stream and 1.1 kWh/m<sup>3</sup> for the NF270 process, respectively. Energy consumption for demineralization in the ED was 9.2 kWh/m<sup>3</sup>, and 12.7 kWh/m<sup>3</sup> when the diluate, concentrate and electrode-rinse circulation pumps were included.

ED energy consumption values are comparable to literature values falling in the range of 3.7–15 kWh/m<sup>3</sup> [48] and significantly increasing with increasing feed salt concentrations [76]. The energy costs also increase with the increasing current density while the required membrane area accordingly decreases. Reduction in energy requirements can be achieved by optimizing ED operating mode via e.g., application of pulse electric field [77], or segmented electrode system of the ED stack [78]. According to the recent study of Severin et al. [79], optimization of the electrode rinsing solution also increases the overall ED process efficiency.

Greiter et al. [80] did an elaborative study regarding the sustainability and cumulative energy demand for why desalination by ED versus IER. The final conclusion was that the ED was preferred due to significantly lower cumulative energy demand, lower effluent volume, and lower total salt discharge. Finally, the investment, operation and maintenance cost, as well as the waste generation, should be considered when calculating a complete economic evaluation.

**Table 6**

The final composition of the pre-treated fermentation effluent meant to be forwarded to EDBM or DD for acid/base recovery.

EDBM Feed	Volume	DOC	Ca <sup>2+</sup>	Mg <sup>2+</sup>	Na <sup>+</sup>	K <sup>+</sup>	NH <sub>4</sub> -N	Cl <sup>-</sup>	SO <sub>4</sub> <sup>2-</sup>	PO <sub>4</sub> -P
	L	mg/L	mg/L	mg/L	mg/L	mg/L	mg/L	mg/L	mg/L	mg/L
NF(DK)	1.5	154.0	2	3	764.0	395.0	1,201.0	91.0	5,987.0	123.3
NF270	1.5	136.7	1	2	283.0	67.0	623.0	86.9	2,767.0	106.3
ED1	0.8	124.8	4	2	2,489.0	446.0	2,571.0	330.0	15,777.0	225.0
ED2	0.8	116.3	11	6	2,423.0	672.0	2,718.0	165.0	16,544.0	235.0
IER*	1.6	1058.0	0	0	1,450.3	195.7	2,068.8	95.0	8,732.0	138.3

\* Each effluent from the three tested IER had the final composition in the similar range

#### 4. Summary and conclusion

EDBM/DD is a system sensitive to fouling and scaling when applied in the treatment of wastewater containing various organic and inorganic pollutants. This research experimentally compared three EDBM/DD pretreatment technologies (NF, ED, IER) for divalent cation reduction to values below 10 ppm and a DOC removal from a fermentation effluent. Assessment of investigated technologies was performed in terms of their removal efficiency for DOC, Mg<sup>2+</sup> and Ca<sup>2+</sup>, selectivity between mono- and divalent cations, ionic fluxes and energy consumption. The obtained results are valuable for designing wastewater treatment and downstream processes in biotechnology.

Table 6 comprises the ionic and DOC composition of the fermentation medium after treatment by NF, ED, and IER.

Both NF membranes had a high removal of divalent cations (95.3 ± 1.6 %) and organic compounds (85.8 ± 0.1 %). However, NF(DK) performed better in permeating sulfates and monovalent cations. The sulfate reduction was 31 % for NF(DK) and 71 % for NF270. Results indicate a possibility of coupling NF(DK) with NF270 for filtering the fermentation effluent. In this case, the NF(DK) permeate would be forwarded to NF270 filtration. Based on the experimental results and rough estimations, NF270 would retain ~50 % of the feed's initial SO<sub>4</sub><sup>2-</sup> and monovalent cations content and concentrate it ~3.4 times. Thus, NF270 retentate could be forwarded to the EDBM for acid/base recovery. Still, the feed treated in this manner would result in higher divalent cation concentrations (above 33 ppm) compared to the ED concentrate (6–17 ppm).

ED technology modified with monovalent CEM had the highest DOC removal (94.1 ± 0.14 %). Mg<sup>2+</sup> and Ca<sup>2+</sup> concentrations were sufficiently low after the first ED run, whereas in the second ED run divalent cations concentration exceeded the limiting 10 ppm. Thus, the ED membrane perm-selectivity decreased in the second run and approached the values of NF membranes' perm-selectivity. ED treatment resulted in a concentration factor of up to 1.9 for monovalent cations, beneficial for the succeeding base production. The major advantage of ED compared to NF was the higher permeation of the SO<sub>4</sub><sup>2-</sup> ions and the concentration factor of 1.6 for SO<sub>4</sub><sup>2-</sup>, providing favorable conditions for sulfuric acid production via EDBM/DD. Concentration factors can be further increased by the addition of multi-stage ED treatment.

All three tested IERs had 100 % removal of Mg<sup>2+</sup> and Ca<sup>2+</sup> until the breakthrough point, among which IER C100E with the sulfonic acid functional group had the highest capacity. There was no DOC removal of the IER effluent, thus, it does not prevent EDBM/DD membranes from biofouling.

According to the energy consumption evaluation, NF requires less energy than ED. Therefore, further optimization of the ED process and membrane stability is needed to reduce energy consumption and increase membrane stability, respectively. Even though the IERs had the highest Mg<sup>2+</sup> and Ca<sup>2+</sup> removal, they are not as feasible as ED and NF due to the absence of DOC removal and requirements for an additional posttreatment and resin regeneration that generates waste.

#### CRedit authorship contribution statement

**Katarina Knežević:** Conceptualization, Methodology, Validation, Formal analysis, Investigation, Visualization. **Ernis Saracevic:** Methodology, Formal analysis, Data curation, Writing – review & editing. **Jörg Krampe:** Resources, Writing – review & editing, Supervision, Project administration, Funding acquisition. **Norbert Kreuzinger:** Conceptualization, Validation, Resources, Funding acquisition.

#### Declaration of Competing Interest

The authors declare that they have no known competing financial interests or personal relationships that could have appeared to influence the work reported in this paper.

#### Data Availability

Data will be made available on request.

#### Acknowledgment

The authors acknowledge TU Wien Bibliothek for financial support through its Open Access Funding Program. The authors acknowledge the "Bioactive" project, TU Wien, under which the study was performed. The special thanks are forwarded to the NovoArc GmbH based at TU Wien, for providing spent culture broth and to Amal Ahmed for the technical support.

#### Appendix A. Supporting information

Supplementary data associated with this article can be found in the online version at [doi:10.1016/j.jece.2022.108423](https://doi.org/10.1016/j.jece.2022.108423).

#### References

- [1] R. Mohammadi, W. Tang, M. Sillanpää, A systematic review and statistical analysis of nutrient recovery from municipal wastewater by electrodialysis, *Desalination* vol. 498 (2021), 114626, <https://doi.org/10.1016/j.desal.2020.114626>.
- [2] W.-Y. Zhao, et al., Waste conversion and resource recovery from wastewater by ion exchange membranes: state-of-the-art and perspective, *Ind. Eng. Chem. Res.* vol. 57 (18) (2018) 6025–6039, <https://doi.org/10.1021/acs.iecr.8b00519>.
- [3] EUR-Lex - 52021DC04002021., Pathway to a Healthy Planet for All EU Action Plan: "Towards Zero Pollution for Air, Water and Soil, 2021.
- [4] A.J. Ward, K. Arola, E. Thompson Brewster, C.M. Mehta, D.J. Batstone, Nutrient recovery from wastewater through pilot scale electrodialysis, *Water Res.* vol. 135 (2018) 57–65, <https://doi.org/10.1016/j.watres.2018.02.021>.
- [5] E.H. Rotta, C.S. Bitencourt, L. Marder, A.M. Bernardes, Phosphorus recovery from low phosphate-containing solution by electrodialysis, *J. Membr. Sci.* vol. 573 (2019) 293–300, <https://doi.org/10.1016/j.memsci.2018.12.020>.
- [6] A. Merkel, L. Čopák, L. Dvořák, D. Golubenko, L. Šeda, Recovery of spent sulphuric acid by diffusion dialysis using a spiral wound module, *Art. no. 21, Int. J. Mol. Sci.* vol. 22 (21) (2021), <https://doi.org/10.3390/jms222111819>.
- [7] A. Merkel, et al., Recovery of hydrochloric acid from industrial wastewater by diffusion dialysis using a spiral-wound module, *Art. no. 11, Int. J. Mol. Sci.* vol. 23 (11) (2022), <https://doi.org/10.3390/jms23116212>.
- [8] J. Wiśniewski, G. Wiśniewska, T. Winnicki, Application of bipolar electrodialysis to the recovery of acids and bases from water solutions, *Desalination* vol. 169 (1) (2004) 11–20, <https://doi.org/10.1016/j.desal.2004.08.003>.

- [9] J. Yang, et al., Porous anion exchange membrane for effective acid recovery by diffusion dialysis, *Processes* vol. 9 (6) (2021), <https://doi.org/10.3390/pr9061049>.
- [10] X. Wang, Y. Wang, X. Zhang, T. Xu, In situ combination of fermentation and electrodialysis with bipolar membranes for the production of lactic acid: Operational compatibility and uniformity, *Bioresour. Technol.* vol. 125 (2012) 165–171, <https://doi.org/10.1016/j.biortech.2012.08.125>.
- [11] X. Zhang, C. Li, Y. Wang, J. Luo, T. Xu, Recovery of acetic acid from simulated acetaldehyde wastewaters: Bipolar membrane electrodialysis processes and membrane selection, *J. Membr. Sci.* vol. 379 (1–2) (2011) 184–190, <https://doi.org/10.1016/j.memsci.2011.05.059>.
- [12] W. Gao, Q. Fang, H. Yan, X. Wei, K. Wu, Recovery of acid and base from sodium sulfate containing lithium carbonate using bipolar membrane electrodialysis, *Membranes* vol. 11 (2) (2021) 152, <https://doi.org/10.3390/membranes11020152>.
- [13] X. Sun, H. Lu, J. Wang, Recovery of citric acid from fermented liquid by bipolar membrane electrodialysis, *J. Clean. Prod.* vol. 143 (2017) 250–256, <https://doi.org/10.1016/j.jclepro.2016.12.118>.
- [14] C. Zhang, W. Zhang, Y. Wang, Diffusion dialysis for acid recovery from acidic waste solutions: anion exchange membranes and technology integration, Art. no. 8, *Membranes* vol. 10 (8) (2020), <https://doi.org/10.3390/membranes10080169>.
- [15] J.G. Wijmans, R.W. Baker, The solution-diffusion model: a review, *J. Membr. Sci.* vol. 107 (1) (1995) 1–21, [https://doi.org/10.1016/0376-7388\(95\)00102-1](https://doi.org/10.1016/0376-7388(95)00102-1).
- [16] H. Yan, S. Xue, C. Wu, Y. Wu, T. Xu, Separation of NaOH and NaAl(OH)<sub>4</sub> in alumina alkaline solution through diffusion dialysis and electrodialysis, *J. Membr. Sci.* vol. 469 (2014) 436–446, <https://doi.org/10.1016/j.memsci.2014.07.002>.
- [17] X. Tongwen, Electrodialysis processes with bipolar membranes (EDBM) in environmental protection—a review, *Resour., Conserv. Recycl.* vol. 37 (1) (2002) 1–22, [https://doi.org/10.1016/S0921-3449\(02\)00032-0](https://doi.org/10.1016/S0921-3449(02)00032-0).
- [18] J. Heinonen, Y. Zhao, B. Van der Bruggen, A process combination of ion exchange and electrodialysis for the recovery and purification of hydroxy acids from secondary sources, *Sep. Purif. Technol.* vol. 240 (2020), 116642, <https://doi.org/10.1016/j.seppur.2020.116642>.
- [19] A. Merkel, A.M. Ashrafi, J. Ecer, Bipolar membrane electrodialysis assisted pH correction of milk whey, *J. Membr. Sci.* vol. 555 (2018) 185–196, <https://doi.org/10.1016/j.memsci.2018.03.035>.
- [20] J. Yan, et al., Ion exchange membranes for acid recovery: diffusion dialysis (DD) or selective electrodialysis (SED), *Desalination* vol. 531 (2022), 115690, <https://doi.org/10.1016/j.desal.2022.115690>.
- [21] S. Mikhaylin, L. Bazinet, Fouling on ion-exchange membranes: Classification, characterization and strategies of prevention and control, *Adv. Colloid Interface Sci.* vol. 229 (2016) 34–56, <https://doi.org/10.1016/j.cis.2015.12.006>.
- [22] M. Bleha, G. Tishchenko, V. Šumberová, V. Kúdela, Characteristic of the critical state of membranes in ED-desalination of milk whey, *Desalination* vol. 86 (2) (1992) 173–186, [https://doi.org/10.1016/0011-9164\(92\)80032-5](https://doi.org/10.1016/0011-9164(92)80032-5).
- [23] H. Ren, Q. Wang, X. Zhang, R. Kang, S. Shi, W. Cong, Membrane fouling caused by amino acid and calcium during bipolar membrane electrodialysis, *J. Chem. Technol. Biotechnol.* vol. 83 (11) (2008) 1551–1557, <https://doi.org/10.1002/jctb.1969>.
- [24] J.-S. Park, T.C. Chilcott, H.G.L. Coster, S.-H. Moon, Characterization of BSA-fouling of ion-exchange membrane systems using a subtraction technique for lumped data, *J. Membr. Sci.* vol. 246 (2) (2005) 137–144, <https://doi.org/10.1016/j.memsci.2004.07.022>.
- [25] W. Cheng, et al., Selective removal of divalent cations by polyelectrolyte multilayer nanofiltration membrane: role of polyelectrolyte charge, ion size, and ionic strength, *J. Membr. Sci.* vol. 559 (2018) 98–106, <https://doi.org/10.1016/j.memsci.2018.04.052>.
- [26] N. Cifuentes-Araya, C. Astudillo-Castro, L. Bazinet, Mechanisms of mineral membrane fouling growth modulated by pulsed modes of current during electrodialysis: evidences of water splitting implications in the appearance of the amorphous phases of magnesium hydroxide and calcium carbonate, *J. Colloid Interface Sci.* vol. 426 (2014) 221–234, <https://doi.org/10.1016/j.jcis.2014.03.054>.
- [27] C. Casademont, G. Pourcelly, L. Bazinet, Effect of magnesium/calcium ratio in solutions subjected to electrodialysis: Characterization of cation-exchange membrane fouling, *J. Colloid Interface Sci.* vol. 315 (2) (2007) 544–554, <https://doi.org/10.1016/j.jcis.2007.06.056>.
- [28] P. Yu. Apel, et al., Fouling and membrane degradation in electromembrane and baromembrane processes, *Membr. Technol.* vol. 4 (2) (2022) 69–92, <https://doi.org/10.1134/S2517751622020032>.
- [29] W. Gao, et al., Membrane fouling control in ultrafiltration technology for drinking water production: a review, *Desalination* vol. 272 (1) (2011) 1–8, <https://doi.org/10.1016/j.desal.2011.01.051>.
- [30] A. Ullah, H.J. Tanudjaja, M. Ouda, S.W. Hasan, J.W. Chew, Membrane fouling mitigation techniques for oily wastewater: a short review, *J. Water Process Eng.* vol. 43 (2021), 102293, <https://doi.org/10.1016/j.jwpe.2021.102293>.
- [31] W. Cai, J. Zhang, Y. Li, Q. Chen, W. Xie, J. Wang, Characterizing membrane fouling formation during ultrafiltration of high-salinity organic wastewater, *Chemosphere* vol. 287 (2022), 132057, <https://doi.org/10.1016/j.chemosphere.2021.132057>.
- [32] X. Shi, G. Tal, N.P. Hankins, V. Gitis, Fouling and cleaning of ultrafiltration membranes: a review, *J. Water Process Eng.* vol. 1 (2014) 121–138, <https://doi.org/10.1016/j.jwpe.2014.04.003>.
- [33] K.S. Barros, M.C. Marti-Calatayud, V. Pérez-Herranz, D.C.R. Espinosa, A three-stage chemical cleaning of ion-exchange membranes used in the treatment by electrodialysis of wastewaters generated in brass electroplating industries, *Desalination* vol. 492 (2020), 114628, <https://doi.org/10.1016/j.desal.2020.114628>.
- [34] H. Li, A. Li, C. Shuang, Q. Zhou, W. Li, Fouling of anion exchange resin by fluorescence analysis in advanced treatment of municipal wastewaters, *Water Res.* vol. 66 (2014) 233–241, <https://doi.org/10.1016/j.watres.2014.08.027>.
- [35] J. Ran, et al., Ion exchange membranes: New developments and applications, *J. Membr. Sci.* vol. 522 (2017) 267–291, <https://doi.org/10.1016/j.memsci.2016.09.033>.
- [36] M. Vasselbehagh, H. Karkhanechi, S. Mulyati, R. Takagi, H. Matsuyama, Improved antifouling of anion-exchange membrane by polydopamine coating in electrodialysis process, *Desalination* vol. 332 (1) (2014) 126–133, <https://doi.org/10.1016/j.desal.2013.10.031>.
- [37] S. Mulyati, R. Takagi, A. Fujii, Y. Ohmukai, H. Matsuyama, Simultaneous improvement of the monovalent anion selectivity and antifouling properties of an anion exchange membrane in an electrodialysis process, using polyelectrolyte multilayer deposition, *J. Membr. Sci.* vol. 431 (2013) 113–120, <https://doi.org/10.1016/j.memsci.2012.12.022>.
- [38] S. Mehdizadeh, M. Yasukawa, T. Abo, Y. Kakihana, M. Higa, Effect of spacer geometry on membrane and solution compartment resistances in reverse electrodialysis, *J. Membr. Sci.* vol. 572 (2019) 271–280, <https://doi.org/10.1016/j.memsci.2018.09.051>.
- [39] K.R. Goode, K. Asteriadou, P.T. Robbins, P.J. Fryer, Fouling and cleaning studies in the food and beverage industry classified by cleaning type, *Compr. Rev. Food Sci. Food Saf.* vol. 12 (2) (2013) 121–143, <https://doi.org/10.1111/1541-4337.12000>.
- [40] G.-Q. Chen, et al., Pretreatment for alleviation of RO membrane fouling in dyeing wastewater reclamation, *Chemosphere* vol. 292 (2022), 133471, <https://doi.org/10.1016/j.chemosphere.2021.133471>.
- [41] Y. Sun, et al., Physical pretreatment of petroleum refinery wastewater instead of chemicals addition for collaborative removal of oil and suspended solids, *J. Clean. Prod.* vol. 278 (2021), 123821, <https://doi.org/10.1016/j.jclepro.2020.123821>.
- [42] H. Ma, et al., An integrated membrane- and thermal-based system for coal chemical wastewater treatment with near-zero liquid discharge, *J. Clean. Prod.* vol. 291 (2021), 125842, <https://doi.org/10.1016/j.jclepro.2021.125842>.
- [43] Y.S. Dzyazko, Purification of a diluted solution containing nickel using electrodeionization, *Desalination* vol. 198 (1) (2006) 47–55, <https://doi.org/10.1016/j.desal.2006.09.008>.
- [44] X. Tong, B. Zhang, Y. Chen, Fouling resistant nanocomposite cation exchange membrane with enhanced power generation for reverse electrodialysis, *J. Membr. Sci.* vol. 516 (2016) 162–171, <https://doi.org/10.1016/j.memsci.2016.05.060>.
- [45] D.A. Vermaas, D. Kunteng, J. Veerman, M. Saakes, K. Nijmeijer, Periodic feedwater reversal and air sparging as antifouling strategies in reverse electrodialysis, *Environ. Sci. Technol.* vol. 48 (5) (2014) 3065–3073, <https://doi.org/10.1021/es4045456>.
- [46] X. Zhang, et al., Near-zero liquid discharge of desulfurization wastewater by electrodialysis-reverse osmosis hybrid system', *J. Water Process Eng.* vol. 40 (2021), 101962, <https://doi.org/10.1016/j.jwpe.2021.101962>.
- [47] T.M. Mubita, S. Porada, P.M. Biesheuvel, A. van der Wal, J.E. Dykstra, Strategies to increase ion selectivity in electrodialysis, *Sep. Purif. Technol.* vol. 292 (2022), 120944, <https://doi.org/10.1016/j.seppur.2022.120944>.
- [48] Y.D. Ahdab, G. Schücking, D. Rehman, J.H. Lienhard, Cost effectiveness of conventionally and solar powered monovalent selective electrodialysis for seawater desalination in greenhouses, *Appl. Energy* vol. 301 (2021), 117425, <https://doi.org/10.1016/j.apenergy.2021.117425>.
- [49] M. Turek, Cost effective electroalytic seawater desalination, *Desalination* vol. 153 (1–3) (2003) 371–376, [https://doi.org/10.1016/S0011-9164\(02\)01130-X](https://doi.org/10.1016/S0011-9164(02)01130-X).
- [50] J. Quehenberger, L. Shen, S.-V. Albers, B. Siebers, O. Spadiut, Sulfolobus – a potential key organism in future biotechnology, *Front. Microbiol.* vol. 8 (2017) 2474, <https://doi.org/10.3389/fmicb.2017.02474>.
- [51] D.A. Cowan, J.H. Brown, Effect of turbulence on limiting current in electrodialysis, *Cells', Ind. Eng. Chem.* vol. 51 (12) (1959) 1445–1448.
- [52] B. Cancino-Madariaga, C.F. Hurtado, R. Ruby, Effect of pressure and pH in ammonium retention for nanofiltration and reverse osmosis membranes to be used in recirculation aquaculture systems (RAS, Aquac. Eng. vol. 45 (3) (2011) 103–108, <https://doi.org/10.1016/j.aquaceng.2011.08.002>.
- [53] C. Niewersch, A.L. Battaglia Bloch, S. Yüce, T. Melin, M. Wessling, Nanofiltration for the recovery of phosphorus — development of a mass transport model, *Desalination* vol. 346 (2014) 70–78, <https://doi.org/10.1016/j.desal.2014.05.011>.
- [54] A.W. Mohammad, Y.H. Teow, W.L. Ang, Y.T. Chung, D.L. Oatley-Radcliffe, N. Hilal, Nanofiltration membranes review: Recent advances and future prospects, *Desalination* vol. 356 (2015) 226–254, <https://doi.org/10.1016/j.desal.2014.10.043>.
- [55] Y. Zhang et al., Using a membrane filtration process to concentrate the effluent from alkaline peroxide mechanical pulping plants, p. 16, 2010.
- [56] B. Van der Bruggen, L. Braeken, C. Vandecasteele, Evaluation of parameters describing flux decline in nanofiltration of aqueous solutions containing organic compounds, *Desalination* vol. 147 (1) (2002) 281–288, [https://doi.org/10.1016/S0011-9164\(02\)00553-2](https://doi.org/10.1016/S0011-9164(02)00553-2).
- [57] U.S. Environmental Protection Agency, '2012 Guidelines for Water Reuse', EPA/600/R-12/618, vol. AR-1530, p. 643, Sep. 2012.
- [58] B. Sun, M. Zhang, S. Huang, J. Wang, X. Zhang, Limiting concentration during batch electrodialysis process for concentrating high salinity solutions: a theoretical and experimental study, *Desalination* vol. 498 (2021), 114793, <https://doi.org/10.1016/j.desal.2020.114793>.
- [59] J.M. Ortiz, et al., Brackish water desalination by electrodialysis: batch recirculation operation modeling, *J. Membr. Sci.* vol. 252 (1) (2005) 65–75, <https://doi.org/10.1016/j.memsci.2004.11.021>.

- [60] H. Selvaraj, P. Aravind, M. Sundaram, Four compartment mono selective electro dialysis for separation of sodium formate from industry wastewater, *Chem. Eng. J.* vol. 333 (2018) 162–169, <https://doi.org/10.1016/j.cej.2017.09.150>.
- [61] V. Hábová, K. Melzoch, M. Rychtera, B. Sekavová, Electro dialysis as a useful technique for lactic acid separation from a model solution and a fermentation broth, *Desalination* vol. 162 (2004) 361–372, [https://doi.org/10.1016/S0011-9164\(04\)00070-0](https://doi.org/10.1016/S0011-9164(04)00070-0).
- [62] F. Gode, E. Pehlivan, A comparative study of two chelating ion-exchange resins for the removal of chromium(III) from aqueous solution, *J. Hazard. Mater.* vol. 100 (1) (2003) 231–243, [https://doi.org/10.1016/S0304-3894\(03\)00110-9](https://doi.org/10.1016/S0304-3894(03)00110-9).
- [63] S. Rengaraj, K.-H. Yeon, S.-H. Moon, Removal of chromium from water and wastewater by ion exchange resins, *J. Hazard. Mater.* vol. 87 (1) (2001) 273–287, [https://doi.org/10.1016/S0304-3894\(01\)00291-6](https://doi.org/10.1016/S0304-3894(01)00291-6).
- [64] K. Suwannahong, et al., Selective chelating resin for copper removal and recovery in aqueous acidic solution generated from synthetic copper-citrate complexes from bioleaching of e-waste, *Adsorpt. Sci. Technol.* vol. 2022 (2022), e5009124, <https://doi.org/10.1155/2022/5009124>.
- [65] T. Sata, T. Sata, W. Yang, Studies on cation-exchange membranes having permselectivity between cations in electro dialysis, *J. Membr. Sci.* vol. 206 (1) (2002) 31–60, [https://doi.org/10.1016/S0376-7388\(01\)00491-4](https://doi.org/10.1016/S0376-7388(01)00491-4).
- [66] C. Casademont, M.A. Farias, G. Pourcelly, L. Bazinet, Impact of electro dialytic parameters on cation migration kinetics and fouling nature of ion-exchange membranes during treatment of solutions with different magnesium/calcium ratios, *J. Membr. Sci.* vol. 325 (2) (2008) 570–579, <https://doi.org/10.1016/j.memsci.2008.08.023>.
- [67] K. Chon, N. Jeong, H. Rho, J.-Y. Nam, E. Jwa, J. Cho, Fouling characteristics of dissolved organic matter in fresh water and seawater compartments of reverse electro dialysis under natural water conditions, *Desalination* vol. 496 (2020), 114478, <https://doi.org/10.1016/j.desal.2020.114478>.
- [68] T. Luo, S. Abdu, M. Wessling, Selectivity of ion exchange membranes: a review, *J. Membr. Sci.* vol. 555 (2018) 429–454, <https://doi.org/10.1016/j.memsci.2018.03.051>.
- [69] M. Irfan, T. Xu, L. Ge, Y. Wang, T. Xu, Zwitterion structure membrane provides high monovalent/divalent cation electro dialysis selectivity: Investigating the effect of functional groups and operating parameters, *J. Membr. Sci.* vol. 588 (2019), 117211, <https://doi.org/10.1016/j.memsci.2019.117211>.
- [70] P. Samanta, H.M. Schönert, H. Horn, F. Saravia, MF–NF treatment train for pig manure: nutrient recovery and reuse of product water, *Membranes* vol. 12 (2) (2022), <https://doi.org/10.3390/membranes12020165>.
- [71] B.A.M. Al-Rashdi, D.J. Johnson, N. Hilal, Removal of heavy metal ions by nanofiltration, *Desalination* vol. 315 (2013) 2–17, <https://doi.org/10.1016/j.desal.2012.05.022>.
- [72] M. Khosravi, G. Badalians Gholikandi, A. Soltanzadeh Bali, R. Riahi, H. R. Tashauoui, Membrane process design for the reduction of wastewater color of the mazandaran pulp-paper industry, *Iran Water Resour. Manag.* vol. 25 (12) (2011) 2989–3004, <https://doi.org/10.1007/s11269-011-9794-1>.
- [73] N.Y. Yip, M. Elimelech, Comparison of energy efficiency and power density in pressure retarded osmosis and reverse electro dialysis, *Environ. Sci. Technol.* vol. 48 (18) (2014) 11002–11012, <https://doi.org/10.1021/es5029316>.
- [74] T. Rottiers, G. De la Marche, B. Van der Bruggen, L. Pinoy, Co-ion fluxes of simple inorganic ions in electro dialysis metathesis and conventional electro dialysis, *J. Membr. Sci.* vol. 492 (2015) 263–270, <https://doi.org/10.1016/j.memsci.2015.05.066>.
- [75] C. Blöcher, C. Niewersch, T. Melin, Phosphorus recovery from sewage sludge with a hybrid process of low pressure wet oxidation and nanofiltration, *Water Res.* vol. 46 (6) (2012) 2009–2019, <https://doi.org/10.1016/j.watres.2012.01.022>.
- [76] H. Strathmann, in: R.D. Noble, S.A. Stern (Eds.), Chapter 6 Electro dialysis and related processes, in *Membrane Science and Technology*, vol. 2, Elsevier, 1995, pp. 213–281, [https://doi.org/10.1016/S0927-5193\(06\)80008-2](https://doi.org/10.1016/S0927-5193(06)80008-2).
- [77] A. Gonzalez-Vogel, J.J. Moltedo, O.J. Rojas, Desalination by pulsed electro dialysis reversal: approaching fully closed-loop water systems in wood pulp mills, *J. Environ. Manag.* vol. 298 (2021), 113518, <https://doi.org/10.1016/j.jenvman.2021.113518>.
- [78] G. Doornbusch, H. Swart, M. Tedesco, J. Post, Z. Borneman, K. Nijmeijer, Current utilization in electro dialysis: electrode segmentation as alternative for multistaging, *Desalination* vol. 480 (2020), 114243, <https://doi.org/10.1016/j.desal.2019.114243>.
- [79] B.F. Severin, T.D. Hayes, Effect of electrode rinse solutions on the electro dialysis of concentrated salts, *Sep. Purif. Technol.* vol. 274 (2021), 119048, <https://doi.org/10.1016/j.seppur.2021.119048>.
- [80] M. Greiter, S. Novalin, M. Wendland, K.-D. Kulbe, J. Fischer, Desalination of whey by electro dialysis and ion exchange resins: analysis of both processes with regard to sustainability by calculating their cumulative energy demand, *J. Membr. Sci.* vol. 210 (1) (2002) 91–102, [https://doi.org/10.1016/S0376-7388\(02\)00378-2](https://doi.org/10.1016/S0376-7388(02)00378-2).

## Supplement 2 – Comparison of ion removal from waste fermentation effluent by nanofiltration, electrodialysis and ion exchange for a subsequent sulfuric acid recovery

Katarina Knežević\*, Ernis Saracevic, Jörg Krampe, Norbert Kreuzinger  
Institute for Water Quality and Resource Management, TU Wien, Vienna, Austria

\*Corresponding author's e-mail: [katarina.knezevic@tuwien.ac.at](mailto:katarina.knezevic@tuwien.ac.at)

### APPENDIX A

It can be assumed that limiting current density (LCD) is governed by the transport of monovalent ions due to their larger transport numbers compared to divalent ions [1]. Thus, four NaCl solutions with decreasing concentration (12.4–0.6 g/L) were prepared to determine the ED stack's LCD with AEM and mCEM. The first NaCl solution matched the conductivity of the treated fermentation effluent, whereas the other three imitated decreasing diluate concentration during the ED demineralization. According to the Cowan and Brown [2] plots, an LCD was found for each NaCl solution and plotted against the solution's conductivity (Figure A1). The obtained correlation was linear, and LCD values were multiplied by a safety factor 0.8 to establish operating current density for the ED experiments with fermentation effluent. These four values were applied step-wise, from highest to lowest, until the diluate conductivity decreased to ~1 mS/cm.

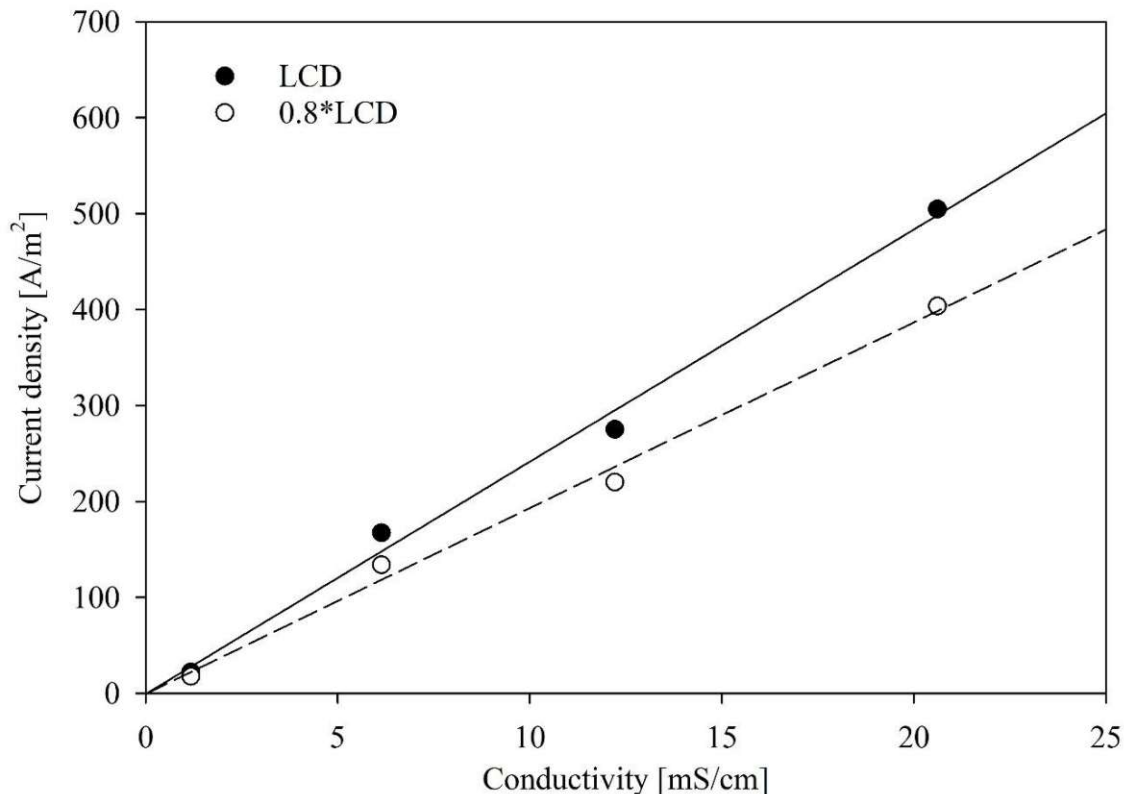
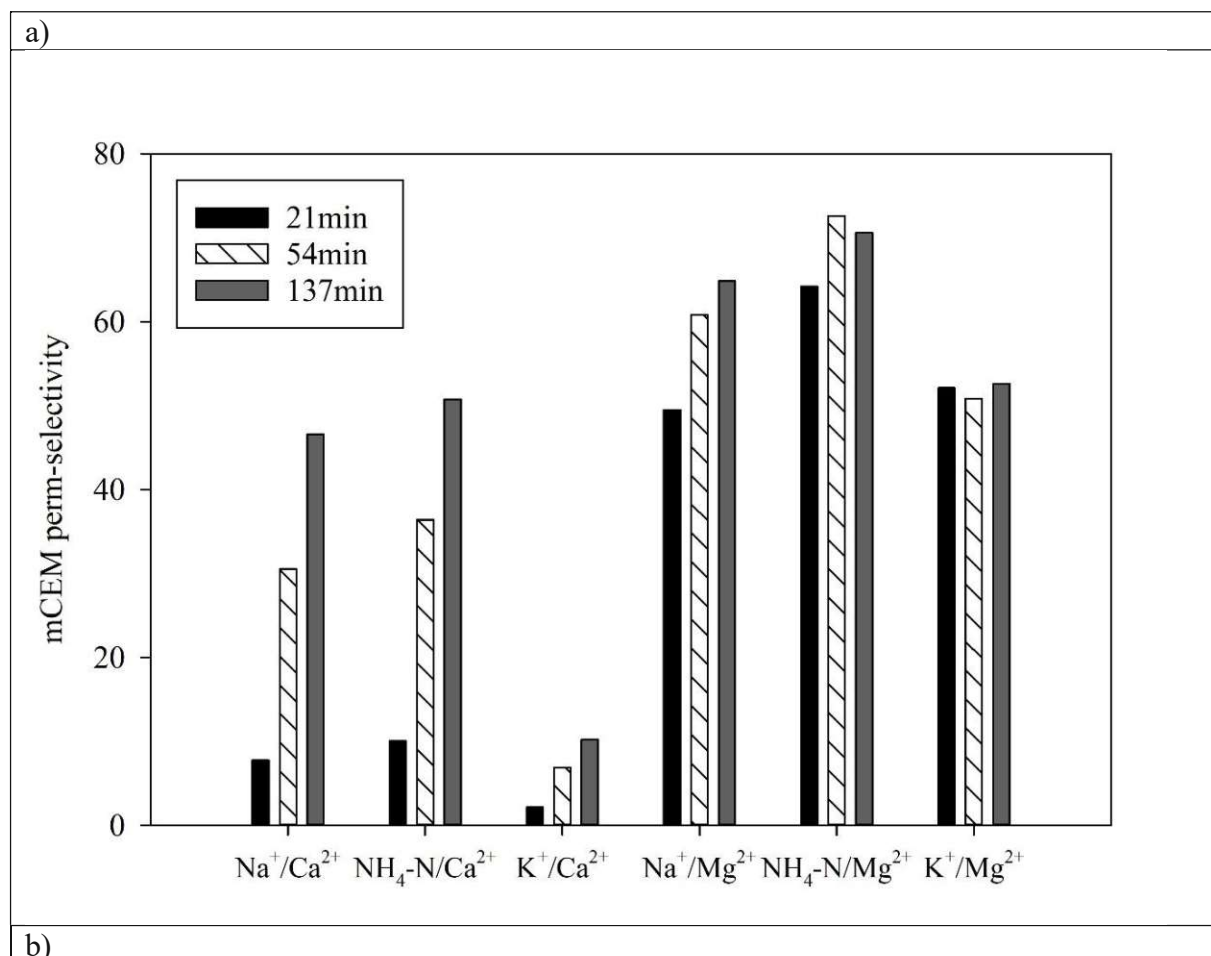
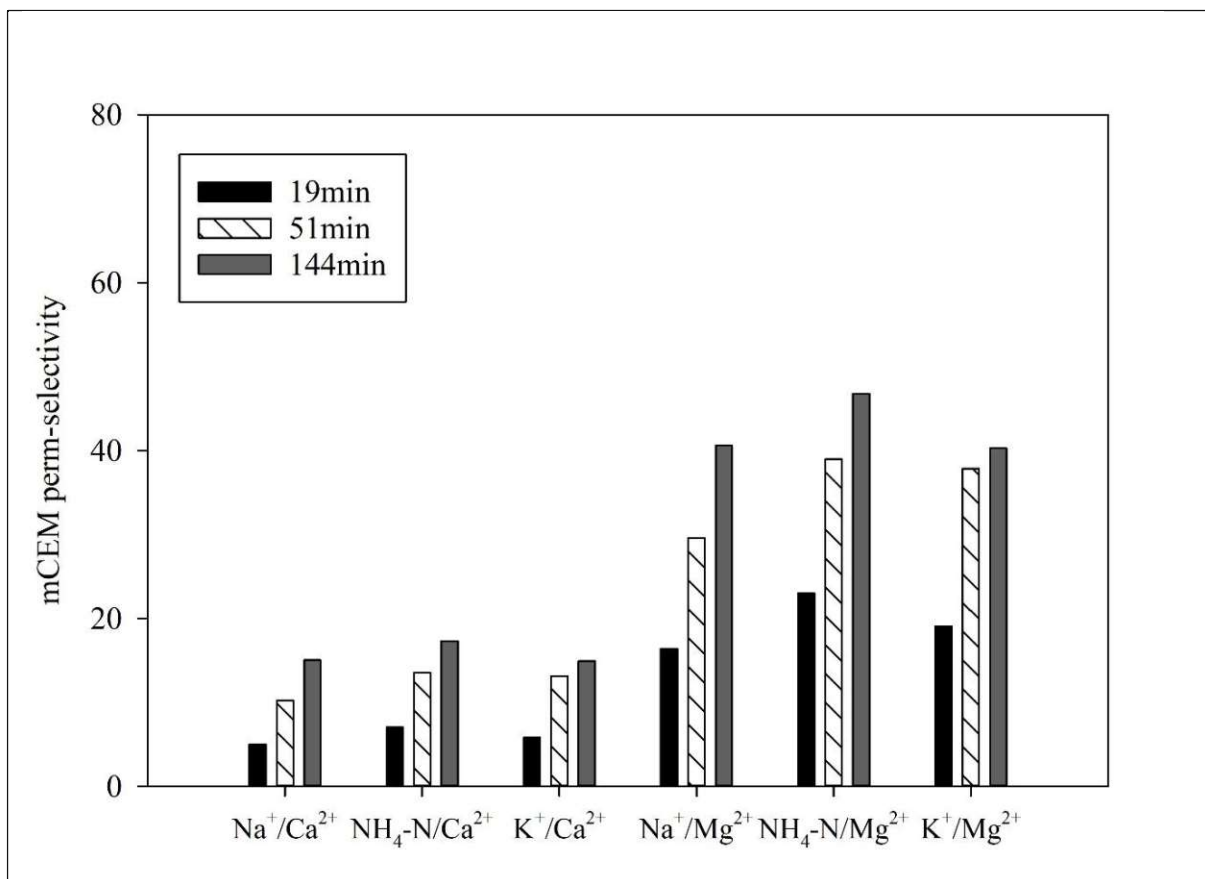


Figure A1. Limiting current density and operating current density (0.8LCD) plotted against the feed conductivity.

## APPENDIX B

Perm-selectivities were determined for three sampling points during the ED process, at average current densities of 209.4 A/m<sup>2</sup>, 143.8 A/m<sup>2</sup> and 78.1 A/m<sup>2</sup>, for both first and the second ED run (Figure B1). The sampling points were accordingly at process time 21 min, 54 min and 137 min for the first ED run (Figure B1a), and 19 min, 51 min and 144 min for the second ED run (Figure B1b). Perm-selectivity of Na<sup>+</sup>, NH<sub>4</sub><sup>+</sup> and K<sup>+</sup> against Mg<sup>2+</sup> was in general higher than for the same monovalent cations against Ca<sup>2+</sup>. This trend can be assigned to the larger Stokes radius (3.47 > 3.10 Å) and smaller self-diffusion coefficient (0.705·10<sup>-9</sup> < 0.793·10<sup>-9</sup> m<sup>2</sup>/s) of Mg<sup>2+</sup> than for Ca<sup>2+</sup> ions [3]. With decreasing diluate ion concentration and current density, the perm-selectivities were increasing, indicating a positive effect of these two parameters on the overall membrane selectivity. However, in the second ED run the perm-selectivities decreased drastically, up to 67% for e.g. Na<sup>+</sup>/Mg<sup>2+</sup> ratio after first 20 min of the ED process when first and the second ED run were compared. With prolonged ED operation time the discrepancy between the membrane selectivity of two ED runs became even more pronounced. When the fluxes of divalent cations through the mCEM of the first and the second ED run were compared, a significant increase could be observed (Figure 4b). The initially higher fluxes (first 20 min) are assigned to the very low ionic strength in the concentrating compared to diluting chamber, as it can be seen from Figure 6 and Figure 2. These values drop by 50% for Ca<sup>2+</sup> and 40% for Mg<sup>2+</sup> with the increasing concentrate concentration. Further on, an above 2 times increased Mg<sup>2+</sup> and Ca<sup>2+</sup> flux in the second ED run was recorded (Figure 4b), as explained in Section 3.5 of the main document.

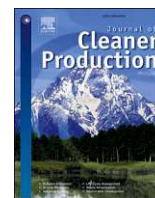




**Figure B1.** Perm-selectivity between mono- and divalent cations through mCEM in ED runs; a) in the first ED run, and b) in the second ED run.

## REFERENCES

- [1] D. Rehman, Y. D. Ahdab, and J. H. Lienhard, ‘Monovalent selective electro dialysis: Modelling multi-ionic transport across selective membranes’, *Water Research*, vol. 199, p. 117171, Jul. 2021, doi: 10.1016/j.watres.2021.117171.
- [2] D. A. Cowan and J. H. Brown, ‘Effect of Turbulence on Limiting Current in Electro dialysis Cells’, *Industrial & Engineering Chemistry*, vol. 51, no. 12, pp. 1445–1448, 1959.
- [3] T. Luo, S. Abdu, and M. Wessling, ‘Selectivity of ion exchange membranes: A review’, *Journal of Membrane Science*, vol. 555, pp. 429–454, Jun. 2018, doi: 10.1016/j.memsci.2018.03.051.



## Circular production – Evaluation of membrane technologies for nutrient recycling from a microbial fermentation effluent

Katarina Knežević<sup>a,\*</sup>, Kerstin Rastädter<sup>b</sup>, Julian Quehenberger<sup>b</sup>, Oliver Spadiut<sup>b</sup>, Jörg Krampe<sup>a</sup>, Norbert Kreuzinger<sup>a</sup>

<sup>a</sup> Institute for Water Quality and Resource Management, TU Wien, 1040, Vienna, Austria

<sup>b</sup> Research Division Biochemical Engineering, Institute of Chemical, Environmental and Bioscience Engineering, Faculty of Technical Chemistry, TU Wien, 1060, Vienna, Austria

### ARTICLE INFO

Handling Editor: Mingzhou Jin

#### Keywords:

Electrodialysis  
Bipolar electro dialysis  
Fermentation  
Wastewater  
Nutrient recovery

### ABSTRACT

The present study demonstrates a detailed analysis of nutrient recovery from the spent fermentation broth of *S. acidocaldarius*, an archaeon with high industrial and pharmaceutical potential. The pathways of the resource recovery by the lately recognized environmental-friendly and cost-effective technologies nanofiltration (NF), electrodialysis (ED), and electrodialysis with bipolar membranes (EDBM) were assessed. In contrast to previous research, this study treated real wastewater and tested the reuse of recovered products in the subsequent batch fermentations. Ions were separated from the rest of the medium by NF, with 78–85% DOC removal and 0.74 kWh/m<sup>3</sup>. ED achieved a 1.7 concentration factor for ions, 96% DOC removal and 0.51–0.74 kWh/kg of removed salts. EDBM coupled with NF removed 94.8–98.1% DOC while recovering 0.11–0.15 M sulfuric acid from the feed containing 6.1–16.7 g/l of SO<sub>4</sub><sup>2-</sup> with energy consumption of 2.7–3 kWh/kgH<sub>2</sub>SO<sub>4</sub>. Recovered media were successfully applied for control fermentations. While NF was less energy-consuming, ED/EDBM offered a selective ion recovery, higher concentration factors and reuse-specific streams. The discharges of NF/ED/EDBM showed reduced negative environmental impacts due to the nutrient removal from the waste fermentation effluent. All applied technologies require a post-treatment to remove organic substances from side streams and close the production loop with a near-to-zero liquid and waste discharge.

### 1. Introduction

The growing and aging world population is driving demand for increased industrial development. Among all industrial sectors, the food and pharmaceutical industries have a major impact on excessive water consumption and increased release of toxic substances into land or water reservoirs (Ahmad et al., 2019; Milanese et al., 2020).

Microbial fermentation processes play a substantial part in producing e.g. alcoholic beverages, lactic acid, proteins, and enzymes. Carbon sources, macronutrients (N, P, S), micronutrients (K, Ca, Mg, Na, Fe), and trace elements (Mn, Zn, Co, Mo, Ni, and Cu) dissolved in water (Stanbury et al., 2017) are needed to ensure microbial growth and a high production rate. The practice of excessive supply of nutrients and trace elements to avoid growth and production limitations results in a

nutrient-rich waste fermentation effluent. The spent culture broth may also contain high organic load or toxic substances (Khan et al., 2020; Wei et al., 2021).

Direct discharge of raw wastewater from industrial processes to inland waters, coastal ecosystems, and oceans causes severe damage to biodiversity, eutrophication, ecosystem unbalances, toxic algal bloom and anoxic zones (ESPP, 2021). The destruction of the environment also presents a serious health risk for humans (Porwal et al., 2015). These effluents require wastewater treatment regulation.

The awareness in the food and pharmaceutical industries of the negative environmental effects of effluents and by-products as well as the need for a cleaner and environmentally friendly production is rising (Chandra et al., 2018; Veleva & W. Cue Jr, 2017).

The pollution control emerging from manufacturing industries

**Abbreviations:** ED, electrodialysis; EDBM, electrodialysis with bipolar membranes; IEM, ion exchange membrane; MF, microfiltration; NF, nanofiltration; SCB, spent culture broth; UF, ultrafiltration; VD, reference medium; CE, % current efficiency; E kWh/kg, energy consumption; Rd %, demineralization rate (total removal efficiency); RE %, removal efficiency; Rs %, recovery/conversion rate; wi, mass fraction.

\* Corresponding author.

E-mail address: [katarina.knezevic@tuwien.ac.at](mailto:katarina.knezevic@tuwien.ac.at) (K. Knežević).

<https://doi.org/10.1016/j.jclepro.2022.134436>

Received 28 April 2022; Received in revised form 6 September 2022; Accepted 28 September 2022

Available online 4 October 2022

0959-6526/© 2022 The Authors. Published by Elsevier Ltd. This is an open access article under the CC BY license (<http://creativecommons.org/licenses/by/4.0/>).

themselves has traditionally aimed to reduce the concentration of organic matter and remove potential pathogens in wastewater (Wheatley, 1984). Genetic modifications of microorganisms and recognition of the side effects of e.g. excess phosphorus, sulfate and nitrogen species released in water bodies has led to the introduction of new requirements for wastewater treatment (Howarth, 2008; Wheatley, 1984). The most common treatment methods are wetland, physico-chemical (coagulation/flocculation) and biological (activated sludge) treatment (Ahmad et al., 2019). These methods are mainly focused on wastewater purification without effective waste utilization.

In last few decades, wastewater has become recognized as containing a valuable store of scarce elements such as P and Mg<sup>2+</sup>. Rather than simply regulating nutrient discharge from a regulatory and legislative perspective (European Environment Agency, 2019), novel approaches are needed to synergize nutrient removal and nutrient recycling (ESPP, 2021). Resource recovery is still challenging for full-scale applications (Hamza et al., 2022), but some centralized wastewater treatment plants have recently been retrofitted as water resource recovery facilities (Faragò et al., 2021). Wet chemical technology, crystallization/precipitation and adsorption are commonly applied in nutrient recovery from sludge or sludge-derived ash (Egle et al., 2016; Liu et al., 2021; H. Wu and Vaneckhaute, 2022). However, end-of-pipe environmental standards should be replaced by pollution prevention through cleaner production, e.g. based on 5 R policy (Olguín et al., 2004). The generation of waste should be tackled at source, comprising reduction, replacement, reuse, recovery and recycling strategies (T. Y. Wu et al., 2009) and diminishing resource scarcity. Membrane technologies, such as nanofiltration (NF), electrodialysis (ED) and electrodialysis with bipolar membranes (EDBM), are seen as attractive methods for nutrient recovery (Blöcher et al., 2012; Wang et al., 2013; Xie et al., 2016; Y. Ye et al., 2020).

NF offers a highly effective means of removing organics and divalent cations. ED is especially promising because it allows removal of organics and concentrates ions and EDBM provides direct acid/base production from ions contained in waste streams (Xie et al., 2016).

The available literature suggests a lack of information derived from experimental research of membrane technologies for nutrient recovery from real wastewater samples. Further challenges include the ability of membranes to retain potentially harmful compounds, which may be present in wastewater but are not included in experiments with synthetic solutions. Moreover, there is a knowledge gap in actual application of recovered nutrients in biotechnological processes. This study offers a path for implementing resource-recovery technologies in the early stage of process planning and optimization to tackle both the resource scarcity and negative environmental impacts of industrial wastewater.

Fermentation with archaeon *Sulfolobus acidocaldarius* is recognized as a future industrial process (Chambers and Patrick, 2015) because archaeal lipids could be used as drug vehicles, vaccine and gene delivery (Benvegnu et al., 2009; Quehenberger et al., 2017). Although the culture medium for *S. acidocaldarius*' growth and biomass yield has been optimized via salt and trace elements reduction (Quehenberger et al., 2019), there are still many valuable compounds in the waste fermentation effluent, also known as a spent culture broth (SCB). Sulfuric acid is commonly used for maintaining pH 3 of the substrate during this fermentation, leading to a generation of wastewater with a low pH value and high sulfate concentration. Decentralized SCB treatment could ensure a maximum recovery of the residual nutrients from SCB and their reuse in the same fermentation process, making production and products fit for a climate-neutral, resource-efficient, circular economy (European Union, 2020).

The present proof-of-concept study applied a circular production concept with near-to-zero liquid and waste discharge to recover water and value products from SCB of the biofermentation with the Archaeon *S. acidocaldarius*. The nutrient recovery also contributes to the reduction of pollution potential. Three emerging technologies were investigated in this regard. The indistinct recovery of macro- and micronutrients was evaluated by nanofiltration and ED. EDBM was assessed for the sulfuric acid recovery and base production. Pre-treatment technologies such as micro- and ultrafiltration of SCB were applied to remove mainly organic SCB constituents. Products resulting from the technical recovery processes were reused within an *S. acidocaldarius* fermentation to prove applicability. Microbial growth and production were compared to those obtained by fresh growth medium. The novelty of this study lies in the detailed analysis of nutrient recovery from spent fermentation broth of *S. acidocaldarius*, an archaeon with high industrial and pharmaceutical potential.

## 2. Material and methods

### 2.1. Experimental set-up

Fig. 1 shows the process scheme with the technologies assessed in this study. Products from the continuous fermentation with *S. acidocaldarius* were separated from SCB with a ceramic filter. The collected SCB was stored at 4 °C until further use. After the pre-filtration in stage I ("I" in Fig. 1), SCB was further treated by ED (stage II) to increase the ionic concentration or by EDBM (stage III) to produce acid/base. The ED concentrate obtained, enriched with nutrients, was finally used as a cultivating medium in shake-flask fermentation experiments to demonstrate its usability. The acid recovered via EDBM from SCB was reused for the fermentation pH adjustment in the same experiments. The base produced via EDBM may be applied to neutralize the diluents from ED and EDBM. Micro- and nanofiltered SCB were used as an additional control cultivation medium to evaluate the media obtained via ED/EDBM.

### 2.2. Pre-treatment

SCB (see Supplement) contains organic compounds such as residual microbial cells, peptones, pyruvate, and metabolites that interfere with cell growth (Soma et al., 2021) and must be removed from the recycling process. SCB was microfiltered (MF) after the storage period to ensure removal of suspended solids and proteins. The pH, conductivity and DOC content of the SCB and microfiltered SCB were almost identical. Ultrafiltration (UF) and nanofiltration (NF-DK) were applied in a separate set-up for further removal of dissolved organics and divalent cations of SCB, as EDBM is sensitive to the precipitation of divalent cations on the EDBM membranes (Irfan et al., 2019; Tongwen, 2002). Applied pressures were 4.5 bar, 9 bar, and 20 bar, for the MF, UF, and NF, respectively. Table 1 shows the specifications of applied membranes. The NF270 membrane was used to provide a substrate for the control cultivation.

### 2.3. ED and EDBM

The experiments were done in a batch laboratory-scale ED system PCCell ED 64-004 (PCCell GmbH, Germany) with ten cell pairs, composed of 9 x PC SA and 10 x PC SK membranes (Table 2). The effective membrane area was 8 x 8 cm<sup>2</sup>. Spacer thickness was 0.45 mm for each stack. Electrodes were Pt/Ir-coated titanium anode and V4A steel cathode, placed in the polypropylene electrode housing material. A

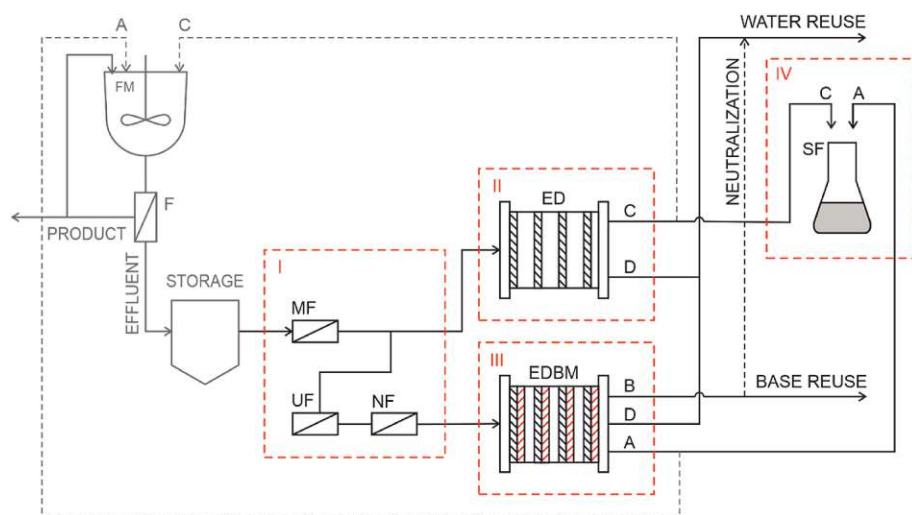


**Fig. 1.** Process scheme with four assessed stages: I Pre-treatment by MF or UF/NF, II Conventional electro dialysis (ED), III Electro dialysis with bipolar membranes (EDBM), IV Shake flask fermentation (SF). Other involved technologies: FM – fermentation, F – filtration, MF – microfiltration, UF – ultrafiltration, NF – nanofiltration. Relevant streams: Product, Effluent, C – concentrate, D – diluate, A – acid, B – base, Neutralization, Water, and Base Reuse. Processes with grey lines are not in the scope of this work.

**Table 1**  
Membranes applied in the pre-treatment of SCB with the specifications of the manufacturers.

Membrane class	Manufacturer	Model	Material	Stabilized salt rejection (%)	pH 25 °C	MWCO (Da)	Max P (bar)	Max. Temp. °C
MF	SUEZ	JX	PVDF	None	1–11	0.3 μm	5	70
UF	SUEZ	PW	PS/PES	None	1–11	20K	10	70
NF	SUEZ	DK	PA-TFC	98% MgSO <sub>4</sub>	2–10	200	40	80
NF	DUPONT	NF270	PA-TFC	>97% MgSO <sub>4</sub>	2–11	200–400	41	45

**Table 2**  
Ion exchange membranes and their specifications from the manufacturer.

Membrane	Type	Thickness, μm	Transference number	Resistance, Ohm cm <sup>2</sup>	Water content (wt%)	pH stability
PC SA	Anion exchange	100–110	>0.95	1.8	14	0–9
PC SK <sup>a</sup>	Cation exchange	100–120	>0.95	2.5	9	0–11
PC MTE	End membrane	220	>0.94	4.5	–	1–13
PC bip <sup>a</sup>	Bipolar	200–350	>0.95 **	–	–	0–12
PC Acid 60 <sup>a</sup>	Anion exchange	100–110	>0.95	2	17	0–9

<sup>a</sup> IEMs of the EDBM stack; \*\*water-splitting efficiency.

direct current power supply was applied to adjust the current/voltage driving force.

Current/voltage control was conducted in a stepwise adaptation of the current density based on the decreasing conductivity of the diluate during the ED separation process. Current density-voltage pairs were estimated based on the Cowan and Brown limiting current density method (Cowan and Brown, 1959). More information on current/voltage control is in Supplement. The diluate chamber was fed with 1 L of microfiltered SCB, while the concentrate was filled with 1 L of deionized water spiked with 250 mg/L Na<sub>2</sub>SO<sub>4</sub> providing initialization ions for ED. The concentrate chamber was used as a receiving medium for ions from SCB feed, whereas contaminants, proteins, and DOC were mostly retained by the ion exchange membranes (IEM).

Generation of mainly H<sub>2</sub>SO<sub>4</sub> acid and bases from the SCB salt content was studied using the same laboratory-scale ED 64-004 PCCell equipment, exchanging the ED stack with an EDBM stack. All IEMs used are described in Table 2 and comprise the same effective area and end

membranes as described above for ED. Diluate was fed with 1 L of nanofiltered SCB (NF-DK), while the acid/base chamber was filled with 0.5 L deionized water. Current/voltage control was conducted by interchanging the constant current/voltage approach. 12 V were applied to induce the separation of water molecules within the bipolar membrane until the conductivity of product solutions reached at least 0.4 mS/cm. Following this, the constant current of 109 A/m<sup>2</sup> was applied until no significant changes in the electrical conductivity of produced acid/base were observable.

The ED/EDBM feed solutions were circulated at 15 L/h flowrate. Electrode rinsing solution was 0.25 M Na<sub>2</sub>SO<sub>4</sub>, circulated at 120 L/h flowrate. Process cooling was achieved with tap water circulating through double-wall tanks containing the solutions. Online monitoring of conductivity and temperature was conducted every 2 s. The pH of the feed solution (SCB) was recorded continuously.

**Table 3**  
Overview of shake flask experiments.

Fermentation	Medium	Medium gained through	Acid to set pH
1	VD	Reference Medium	H <sub>2</sub> SO <sub>4</sub> (4.8%)
2	ED 1	Electrodialysis	H <sub>2</sub> SO <sub>4</sub> (4.8%)
3	ED 2	Electrodialysis	H <sub>2</sub> SO <sub>4</sub> (4.8%)
4	NF270	Nanofiltration	H <sub>2</sub> SO <sub>4</sub> (4.8%)
5	MF	Microfiltration	Base B2 (EDBM2)
6	VD	Reference Medium	Acid A1 (EDBM1)
7	VD	Reference Medium	Acid A2 (EDBM2)
8	ED 1	Electrodialysis	Acid A2 (EDBM2)

#### 2.4. Analytical methods

Ions in all liquid streams were analyzed by ion chromatography for the following ions: PO<sub>4</sub>-P, NH<sub>4</sub>-N, anions (Cl<sup>-</sup>, SO<sub>4</sub><sup>2-</sup>) and cations (Na<sup>+</sup>, K<sup>+</sup>, Ca<sup>2+</sup>, Mg<sup>2+</sup>), based on DIN EN ISO 6878, DIN EN ISO 11732, DIN EN ISO 10304-1 and DIN EN ISO 14911, respectively. Trace elements (Co, Cu, Zn, Mo, Cr, and Ni) were below detection limits. Dissolved organic carbon (DOC) was analyzed using the standard DIN EN 1484 method.

#### 2.5. Cultivation of *Sulfolobus acidocaldarius* in recycled media

To minimize evaporation, *S. acidocaldarius* DSM 639 was grown aerobically in a 75 °C temperate shaking oil bath in 100 mL long-neck Erlenmeyer flasks. Shake-flasks were filled with 50 mL medium. The medium described by Quehenberger et al. (2019) was used as a reference medium and is denoted as “VD basal” (= medium without carbon sources). Recovered media used for the growth experiments were from all process steps, including ED1, ED2, NF, and MF gained from SCB, as described in Table 3. Acid A1&2 and Base B2 are recovered/produced solutions from SCB by EDBM1&2 (see Section 3.3). The following carbon sources were added to 50 mL of medium (recovered and reference): 1.79 g/L monosodium glutamate (MSG), 3 g/L D-glucose, and 0.5 g/L citric acid. The initial pH was set to 3.0, either with 4.8% H<sub>2</sub>SO<sub>4</sub> or recovered acid. All shake-flask fermentations were conducted in duplicate except the reference medium, which was conducted in triplicate. Since the oil bath only holds a limited number of shake flasks, the experiments were performed in two runs. Each run contained a set of three reference medium shake flasks.

2 mL of the culture broth from the shake-flasks were extracted after the lag-phase approximately every 24 h (see Results) to compare the growth of *S. acidocaldarius* in the fermentation experiments using the media described in Table 3. Optical density, OD<sub>600</sub>, was determined with a spectrophotometer (ONDA V-10 PLUS, XS instruments, Italy) at 600 nm against a blank of distilled water. Samples were diluted with deionized water to ensure they remained within the linear range of the photometer. 1 mL of culture broth was centrifuged for 10 min at 10,000 g and 4 °C. The obtained supernatant was used for substrate and metabolite determination by chemical analysis. Glutamic acid and D-glucose concentrations were determined via a photometric assay using a Cedex Bio HT Analyzer (Roche, Switzerland). The concentration of glutamic acid obtained was converted to the used substrate MSG by multiplication by the factor 1.15. Possible metabolites, such as pyroglutamic acid, were identified with an Aminex HPX-87H column (300 × 7.8 mm, Bio-Rad, USA) employing an Ultimate 3000 high-performance liquid chromatography (HPLC) system (Thermo Fisher Scientific, USA). 10 µL samples were analyzed at a flow rate of 0.6 mL/min, and a column temperature of 60 °C. 4 mM H<sub>2</sub>SO<sub>4</sub> served as the mobile phase. A RI detector (RefractoMax 520, Thermo Fisher Scientific, USA) and a UV

detector (VH-D10-A, Thermo Fisher Scientific, USA) at 210 nm were used for quantitative determination. The Chromeleon 7.2.6 Chromatography Data System (Thermo Fisher Scientific, Waltham/MA, USA) was used for control and data analysis.

#### 2.6. Data analysis

The slopes of the diluate/concentrate electrical conductivities were calculated to estimate the average rate of total ion migration from the diluate to the concentrate, depending on the ED operation time. Slopes were determined for a specific segment of applied current density as follows:

$$s = \frac{y_n - y_{n-1}}{x_n - x_{n-1}} \quad (1)$$

where  $x$  is the ED operation time at two subsequent time points  $n$  and  $n-1$  on the  $x$ -axis, and  $y$  are the corresponding diluate/concentrate conductivity values on the  $y$ -axis.

Transport phenomena such as osmosis and electro-osmosis were determined from the differences between the slopes ( $\Delta s$ ) of the diluate and concentrate for the same ED timeframe and applied current density according to the following equation:

$$\Delta s = s_{\text{diluate}} + s_{\text{concentrate}} \quad (2)$$

where the diluate ( $s_{\text{diluate}}$ ) has a negative slope due to the ionic depletion, and the concentrate ( $s_{\text{concentrate}}$ ) has a positive slope due to the increasing conductivity with increasing ionic concentration.

Total desalination rate ( $RE$ ), removal efficiency ( $RE_i$ ), and the ratio of ions present in the ED feed and the ED concentrate (mass fractions  $w_i$ ) were calculated to assess the ED performance.

Removal efficiency (%):

$$RE = \frac{\lambda_D^0 - \lambda_D^f}{\lambda_D^0} \cdot 100\%$$

or

$$RE_i = \frac{n_i^0 - n_i^f}{n_i^0} \cdot 100\% \quad (3)$$

$\lambda_D$  [mS/cm] is the conductivity of the feed solution (diluate) at the time 0 and final desalination point;  $n_i^0$  and  $n_i^f$  are the molar concentrations [mol/L] of the ion  $i$  at the time 0 and the final time, respectively.  $RE_i$  in EDBM was calculated based on the number of milliequivalents of anions/cations  $n_{Eq,i}$  [mEq] in the initial and final diluate.

Mass fraction:

$$w_i = \frac{m_i^c}{m_i^f} \quad (4)$$

where  $m_i^c$  [g] is the mass of ion  $i$  transported in each desalination step from diluate to the concentrate solution,  $m_i^f$  [g] is the mass of ion  $i$  in feed. In the first ED run, the maximum possible value of  $w_i$  is 1, meaning that all of the ionic species  $i$  is removed from the feed and transferred to the concentrate. The ions were concentrated in the subsequent ED run and the maximum possible value of  $w_i$  is 2, denoting the doubled concentration of ion  $i$  in the concentrate compared to its content in SCB.

The current efficiency ( $CE$ ) was calculated to determine how much of the externally applied electrical field is used for the removal of ions from the diluate compartment:

$$CE = \frac{F \sum (n_i^0 - n_i^f)}{N \cdot \int_0^t Idt} \cdot 100\% \quad (5)$$

where  $n_i$  [mol] is the mole number of each anion/cation at time 0 and final desalination point.  $CE$  is calculated separately either for all cations or all anions, as their removal happens simultaneously but in the opposite directions.  $F$  is the Faraday constant (96485 sA/mol).  $N$  is the number of cell pairs ( $N = 10$  in this case).  $I$  [A] is the stack current, and  $t$  [s] is the desalination time.

Energy consumption to remove and concentrate ions in the ED set-up and the energy consumption to produce sulfuric acid in the EDBM set-up was calculated:

$$E = \int \frac{UIdt}{c_i V}$$

or

$$E = \int \frac{UIdt}{Mc_i V} \quad (6)$$

where  $U$  [A] is the voltage across ED/EDBM stack,  $c_i$  [kg/L] is the salt concentration,  $M$  [g/mol] is the molar mass of  $H_2SO_4$  ( $M = 98.079$  g/mol).

Recovery/conversion rate of salts to acid/base (%) was calculated to determine how efficient the anions/cations are transferred to the corresponding acid/base in the EDBM set-up:

$$R_s = \frac{n_a^f}{n_s^0} \cdot 100\% \quad (7)$$

where  $n_a^f$  [mEq] is the final equivalent mole number of acids/bases, and  $n_s^0$  [mEq] is the initial equivalent mole number of anions/cations in feed.

### 3. Results

#### 3.1. Results of membrane filtration

Filtration steps (Table S2) resulted in 31% DOC removal by UF, 78% by NF(DK) and 89% by NF270. NF(DK) removed above 98% divalent cations, around 30% of the monovalent  $Na^+$  and  $K^+$ , and 40% of  $SO_4^{2-}$ . NF270 had lower divalent cation retention (90%) than NF(DK). Thus, the NF(DK) permeate was forwarded to EDBM, whereas the NF270 permeate was directly subjected to the fermentation trials. The energy required for pumps in UF was 0.85 kWh/m<sup>3</sup> and in NF was 0.74 kWh/m<sup>3</sup> of SCB.

#### 3.2. Results from ED

Microfiltered SCB was introduced to the batch ED to remove the organic matter and concentrate the ions that were later reused as a substrate for the fermentation. The concentrate/diluate quality and the ED process characteristics are analyzed in the following subsections.

##### 3.2.1. Salt and water transport

Desalination of SCB was analyzed in ED1 to understand the behavior of concentrate/diluate, ion migration, water transport and retention of organic compounds. The desalination was aborted after 103 min, when the concentrate volume increased by 59 ml from the initial 1000 ml, and the total desalination rate was 85%. The ion migration from the diluate to the concentrate was monitored by conductivity measurements for each regime of applied current density (Fig. 2a). The differences ( $\Delta m$ )

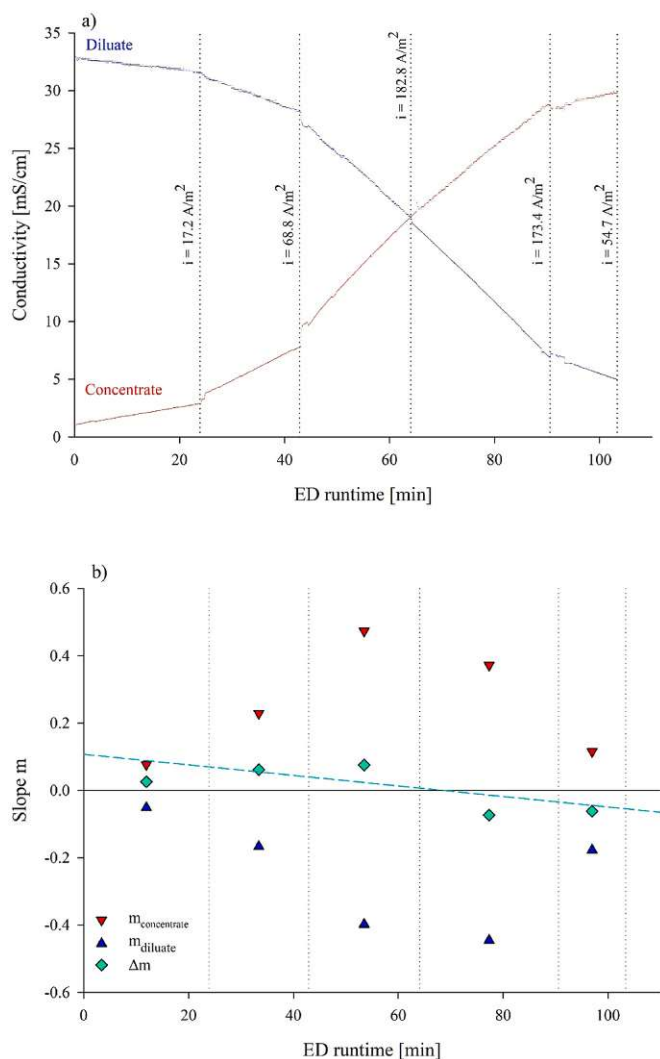
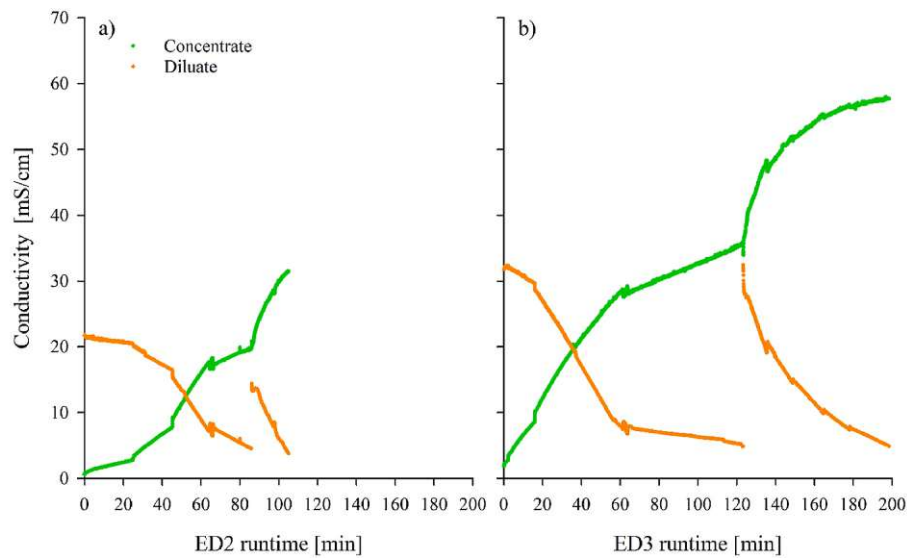


Fig. 2. ED1 desalination process with a) conductivity change in the diluate (SCB) and concentrate over time. Denoted segments correspond to different current densities applied in consecutive steps (dotted line); b) desalination/concentration slopes and their differences for each desalination segment.

between the desalination and concentration slopes indicate the osmotic and electro-osmotic water transport (Fig. 2b). The osmosis and electro-osmosis acted in opposite directions before the conductivities equalized ( $\Delta m > 0$ ) and in the same direction after ( $\Delta m < 0$ ), intensifying water transport from SCB to the concentrate and leading to the limiting concentrate concentration. Besides diluting the concentrate, the water diffusion increased the transport of uncharged pollutants (organic matter and proteins) from SCB that contaminated the concentrate. The DOC measured in the final concentrate was 68.7 mg/l. Since the initial DOC in SCB was 1735 mg/l, the ED thus achieved 96% DOC removal. Energy consumption for SCB desalination was 0.51 kWh/kg of total removed ions (12.5 kWh/m<sup>3</sup> of SCB).

##### 3.2.2. Concentrating salts from SCB

Doubling the ion concentration from SCB was aimed for in further ED experiments because the microorganisms consume up to 27% of



**Fig. 3.** Doubling the ionic content of the receiving medium from two different feed solutions: a) with lower initial ionic content (ED2 = ED2<sub>1</sub>+ED2<sub>2</sub>) and b) with higher ionic content (ED3 = ED3<sub>1</sub>+ED3<sub>2</sub>).

**Table 4**  
Process characteristics of ED2 and ED3.

ED run	Process time	Volume increase in concentrate	RE	CE	Energy consumption
	<i>min</i>	<i>ml</i>	%	%	<i>kWh/kg<sup>a</sup></i>
ED2	105	100	78.6	85.6	0.72
ED3	198	30	84.9	78.1	0.74

<sup>a</sup> kg of removed salts.

macronutrient P and 58% of micronutrients ( $K^+$ ,  $Ca^{2+}$ ,  $Mg^{2+}$ ) from the reference culture medium (Supplement, Table S1). Concentrating the remaining salts from SCB was necessary to provide the ideal conditions for a new fermentation. Fig. 3 compares concentrating of a lower (ED2) and higher (ED3) concentrated feed (SCB) because waste fermentation effluents often vary in composition. Table 4 summarizes the desalination characteristics. The ions were firstly transferred (ED2<sub>1</sub>, ED3<sub>1</sub>) and then concentrated in the subsequent batch (ED2<sub>2</sub>, ED3<sub>2</sub>) by addition of 1 L of SCB to the diluate while retaining the concentrate from the first batch. In both ED2 and ED3, the concentrate conductivity increased ~1.7 times compared to the initial feed conductivity (Fig. 3).

Table 5 presents the ionic mass fractions in each ED run for each ion observed separately as a whole part in feed (SCB). There was a higher fraction of sulfates from SCB (~0.9) and a lower fraction of phosphorus (~0.5) in the first and in the concentrating batch. There was almost no increase of  $Ca^{2+}$  and  $Mg^{2+}$  fractions when ED3<sub>1</sub> and ED3<sub>2</sub> were compared and  $K^+$  fractions of ED2<sub>1</sub>, ED2<sub>2</sub> and ED3<sub>2</sub> solutions exceeded the maximum reference values.

**Table 5**  
Fraction of ions from SCB transferred to the concentrate for each ED run separately. Reference values denote the maximum theoretical values for each stage.

Ionic mass fraction	PO <sub>4</sub> -P	NH <sub>4</sub> -N	Cl <sup>-</sup>	SO <sub>4</sub> <sup>2-</sup>	Na <sup>+</sup>	K <sup>+</sup>	Ca <sup>2+</sup>	Mg <sup>2+</sup>	Reference
ED1	0.52	0.86	0.99	0.91	0.99	0.70	0.99	0.40	$X \leq 1$
ED2 <sub>1</sub>	0.43	0.82	0.80	0.91	0.98	1.32	0.69	0.57	$X \leq 1$
ED2 <sub>2</sub>	0.84	1.52	1.77	1.73	1.79	2.65	0.81	0.78	$1 < X \leq 2$
ED3 <sub>1</sub>	0.54	0.83	0.54	0.92	1.08	0.63	0.63	0.49	$X \leq 1$
ED3 <sub>2</sub>	1.05	1.66	1.14	2.08	2.16	2.40	0.58	0.59	$1 < X \leq 2$

### 3.2.3. Removal of ions in the diluate

The ED diluate was surveyed for any patterned behavior of ionic removal in the first ED batch (ED1, ED2<sub>1</sub>, and ED3<sub>1</sub>) and subsequent second batch (ED2<sub>2</sub> and ED3<sub>2</sub>). The total RE was  $82.4 \pm 3.4\%$  in all batches, with final diluate conductivities of  $4.5 \pm 0.5$  mS/cm. Fig. 4 shows RE<sub>i</sub> of the analyzed cations and anions from SCB. Removal of

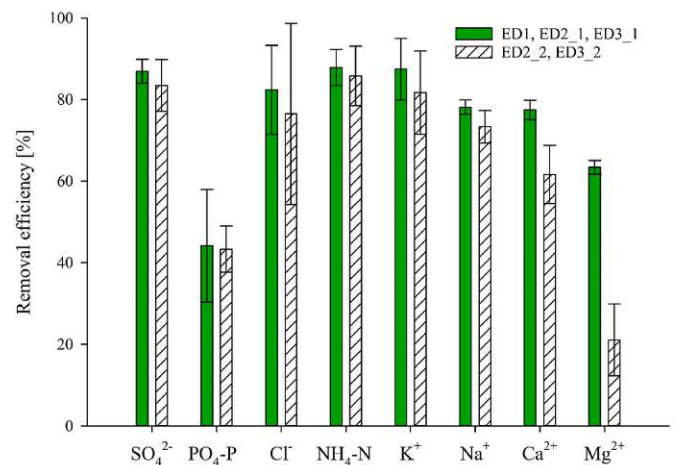


**Fig. 4.** Removal efficiency of each analyzed ion with the standard deviation bars in the first ED runs (ED1, ED2<sub>1</sub> and ED3<sub>1</sub>) for transferring ions, and subsequent ED runs (ED2<sub>2</sub> and ED3<sub>2</sub>) for concentrating ions.

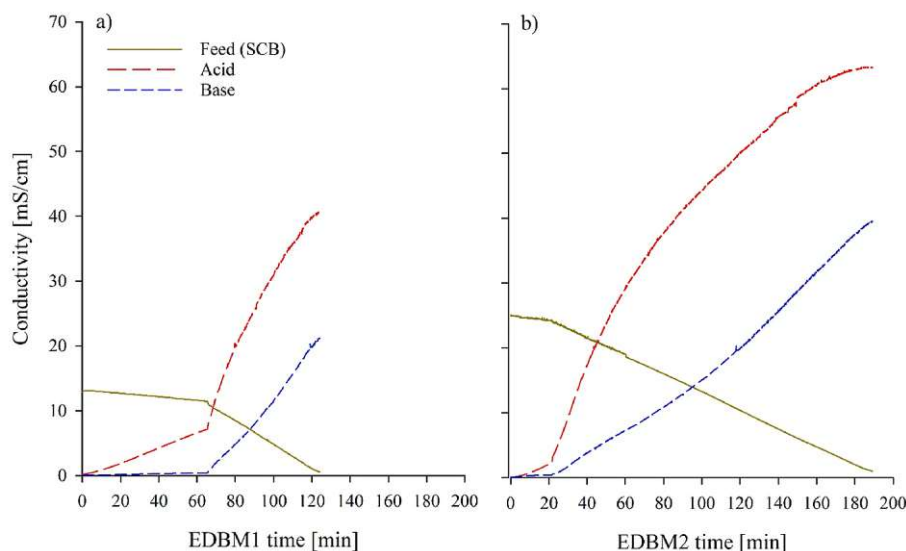


**Fig. 5.** Conversion of two fermentation effluents with various ionic strengths to corresponding acid/base produced via bipolar membranes in a) EDBM1 and b) EDBM2.

**Table 6**

Parameters for evaluation of EDBM fed with lower ionic feed concentration (EDBM1) and higher ionic feed concentration (EDBM2).

Parameter	Unit	EDBM1	EDBM2
SO <sub>4</sub> <sup>2-</sup> in feed	mg/L	6512.4	12,172.6
pH acid		1.7	1.5
Anions in feed	mEq/L	133.2	360.9
H <sub>2</sub> SO <sub>4</sub> concentration	mol/L	0.11	0.15
DOC in acid	mg/L	8.3	7.5
R <sub>s</sub> theoretical	%	52.0	36.3
R <sub>s</sub> <sup>a</sup>	%	42.0	22.5
pH base		12.4	12.6
Cations in feed	mEq/L	108.5	280.5
NaOH concentration	mol/L	0.12	0.22
DOC in base	mg/L	13.8	21.6
R <sub>s</sub> theoretical	%	54.1	43.4
R <sub>s</sub> <sup>a</sup>	%	52.6	41.4
RE	%	95.8	96.1
CE	%	43.2	48.3
Energy Consumption	kWh/kgH <sub>2</sub> SO <sub>4</sub>	2.7	3.0

<sup>a</sup> included intrusion of co-ions, that decreases the actual acid/base concentration.

phosphates was the lowest and remained lower in the subsequent batch. The removal of Ca<sup>2+</sup> decreased from ~80% to ~60% and of Mg<sup>2+</sup> from ~60% to ~20%. The concentration of all ions in the diluate/concentrate and the applied current densities are in Supplement, Table S2.

### 3.3. Results from EDBM

EDBM1 treated the higher concentrated SCB (13.1 mS/cm, pH 3) and EDBM2 treated the lower concentrated SCB (25.1 mS/cm, pH 2.8) (Fig. 5). EDBM2 desalination time was prolonged by 65 min, compared to the EDBM1 process duration of 124 min, due to the almost doubled ionic load of EDBM2 feed.

Table 6 compares the EDBM parameters. The almost double

increased feed conductivity led to 1.8 times higher concentration of produced base, whereas the concentration of recovered acid was 1.3 times higher. Increasing desalination time for EDBM2 slightly increased the concentration of organic compounds in the base. The total removal of organics after EDBM was 98.1% for the acid and 94.8% for the base. Recovery rates (R<sub>s</sub>) of acids/bases decreased with increased feed concentration. The acid compartment was especially affected by the co-ion intrusion, with the R<sub>s</sub> decreasing by 19.2% and 37.9% compared to the theoretical R<sub>s</sub> values for EDBM1 and EDBM2, respectively. Both produced bases contained ~44% of NH<sub>4</sub>OH and ~50% of NaOH, corresponding to the concentration of mainly NH<sub>4</sub><sup>+</sup> and Na<sup>+</sup> cations in SCB. For the same removal efficiency (RE ~96%), CE and energy consumption were slightly higher for the more concentrated feed in EDBM2 than for EDBM1.

Removal of all assessed ions in the EDBM feed (Supplement, Fig. S1) was in the same range as in the conventional ED (Fig. 4).

### 3.4. Fermentation with *S. Acidocaldarius* in recycled SCB

Fig. 6 shows the results from the first batch fermentation. From SCB recovered media: ED1, ED2, and NF270 were tested for their usability of cultivation *S. acidocaldarius* compared to the standard medium (VD). NF270 medium showed the most similar results to the standard medium regarding biomass growth measured by the OD<sub>600</sub> (Fig. 6a). *S. acidocaldarius* growth in ED1 and ED2 medium were close to the reference medium and similar in the substrate uptake (Fig. 6b).

With regard to the outcome of the second run with cultures growing on the MF medium, recovered acids, and a mixture of ED2 and pH set with recovered acid A2 can be seen in Fig. 7. Growth on the MF medium could not be achieved. Both recovered acids procured similar results in terms of growth (Fig. 7a) and substrate uptake (Fig. 7b). The recovered acid combined with ED1 medium did not improve the growth (Fig. 7) compared to ED1 with 4.8% sulfuric acid (Fig. 6).

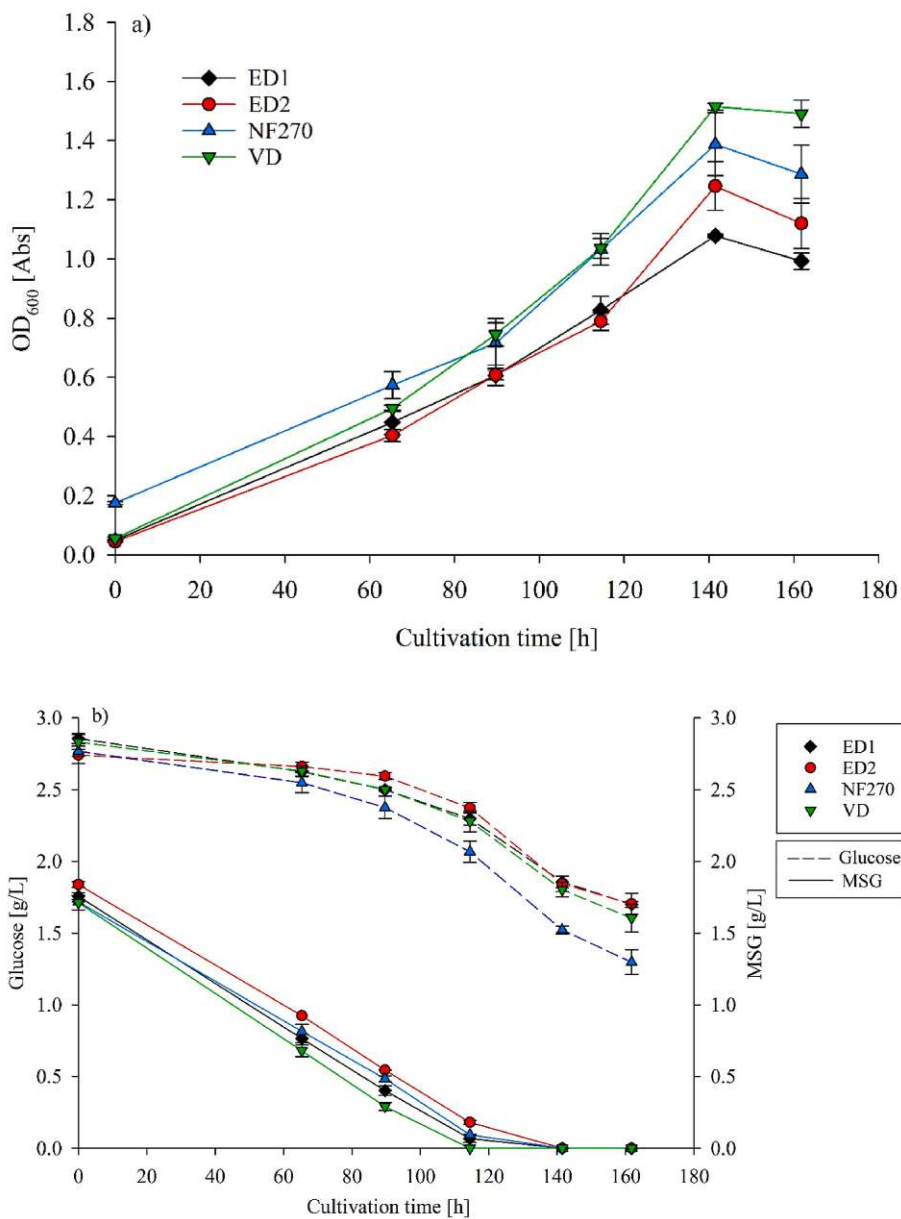


Fig. 6. Results of optical density (OD<sub>600</sub>) measurements in a) and substrate concentration in b) at each sampling point of cultures grown in ED1, ED2 and NF medium compared to fresh medium (VD).

Die approbierte gedruckte Originalversion dieser Dissertation ist an der TU Wien Bibliothek verfügbar. The approved original version of this doctoral thesis is available in print at TU Wien Bibliothek.

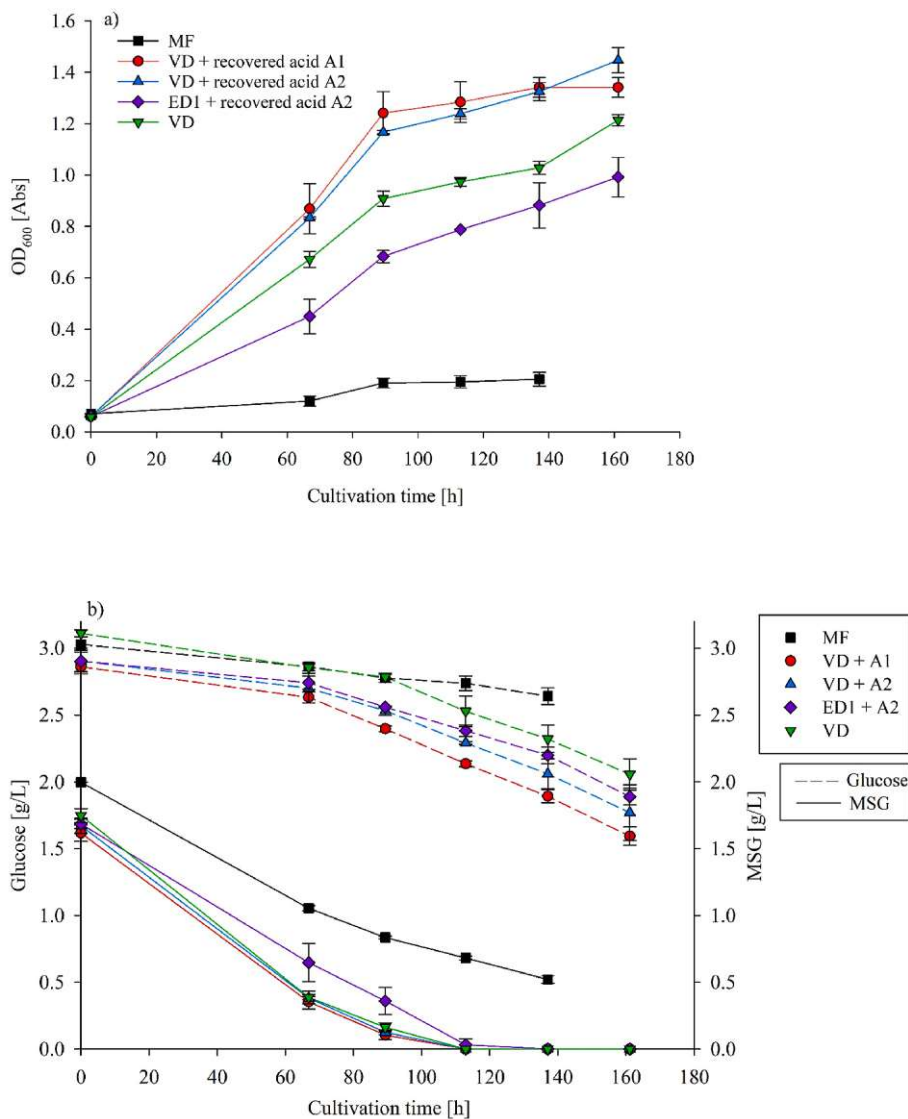


Fig. 7. Results of optical density (OD<sub>600</sub>) measurements in a) and substrate concentration in b) at each sampling point of cultures grown in MF, VD + recovered acids and mix of ED1 and recovered acid medium. A1 and A2 are the acids recovered by EDBM.

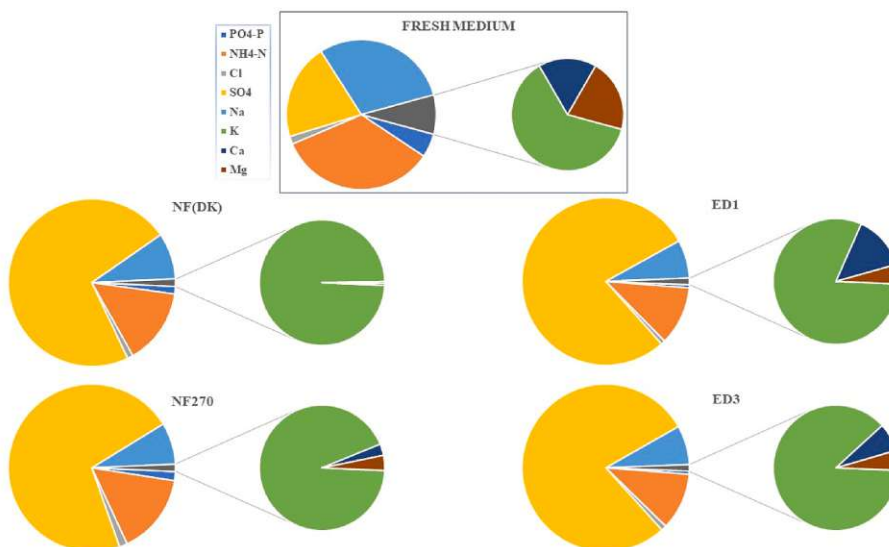


Fig. 8. Contribution of the recovered ions to the total ionic content of recovered media compared to the fresh media composition.

## 4. Discussion

### 4.1. Fermentation

Growth on only microfiltered SCB was not achieved. This was probably due to unknown inhibiting metabolites formed in the initial fermentation. Nevertheless, a decrease in MSG concentration over time (Fig. 7b) could be observed. This decrease can be explained by the spontaneous formation of pyroglutamate under high temperatures and low pH (Park et al., 2001). Also, it is possible that MSG was still consumed by the cells, but the uptake did not translate into significant proliferation due to a reduced biomass yield under the inhibiting conditions of the MF medium. Subsequent treatment of SCB via NF or ED can apparently diminish these not yet identified inhibiting compounds. After replenishing the carbon sources MSG and D-glucose, growth on all recovered media, except MF, was possible (Figs. 6a and 7a). The higher recovery rate of  $\text{SO}_4^{2-}$  in ED compared to NF might slightly decrease the growth curve. Recovered acid by EDMB even showed an improved growth curve (Fig. 7a) as to the reference medium (VD). This effect can be assigned to the impurity of the sulfuric acid and co-ion transport that supply additional P and N sources for microbial growth.

### 4.2. Pretreatment

Biomass is commonly separated by microfiltration, while fermentation inhibiting substances permeate to SCB (Fig. 7). UF can be excluded from the process (Fig. 1) due to the low DOC removal. NF membranes set off microbial growth and satisfied the EDBM requirements. The permeates had significantly reduced divalent cations and organic foulants, thus decreasing the need for frequent IEM cleaning steps (Merino-Garcia and Velizarov, 2021).

### 4.3. Nutrient recovery

The composition of macro- and micronutrients recovered by nanofiltration (NF(DK)), single run electro dialysis (ED1) and double run electro dialysis (ED3) from the SCB was compared to the fresh fermentation medium shown in Fig. 8. Pie charts represent only the contribution of individual nutrients to the total amount of nutrients in the medium. Exact values can be found in Table S2.

The ratio of nutrients in recovered media differed strongly compared to the fresh medium due to the sulfuric acid additions and nutrient consumption by microorganisms during the fermentation and losses during the recovery treatment. The microbial growth and production was possible in the media recovered by NF270 and ED (Figs. 6 and 7) as

~40% of P and K sources and ~75% of N sources compared to the fresh medium were available for the microbial growth. This study showed lower P-recovery in ED compared to other ions due to the low pH (3) of SCB wherein phosphorus appears mainly as a monovalent dihydrogen phosphate ion and partially as phosphoric acid (Rotta et al., 2019). The competing transport of other in SCB present ions also decreased the P-removal efficiency (Tran et al., 2015; Zhang et al., 2009). P-recovery rate can be improved by increasing the voltage (Wang et al., 2013), increasing the total effective membrane area (Mohammadi et al., 2021), multistaged ED (Tsiakis and Papageorgiou, 2005), prolonging the desalination time (Tran et al., 2015), or by applying a subsequent ED batch to increase the concentration factor as it was done in this study (ED3 in Fig. 3). The prolonged desalination time would increase the diffusion of nonionic pollutants from SCB towards the concentrate and contaminate it, as shown in Section 3.2.1 and Fig. 2.

ED performed better for micronutrient recovery than nanofiltration with up to 43 times higher  $\text{Ca}^{2+}$ , 30 times higher  $\text{Mg}^{2+}$  and 3 times higher  $\text{K}^+$  and  $\text{Na}^+$  concentrations. Still, divalent cations were significantly less recovered from the SCB (Fig. 4 and Table 5, ED2.2 and ED3.2) due to their lower diffusion coefficients and lower initial concentrations compared to monovalent cations (Długolecki et al., 2010; Feijoo et al., 2021).

The ions initially present in the highest concentration ( $\text{SO}_4^{2-}$  and  $\text{Na}^+$ ) were effectively concentrated, with a doubled concentration in the receiving medium, followed by other monovalent ions (Table 5). However, all recovered media were unbalanced by the presence of sulfates, which might reach toxic levels to the microorganism in succeeding recovering cycles (Soucek and Kennedy, 2005). Fractionating various nutrient anions and cations from SCB by the application of monovalent selective ion membranes could deliver balanced recovered medium (Z.-L. Ye et al., 2019).

Organic substances were removed up to 96% by ED and up to 89% by NF. Inhibiting substances that were initially present in the SCB were removed by both membrane technologies, allowing the biomass growth (Fig. 6).

### 4.4. Acid/base recovery

Accumulation of sulfates in the recovered medium (Fig. 8) indicated the alternative applications of EDBM for the sulfuric acid recovery. Bipolar electro dialysis yielded an acidic stream mainly containing sulfuric acid, with around 97% of  $\text{SO}_4^{2-}$  among all present anionic equivalents. Both bases produced contained 44% of  $\text{NH}_4\text{OH}$  and 50% of  $\text{NaOH}$  compared to the total concentration of all equivalent cations, corresponding to the high  $\text{NH}_4^+$  and  $\text{Na}^+$  initial concentrations in the SCB. In

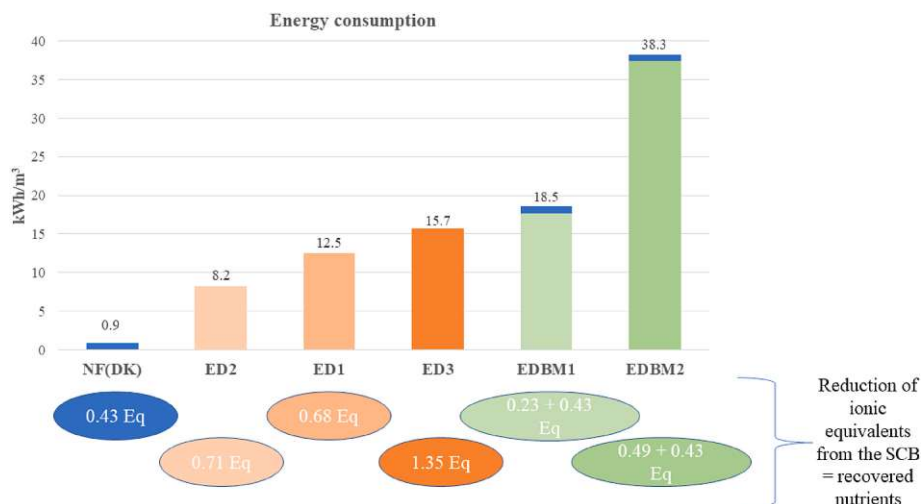


Fig. 9. Energy consumed per  $\text{m}^3$  of treated SCB and the ionic equivalents that were removed from the effluents of the each tested technology.

the study by Gao et al. up to 0.9 mol/L H<sub>2</sub>SO<sub>4</sub> and 1.6 mol/L NaOH with ~98% purity were recovered by EDBM from the feed with 0.5 mol/L salt concentration (Gao et al., 2021). Concentration of recovered acids/bases in our study were about 10 times lower (Table 6) due to the 10-fold lower initial salt concentration (Table S2), and are similar to those obtained in the study by Marti-Calatayud et al. (Marti-Calatayud et al., 2014) and Lemair et al. (Lemair et al., 2016). Higher concentrated prefiltered feed delivered higher concentrated acid/base (Table 6). The adverse effect of the increasing feed concentrations was the increased co-ion transport, decreasing the final acid/base concentration than theoretically possible (Öner et al., 2021; Tongwen, 2002). Adequate pretreatment with selective increase of the feed salt concentration while decreasing DOC can lead to higher concentrated and purer recovered acid/base, such as ED with monovalent selective anion exchange membranes, as demonstrated in our previous research (Knežević et al., 2022), as well as current density and pH increase of the SCB (Zhang et al., 2012), or increments of volume ratio (Gao et al., 2021).

The pH adjustment with recovered acid was applicable to the batch fermentation, as observed in Fig. 7, but in continuous application it might dilute the substrate and hamper the microbial growth.

The DOC removal was remarkably high for all evolved product streams due to the preceding NF, achieving 98.1% DOC removal for acids and 94.8% DOC removal for bases from the initial SCB organic content.

#### 4.5. Characteristics of discharge streams

A secondary stream evolved after each of the applied membrane technologies for the SCB treatment. The environmental impact and the potential use of discharge streams needs to be taken into account when comparing the applied technologies. NF had a concentrate whereas the ED and EDBM had a diluate stream as the discharge. ED and EDBM significantly decreased the concentrations of nutrients in SCB (Fig. 4 and Fig. S1), preventing severe environmental degradation in case of untreated SCB discharge into receiving water bodies. The greater environmental benefit of e.g. P reduction in the effluent than the resource recovery optimization was presented in the LCA of novel resource-recovery approaches (Faragò et al., 2021). The ionic content of EDBM diluate was lower compared to the conventional ED due to the NF pretreatment (Table S2). The remaining nutrients in NF, ED and EDBM effluents may be suitable for the irrigation purposes if the pH is adjusted by the recovered base obtained in the EDBM experiments. The results of this study also indicate the necessity of a posttreatment application, such as activated carbon or ozonation, for the removal of the inhibiting compounds and DOC reduction.

#### 4.6. Energy requirements

The energy needed for SCB treatment increased with the selectivity of tested technologies NF < ED < EDBM and with the increase of the total ionic content (ED2 < ED1 < ED3; EDBM1 < EDBM2) (Fig. 9). Ionic equivalents removed from SCB have a positive environmental impact due to the waste reduction and their reuse in the fermentation process, resulting in savings for the purchase of new chemicals.

The high energy requirements for ED/EDBM are comparable to the values reported in the literature (Al-Amshawee et al., 2020, p.; Lei et al., 2020; Mohammadi et al., 2021), and most probably offset the benefits of the nutrient recovery, as demonstrated in the study by Fargo et al. (Faragò et al., 2021). Renewable energy to power desalination processes (Al-Karaghoul and Kazmerski, 2013), an increased market for recovered resources, process and membrane optimization can decrease the negative environmental impacts.

## 5. Conclusions

Our study offers a concept for sustainable production in the future industrial fermentation with *Sulfolobus acidocaldarius*, an archaeon with high pharmaceutical potential. Three technological pathways were contrasted to provide recycled substrate and close the material loop by nutrient and water recovery from the real waste fermentation effluent. Cultivation on the nanofiltered and by ED recovered medium was possible and similar to the reference medium. ED enabled higher concentration factors of recovered macro- and micronutrients with higher DOC removal than NF. Acid recovered by EDBM even exhibited an improved growth curve compared to the reference medium, most probably due to the impurity of the recovered sulfuric acid and co-ion transport that supply additional P and N sources. The recovered nutrients performed well in the batch fermentation, but future studies should seek to integrate the recovery cycle in the continuous fermentation.

NF was economically more feasible than ED/EDBM, but ED/EDBM offered a selective ion separation, higher concentration factors and recovery of high-value products. Further research is needed to reduce the energy consumption of electro-membrane processes and to increase the membrane selectivity in ED for obtaining balanced ion-fractions in the recovered medium and acid/base purity in EDBM.

### CRedit authorship contribution statement

**Katarina Knežević:** Conceptualization, Methodology, Validation, Formal analysis, Investigation, Data curation, Writing – original draft, Visualization. **Kerstin Rastädter:** Methodology, Validation, Formal analysis, Investigation, Data curation, Writing – review & editing. **Julian Quehenberger:** Conceptualization, Methodology, Validation, Data curation, Writing – review & editing. **Oliver Spadiut:** Validation, Writing – review & editing, Supervision. **Jörg Krampe:** Validation, Resources, Writing – review & editing, Supervision, Project administration, Funding acquisition. **Norbert Kreuzinger:** Conceptualization, Validation, Resources, Writing – review & editing, Supervision, Project administration, Funding acquisition.

### Declaration of competing interest

The authors declare that they have no known competing financial interests or personal relationships that could have appeared to influence the work reported in this paper.

### Data availability

Data will be made available on request.

### Acknowledgments

The authors acknowledge TU Wien Bibliothek for financial support for editing/proofreading and for financial support through its Open Access Funding Program. The authors want to acknowledge the Bioactive project within this research was done. The special thanks are forwarded to the Water Research Laboratory, headed by Ernis Saracevic, for performing chemical analysis of water samples, to the NovoArc GmbH based at TU Wien, for providing spent culture broth, and to the Bachelor student Leonard Kern for performing fermentation processes in the scope of his Bachelor thesis.

### Appendix A. Supplementary data

Supplementary data to this article can be found online at <https://doi.org/10.1016/j.jclepro.2022.134436>.

org/10.1016/j.jclepro.2022.134436.

## References

- Ahmad, T., Aadil, R.M., Ahmed, H., Rahman, U. ur, Soares, B.C.V., Souza, S.L.Q., Pimentel, T.C., Scudino, H., Guimaraes, J.T., Emerino, E.A., Freitas, M.Q., Almada, R.B., Vendramel, S.M.R., Silva, M.C., Cruz, A.G., 2019. Treatment and utilization of dairy industrial waste: a review. *Trends Food Sci. Technol.* 88, 361–372. <https://doi.org/10.1016/j.tifs.2019.04.003>.
- Al-Amshawee, S., Yunus, M.Y.B.M., Azoddein, A.A.M., Hassell, D.G., Dakhlil, I.H., Hasan, H.A., 2020. Electrodialysis desalination for water and wastewater: a review. *Chem. Eng. J.* 380, 122231 <https://doi.org/10.1016/j.cej.2019.122231>.
- Al-Karaghoul, A., Kazmerski, L.L., 2013. Energy consumption and water production cost of conventional and renewable-energy-powered desalination processes. *Renew. Sustain. Energy Rev.* 24, 343–356. <https://doi.org/10.1016/j.rser.2012.12.064>.
- Benvegnu, T., Lemiegre, L., Cammas-Marion, S., 2009. New generation of liposomes called archaeosomes based on natural or synthetic archaeal lipids as innovative formulations for drug delivery. *Recent Pat. Drug Deliv. Formulation* 3 (3), 206–220. <https://doi.org/10.2174/187221109789105630>.
- Blöcher, C., Niewersch, C., Melin, T., 2012. Phosphorus recovery from sewage sludge with a hybrid process of low pressure wet oxidation and nanofiltration. *Water Res.* 46 (6), 2009–2019. <https://doi.org/10.1016/j.watres.2012.01.022>.
- Chambers, C.R., Patrick, W.M., 2015. Archaeal nucleic acid ligases and their potential in biotechnology. *Archaea*, e170571. <https://doi.org/10.1155/2015/170571>, 2015.
- Chandra, R., Castillo-Zacarias, C., Delgado, P., Parra-Saldívar, R., 2018. A biorefinery approach for dairy wastewater treatment and product recovery towards establishing a biorefinery complexity index. *J. Clean. Prod.* 183, 1184–1196. <https://doi.org/10.1016/j.jclepro.2018.02.124>.
- Cowan, D.A., Brown, J.H., 1959. Effect of turbulence on limiting current in electrodialysis cells. *Ind. Eng. Chem.* 51 (12), 1445–1448.
- Długolecki, P., Anet, B., Metz, S.J., Nijmeijer, K., Wessling, M., 2010. Transport limitations in ion exchange membranes at low salt concentrations. *J. Membr. Sci.* 346 (1), 163–171. <https://doi.org/10.1016/j.memsci.2009.09.033>.
- Egle, L., Rechberger, H., Krampe, J., Zessner, M., 2016. Phosphorus recovery from municipal wastewater: an integrated comparative technological, environmental and economic assessment of P recovery technologies. *Sci. Total Environ.* 571, 522–542. <https://doi.org/10.1016/j.scitotenv.2016.07.019>.
- ESPP, 2021. *ESPP Input for the EU's "Integrated Nutrient Management Action Plan" (INMAP)*. European Sustainable Phosphorus Platform (ESPP). [https://phosphorusplatform.eu/images/ESPP\\_input\\_INMAP\\_v27\\_3\\_21.pdf](https://phosphorusplatform.eu/images/ESPP_input_INMAP_v27_3_21.pdf).
- European Environment Agency, 2019. *Industrial Waste Water Treatment: Pressures on Europe's Environment*. Publications Office. <https://data.europa.eu/doi/10.2800/496223>.
- Faragó, M., Damgaard, A., Madsen, J.A., Andersen, J.K., Thornberg, D., Andersen, M.H., Rygaard, M., 2021. From wastewater treatment to water resource recovery: environmental and economic impacts of full-scale implementation. *Water Res.* 204, 117554 <https://doi.org/10.1016/j.watres.2021.117554>.
- Feijoo, G.C., Barros, K.S., Scarazzato, T., Espinosa, D.C.R., 2021. Electrodialysis for concentrating cobalt, chromium, manganese, and magnesium from a synthetic solution based on a nickel laterite processing route. *Separ. Purif. Technol.* 275, 119192 <https://doi.org/10.1016/j.seppur.2021.119192>.
- Gao, W., Fang, Q., Yan, H., Wei, X., Wu, K., 2021. Recovery of acid and base from sodium sulfate containing lithium carbonate using bipolar membrane electrodialysis. *Membranes* 11 (2), 152. <https://doi.org/10.3390/membranes11020152>.
- Hamza, R., Rabihi, A., Ezzahraoui, F., Morgan, G., Iorhemen, O.T., 2022. A review of the state of development of aerobic granular sludge technology over the last 20 years: full-scale applications and resource recovery. *Case Studies Chem. Environ. Eng.* 5, 100173 <https://doi.org/10.1016/j.csee.2021.100173>.
- Howarth, R.W., 2008. Coastal nitrogen pollution: a review of sources and trends globally and regionally. *Harmful Algae* 8 (1), 14–20. <https://doi.org/10.1016/j.hal.2008.08.015>.
- Irfan, M., Xu, T., Ge, L., Wang, Y., Xu, T., 2019. Zwitterion structure membrane provides high monovalent/divalent cation electrodialysis selectivity: investigating the effect of functional groups and operating parameters. *J. Membr. Sci.* 588, 117211 <https://doi.org/10.1016/j.memsci.2019.117211>.
- Khan, H.K., Rehman, M.Y.A., Malik, R.N., 2020. Fate and toxicity of pharmaceuticals in water environment: an insight on their occurrence in South Asia. *J. Environ. Manag.* 271, 111030 <https://doi.org/10.1016/j.jenvman.2020.111030>.
- Knežević, K., Saracevic, E., Krampe, J., Kreuzinger, N., 2022. Comparison of ion removal from waste fermentation effluent by nanofiltration, electrodialysis and ion exchange for a subsequent sulfuric acid recovery. *J. Environ. Chem. Eng.* 10 (5), 108423 <https://doi.org/10.1016/j.jece.2022.108423>.
- Lei, C., Li, Z., Gao, Q., Fu, R., Wang, W., Li, Q., Liu, Z., 2020. Comparative study on the production of gluconic acid by electrodialysis and bipolar membrane electrodialysis: effects of cell configurations. *J. Membr. Sci.* 608, 118192 <https://doi.org/10.1016/j.memsci.2020.118192>.
- Lemaire, J., Blanc, C.-L., Duval, F., Théoleyre, M.-A., Pareau, D., 2016. Purification of pentoses from hemicellulosic hydrolysates with sulfuric acid recovery by using electrodialysis. *Separ. Purif. Technol.* 166, 181–186. <https://doi.org/10.1016/j.seppur.2016.04.030>.
- Liu, H., Hu, G., Basar, I.A., Li, J., Lyczko, N., Nzihou, A., Eskicioglu, C., 2021. Phosphorus recovery from municipal sludge-derived ash and hydrochar through wet-chemical technology: a review towards sustainable waste management. *Chem. Eng. J.* 417, 129300 <https://doi.org/10.1016/j.cej.2021.129300>.
- Martí-Calatayud, M.C., Buzzi, D.C., García-Gabaldón, M., Ortega, E., Bernardes, A.M., Tenório, J.A.S., Pérez-Herranz, V., 2014. Sulfuric acid recovery from acid mine drainage by means of electrodialysis. *Desalination* 343, 120–127. <https://doi.org/10.1016/j.desal.2013.11.031>.
- Merino-García, I., Velizarov, S., 2021. New insights into the definition of membrane cleaning strategies to diminish the fouling impact in ion exchange membrane separation processes. *Separ. Purif. Technol.* 277, 119445 <https://doi.org/10.1016/j.seppur.2021.119445>.
- Milanesi, M., Runfola, A., Guercini, S., 2020. Pharmaceutical industry riding the wave of sustainability: review and opportunities for future research. *J. Clean. Prod.* 261, 121204 <https://doi.org/10.1016/j.jclepro.2020.121204>.
- Mohammadi, R., Tang, W., Sillanpää, M., 2021. A systematic review and statistical analysis of nutrient recovery from municipal wastewater by electrodialysis. *Desalination* 498, 114626. <https://doi.org/10.1016/j.desal.2020.114626>.
- Olguín, E.J., Sánchez, G., Mercado, G., 2004. Cleaner production and environmentally sound biotechnology for the prevention of upstream nutrient pollution in the Mexican coast of the Gulf of México. *Ocean Coast Manag.* 47 (11), 641–670. <https://doi.org/10.1016/j.ocecoaman.2004.12.006>.
- Öner, M.R., Kanca, A., Ata, O.N., Yapıcı, S., Yaylı, N.A., 2021. Bipolar membrane electrodialysis for mixed salt water treatment: evaluation of parameters on process performance. *J. Environ. Chem. Eng.* 9 (4), 105750 <https://doi.org/10.1016/j.jece.2021.105750>.
- Park, C.B., Lee, S.B., Ryu, D.D.Y., 2001. L-pyroglutamate spontaneously formed from L-glutamate inhibits growth of the hyperthermophilic archaeon *Sulfolobus solfataricus*. *Appl. Environ. Microbiol.* 67 (8), 3650–3654. <https://doi.org/10.1128/AEM.67.8.3650-3654.2001>.
- Porwal, H.J., Mane, A.V., Velhal, S.G., 2015. Biodegradation of dairy effluent by using microbial isolates obtained from activated sludge. *Water Resour. Industry* 9, 1–15. <https://doi.org/10.1016/j.wri.2014.11.002>.
- Quehenberger, J., Shen, L., Albers, S.-V., Siebers, B., Spadiut, O., 2017. *Sulfolobus* – a potential key organism in future biotechnology. *Front. Microbiol.* 8, 2474. <https://doi.org/10.3389/fmicb.2017.02474>.
- Quehenberger, J., Albersmeier, A., Glatzel, H., Hackl, M., Kalinowski, J., Spadiut, O., 2019. A defined cultivation medium for *Sulfolobus acidocaldarius*. *J. Biotechnol.* 301, 56–67. <https://doi.org/10.1016/j.jbiotec.2019.04.028>.
- Rotta, E.H., Bitencourt, C.S., Marder, L., Bernardes, A.M., 2019. Phosphorus recovery from low phosphate-containing solution by electrodialysis. *J. Membr. Sci.* 573, 293–300. <https://doi.org/10.1016/j.memsci.2018.12.020>.
- Soucek, D.J., Kennedy, A.J., 2005. Effects of hardness, chloride, and acclimation on the acute toxicity of sulfate to freshwater invertebrates. *Environ. Toxicol. Chem.* 24 (5), 1204–1210. <https://doi.org/10.1897/04-142.1>.
- Stanbury, P.F., Whitaker, A., Hall, S.J., 2017. *Principles of Fermentation Technology, third ed.* Butterworth-Heinemann, an imprint of Elsevier.
- Tongwen, X., 2002. Electrodialysis processes with bipolar membranes (EDBM) in environmental protection—a review. *Resour. Conserv. Recycl.* 37 (1), 1–22. [https://doi.org/10.1016/S0921-3449\(02\)00032-0](https://doi.org/10.1016/S0921-3449(02)00032-0).
- Tran, A.T.K., Zhang, Y., Lin, J., Mondal, P., Ye, W., Meesschaert, B., Pinoy, L., Van der Bruggen, B., 2015. Phosphate pre-concentration from municipal wastewater by select rodialysis: effect of competing components. *Separ. Purif. Technol.* 141, 38–47. <https://doi.org/10.1016/j.seppur.2014.11.017>.
- Tsiakis, P., Papageorgiou, L.G., 2005. Optimal design of an electrodialysis brackish water desalination plant. *Desalination* 173 (2), 173–186. <https://doi.org/10.1016/j.desal.2004.08.031>.
- Union, European, 2020. *Circular Economy Action Plan. For a Cleaner and More Competitive Europe*. European Union (EU), European Commission (EC), Brussels, Belgium. [https://ec.europa.eu/environment/pdf/circular-economy/new\\_circular\\_economy\\_action\\_plan.pdf](https://ec.europa.eu/environment/pdf/circular-economy/new_circular_economy_action_plan.pdf).
- Veleva, V., Cue Jr., W., B., 2017. Benchmarking green chemistry adoption by “big pharma” and generics manufacturers. *Benchmark Int. J.* 24 (5), 1414–1436. <https://doi.org/10.1108/BLJ-01-2016-0003>.
- Wang, X., Wang, Y., Zhang, X., Feng, H., Li, C., Xu, T., 2013. Phosphate recovery from excess sludge by conventional electrodialysis (CED) and electrodialysis with bipolar membranes (EDBM). *Ind. Eng. Chem. Res.* 52 (45), 15896–15904. <https://doi.org/10.1021/ie4014088>.
- Wei, F., Mortimer, M., Cheng, H., Sang, N., Guo, L.-H., 2021. Parabens as chemicals of emerging concern in the environment and humans: a review. *Sci. Total Environ.* 778, 146150 <https://doi.org/10.1016/j.scitotenv.2021.146150>.
- Wheatley, A.D., 1984. Biotechnology and effluent treatment. *Biotechnol. Genet. Eng. Rev.* 1 (1), 261–310. <https://doi.org/10.1080/02648725.1984.10647788>.
- Wu, H., Vaneckhaute, C., 2022. Nutrient recovery from wastewater: a review on the integrated Physicochemical technologies of ammonia stripping, adsorption and struvite precipitation. *Chem. Eng. J.* 433, 133664 <https://doi.org/10.1016/j.cej.2021.133664>.
- Wu, T.Y., Mohammad, A.W., Jahim, J.M., Anuar, N., 2009. A holistic approach to managing palm oil mill effluent (POME): biotechnological advances in the sustainable reuse of POME. *Biotechnol. Adv.* 27 (1), 40–52. <https://doi.org/10.1016/j.biotechadv.2008.08.005>.
- Xie, M., Shon, H.K., Gray, S.R., Elimelech, M., 2016. Membrane-based processes for wastewater nutrient recovery: technology, challenges, and future direction. *Water Res.* 89, 210–221. <https://doi.org/10.1016/j.watres.2015.11.045>.
- Ye, Z.-L., Ghyselsbrecht, K., Monballiu, A., Pinoy, L., Meesschaert, B., 2019. Fractionating various nutrient ions for resource recovery from swine wastewater using simultaneous anionic and cationic selective-electrodialysis. *Water Res.* 160, 424–434. <https://doi.org/10.1016/j.watres.2019.05.085>.

Ye, Y., Ngo, H.H., Guo, W., Chang, S.W., Nguyen, D.D., Zhang, X., Zhang, J., Liang, S., 2020. Nutrient recovery from wastewater: from technology to economy. *Bioresour Technol. Rep.* 11, 100425 <https://doi.org/10.1016/j.biteb.2020.100425>.

Zhang, Y., Van der Bruggen, B., Pinoy, L., Meesschaert, B., 2009. Separation of nutrient ions and organic compounds from salts in RO concentrates by standard and

monovalent selective ion-exchange membranes used in electrodialysis. *J. Membr. Sci.* 332 (1), 104–112. <https://doi.org/10.1016/j.memsci.2009.01.030>.

Zhang, Y., Paepen, S., Pinoy, L., Meesschaert, B., Van der Bruggen, B., 2012. Selectrodialysis: fractionation of divalent ions from monovalent ions in a novel electrodialysis stack. *Separ. Purif. Technol.* 88, 191–201. <https://doi.org/10.1016/j.seppur.2011.12.017>.

### Supplement 3 – Circular production – Evaluation of membrane technologies for nutrient recycling from a microbial fermentation effluent

*The cultivation of S. acidocaldarius was performed as follows:*

*S. acidocaldarius* was cultivated continuously in a Biostat A-plus bioreactor (Sartorius, Germany) with 2 L working volume and a dilution rate of 0.03 h<sup>-1</sup>. The reactor was supplied with 0.23 vvm pressurized air and stirred at 350 rpm. The temperature was set to 75 °C. The pH was kept constant at pH 3.0 and adjusted by adding 4.8% sulfuric acid automatically. Supplied feed contained a 5-times concentrated VD Medium (Quehenberger et al., 2019) with modified carbon source concentrations (9.5 g/L monosodium glutamate (MSG) and 4.5 g/L D-glucose). Cell broth was pumped via a bleed tube mounted at a fixed height for harvesting and maintaining the constant volume. The grown biomass is considered the product and harvested for its intracellular components. The biomass was separated from the surrounding liquid via Al<sub>2</sub>O<sub>3</sub>-coated ceramic filter (0.2 µm pore size, Deltapore, Netherlands) for further extraction steps. SCB is the liquid permeate of this filtration step and still contains ions from the initial culture medium (Table S1) targeted for reuse in this study. SCB also contains organic compounds such as residual microbial cells, peptones, pyruvate, and metabolites that interfere with cell growth (Soma et al., 2021) and must be removed from the recycling process. SCB has a yellowish color, a density of 1.02 g/cm<sup>3</sup> at 20 °C, and a sweet sugary smell. It was stored for up to one week at 4° C until further usage in the technical recovery steps of this study.

The concentration of macro - and micronutrients was analyzed in a sample of the reference culture media (VD Medium) before and after the fermentation (Table S1).

**Table S1.** Concentration of ions before and after the fermentation with the percentage change

Parameter	DOC	PO <sub>4</sub> -P	NH <sub>4</sub> -N	Cl <sup>-</sup>	SO <sub>4</sub> <sup>2-</sup>	Na <sup>+</sup>	K <sup>+</sup>	Ca <sup>2+</sup>	Mg <sup>2+</sup>
mg/L									
<b>Culture medium</b>	14,973.30	503.3	3,366.70	168.8	2,028.00	2,933.00	516.7	138.7	172.7
<b>Spent culture medium</b>	1887	369.2	3,762.00	237.7	24,784.80	2,582.00	399	62	72
%									
<b>Removal</b>	87.4	26.6	/	/	/	12.0	22.8	55.3	58.3
<b>Increase</b>	/	/	11.7	40.8	1122.1	/	/	/	/

Ions were analyzed by ion chromatography for the following ions: PO<sub>4</sub>-P, NH<sub>4</sub>-N, anions (Cl<sup>-</sup>, SO<sub>4</sub><sup>2-</sup>) and cations (Na<sup>+</sup>, K<sup>+</sup>, Ca<sup>2+</sup>, Mg<sup>2+</sup>), based on the following standards: DIN EN ISO 6878, DIN EN ISO 11732, DIN EN ISO 10304-1 and DIN EN ISO 14911, respectively. Total and dissolved organic carbon (TOC and DOC) were analyzed using the standard DIN EN 1484 method.

In ED and EDBM the ions were analyzed at the beginning and end of the demineralization process and can be seen in Table S1 and Table S2, respectively. The same methods and standards as noted above were applied.

**Table S2.** Ionic composition of permeates, NF(DK) retentate, diluate (d) and concentrate (c) solutions in each of the ED and EDBM (BM) runs.

Parameter	PO <sub>4</sub> -P	NH <sub>4</sub> -N	Cl <sup>-</sup>	SO <sub>4</sub> <sup>2-</sup>	Na <sup>+</sup>	K <sup>+</sup>	Ca <sup>2+</sup>	Mg <sup>2+</sup>
	mg/l							
<b>UF perm.</b>	256	2,914.40	158.8	16,339.00	1,908.00	282	63	64
<b>NF270 perm.</b>	258.2	2,296.20	228	10,525.00	1,182.00	191	6	8
<b>NF(DK)perm.</b>	206.4	2,059.10	158.3	10,170.10	1,258.00	199	1	1
<b>NF(DK)ret.</b>	267.2	2985.6	151.9	13777.4	1936	310	67	74
<b>ED1_d0</b>	293.8	3321	205	21833	1882	366	45	40
<b>ED1_d1</b>	157.6	360.2	24	2703	439	25	10	14
<b>ED1_c0</b>	3	27.97	28	214	50	2	0	0
<b>ED1_c1</b>	143.8	2699	192	18684	1756	243	42	15
<b>ED2_d0</b>	178.8	1908.8	116	12199	1243	104	32	33
<b>ED2_d1</b>	126.2	324.4	35	1981	277	22	8	12
<b>ED2_d2</b>	74.6	292	36	2026	290	21	11	19
<b>ED2_c0</b>	0.87	17.34	35	210	121	11	5	4
<b>ED2_c1</b>	74.6	1536.4	123	10891	1290	143	26	22
<b>ED2_c2</b>	137.8	2655	218	19361	2129	261	28	27
<b>ED3_d0</b>	274.8	3196.8	386	18243	1684	218	69	47
<b>ED3_d1</b>	118.6	269.4	42	1914	335	21	14	18
<b>ED3_d2</b>	166.8	287.2	30	2189	401	24	23	40
<b>ED3_c0</b>	7.56	90.6	62	557	79	8	4	3
<b>ED3_c1</b>	171.8	3032	301	19284	2112	162	53	29
<b>ED3_c2</b>	286.2	5245	489	37318	3603	516	43	30
<b>BM1_f0</b>	103.4	1154.7	98	6104	523	112	5	1
<b>BM1_f1</b>	68.4	15.19	23	220	83	4	0	0
<b>BM1_a</b>	29.6	702.2	173	13309	93	0	5	0
<b>BM1_b</b>	0.11	785.6	24	132	1470	153	13	0
<b>BM2_f0</b>	252.2	2927.2	192	16683	1463	274	5	5
<b>BM2_f1</b>	151.8	16.13	26	231	122	4	5	1
<b>BM2_a</b>	73.8	2263.2	464	22132	386	56	12	0
<b>BM2_b</b>	0.1	1417.2	120	352	2696	362	34	0

The ED processes were controlled by adjusting the current density with decreasing diluate conductivity, as shown in **Table S3**.

**Table S3.** Current density control in a step-wise mode with decreasing diluate conductivity.

	Concentrate Conductivity	Diluate conductivity	Current density

	mS/cm	mS/cm	A/m <sup>2</sup>
ED1	0.69	32.95	18
	3.28	31.37	68
	7.79	28.21	182
	19.05	19.05	173
	29.46	6.21	54
	29.78	4.97	
ED2	0.57	21.69	19
	3.02	20.32	66
	7.75	16.43	183
	12.44	12.44	180
	17.64	7.13	59
	19.64	4.53	
	19.86	14.38	310
	26.87	9.66	253
	29.89	5.93	231
	31.51	3.75	
ED3	1.82	31.73	21
	2.72	32.37	66
	8.54	29.59	183
	19.64	19.55	181
	28.7	7.5	59
	35.56	4.85	
	34.63	32.48	385
	48.23	19.12	169
	55.32	9.88	73
	57.64	4.87	

An initial constant voltage of 12 V was applied at the beginning of both EDBM processes because the starting solution in acid and base tanks was only deionized water. When the electrical conductivity of at least 0.4 mS/cm was reached in both acid and base tank, the control was switched to the constant current as denoted in Table S4.

**Table S4.** Average voltage and current density adjustment for EDBM processes for acid and base production.

	Feed Conductivity	Acid conductivity	Base conductivity	Voltage	Current density
	mS/cm	mS/cm	mS/cm	V	A/m <sup>2</sup>
EDBM1	12.93	0.13	0.02	12	15
	11.42	7.14	0.4	27.05	107
	0.54	40.57	21.2		
EDBM2	24.89	0.06	0.05	12	13
	24.25	2.29	0.4	19.5	107
	0.98	63.22	39.57		

Removal efficiencies of the ions removed from the EDBM feed are shown in Figure S1.

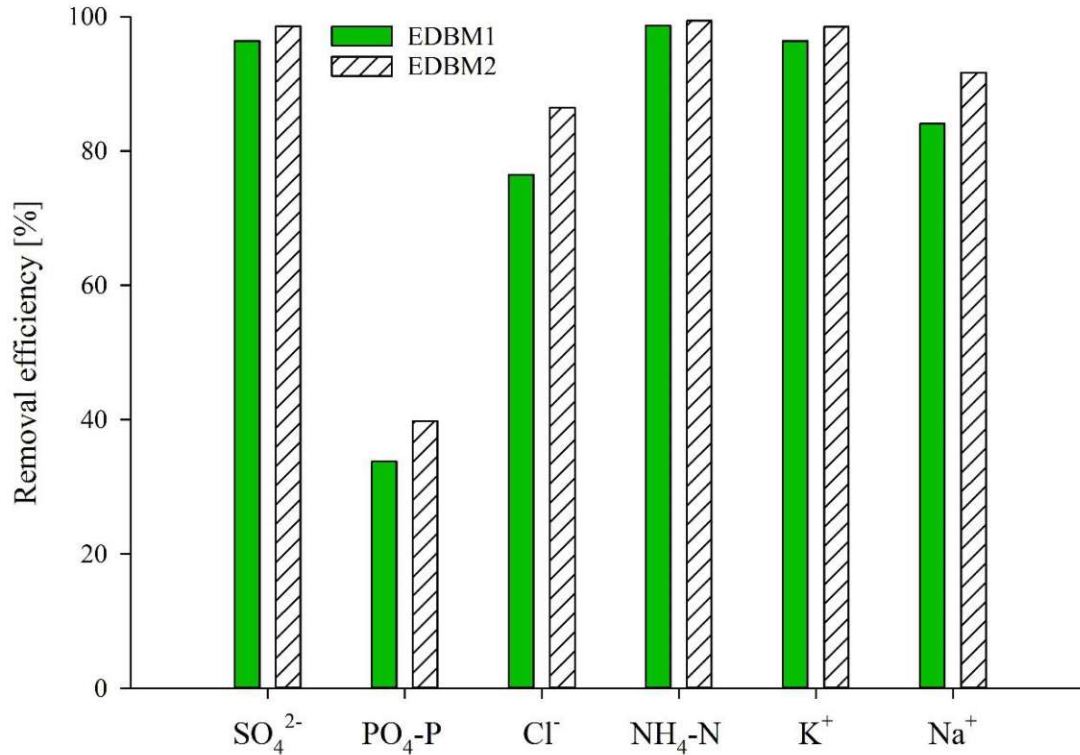


**Figure S1.** Removal efficiencies of specific ions from the feed solutions of the EDBM1 and EDBM2.

#### References:

- Quehenberger, J., Albersmeier, A., Glatzel, H., Hackl, M., Kalinowski, J., Spadiut, O., 2019. A defined cultivation medium for *Sulfolobus acidocaldarius*. *Journal of Biotechnology* 301, 56–67. <https://doi.org/10.1016/j.jbiotec.2019.04.028>
- Soma, Y., Yamaji, T., Hanai, T., 2021. Dynamic metabolic engineering of *Escherichia coli* improves fermentation for the production of pyruvate and its derivatives. *Journal of Bioscience and Bioengineering*. <https://doi.org/10.1016/j.jbiosc.2021.09.015>

# Investigation of ion-exchange membranes and erythritol concentration for the desalination of erythritol culture broth by electro dialysis

Katarina Knežević<sup>1\*</sup>, Laura Daza-Serna<sup>2</sup>, Astrid Rosa Mach-Aigner<sup>2,3</sup>, Robert L. Mach<sup>3</sup>, Anton Friedl<sup>4</sup>, Jörg Krampe<sup>1</sup> and Norbert Kreuzinger<sup>1</sup>

1 Research Unit for Water Quality Management. Institute for Water Quality and Resource Management, TU Wien, 1040 Vienna, Austria.

2 Christian Doppler Laboratory for Optimized Expression of Carbohydrate-active Enzymes, Research Division Biochemical Technology, Institute of Chemical, Environmental and Bioscience Engineering, TU Wien, 1060 Vienna, Austria.

3 Research Division Biochemical Technology, Institute of Chemical, Environmental and Bioscience Engineering, TU Wien, 1060 Vienna, Austria.

4 Research Division Bioresource and Plant Science, Institute of Chemical, Environmental and Bioscience Engineering, TU Wien, 1060 Vienna, Austria.

\* Corresponding author: [katarina.knezevic@tuwien.ac.at](mailto:katarina.knezevic@tuwien.ac.at)

## Abstract

Erythritol is a zero-calorie sugar substitute, safe for people with diabetes, that occurs naturally but is also commercially produced. Erythritol produced by fermentation must be separated from the rest of the cultivation broth. Electrodialysis (ED) may be used to separate and purify fermentation products, allowing simultaneous salt removal from the cultivation broth and generation of saline concentrate solution for reuse in a subsequent fermentation process. In the first stage, this study tested the performance of three membrane stacks and compared them to

the reference membrane for erythritol purification. The diffusion of products and by-products was analyzed for the synthetic broth containing 5–25 g/L of erythritol. Product and by-product losses, current efficiency and energy consumption were compared among the tested membranes for the same salt removal rate. Step-wise voltage approach was demonstrated to have fewer product losses than the ED controlled by the constant current approach. Finally, erythritol culture broth after cultivation was treated with selected membranes and ED control based on the findings from the first experimental stage. The erythritol losses were only 2% for the 94.8% desalination rate.

**Keywords:** erythritol separation; fermentation; electrodialysis; ion-exchange membranes; salt recovery.

## 1 Introduction

Erythritol is a polyol naturally occurring in small amounts in some fermented food and fruits (Tiefenbacher, 2017). At industrial scale it is produced through biotechnological processes, likewise other polyols as sorbitol, mannitol, xylitol, maltitol, etc., (Moon et al., 2010). Erythritol is a zero-calorie sweetener with a small molecular size. Erythritol cannot be broken by enzymatic batteries of the human body, because of that it is absorbed and excreted in the urine without changes (Park et al., 2016). Because it does not affect glucose and insulin levels, erythritol has been declared as a safe sugar substitute for people with diabetes (Ishikawa et al., 1996; Wölnerhanssen et al., 2020).

Erythritol is produced at industrial scale by several microorganisms including osmophilic yeasts as *Yarrowia lipolytica*, *Moniliella pollinis*, *Zygosaccharomyces* or *Hansenula*. Glucose is commonly used as a primary carbon source in the culture medium. Besides the carbon source, a mixture of macro- and micronutrients is required to allow yeasts' growth and efflux of osmolyte compounds. The production of osmolytes such as glycerol (considered the main by-product) and sugar alcohols (i.e. erythritol or mannitol), is induced when the osmophilic yeasts are exposed to high sugar or salt concentrations (Moon et al., 2010).

After the cultivation stage, erythritol needs to be purified. Firstly, the cultivation broth is membrane-filtered to remove microorganisms, followed by the treatments with ion-exchange resins (IER) to remove charged impurities. In the final step, the solution is discoloured on activated carbon, then the erythritol fraction is separated by preparative chromatography and concentrated by rotary evaporation to allow the crystallization of pure polyol (Daza-Serna et al., 2021; Moon et al., 2010; Rakicka et al., 2016). Although IER achieve almost complete ion

removal from the culture liquid, they eventually get saturated and require a regeneration step with acids and bases (Daza-Serna et al., 2021; González et al., 2006; Rakicka et al., 2016). The intensive requirements of chemicals for the regeneration of IER lead to the generation of large amounts of waste, having a negative environmental impact. Further disadvantages of IER application are the high cumulative energy demand consisting in the energy required for pumping, regenerants production and wastewater treatment (Greiter et al., 2004).

Along with circular and green economy goals rises the demand for improvements in downstream technologies of bioprocesses. For the biotechnological production of erythritol, the focus shall be put on reducing the waste and recovering the salts from culture broth for their reuse in subsequent culture stages. Thus, erythritol culture broth can be treated by electrodialysis (ED) for its desalination and product purification. ED is an electro-membrane process that contains a membrane stack composed of pairs of anion- and cation-exchange membranes. Ion-exchange membranes (IEMs) can selectively remove cations and anions while uncharged components remain in the feed on the diluate side of the ED system.

The advantage of ED used for the downstream of the erythritol broth is threefold. Firstly, the broth can be desalted, enhancing the erythritol isolation in subsequent steps. Secondly, the salts removed from the feed can be concentrated in the concentrate chamber and reused in the following culture batch. Thirdly, ED has almost zero discharge and less need for maintenance chemicals compared to the commonly used IER in the purification of culture broths (Zhang et al., 2021). Additionally, ED can be driven by green energy, lowering the carbon footprint (Al-Amshawee et al., 2020; Bian, 2019).

IEMs are polymeric membranes with embedded charged groups that allow the passage of counter-ions while rejecting co-ions (Ran et al., 2017). The transport of counter-ions is well described by the extended Nernst-Planck equation comprehending electromigration, convection and diffusion of ions through the membrane phase (Luo et al., 2018). Although electromigration is the main constituent of ion transport, IEMs have an interstitial phase between the fixed charged groups within which co-ion transport is possible (Luo et al., 2018). These voids in the membrane structure are electro-neutral. Thus, when the membranes get in contact with a feed solution, some of the non-ionic compounds can diffuse from the feed towards the concentrate chamber. The diffusional phenomenon leads to product losses in the separation process. Erythritol's diffusional potential is increased due to its concentration in solution and its molecular size, which may be especially concerning in the ED treatment.

Erythritol diffusion is also influenced by other operational and setup parameters such as current/voltage application mode and IEM characteristics. The regulation of the applied current/voltage may have a direct effect in the control of the diffusional effects. In this regard, a step-wise current/voltage control may reduce diffusional effects compared to the common constant current/voltage approach (Albornoz et al., 2019; Hábová et al., 2004).

Properties of ion-exchange membranes in ED strongly differ depending on fabrication method, membrane material and its homogeneity, ion-exchange group and capacity, membrane thickness and swelling, etc., (Ran et al., 2017; Yaroslavtsev & Nikonenko, 2009). Various manufacturers, such as Fumatech GmbH (Germany), SUEZ (United States), PCCell (Germany), offer commercial IEMs for broad applications, always striving to develop products with high ion selectivity, low resistance, low swelling, etc.

Our previous research assessed ED as an alternative process for removing ions from a synthetic erythritol culture broth with low levels ( $\leq 2\%$ ) of losses in products and by-products and 53 % current efficiency (Daza-Serna et al., 2022). The conclusions of our previous work led to new questions about the separation performance at different concentration of products, and the current efficiency that we could reach using different membrane stacks. In this work, we aimed to get a better understanding of the product losses and the ED current efficiency. For this, three new membrane stacks were assembled and their performance and response to different erythritol concentrations were evaluated. The results of newly purchased membranes were compared to the reference membrane stack used in the previous study (Daza-Serna et al., 2022). The limiting current density and the membrane resistance were done as prerequisite tests for investigated membranes. Diffusional phenomena, product losses, current efficiency and energy consumption were compared among four membrane stacks in the first stage to select an optimal membrane for the second stage of the experiments. In the second stage, the focus was put more on the behaviour of the chosen membrane stack with increments of product concentration. Further on, step-wise voltage and constant current ED control were compared. Finally, erythritol culture broth after cultivation was treated by ED based on the previously obtained parameters.

## 2 Materials and Methods

### 2.1 Technical equipment

Laboratory scale electrodialysis ED 64004 (PCCell GmbH, Heusweiler, Deutschland) with built-in pH, temperature and electrical conductivity probes was used for this study. 1.5 L of

diluate and 1.5 L of concentrate were circulated with a flow rate of 15 L/h (linear velocity of 0.012 m/s), and the electrode-rinse solution (0.25 M Na<sub>2</sub>SO<sub>4</sub>) with a flow rate of 150 L/h, in all ED experiments. ED outlet pipes were adjoined for the limiting current density tests in order to achieve stationary conditions. On the contrary, the concentrate and diluate streams were completely separated in the erythritol purification experiments and diffusion analysis. The temperature was controlled with cooling water to maintain 22.5±1°C throughout all experiments.

## 2.2 Membranes

A 10 cell pair ED stack was assembled from different cation- (9xCEM) and anion-exchange membranes (10xAEM) to test them for erythritol purification. Membranes were cut to the active membrane area of 64 cm<sup>2</sup>. The reference membrane (M0) was from the previous research on the erythritol broth treatment by electrodialysis (Daza-Serna et al., 2022). Membrane stacks M1 (SUEZ Water Technologies & Solutions, Pennsylvania, United States), M2 and M3 (Fumatech GmbH, Bietigheim-Bissingen, Germany) were tested in this study. All tested membrane stacks had the same end-membranes (End-M in Table 1) and polypropylene spacers (0.45 mm). Membrane specifications are presented in Table 1.

**Table 1.** Membrane characteristics of the reference membrane stack (M0) and tested membrane stacks (M1-M3):

Membrane stack	Membrane	Type	Thickness	Resistance	Selectivity	Ion-
						exchange capacity
			[μm]	[Ω cm <sup>2</sup> ]	[%]	[meq/g]
M0	PC-SA	AEM	100-110	~ 1.8	>95	0.1-1.2
	PC-SK	CEM	100-120	~ 2.5	>96	3
M1	AER103P	AEM	570	9.4	92	2.4
	CR61P	CEM	580	10	94	2.2
M2	FAS-PET-130	AEM	120-140	1.7-3.0	93-97	1.0-1.3
	FKS-PET-130	CEM	120-140	2.4-4.0	96-99	0.8-1.0
M3	FAB-PK-130	AEM	115-138	<4	95	0.8
	FKL-PK-130	CEM	120-140	3-10	96-99	0.6-0.8
End-M	PC-MTE	CEM	220	~ 4.5	>94	1.8

## 2.3 Experimental setup

Figure 1 depicts the experimental methods performed within this study. The criteria for selecting an ion-exchange membrane embraced results from LCD tests and first experimental stage (1<sup>st</sup>). 1<sup>st</sup> stage included diffusion tests and erythritol separation of 5 g/L erythritol from a synthetic erythritol broth (SEB). Erythritol concentrations were increased to 15 g/L and to 25 g/L in the second experimental stage (2<sup>nd</sup>), that included diffusion tests and erythritol separation. Step-wise voltage and constant current ED operating mode were compared and finally erythritol was separated from a real erythritol culture broth.

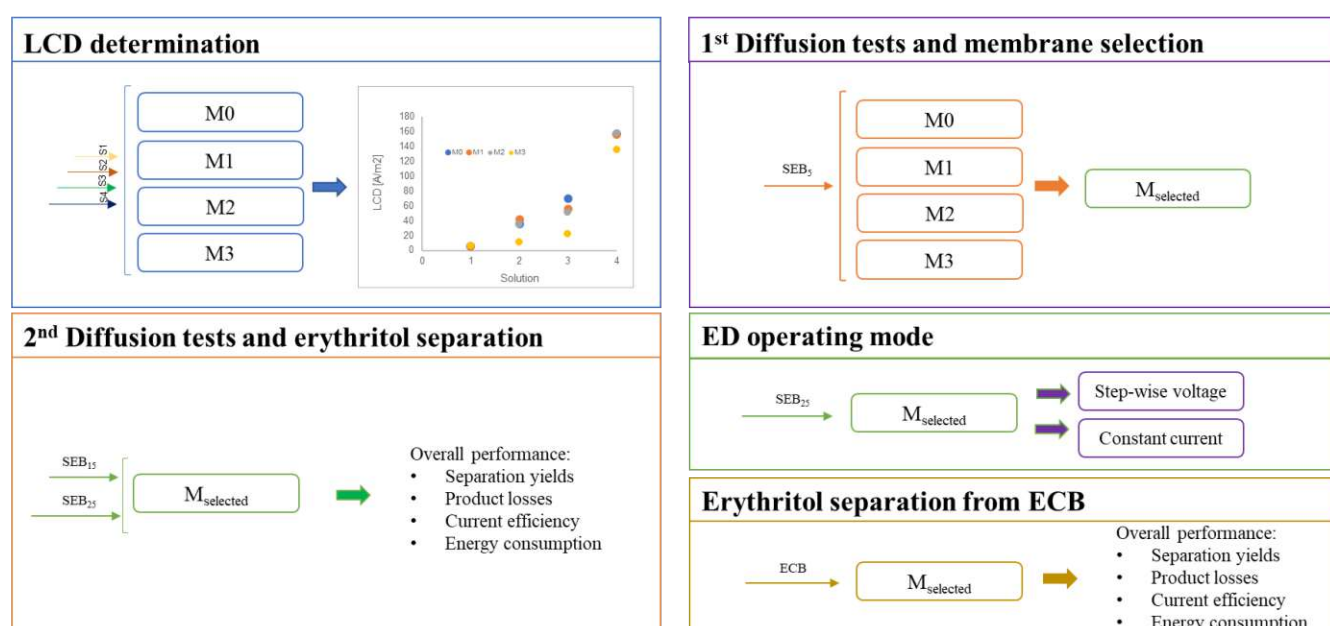


**Figure 1.** Scheme of experimental methods for the membrane selection and overall performance of erythritol separation by electrodialysis under various erythritol concentrations and operating conditions. SEB – synthetic erythritol broth containing 5 g/L (SEB<sub>5</sub>), 15 g/L (SEB<sub>15</sub>) or 25 g/L (SEB<sub>25</sub>) erythritol; ECB -erythritol culture broth.

### Limiting current density (LCD)

Synthetic solutions S1–S4 without products and by-products were put in both diluate and concentrate chambers to define LCDs of each tested membrane stack. It was adopted that the LCD is mainly governed by the salt content, while uncharged molecules have a minor impact on LCD when other parameters (i.e., temperature, flow) are maintained constant. The steady-state condition was achieved by mixing the membrane outlets and evenly distributing the mixed

solution in the diluate and concentrate inlet. The voltage was increased step-wise from 3 – 29 V in 0.5 V increments. LCD was determined based on the Cowan and Brown method (Cowan & Brown, 1959).

The same LCD experiments were done for the reference membrane stack M0. The ED operation mode was determined based on the M0 results for the first stage of experiments – testing M1–M3 performances in erythritol purification.

### First stage

Three membranes M1-M3 were tested for diffusional behaviour of erythritol, glycerol and glucose from the diluate towards concentrate. The solution containing salts, products and by-products (SEB) was placed on the diluate side, whereas salt solution (S4) was placed in the concentrate chamber. Both feeds were circulated (15 L/h) for 80 minutes without applying an external electrical field. Samples were taken every 20 minutes for product/by-product analysis.

Three ED membrane stacks M1–M3 were tested for the erythritol separation from the salt content in the culture broth (Table 2) and compared to the reference membrane M0 (Table 1). Step-wise voltage was applied for the ED control, as explained in the previous research (Daza-Serna et al., 2022), until the 94% desalination rate. The outcomes assessed were: product and by-product leakage from the diluate to the concentrate, salt removal efficiency, current efficiency, and energy consumption.

### Second stage

The ED stack with the lowest product losses, highest current efficiency and lowest energy consumption was applied for further experiments in the second stage. Ideally, the erythritol concentrations are high, whereas the by-product and remaining glucose concentrations are low in an optimized cultivation for erythritol production. The membranes need to retain the products and by-products, inhibiting their diffusion and passage towards the concentrate.

Diffusion tests were also done in the second stage of testing the M2 membrane, with increased erythritol concentration to 15 g/L and 25 g/L. On the contrary, the by-product and glucose concentrations remained the same as in the first stage.

Erythritol from SEB containing 15 g/L and 25 g/L of erythritol were separated with M2 membrane stack and the same stepwise voltage control as in the first stage.

## ED operating mode

Besides choosing an optimal ion-exchange membrane, as defined before, the ED operating conditions may impact the transport mechanisms of charged and uncharged particles from the diluate towards the concentrate. Thus, the variations in current density, constant current (21.9 A/m<sup>2</sup>) and step-wise voltage (10V, 9V, 7V, 6V) were compared in the scope of this study. Step-wise voltage was regulated based on the online measurements of the diluate conductivity to prevent exceeding current densities (in results section).

## Treatment of the erythritol culture broth

A real erythritol culture broth (ECB) was treated by ED with M2 membrane stack and step-wise voltage control.

### 2.4 Solutions (synthetic and culture broth)

A synthetic solution containing only salt fractions from the erythritol culture broth was used as a fundamental solution in all the experiments with the synthetic broth. The composition of the fundamental solution (S4) is presented in Table 2. Reagents used in this study were purchased from Merck KGaA (Darmstadt, Germany). S4 solution was diluted for the purposes of LCD test, as explained later on. In all the other experiments S4 solutions was placed in the concentrate chamber as the receiving medium for recovered salts. Alterations of S4 were made for the diluate compartment in diffusion tests and other experiments of the first and the second stage, as explained in the further text.

**Table 2.** Salt fraction of the synthetic erythritol culture broth for membrane testing in LCD, stage one and stage two.

<b>Compounds in S4</b>	<b>Molecular formula</b>	<b>[g/L]</b>
Ammonium sulphate	(NH <sub>4</sub> ) <sub>2</sub> SO <sub>4</sub>	1.4
Magnesium sulphate heptahydrate	MgSO <sub>4</sub> 7H <sub>2</sub> O	0.5
Potassium dihydrogen phosphate	KH <sub>2</sub> PO <sub>4</sub>	4.2
Ferrous sulphate heptahydrate	FeSO <sub>4</sub> 7H <sub>2</sub> O	0.0025

Manganese sulphate monohydrate	MnSO <sub>4</sub> H <sub>2</sub> O	0.00085
Zinc sulphate heptahydrate	ZnSO <sub>4</sub> 7H <sub>2</sub> O	0.0007
Calcium chloride dihydrate	CaCl <sub>2</sub> 2H <sub>2</sub> O	0.001
Sodium chloride	NaCl	0.8

### *Solutions for the LCD determination*

S4 solution was diluted with dilution factors of 18, 3.9 and 1.7, to obtain S1–S3 solution, respectively. S1–S4 were used for limiting current density tests and for setting the step-wise operating mode for ED.

### *Solutions for the first experimental stage*

S4 solution in the diluate compartment was enriched with 5 g/L erythritol (C<sub>4</sub>H<sub>10</sub>O<sub>4</sub>), 5 g/L glycerol (C<sub>3</sub>H<sub>8</sub>O<sub>3</sub>) and 2 g/L glucose (C<sub>6</sub>H<sub>12</sub>O<sub>6</sub>) (SEB<sub>5</sub> in Figure 1).

### *Solutions for the second experimental stage*

S4 solution in the diluate compartment was firstly enriched with 15 g/L erythritol (SEB<sub>15</sub> in Figure 1), and in the following experiments the erythritol concentration was increased to 25 g/L (SEB<sub>25</sub> in Figure 1). Glycerol and glucose concentrations remained unchanged, 5 g/L and 2 g/L, respectively.

### *Erythritol culture broth*

Final experiments were done with a real erythritol culture broth (ECB) that was prefiltered (microfiltration with 0.3 µm pore size) and placed in the diluate side, whereas S4 solution was in the concentrate chamber for receiving the salts from the culture broth.

## 2.5 Analytics

PO<sub>4</sub>-P and NH<sub>4</sub>-N were determined with continuous flow analysis and photometrical detection (Skalar, Netherlands) according to DIN EN ISO 6878 and DIN EN ISO 11732 standards, respectively. Anions (Cl<sup>-</sup>, SO<sub>4</sub><sup>2-</sup>) were analyzed according to DIN EN ISO 10304-1 and cations (Na<sup>+</sup>, K<sup>+</sup>, Ca<sup>2+</sup>, Mg<sup>2+</sup>) according to DIN EN ISO 14911 standard, using high performance ion chromatography (Metrohm AG, Switzerland).

Erythritol, glycerol and glucose analysis were performed in high performance liquid chromatography (HPLC) as explained in the previous study (Daza-Serna et al., 2022).

## 2.6 Data analysis and calculations

The convective diffusion and flux [mmol/(m<sup>2</sup>s)] of products and by-products through the membrane were calculated by the following equation:

$$J = \frac{V_c c_c^i}{ANt} \quad (1)$$

Where  $V_c$  [L] is the concentrate volume;  $c_c^i$  [mmol/L] is the concentration of component  $i$  that diffused to the concentrate solution;  $A$  [m<sup>2</sup>] is the effective area of a single membrane;  $N$  is the number of membranes ( $N = 19$ );  $t$  [s] is the ED process time.

Energy consumed [kWh/m<sup>3</sup>] for the desalination of the erythritol broth was calculated as follows:

$$E = \int_0^t \frac{U_t I d_t}{V_d} \quad (2)$$

Where  $U_t$  [V] is the voltage drop at time  $t$  [h];  $I$  [A] is the electrical current;  $V_d$  [L] is the diluate volume.

Current efficiency [%] was calculated according to the following equation:

$$CE = \frac{(c_t - c_0)zVF}{NIt} * 100 \quad (3)$$

Where  $c_0$  and  $c_t$  are the concentration of ionic species at time zero and time  $t$  in the diluate;  $z$  is the ionic valence;  $F$  is the Faraday constant [96,485 C/mol].

## 3 Results and Discussion

### 3.1 LCD determination

#### Membranes' resistance and limiting current density

The membrane stack resistance among the tested membranes in LCD experiments is demonstrated for the applied 12 V in Figure 2. The trend was the same for the whole diapason of applied voltages 3 – 29 V. The overall resistance was very high ( $1.1 \Omega\text{m}^2$ ) and equal in M0–M3 stack for S1 solution, representing the desired final diluate quality, due to its low ionic strength. In general, the resistance decreased and the LCD increased with an increasing salt concentration of the treated feed. At the low salt concentrations ( $<1 \text{ mol/L}$ ) the overall resistance is high and the contribution of the concentration boundary layer at the membrane/solution surface should not be neglected (Sun et al., 2022). High resistances are reasonable as the S4 solution has the salt concentration of  $0.1 \text{ mol/L}$ . Additionally, diffusional transport is expected to have a high contribution to the transmembrane ion transport.

A clear inflection point in ED stack resistance with increasing current density was observed for all ran experiments of the LCD assessment. The obtained LCD values of each tested membrane stack depending on the solution's conductivity are presented in Table 3. M1 membrane was expected to have the lowest LCDs due to the largest membrane thickness and the highest specific membrane resistance (Table 1). However, the highest ion exchange capacity of the M1 membrane stack led to the lowest overall resistance. Conversely, the M3 stack had the highest overall resistance for S2–S4 solutions (Figure 2). M3 are polyketone reinforced membranes with high proton and hydroxyl blocking capability and low ion exchange capacity that resulted in low LCDs (Table 3).

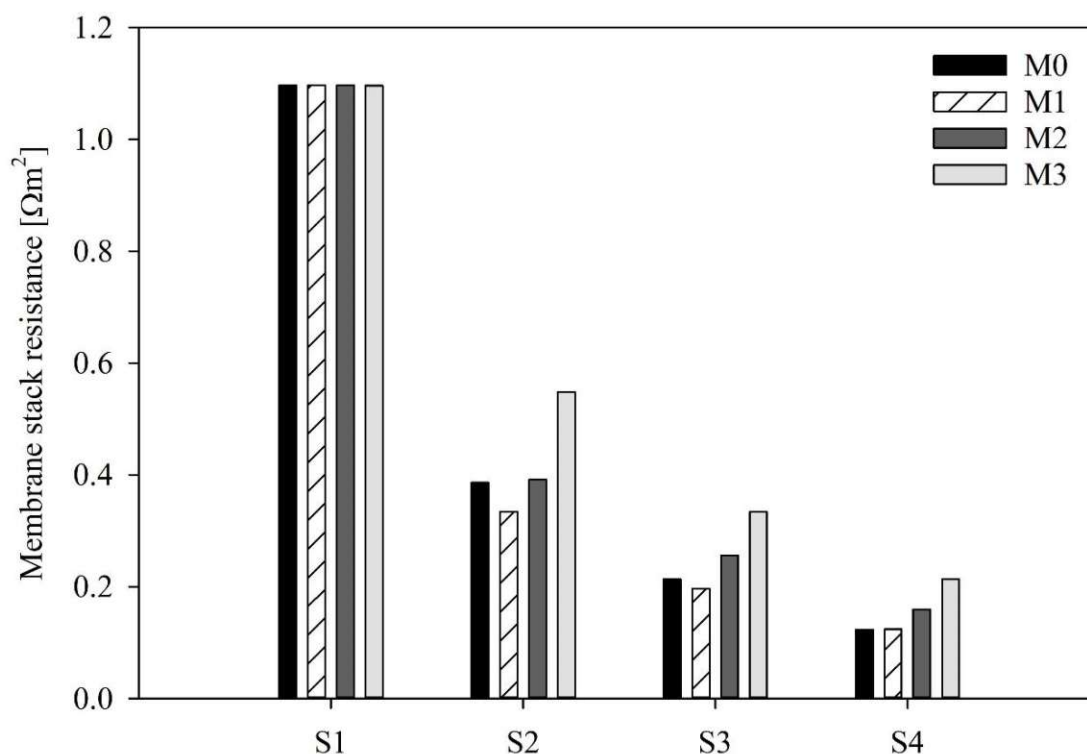


**Figure 2.** The resistance of M0–M3 membrane stacks for applied 12V in LCD test of four salt solutions with increasing salt content. S4 is the initial solution to be treated, whereas S1 represents the desired final solution after the ED treatments.

**Table 3.** LCDs reached within M0–M3 membrane stacks for salt solutions S1–S4 with their measured electrical conductivities.

Solution	Conductivity [mS/cm]	LCDs			
		M0	M1	M2	M3
S1	0.3	6.2	6.2	6.2	6.2
S2	1.4	35.9	42.2	35.9	10.9
S3	3.0	70.3	56.2	51.6	21.9
S4	5.6	157.8	156.2	157.8	135.9

Among the membranes, the LCD progression for a particular salt solution (S1–S4) could not be correlated to the membrane-specific thickness, resistance, or ion exchange capacity. M1 and

M2 membrane stacks had the most similarities with the reference membrane M0, whereas M3 had up to 70 % lower LCDs.

## 3.2 First stage – Membrane selection

### 3.2.1 Diffusion of products and by-products

Diffusion experiments were done as a single run, without current/voltage application. Diluate, containing salts, products and by-products (SEB), and concentrate, containing salts only (S4), were circulated for 80 min. The diffusion of erythritol (5 g/L), glycerol (5 g/L) and glucose (2 g/L) from the diluate to the concentrate solution was not detected in M2 and M3. The initial sample of M1 concentrate was contaminated with products, however, after the mass balance of initial and final samples there was no indication of diffusional phenomena. The non-ionic compounds did not diffuse to the electrode-rinsing solution neither.

### 3.2.2 Desalination of synthetic erythritol broth (SEB)

The set endpoint of the ED process was 93.6% feed desalination based on the online conductivity measurements. However, the desalination velocity (% removed salts/min) varied between the membrane stacks. The highest desalination velocity was for the reference membrane M0 (1.1 %/min), followed by M1 (1 %/min) and M2 (0.97 %/min), whereas M3 had a significantly lower salt removal velocity (0.51 %/min) for the same applied electrical field. M3 contains CEMs and AEMs with lower ion exchange capacity compared to M0–M2 membranes, which significantly prolonged the desalination time.

The average desalination rate for individual ions had the same trend at the end of ED in all tested membrane stacks (Table 4):

**Table 4.** Average desalination rate of anions and cations using four different membrane stacks (M0-M3)

<b>Membrane stack</b>	<b>PO<sub>4</sub>-P</b>	<b>NH<sub>4</sub>-N</b>	<b>Cl</b>	<b>SO<sub>4</sub></b>	<b>Na</b>	<b>K</b>	<b>Ca</b>	<b>Mg</b>
	<b>%</b>	<b>%</b>	<b>%</b>	<b>%</b>	<b>%</b>	<b>%</b>	<b>%</b>	<b>%</b>
M0	91.0	91.8	99.0	95.4	88.4	95.0	n.d.	93.7
M1	86.7	94.9	93.9	98.2	68.1	94.2	100	100
M2	86.3	96.3	92.4	98.2	88.0	93.9	100	97.1
M3	89.8	99.9	94.1	96.5	87.7	97.5	100	100

Only phosphates and sodium ions had removal efficiencies below 90 % in M1–M3 experiments. PO<sub>4</sub>-P was less removed due to the increased presence of H<sub>3</sub>PO<sub>4</sub> at the pH < 4 (Chen et al., 2021; Roman et al., 2020). Namely, the diluate pH dropped from ~4.6 to ~3.7 in M1–M3. In the M0 serial, the diluate pH did not drop below 4, having the complete fraction of H<sub>2</sub>PO<sub>4</sub><sup>1-</sup> that led to the higher P removal. K<sup>+</sup> was better removed than Na<sup>+</sup> because of the feed's two times higher potassium molar concentration and its higher electrical mobility (Alakhras et al., 2021; Robinson et al., 1970). The electrostatic attraction between the membrane and ions increased with increased ionic charge. Thus, almost all performed experiments achieved complete removal of divalent cations and above 95.4% of sulphate removal.

### 3.2.3 Product purification

Product and by-product losses were observed in M1, similar to the reference M0 (Daza-Serna et al., 2022). Higher concentrated erythritol and glycerol (~5 g/L) started permeating towards concentrate between 60 and 90 min of the processing time.  $1.3 \pm 0.05$  % of erythritol and  $1.8 \pm 0.02$ % of glycerol losses were recorded in M1 experiments. In the reference membrane, less than 2 % of products were found in the concentrate after 40 min of treatment (Daza-Serna et al., 2022). Contrary, glucose (~2 g/L) was not detected in the concentrate of M1–M3 experiments. This behaviour can be assigned to the lower initial glucose concentration. Steric exclusion mechanisms (Kingsbury et al., 2020; Lanteri et al., 2008) might also impact the permeation of non-ionic species. For example, glucose is a molecule with six carbon atoms existing mainly as pyranose cyclic form in aqueous solutions (>99%). Thus, the ion exchange membranes may block the passage of bigger glucose molecules better than the four-carbon erythritol and three-carbon glycerol. However, this study could not thoroughly analyze steric effects due to the other governing transport mechanism. The concentrate of M2 and M3 runs remained pure saline until the end of the feed desalination, performing even better than M0–M1 membranes. The advantage of the M2 membrane was a significantly lower resistance (Figure 2) and a shorter process time (97 min) than ED with the M3 stack (184 min).

A concentration factor of 1.8 was reached for the ions in the concentrate of all (M0–M3) experiments. The maximum recorded decrease of diluate volume was 4.7 %, caused mainly by sample uptake and partially by the osmotic water transport from the diluate towards the concentrate (Sun et al., 2021). The diluate densities dropped by  $0.32 \pm 0.017$ % from the average value of 1.005 g/cm<sup>3</sup> due to the salt removal, and the concentrate densities increased for  $0.34 \pm 0.018$ % from the average value of 1.002 g/cm<sup>3</sup> with increased salt concentration.

The current efficiency was the lowest for the reference M0 membranes (53%), and the highest for the M2 membrane stack (71.9%), as shown in Figure 3. The current efficiency trend among M0–M3 membranes could not be correlated to the operational current, charge or membrane resistance. The higher ion-exchange capacity of AEMs of M1 and M2 membrane stacks had a major impact on the higher current efficiency compared to M0 and M3 membranes (Table 1). The M0–M2 had lower resistance than M3 membranes (Figure 2) and, followingly, the shorter desalination time (81–98 min) and lower energy demand. The energy consumption for desalination of synthetic erythritol broth was the lowest in the ED assembled with M2 membranes (Figure 3).

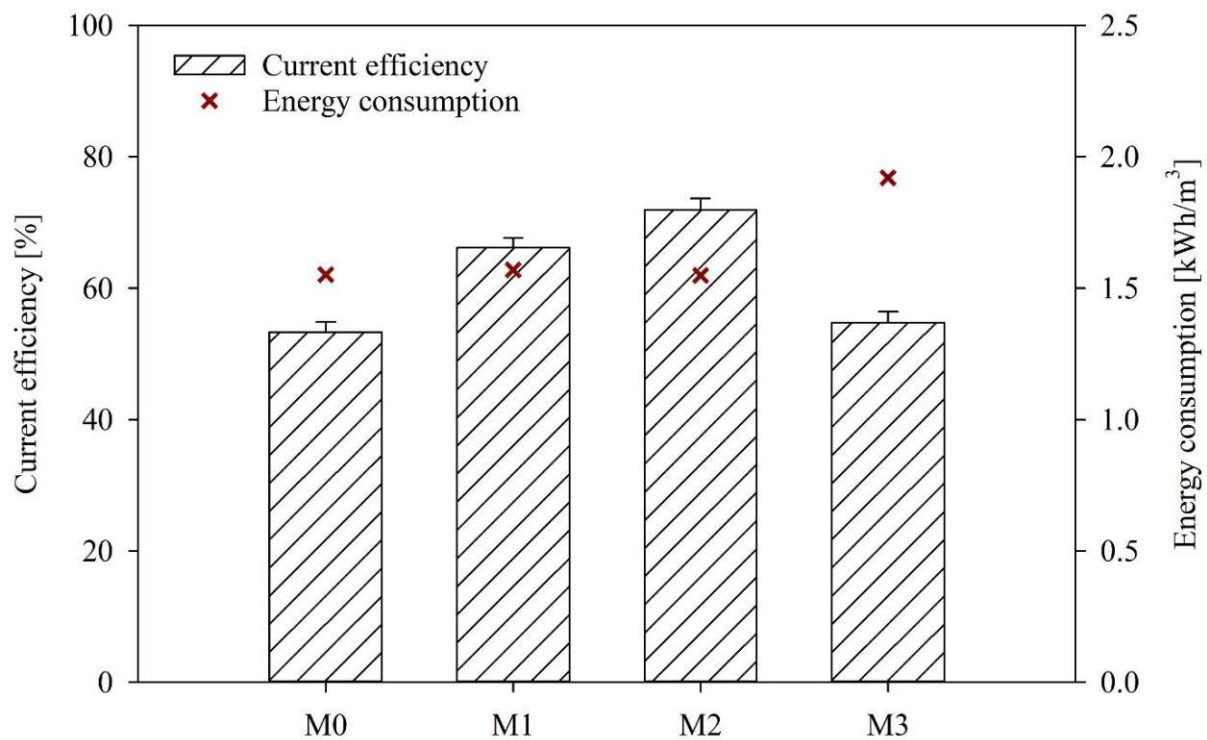


**Figure 3.** Comparison of current efficiency and energy consumption for desalination of erythritol broth among four tested membranes (M0–M3).

Finally, M2 membranes outperformed reference and other tested membranes (M0, M1 and M3) regarding higher current efficiency and high retention of products and by-products. The membrane resistance and energy consumption were in the range of values obtained in M0 and M1 and lower than in M3. The results from the first stage of experiments indicate a preferable selection of the M2 membrane stack for further ED investigation in erythritol isolation.

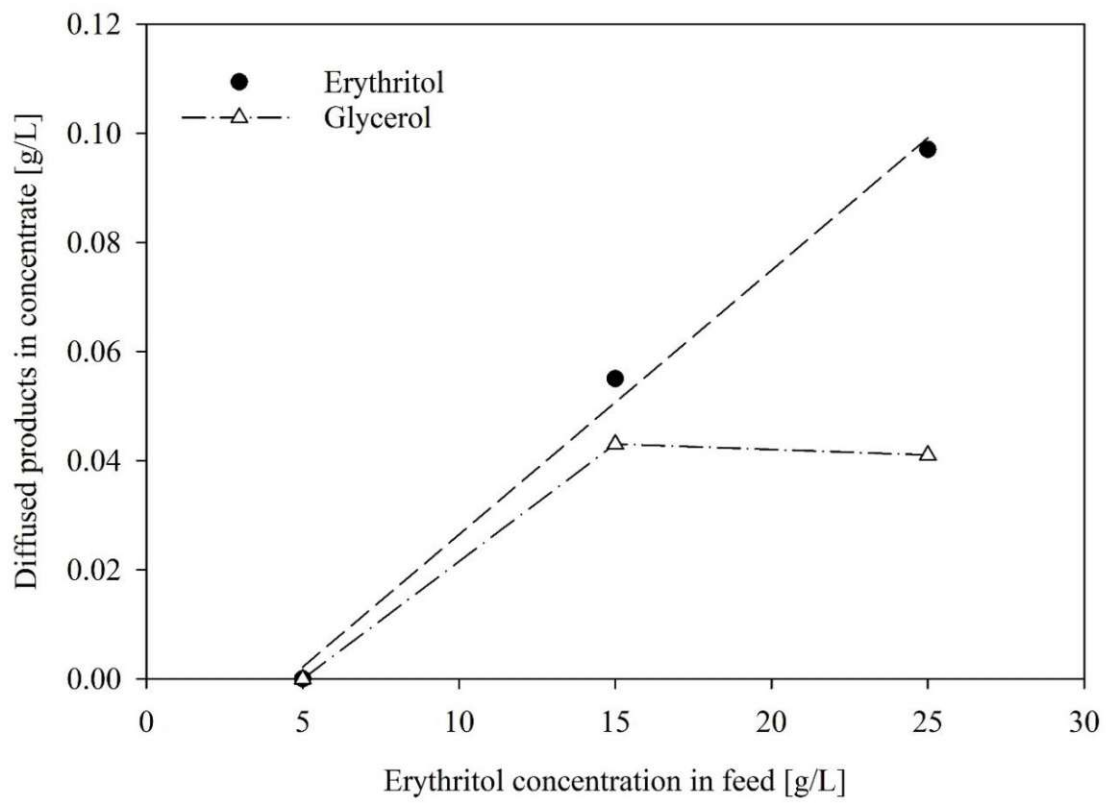
### 3.3 Second stage – Effect of the increase in erythritol concentration

Based on the results from the previous section, the M2 membranes were applied for further experiments on the optimization of the erythritol purification step. Effects of the increments in the product concentration and the current application were analyzed in the ED desalination with the M2 stack.

#### 3.3.1 Diffusion of products and by-products

Ideally, cultivation processes are optimized to intensify erythritol production and to minimize the evolution of by-product. Thus, diffusion tests were also done in the second stage of testing the M2 membrane, increasing the erythritol concentration from 5 g/L to 15 g/L and 25 g/L in SEB. On the contrary, the by-product concentrations remained the same as in the first stage. As previously reported, with 5 g/L of erythritol in the feed, no detectable amounts were measured in the concentrate fraction. The diffusion of the erythritol increased with increased initial erythritol concentration (Figure 4a) and increased contact time between the feed and the membrane surface (Figure 4b). The convective erythritol diffusion was  $1.2 \cdot 10^{-6}$  mol/(m<sup>2</sup>s) and  $2.1 \cdot 10^{-6}$  mol/(m<sup>2</sup>s) for 0.00045 mol/L (15 g/L) and 0.00079 mol/L (25 g/L), respectively. Interestingly, the diffusion of the glycerol (5 g/L) appeared with the increased erythritol concentration, but it remained at the same rate for the feed containing 15 g/L and 25 g/L of erythritol (Figure 4). Therefore, a co-transport of glycerol with erythritol diffusion was observed, but it reached its limiting convective diffusional rate of  $1.2 \cdot 10^{-6}$  mol/(m<sup>2</sup>s). The results show a clear dependence of diffusional rate on the molar concentration of carbon compounds as dominating effect (molar glycerol concentration was 0.00045 mol/L).

a)



b)

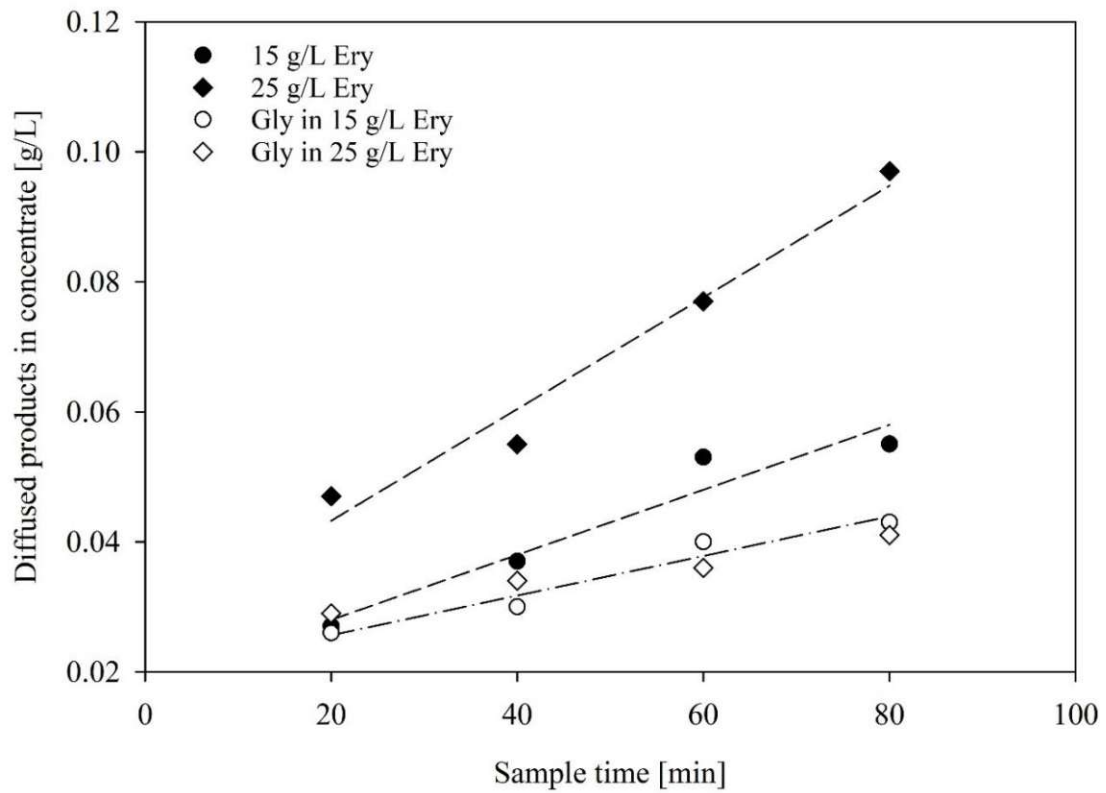


**Figure 4.** a) Diffusion of erythritol and glycerol from the feed towards concentrate depending on the erythritol concentration in the feed; b) Evolution of erythritol and glycerol diffusion over circulation time. "Ery" stays for erythritol and "Gly" for glycerol.

Erythritol losses of 0.36 % and 0.41 % were recorded for the feeds containing initially 15 g/L and 25 g/L of erythritol, respectively. The glycerol losses were 0.84% in both cases. Diffusion is concentration-dependent, thus, glucose (2 g/L) remained in the diluate for all performed experiments.

### 3.3.2 Erythritol purification and conservation

SEB containing 15 g/L and 25 g/L erythritol were desalinated by ED and compared as single runs, although the experiments in the second stage were done in duplicates. The reason for this was the contamination of the concentrate with products and by-products in the subsequent ED run. The presence of non-ionic compounds in the first samples taken from the concentrates of the second runs indicates the insufficient cleaning procedure before the experiments. More thorough cleaning is required for the ED system with higher erythritol concentrations. Cleaning steps depend on the characteristics of the treated feed and some cleaning strategies are suggested in the study of Merino-Garcia et al., (Merino-Garcia & Velizarov, 2021).

In Figure 5, the erythritol flux in ED desalination and its diffusional rate from previous experiments increased with increasing initial concentrations. The transport of erythritol was intensified with the application of the external electrical field, although the desalination time for 15 g/L and 25 g/L was prolonged for only 5–8 min compared to the diffusion experiments (80 min). The product losses increased from ~0.4 % (only diffusion) to 0.53 % due to the co-transport with ion migration through ion-exchange membranes. Ions are surrounded by water molecules that enable some non-ionic compounds to pass through the membrane matrix beside their diffusion through the interstitial membrane phase. Molar flux of glycerol was slightly higher ( $1.3 \cdot 10^{-6}$  mol/(m<sup>2</sup>s)) than its convective diffusional rate of ( $1.2 \cdot 10^{-6}$  mol/(m<sup>2</sup>s)). Thus, the glycerol losses were 0.98–1.1%.

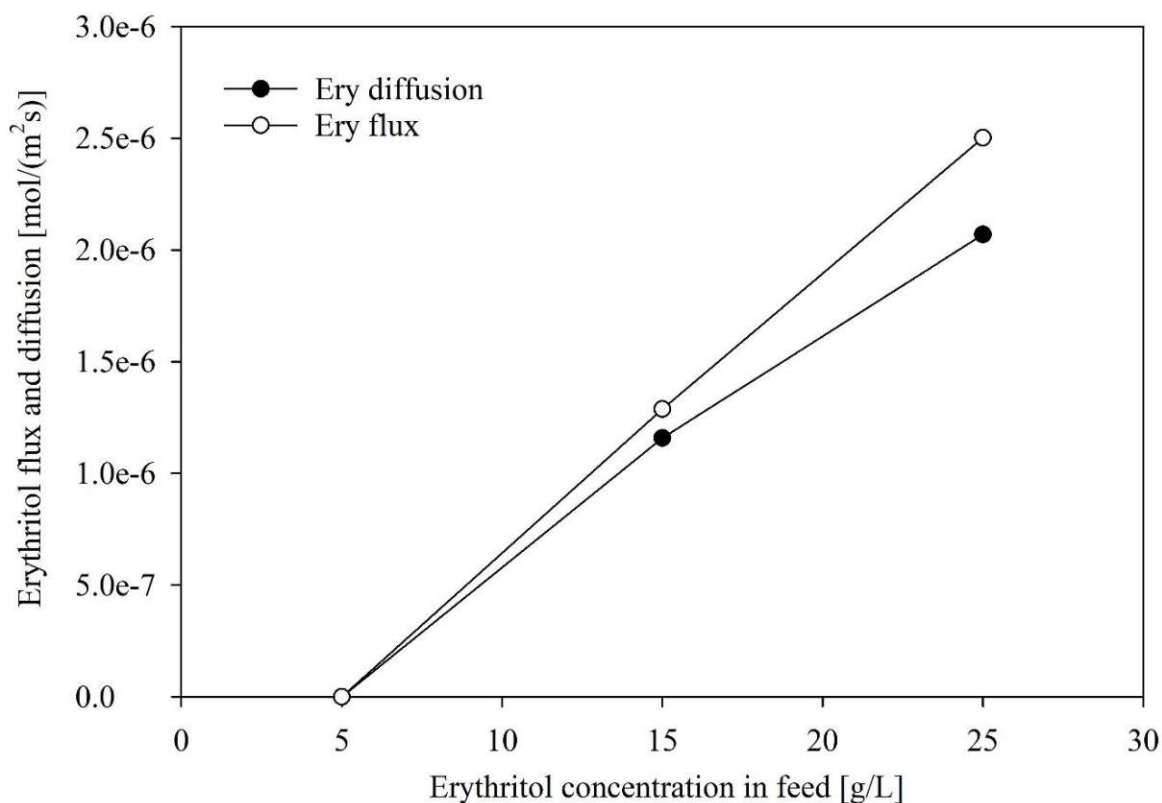


**Figure 5.** Diffusion of erythritol from the feed containing 5 g/L, 15 g/L and 25 g/L of erythritol towards the concentrate solution (black circles); Erythritol flux in the ED desalination that includes convective diffusion and co-transport with ionic species driven by the external electrical field (white circles).

The current efficiency and the energy consumption remained in the same range, 70% and 1.5 kWh/m<sup>3</sup>, respectively, for the desalination of the feed containing 5–25 g/L erythritol. Thus, the membrane characteristics and the salt content were the major factors impacting the current efficiency, desalination duration and energy demand.

### 3.4 ED operating mode

The previous experiments showed that the erythritol diffusion from the feed to the concentrate increases with the increasing contact time between the feed and the membranes (Figure 4a). Thus, the step-wise voltage control was adopted for the erythritol purification in order to intensify the ED process and reduce the product losses. Commonly, a low current density corresponding to 75 – 80 % of the limiting current density determined for the final feed quality (S1 in this case) is applied throughout the desalination process (Hábová et al., 2004; Meng et al., 2005; Sun et al., 2022). Therefore, the step-wise voltage approach was compared with the constant current approach within this research. The applied constant current density was 21.9 A/m<sup>2</sup> and the M2 membrane stack was utilized. Normally, 6.2 A/m<sup>2</sup> would be adopted

according to Table 3 for S1 solution. However, the current density between S1 and S2 solutions was chosen due to the very high membrane stack resistance when treating S1 solution.

The 93.6% desalination rate of 25 g/L erythritol broth was prolonged 1.5 times for constant current versus step-wise voltage approach (Figure 6). Although the diffusional rate was somewhat lower in the ED controlled by the constant current approach ( $2.4 \cdot 10^{-6}$  mol/(m<sup>2</sup>s)), the product and by-product escape towards concentrate was higher due to the prolonged membrane/feed contact time. The losses of erythritol were 0.78% and of glycerol 1.2%, whereas the glucose was not detected in the concentrated fraction. On the contrary, losses of erythritol were 0.53% and of glycerol 0.98% in the step-wise controlled ED. The current efficiency for ED with constant current dropped to 55%, whereas the energy consumption was slightly reduced to 1.38 kWh/m<sup>3</sup>. Current density has insignificant role in salt transport number, but the increased current density, as it was in the step-wise approach, increased the current efficiency (Sun et al., 2022). The salt removal velocity was 0.72 %/min and lower than in the step-wise ED (1 %/min).

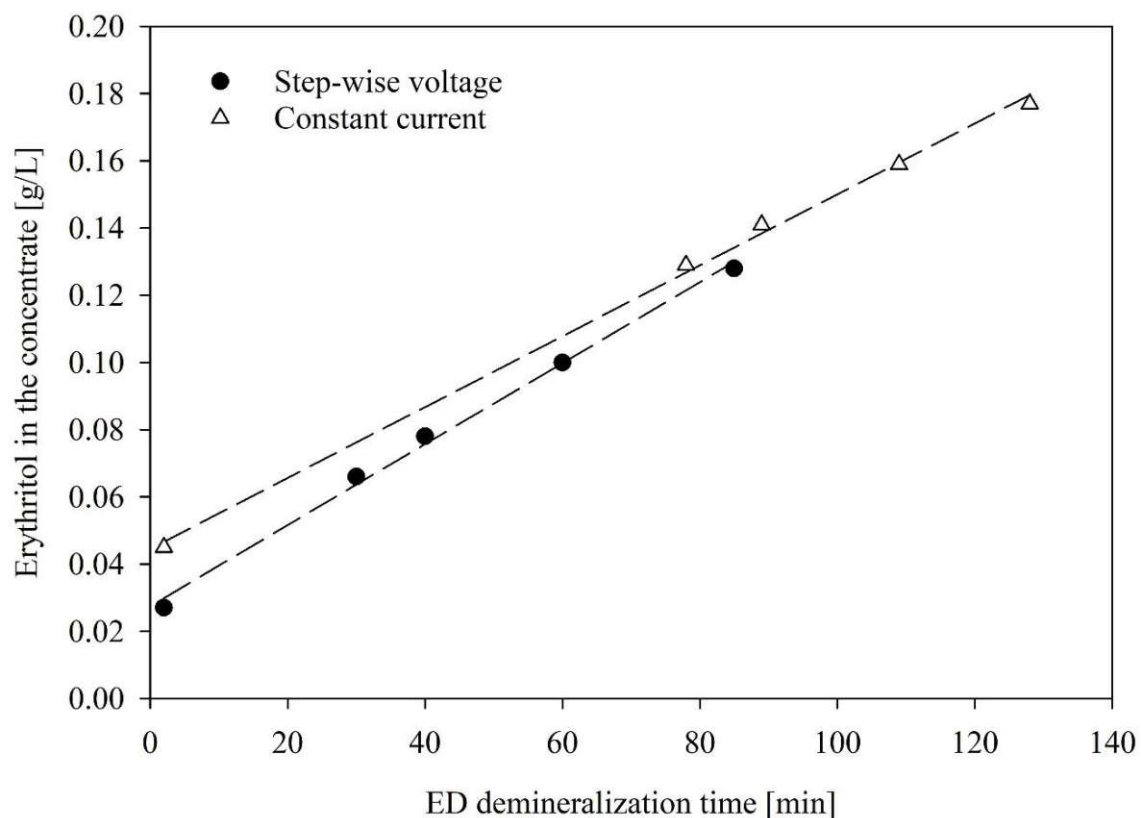


**Figure 6.** Evolution of erythritol in the concentrate during the desalination of 25 g/L erythritol broth by ED with applied step-wise voltage vs. constant current.

### 3.5 Erythritol culture broth

In the final step, erythritol was separated from the culture broth (ECB) by ED adjusted according to the previously obtained results. M2 membranes and step-wise voltage were used to minimize product losses. The feed contained 23.81 g/L erythritol, 37.92 g/L glucose and 0.99 g/L glycerol. Some other polyols were found in the culture broth, but they remained at the same concentration level in the feed during the entire desalination. The ECB treated in this work did not present a complete glucose consumption. The ionic content of the real broth was: 610 mg (PO<sub>4</sub>-P)/L, 729 mg (NH<sub>4</sub>-N)/L, 444 mg (Cl<sup>-</sup>)/L, 419 mg (SO<sub>4</sub><sup>2-</sup>)/L, 224 mg (Na<sup>+</sup>)/L, 996 mg (K<sup>+</sup>)/L, 21 mg (Ca<sup>2+</sup>)/L, 4 mg (Mg<sup>2+</sup>)/L. The same S4 solution as used in previous experiments, containing salts solely, was placed on the concentrate side.

The desalination rate was 94.8% and the ED time was 241 min. The removal efficiency for specific ions was: 95.7 % PO<sub>4</sub>-P, 90.8 % NH<sub>4</sub>-N, 94.8 % Cl<sup>-</sup>, 89 % SO<sub>4</sub><sup>2-</sup>, 92 % Na<sup>+</sup>, 95.7 % K<sup>+</sup> and 100 % for Ca<sup>2+</sup> and Mg<sup>2+</sup>, and similar to the values obtained in Table 4.

The transport of glucose and erythritol from the feed towards the concentrate was recorded already after one minute of the circulation step, and it gradually increased over the ED process time (Figure 7). Both glucose and erythritol molar fluxes decreased over ED time as their concentration in the feed decreased and as the ionic transport decreased. The erythritol and glucose molar fluxes significantly differed with the desalination time. Glucose molar flux was lower, although the initial molar concentration of glucose in the feed was higher (0.21 mol/L) than erythritol (0.19 mol/L). Differences in molecular structure and properties led to divergences in molar fluxes (Zhao et al., 2019). Erythritol is a smaller (~0.4nm) and open-chain molecule compared to glucose (~1nm) that appears in cyclic form in solutions. These chemical properties allow higher erythritol transmembrane migration. Erythritol flux was eventually the same as in the experiments performed with the synthetic solution (Figure 5 and Figure 7). The glucose and erythritol losses from the real culture broth were 4.7% and 5.6%, respectively. However, only 1.2% glucose and 2% erythritol from the feed were detected in the concentrate compartment. Therefore, it should be concluded that the remained polyol losses adsorbed in the IEMs, blocking the membrane-free volume (Roman et al., 2020; Tanaka et al., 2012). IEM fouling leads to poorer desalination performance, lower current efficiency, and higher energy consumption (Merino-Garcia & Velizarov, 2021; Pawlowski et al., 2020; Zhao et al., 2019). The effects of membrane fouling by erythritol and glucose require further research. Glycerol was not detected in the concentrate fraction.

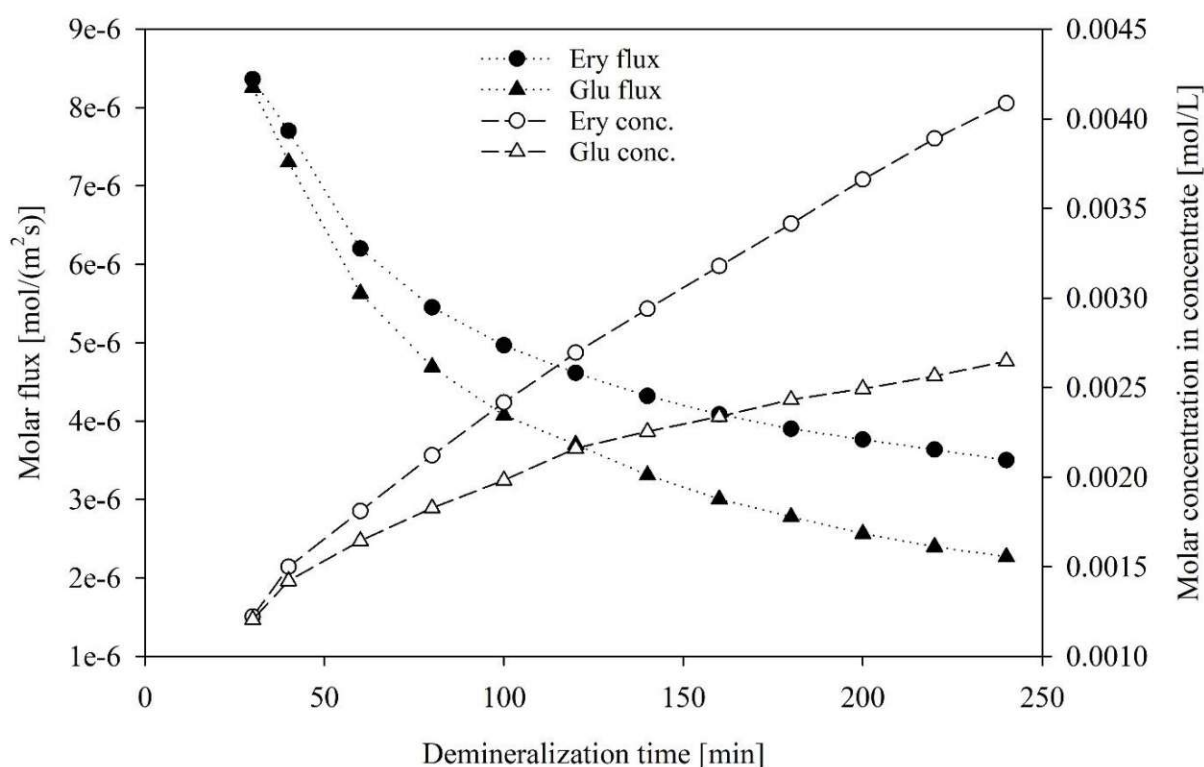


**Figure 7.** Evolution of the erythritol (Ery) and glucose (Glu) molar fluxes from the feed to the concentrate in the ED desalination of the real erythritol culture broth. The evolution of Ery and Glu concentrations in the concentrate is on the right y-axis.

The salt concentration factor in the concentrate was 2.6 due to the higher ionic content of the real culture broth (7.9 mS/cm) compared to the synthetic one (5.6 mS/cm). The 1.3 times increased salt content of the real broth led to 82 % higher energy consumption than the M2 trials with the synthetic culture broth. The presence of polyols and other organic compounds originating from microbial cells may have also prolonged the desalination process. The lower current efficiency (51%) may be assigned to the higher concentration of by-products and to the possible remains of microbial cells.

## 4 Conclusion

This research investigated membrane performance for erythritol broth desalination by electro dialysis to reduce erythritol losses and increase current efficiency. Afterward, the best-performing membrane pair was further investigated for the treatment of feeds with higher erythritol concentrations.

Limiting current density was in a similar range for M0–M2 membrane stack, whereas the M3 had up to 70 % lower values due to the higher stack resistance. M2 membrane pair, composed of FAS-PET-130 (AEM) and FKS-PET-130 (CEM) (Fumatech GmbH, Germany), had higher current efficiency (79.1%) and high retention of products and by-products (100% for the feed containing 5 g/L erythritol), while the membrane resistance and energy consumption (1.5 kWh/m<sup>3</sup>) were in the range of values obtained in M0 and M1 and lower than in M3. Thus, M2 was applied in the second experimental stage for the purification of higher concentrated synthetic erythritol broth. Erythritol losses increased from 0% to 0.36% and 0.41% for the feeds containing initially 5 g/L, 15 g/L and 25 g/L of erythritol, respectively. Additionally, erythritol losses increased by ~0.1 % under the electrical field compared to solely convective diffusion.

Step-wise voltage control of the ED process showed better results than constant current control because of the reduced product losses, mainly governed by the reduced contact time between the feed and the ion-exchange membranes. The energy consumption was similar for the same desalination rate performed with lower constant current and step-wise voltage (1.4 – 1.5 kWh/m<sup>3</sup>). In contrast, the current efficiency was higher for the step-wise approach (70 %) compared to the constant current (55 %).

Finally, optimized ED operation was applied for the desalination of the erythritol culture broth after cultivation, containing almost the same erythritol and glucose molar concentrations (~0.2 mol/L). Erythritol molar flux was higher than glucose due to the smaller molecular size. 1.2 % glucose and 2 % erythritol from the feed were detected in the concentrate compartment. The higher salt content in the culture broth led to higher product and by-product losses because of the prolonged desalination time.

### Acknowledgment

The authors want to acknowledge: MSc. Audrey Masi and MSc. Johanna Pfinier for providing the culture broth; BSc Raj Mailaram for helping to perform experiments; TU Wien and the Institutional Open Access Program (IOAP) for financial support (Open Access Funding by TU Wien).

## **Funding**

The financial support was provided by the Doctoral College “Bioactive” and the Christian Doppler Research Association, the Austrian Federal Ministry for Digital and Economic Affairs, the National Foundation for Research, Technology and Development, and Conzil Estate GmbH is gratefully acknowledged.

## **Competing interest**

Conzil Estate GmbH filed a patent (EPO application no. 21 216 448.7) related to the content of this study.

## **Author contributions**

Conceptualization: K.K. and L.D.; methodology: K.K. and L.D.; validation: K.K., L.D., N.K., J.K., A.F., A.M., and R.M.; formal analysis: K.K.; investigation: K.K. and L.D.; resources: A.F., A.M., R.M., J.K., and N.K.; data curation: K.K. and L.D.; writing-original draft preparation: K.K.; writing-review and editing, L.D., A.M., A.F., R.M., J.K., and N.K.; visualization, K.K.; supervision: A.F., A.M., R.M., and J.K.; project administration: A.F., A.M., R.M., J.K.; funding acquisition: A.F., A.M., R.M., J.K., and N.K. All authors have read and agreed to the published version of the manuscript.”

## References

- Alakhras, F., Bel Hadj Hmida, E. S., Anastopoulos, I., Trabelsi, Z., Mabrouk, W., Ouerfelli, N., & Fauvarque, J. F. (2021). Diffusion analysis and modeling of kinetic behavior for treatment of brine water using electro dialysis process. *Water Science and Engineering*, *14*(1), 36–45. <https://doi.org/10.1016/j.wse.2020.05.002>
- Al-Amshawee, S., Yunus, M. Y. B. M., Azoddein, A. A. M., Hassell, D. G., Dakhil, I. H., & Hasan, H. A. (2020). Electro dialysis desalination for water and wastewater: A review. *Chemical Engineering Journal*, *380*, 122231. <https://doi.org/10.1016/j.cej.2019.122231>
- Albornoz, L. L., Marder, L., Benvenuti, T., & Bernardes, A. M. (2019). Electro dialysis applied to the treatment of an university sewage for water recovery. *Journal of Environmental Chemical Engineering*, *7*(2), 102982. <https://doi.org/10.1016/j.jece.2019.102982>
- Bian, D. W. (2019). *Optimization and design of a low-cost, village-scale, photovoltaic-powered, electro dialysis reversal desalination system for rural India*. 14.
- Chen, R.-F., Liu, T., Rong, H.-W., Zhong, H.-T., & Wei, C.-H. (2021). Effect of Organic Substances on Nutrients Recovery by Struvite Electrochemical Precipitation from Synthetic Anaerobically Treated Swine Wastewater. *Membranes*, *11*(8), 594. <https://doi.org/10.3390/membranes11080594>
- Cowan, D. A., & Brown, J. H. (1959). Effect of Turbulence on Limiting Current in Electro dialysis Cells. *Industrial & Engineering Chemistry*, *51*(12), 1445–1448.
- Daza-Serna, L., Knežević, K., Kreuzinger, N., Mach-Aigner, A. R., Mach, R. L., Krampe, J., & Friedl, A. (2022). Recovery of Salts from Synthetic Erythritol Culture Broth via Electro dialysis: An Alternative Strategy from the Bin to the Loop. *Sustainability*, *14*(2), 734. <https://doi.org/10.3390/su14020734>
- Daza-Serna, L., Serna-Loaiza, S., Masi, A., Mach, R. L., Mach-Aigner, A. R., & Friedl, A. (2021). From the culture broth to the erythritol crystals: An opportunity for circular economy. *Applied Microbiology and Biotechnology*, *105*(11), 4467–4486. <https://doi.org/10.1007/s00253-021-11355-2>
- González, M. I., Álvarez, S., Riera, F. A., & Álvarez, R. (2006). Purification of Lactic Acid from Fermentation Broths by Ion-Exchange Resins. *Industrial & Engineering Chemistry Research*, *45*(9), 3243–3247. <https://doi.org/10.1021/ie051263a>
- Greiter, M., Novalin, S., Wendland, M., Kulbe, K.-D., & Fischer, J. (2004). Electro dialysis versus ion exchange: Comparison of the cumulative energy demand by means of two

applications. *Journal of Membrane Science*, 233(1), 11–19.

<https://doi.org/10.1016/j.memsci.2003.11.027>

Hábová, V., Melzoch, K., Rychtera, M., & Sekavová, B. (2004). Electrodialysis as a useful technique for lactic acid separation from a model solution and a fermentation broth. *Desalination*, 162, 361–372. [https://doi.org/10.1016/S0011-9164\(04\)00070-0](https://doi.org/10.1016/S0011-9164(04)00070-0)

Ishikawa, M., Miyashita, M., Kawashima, Y., Nakamura, T., Saitou, N., & Modderman, J. (1996). Effects of Oral Administration of Erythritol on Patients with Diabetes. *Regulatory Toxicology and Pharmacology*, 24(2), S303–S308.

<https://doi.org/10.1006/rtp.1996.0112>

Kingsbury, R. S., Wang, J., & Coronell, O. (2020). Comparison of water and salt transport properties of ion exchange, reverse osmosis, and nanofiltration membranes for desalination and energy applications. *Journal of Membrane Science*, 604, 117998. <https://doi.org/10.1016/j.memsci.2020.117998>

Lanteri, Y., Szymczyk, A., & Fievet, P. (2008). Influence of Steric, Electric, and Dielectric Effects on Membrane Potential. *Langmuir*, 24(15), 7955–7962.

<https://doi.org/10.1021/la800677q>

Luo, T., Abdu, S., & Wessling, M. (2018). Selectivity of ion exchange membranes: A review. *Journal of Membrane Science*, 555, 429–454.

<https://doi.org/10.1016/j.memsci.2018.03.051>

Meng, H., Deng, D., Chen, S., & Zhang, G. (2005). A new method to determine the optimal operating current (I<sub>lim</sub>) in the electrodialysis process. *Desalination*, 181(1–3), 101–108. <https://doi.org/10.1016/j.desal.2005.01.014>

Merino-Garcia, I., & Velizarov, S. (2021). New insights into the definition of membrane cleaning strategies to diminish the fouling impact in ion exchange membrane separation processes. *Separation and Purification Technology*, 277, 119445.

<https://doi.org/10.1016/j.seppur.2021.119445>

Moon, H.-J., Jeya, M., Kim, I.-W., & Lee, J.-K. (2010). Biotechnological production of erythritol and its applications. *Applied Microbiology and Biotechnology*, 86(4), 1017–1025. <https://doi.org/10.1007/s00253-010-2496-4>

Park, Y.-C., Oh, E. J., Jo, J.-H., Jin, Y.-S., & Seo, J.-H. (2016). Recent advances in biological production of sugar alcohols. *Current Opinion in Biotechnology*, 37, 105–113.

<https://doi.org/10.1016/j.copbio.2015.11.006>

Pawlowski, S., Huertas, R. M., Galinha, C. F., Crespo, J. G., & Velizarov, S. (2020). On operation of reverse electrodialysis (RED) and membrane capacitive deionisation

(MCDI) with natural saline streams: A critical review. *Desalination*, 476, 114183.  
<https://doi.org/10.1016/j.desal.2019.114183>

Rakicka, M., Rukowicz, B., Rywińska, A., Lazar, Z., & Rymowicz, W. (2016). Technology of efficient continuous erythritol production from glycerol. *Journal of Cleaner Production*, 139, 905–913. <https://doi.org/10.1016/j.jclepro.2016.08.126>

Ran, J., Wu, L., He, Y., Yang, Z., Wang, Y., Jiang, C., Ge, L., Bakangura, E., & Xu, T. (2017). Ion exchange membranes: New developments and applications. *Journal of Membrane Science*, 522, 267–291. <https://doi.org/10.1016/j.memsci.2016.09.033>

Robinson, R. A., Stokes, R. H., & Marsh, K. N. (1970). Activity coefficients in the ternary system: Water + sucrose + sodium chloride. *The Journal of Chemical Thermodynamics*, 2(5), 745–750. [https://doi.org/10.1016/0021-9614\(70\)90050-9](https://doi.org/10.1016/0021-9614(70)90050-9)

Roman, M., Gutierrez, L., Van Dijk, L. H., Vanoppen, M., Post, J. W., Wols, B. A., Cornelissen, E. R., & Verliefde, A. R. D. (2020). Effect of pH on the transport and adsorption of organic micropollutants in ion-exchange membranes in electrodialysis-based desalination. *Separation and Purification Technology*, 252, 117487. <https://doi.org/10.1016/j.seppur.2020.117487>

Sun, B., Zhang, M., Huang, S., Cao, Z., Lu, L., & Zhang, X. (2022). Study on mass transfer performance and membrane resistance in concentration of high salinity solutions by electrodialysis. *Separation and Purification Technology*, 281, 119907. <https://doi.org/10.1016/j.seppur.2021.119907>

Sun, B., Zhang, M., Huang, S., Wang, J., & Zhang, X. (2021). Limiting concentration during batch electrodialysis process for concentrating high salinity solutions: A theoretical and experimental study. *Desalination*, 498, 114793. <https://doi.org/10.1016/j.desal.2020.114793>

Tanaka, N., Nagase, M., & Higa, M. (2012). Organic fouling behavior of commercially available hydrocarbon-based anion-exchange membranes by various organic-fouling substances. *Desalination*, 296, 81–86. <https://doi.org/10.1016/j.desal.2012.04.010>

Tiefenbacher, K. F. (2017). Chapter Three—Technology of Main Ingredients—Sweeteners and Lipids. In K. F. Tiefenbacher (Ed.), *Wafer and Waffle* (pp. 123–225). Academic Press. <https://doi.org/10.1016/B978-0-12-809438-9.00003-X>

Wölnerhanssen, B. K., Meyer-Gerspach, A. C., Beglinger, C., & Islam, Md. S. (2020). Metabolic effects of the natural sweeteners xylitol and erythritol: A comprehensive review. *Critical Reviews in Food Science and Nutrition*, 60(12), 1986–1998. <https://doi.org/10.1080/10408398.2019.1623757>

- Yaroslavtsev, A. B., & Nikonenko, V. V. (2009). Ion-exchange membrane materials: Properties, modification, and practical application. *Nanotechnologies in Russia*, 4(3), 137–159. <https://doi.org/10.1134/S199507800903001X>
- Zhang, X., Zhang, C., Meng, F., Wang, C., Ren, P., Zou, Q., & Luan, J. (2021). Near-zero liquid discharge of desulfurization wastewater by electro dialysis-reverse osmosis hybrid system. *Journal of Water Process Engineering*, 40, 101962. <https://doi.org/10.1016/j.jwpe.2021.101962>
- Zhao, Z., Shi, S., Cao, H., Li, Y., & Van der Bruggen, B. (2019). Comparative studies on fouling of homogeneous anion exchange membranes by different structured organics in electro dialysis. *Journal of Environmental Sciences*, 77, 218–228. <https://doi.org/10.1016/j.jes.2018.07.018>